



**A study of genetic polymorphism underlying
idiosyncratic hepatotoxicity due to
anti-tuberculosis medications**

Ching Soon, Ng

**Thesis submitted in partial fulfilment of the requirements for the
degree of Doctor of Philosophy**

**Newcastle University
Faculty of Medical Sciences
Institute of Cellular Medicine
June 2011**

Abstract

Anti-tuberculosis drug-induced liver injury is a rare but serious adverse drug reaction. This study aimed to identify specific genes conferring susceptibility to this serious adverse drug reaction, especially in relation to isoniazid treatment and to study the underlying mechanism for toxicity.

Anti-tuberculosis drug-induced liver injury cases (n=26) and community controls (n=90) from Europe and South Asia were genotyped for polymorphisms in *NAT2*, *GST* genes, *CYP2E1*, *PXR* and *SOD2*. *NAT2* slow acetylators were more susceptible to liver injury (OR=4.60; 95% CI=1.47-14.44). The *GSTM1* null genotype was more common in cases than controls (OR=2.91; 95% CI=1.14-7.43). Risk of liver injury was significantly increased in subjects with combined *NAT2* slow acetylator and *GSTM1* null genotype (OR=3.71; 95% CI=1.48-9.31). No significant effects were seen for the other genotypes studied except that a *GSTA4* haplotype was slightly more common in liver injury cases.

The contribution of *NAT2* genotype to isoniazid toxicity was examined using an *in vitro* overexpression approach. Stable expression of either *NAT2*4* or *NAT*5* constructs in HepG2 cells had small effects on reduced glutathione to oxidised glutathione ratio and apoptosis. These changes were consistent with higher *NAT2* activity increasing isoniazid toxicity. In addition, overexpression and siRNA knockdown approaches showed protective roles for *GSTA1* and *A4* against isoniazid toxicity.

The relevance of combinations of anti-tuberculosis drugs to overall toxicity was investigated by studies in human hepatocytes and LS180 cells. In the LS180 cells, rifampicin coadministration with isoniazid resulted in a small but significant decrease in both isoniazid and pyrazinamide toxicity. Studies on the isoniazid-rifampicin combination in human hepatocytes gave inconsistent findings but a decrease in cell toxicity due to isoniazid by pretreatment with rifampicin was seen in some donors. Increased expression of the carboxyesterase gene *CES2* was seen in LS180 cells and in some hepatocytes and could represent a protective effect.

CONTENTS

LIST OF FIGURES	VIII
LIST OF TABLES	X
ACKNOWLEDGEMENTS.....	XII
1. INTRODUCTION.....	2
1.1 Adverse drug reactions	2
1.2 Drug-induced liver injury.....	5
1.2.1 The epidemiology of DILI	8
1.2.2 Types of DILI.....	9
1.2.2.1 Hepatocellular injury.....	9
1.2.2.2 Cholestatic injury	10
1.2.2.3 Mixed pattern of liver injury	10
1.3 Causality assessment in DILI.....	11
1.3.1 International Organisation of Medical Sciences (CIOMS) scale/ RUCAM ...	12
1.3.2 DILIN expert opinion.....	13
1.4 Mechanism of DILI.....	14
1.4.1 Overview of DILI mechanism	14
1.4.2 Immunological idiosyncratic reactions	16
1.4.2.1 The hapten hypothesis.....	16
1.4.2.2 Danger hypothesis.....	16
1.4.2.3 Activation of the adaptive immune response	17
1.4.2.4 Stimulation of innate immune response.....	17
1.4.2.5 Autoimmunity	18
1.4.3 Metabolic idiosyncratic reactions	18
1.4.3.1 Toxic metabolites	18
1.4.3.2 Disruption of intracellular calcium homeostasis.....	19
1.4.3.3 Mitochondrial damage	19
1.5 Pharmacogenomics in DILI	20
1.5.1 Xenobiotic metabolism	20
1.5.2 Phase I metabolising enzymes	21
1.5.3 Phase II metabolising enzymes	22
1.5.3.1 UDP-glucuronosyltransferases (UGTs).....	22
1.5.3.2 Arylamine N-acetyltransferase 2 (NAT2).....	22
1.5.3.3 Glutathione S-transferases	23
1.5.4 Drug transporters.....	23
1.5.5 Oxidative stress	26
1.5.6 Immune related genes	27
1.5.6.1 Human leukocytes antigen (HLA)	27
1.5.6.2 Cytokine genes	28
1.6 Anti-tuberculosis drugs-induced liver injury	28
1.6.1 The burden of tuberculosis (TB)	28

1.6.2	Anti-TB drugs (ATD)	29
1.6.3	Metabolism of anti-TB drugs (ATD)	32
1.6.3.1	Isoniazid (INH)	32
1.6.3.2	Rifampicin (RMP)	33
1.6.3.3	Pyrazinamide (PZA)	34
1.6.4	Anti-TB drugs-induced liver injury (ATD-DILI)	35
1.7	Candidate genes for ATD-DILI	37
1.7.1	N-acetyltransferase 2 (NAT2)	38
1.7.2	<i>CYP2E1</i>	40
1.7.3	Glutathione S-transferase enzymes (GSTs)	41
1.8	Aims of the study	42
2	GENERAL MATERIALS AND METHODS	44
2.1	General Laboratory Practice	44
2.2	Chemical Reagents	44
2.3	Mammalian Cell culture	46
2.3.1	General Materials	46
2.3.2	Routine Passage	46
2.3.3	Cell line maintenance	46
2.3.4	Cell line storage	46
2.3.5	Microscopy and cell counting	47
2.3.6	Cell lines	47
2.4	Genomic DNA preparation and analysis	47
2.4.1	DNA extraction	47
2.4.2	Determinants of DNA yield and purity	48
2.4.3	DNA sample storage	48
2.4.4	Polymerase Chain Reaction (PCR)	48
2.4.4.1	Primers	48
2.4.4.2	PCR procedure	49
2.4.5	Electrophoresis and visualisation of DNA fragments	49
2.4.5.1	Agarose gel electrophoresis	49
2.4.5.2	Polyacrylamide gel electrophoresis (PAGE)	49
2.4.5.3	Gel visualisation	50
2.4.6	DNA purification and sequencing	50
2.5	Recombinant cell line construction	50
2.5.1	Insertion of PCR product into plasmid vector	50
2.5.2	Transformation	52
2.5.3	Isolating recombinant plasmid DNA	52
2.5.4	Transfection and generation of stable cell lines	52
2.6	RNA isolation and analysis	53
2.6.1	RNA isolation and quantification	53
2.6.2	Synthesis of cDNA	53
2.6.3	Semiquantitative reverse transcription-PCR (Semiquantitative RT-PCR)	54
2.6.4	Quantitative real-time PCR (Quantitative RT-PCR)	56

2.7	Protein analysis	63
2.7.1	Protein extraction and quantification	63
2.7.2	SDS polyacrylamide Gel Electrophoresis (SDS-PAGE)	63
2.7.3	Western Blotting	64
2.7.4	Quantitation of protein bands	65
2.8	Assessment of cell viability	65
2.9	Determination of intracellular glutathione content	66
2.10	DNA fragmentation assay	69
2.11	Caspase-3 activity assay	71
3	GENETIC POLYMORPHISMS OF ANTI-TUBERCULOSIS DRUGS METABOLIZING ENZYMES.....	75
3.1	Introduction	75
3.2	Materials and Methods	76
3.2.1	Patient recruitment	76
3.2.2	PCR-restriction fragment length polymorphism (PCR-RFLP).....	78
3.2.3	Genotyping of <i>NAT2</i>	78
3.2.4	Genotyping of <i>CYP2E1</i>	83
3.2.5	<i>PXR</i> -25385 SNP genotyping	89
3.2.6	Genotyping of anti-oxidative stress-related genes	91
3.2.6.1	<i>GSTA1</i>	91
3.2.6.2	<i>GSTA4</i>	92
3.2.6.3	<i>GSTT1</i>	100
3.2.6.4	<i>GSTM1</i>	101
3.2.6.5	<i>SOD2</i>	102
3.2.7	Taqman SNP genotyping assay for <i>NAT1</i> (rs2739685)	106
3.2.8	Statistical analysis	108
3.2.8.1	Power Calculations.....	108
3.2.8.2	Hardy-Weinberg Equilibrium	108
3.2.8.3	Genotype analysis	111
3.2.8.4	Haplotype analysis	111
3.2.8.5	Multiple testing	112
3.3	Results	115
3.3.1	<i>NAT2</i>	115
3.3.1.1	Investigation of a possible association between <i>NAT2</i> genotype and susceptibility to ATD-DILI.....	115
3.3.1.2	Sensitivity analysis on <i>NAT2</i> genotype as a predictor of anti-TB DILI.....	123
3.3.2	Genotyping for additional candidate genes for ATD-DILI.....	123
3.3.2.1	Genes chosen for study	123
3.3.2.2	<i>CYP2E1</i>	125
3.3.2.3	<i>PXR</i>	127
3.3.2.4	<i>GSTA1</i>	128
3.3.2.5	<i>GSTA4</i>	129
3.3.2.6	<i>GSTT1</i>	134

3.3.2.7	GSTM1.....	135
3.3.2.8	SOD2.....	138
3.3.3	<i>NAT1</i>	140
3.4	Discussion.....	142
4	<i>IN VITRO</i> HEPATOTOXICITY AND INTERACTIONS BETWEEN ANTI-TUBERCULOSIS DRUGS	150
4.1	Introduction.....	150
4.2	Materials and Methods	152
4.2.1	Cell culture of human hepatocytes.....	152
4.2.2	Cell proliferation effects of RMP combined with INH and PZA	152
4.2.2.1	LS180 cells.....	152
4.2.2.2	Human hepatocytes	152
4.2.3	Effects of Rifampicin on mRNA expression profile.....	153
4.2.3.1	LS180 cells.....	153
4.2.3.2	Human hepatocytes	153
4.2.4	NAT2 genotyping	153
4.3	Results	154
4.3.1	Cell proliferation effects of RMP combined with other anti-TB medications	154
4.3.1.1	LS180 cells.....	154
4.3.1.2	Human primary hepatocytes	157
4.3.2	Effects of Rifampicin on mRNA expression profile.....	159
4.3.2.1	LS180 cells.....	159
4.3.2.2	Human primary hepatocytes	161
4.3.3	Determination of NAT2 genotype	161
4.4	Discussion.....	163
5	<i>IN VITRO</i> EFFECTS OF <i>NAT2</i> ALLELIC VARIANTS ON ISONIAZID TOXICITY	168
5.1	Introduction.....	168
5.2	Materials and Methods	171
5.2.1	Choice of Cell line	171
5.2.2	Construction of NAT2 recombinant stable cells.....	171
5.2.3	Recombinant expression of NAT2 alleles.....	174
5.2.4	N-acetyltransferase-2 enzyme assay	174
5.2.5	Rat liver lysate preparation	177
5.2.6	Functional characterisation of <i>NAT2</i> acetylation phenotypes.....	177
5.3	Results	177
5.3.1	Sequencing	177
5.3.2	Determination of NAT2 enzyme activity.....	182
5.3.3	Functional characterisation of <i>NAT2</i> acetylation phenotypes.....	184
5.3.3.1	Effects of NAT2 overexpression on cell proliferation.....	184
5.3.3.2	Effects of NAT2 overexpression on cellular GSH and GSSG.....	185

5.3.3.3	Effects of NAT2 overexpression on INH-induced apoptosis	188
5.4	Discussion.....	190
6	THE PROTECTIVE ROLE OF GLUTATHIONE S-TRANSFERASE A CLASS AGAINST CYTOTOXIC EFFECTS OF ISONIAZID	195
6.1	Introduction.....	195
6.2	Materials and Methods	196
6.2.1	The overexpression effect of hGSTA4 on INH toxicity	196
6.2.1.1	Construction of hGSTA4 recombinant stable cell lines.....	196
6.2.1.2	Functional analysis of GSTA4 overexpression in HepG2 cell line against isoniazid hepatotoxicity	196
6.2.2	Effects of GSTA1 inhibition in INH Cytotoxicity	198
6.2.2.1	Detection of GSTA1 expression in mammalian cells.....	198
6.2.2.2	Small interfering RNA (siRNA) knockdown of GSTA1	198
6.2.2.3	Analysis of the effects of GSTA1 inhibition in INH cytotoxicity	199
6.3	Result.....	199
6.3.1	The effect of hGSTA4 in INH toxicity	199
6.3.1.1	Evaluation of GSTA4 expression in stably transfected HepG2 cells with GSTA4 plasmid	199
6.3.1.2	Functional role of GSTA4 against INH-decreased cell proliferation in HepG2 cells.....	201
6.3.1.3	Inhibitory effect of INH-induced apoptosis in HepG2 overexpressing GSTA4	202
6.3.2	The effect of isoniazid on <i>GSTA1</i> expression profile in human cell line.....	204
6.3.2.1	GSTA1 expression in mammalian cell lines.....	204
6.3.2.2	GSTA1 silencing decreased GSTA1 transcript levels	206
6.3.2.3	GSTA1 silencing decreased GSTA1 total protein levels.....	208
6.3.2.4	GSTA1 silencing abolished protection against INH-induced cell proliferation inhibition	210
6.3.2.5	GSTA1 silencing promotes INH-induced apoptosis.....	211
6.4	Discussion.....	212
7	GENERAL DISCUSSION	216
8	APPENDICES.....	221
9	REFERENCES.....	229

LIST OF FIGURES

Figure 1.1	The six mechanisms of DILI.....	15
Figure 1.2	Transport proteins for drugs and endogenous substances in basolateral and apical membranes of hepatocytes	25
Figure 1.3	Schematic diagrams of molecular structures of isoniazid, rifampicin, pyrazinamide, streptomycin and ethambutol.....	31
Figure 1.4	Isoniazid metabolic pathways.....	33
Figure 1.5	Pyrazinamide metabolic pathways	35
Figure 2.1	Map of the pTARGET mammalian expression vector.....	51
Figure 2.2	Comparison of Taqman®- and SYBR®-Green based detection.....	59
Figure 2.3	Representative amplification plot quantitative RT-PCR using SYBR Green I detection dye.....	60
Figure 2.4	Melting curve (a) and derivative melting curve (b) analyses	61
Figure 2.5	GSH calibration curve as absorbance values versus glutathione concentrations.....	68
Figure 2.6	Camptothecin induces apoptotic DNA fragmentation in HepG2 cells ...	70
Figure 2.7	AMC reference standard calibration curve.....	72
Figure 3.1	PCR-RFLP analysis of <i>NAT2</i> *5 (481C>T) polymorphism.....	79
Figure 3.2	PCR-RFLP analysis of <i>NAT2</i> *6 (590G>A) polymorphism	80
Figure 3.3	PCR-RFLP analysis of <i>NAT2</i> *7(857G>A) polymorphism.....	81
Figure 3.4	PCR-RFLP analysis of <i>NAT2</i> (rs4646244)	82
Figure 3.5	The position of four studied SNPs in <i>CYP2E1</i>	84
Figure 3.6	PCR-RFLP analysis of <i>CYP2E1</i> -1293G>C (rs3813867).....	85
Figure 3.7	PCR-RFLP analysis of <i>CYP2E1</i> (rs2031920).....	86
Figure 3.8	PCR-RFLP analysis of <i>CYP2E1</i> (rs6413420).....	87
Figure 3.9	PCR-RFLP analysis of <i>CYP2E1</i> (rs2070676).....	88
Figure 3.10	PCR-RFLP analysis of <i>PXR</i> -25385 C/T (rs3814055).....	90
Figure 3.11	PCR-RFLP analysis of <i>GSTA1</i> -69C>T (rs3957357).....	91
Figure 3.12	LD plot of <i>GSTA4</i> tag SNPs and their position in the gene	93
Figure 3.13	PCR-RFLP analysis of <i>GSTA4</i> (rs316141)	95
Figure 3.14	PCR-RFLP analysis of <i>GSTA4</i> (rs4147618)	96
Figure 3.15	PCR-RFLP analysis of <i>GSTA4</i> (rs316128)	97
Figure 3.16	PCR-RFLP analysis of <i>GSTA4</i> (rs3756980)	98
Figure 3.17	PCR-RFLP analysis of <i>GSTA4</i> (rs13207376)	99
Figure 3.18	PCR analysis of <i>GSTT1</i> genotype	100
Figure 3.19	PCR analysis of <i>GSTM1</i> genotype.....	101
Figure 3.20	LD plot of <i>SOD2</i> tag SNPs and their position in the gene.....	103
Figure 3.21	PCR-RFLP analysis of <i>SOD2</i> V16A (rs4880)	104
Figure 3.22	PCR-RFLP analysis of <i>SOD2</i> (rs5746136)	105
Figure 3.23	Sequence electropherogram of the forward and reverse sequence traces in <i>NAT1</i>	107
Figure 3.24	Detection of the <i>NAT2</i> 191G>A nucleotide change in a liver transplant patient from African origin	122
Figure 3.25	Allelic discrimination plot of the DNA samples	141
Figure 4.1	The influence of rifampicin co-administration on INH-induced decreased cell proliferation in LS180 cells	155
Figure 4.2	The influence of rifampicin co-administration on PZA-induced decreased cell proliferation in LS180 cells	156
Figure 4.3	Effect of Rifampicin pre-treatment in hepatocytes	158

Figure 4.4	Quantitative RT-PCR analysis of the effect of 50 μ M of RMP on mRNA expression level in LS180 cells.....	160
Figure 4.5	Quantitative RT-PCR of CYP3A4, CYP2E1 and CES2 transcript level in human hepatocytes exposed to rifampicin (50 μ M)	162
Figure 5.1	Comparison of DNA sequences of rapid acetylator recombinant (RAR) and slow acetylator recombinant (SAR) plasmids.	172
Figure 5.2	Ethidium bromide-stained agarose gel pattern showing digested pTARGET plasmids	173
Figure 5.3	Detection of NAT2 enzyme activity using Luciferin-NAT2	175
Figure 5.4	NAT2 activity in rat liver lysate using Luciferin-NAT2.....	176
Figure 5.5	Sequencing result of the RAR and SAR plasmids	178
Figure 5.6	SQ-RTPCR analysis of NAT2 mRNA expressions	180
Figure 5.7	Western blot of NAT2 protein expressions in stably transfected cells .	181
Figure 5.8	Time course of NAT2 activity with Luciferin-NAT2	183
Figure 5.9	INH-induced decreased cell proliferation at 48 h in RAR, SAR and non-transfected cells	184
Figure 5.10	The effect of NAT2 overexpression on total glutathione depletion in RAR, SAR and non-transfected cells	186
Figure 5.11	The effect of NAT2 overexpression on GSH/GSSG ratio in RAR, SAR and non-transfected cells	187
Figure 5.12	Effects of NAT2 overexpression on INH-induced DNA fragmentation.....	188
Figure 5.13	INH-induced increased caspase-3 activity in RAR, SAR and non-transfected cells	189
Figure 6.1	Nucleotide sequences of plasmid insert possessing GSTA4 coding region.....	197
Figure 6.2	Semiquantitative RT-PCR analysis of GSTA4 mRNA expressions in non-transfected (A) and hGSTA4-stably transfected	200
Figure 6.3	Immunoblot of GSTA4 protein expressions in non-transfected (A) and GSTA4-stably transfected HepG2.....	200
Figure 6.4	INH-induced decreased cell proliferation at 48 h in hGSTA4-transfected and non-transfected HepG2 cells	201
Figure 6.5	INH-induced DNA fragmentation in hGSTA4-stably transfected cells.....	202
Figure 6.6	INH-induced increased caspase-3 activity in hGSTA4- and non-transfected HepG2 cells.....	203
Figure 6.7	Immunoblot of GSTA1 protein level in mammalian cell lines	205
Figure 6.8	Silencing effect of GSTA1 siRNA on GSTA1 transcription levels at 72 hours by quantitative RT-PCR	207
Figure 6.9	Effect of GSTA1 siRNA on GSTA1 protein levels	209
Figure 6.10	INH-induced decreased cell proliferation in GSTA1 siRNA knockdown cells (GSTA1s)	210
Figure 6.11	DNA fragmentation analysis in Caco-2 cells transfected with NSCs and GSTA1s cells	211
Figure 6.12	INH-induced increased caspase-3 activity in GSTA1 siRNA knockdown cells (GSTA1s)	212

LIST OF TABLES

Table 1.1	Risk factors that contribute to the development of ADRs	4
Table 1.2	Commonly-used drugs associated with DILI.....	7
Table 1.3	Recommended doses of first-line anti-tuberculosis drugs for adults	32
Table 1.4	Previous published genotyping studies of <i>NAT2</i> acetylator status and their association with ATD-DILI	39
Table 2.1	List of suppliers and addresses.....	45
Table 2.2	Semiquantitative RT-PCR primer sequences and conditions	55
Table 2.3	Quantitative RT-PCR primer sequences	62
Table 2.4	Antibodies used for Western blotting	65
Table 2.5	Reaction scheme for caspase 3 assay	73
Table 3.1	Clinical and biochemical parameters of DILI patients exposed to INH.....	77
Table 3.2	Description of <i>CYP2E1</i> alleles and their PCR-RFLP conditions.....	84
Table 3.3	PCR-RFLP primer sequences and conditions of <i>GSTA4</i> tag SNPs	94
Table 3.4	Punnett square for Hardy-Weinberg equilibrium.....	110
Table 3.5	Contingency table showing Type I and Type II errors	112
Table 3.6	Association of <i>NAT2</i> genotypes and the risk of ATD-DILI in combined European and South Asian cohorts	116
Table 3.7	Association of <i>NAT2</i> genotypes and the risk of ATD-DILI in European cohort	116
Table 3.8	Association of <i>NAT2</i> genotypes and the risk of ATD-DILI in South Asian subjects	117
Table 3.9	Association of <i>NAT2</i> genotypes and the risk of ATD-DILI	119
Table 3.10	Predicted <i>NAT2</i> acetylator phenotype and the risk of ATD-DILI	120
Table 3.11	The relationship between 9796T>A and the other <i>NAT2</i> polymorphisms	120
Table 3.12	Statistical analysis of the association between -9796T>A and other <i>NAT2</i> alleles	121
Table 3.13	<i>NAT2</i> genotypes (for *5, *6 and *7) and predicted phenotypes in 6 liver-transplanted patients	121
Table 3.14	Sensitivity analysis for <i>NAT2</i> genotyping	123
Table 3.15	Additional candidate genes chosen for study.....	124
Table 3.16	Association of <i>CYP2E1</i> genotypes and the risk of ATD-DILI in combined European-South Asian cohorts.....	126
Table 3.17	Association of <i>CYP2E1</i> genotypes and the risk of ATD-DILI in European cohorts.....	126
Table 3.18	Association of <i>CYP2E1</i> genotypes and the risk of ATD-DILI in South Asian subjects	127
Table 3.19	Association of <i>PXR</i> genotypes and the risk of ATD-DILI	128
Table 3.20	Association of <i>GSTA1</i> genotypes and the risk of ATD-DILI	129
Table 3.21	Association of <i>GSTA4</i> genotypes and the risk of ATD-DILI in combined European-South Asian cohorts.....	130
Table 3.22	Association of <i>GSTA4</i> genotypes and the risk of ATD-DILI in European cohorts.....	131
Table 3.23	Association of <i>GSTA4</i> genotypes and the risk of ATD-DILI in South Asian subjects	132
Table 3.24	Association of the most common <i>GSTA4</i> haplotypes and the risk of ATD-DILI in c	133

Table 3.25	Association of the most common <i>GSTA4</i> haplotypes and the risk of ATD-DILI in European cohorts	133
Table 3.26	Statistical analysis of <i>GSTT1</i> ‘null’ polymorphism and the risk of ATD	134
Table 3.27	Statistical analysis of <i>GSTM1</i> ‘null’ polymorphism and the risk of ATD-DILI	136
Table 3.28	Statistical analysis of combined effect of <i>NAT2</i> acetylator status and <i>GSTM1</i> ‘null’ polymorphism in ATD-DILI	137
Table 3.29	Association of <i>SOD2</i> genotypes and the risk of ATD-DILI in combined European.....	138
Table 3.30	Association of <i>SOD2</i> genotypes and the risk of ATD-DILI in European cohorts.....	139
Table 3.31	Association of <i>SOD2</i> genotypes and the risk of ATD-DILI in South Asian subjects	139
Table 3.32	Association of <i>NAT1</i> genotypes and the risk of ATD-DILI	142
Table 5.1	Non-synonymous SNPs in human <i>NAT2</i> function and structure	170
Table 5.2	Quantitative RT-PCR of <i>NAT2</i> transcript level in non-transfected, RAR and SAR stably transfected cells.....	180
Table 5.3	Quantification of recombinant protein expressions of <i>NAT2</i> alleles in HepG2 cells normalized to <i>GAPDH</i> expression using ImageJ software	181
Table 5.4	<i>NAT2</i> activities of RAR, SAR and non-transfected cells as evaluated by the bioluminescent <i>NAT2</i> enzyme assay	183
Table 6.1	Quantitative RT-PCR of <i>GSTA4</i> transcript level in non-transfected and stably transfected HepG2 with h <i>GSTA4</i> plasmid	200
Table 6.2	Quantitative RT-PCR of <i>GSTA1</i> transcript level in Caco-2, HepG2, Huh7.5, and LS180 cell lines	205
Table 6.3	Quantitative RT-PCR analysis of the effect of <i>GSTA1</i> siRNA on <i>GSTA1</i> transcript levels at 72 h.....	206
Table 6.4	Quantification of protein expression of <i>GSTA1</i> normalized to β -actin level using ImageJ software.....	209

ACKNOWLEDGEMENTS

I would like to thank:

- My supervisor, Prof. Ann Daly for giving me this opportunity to work under her supervision. I am truly grateful for her constant guidance and encouragement that helped me in my work and writing of this thesis.
- My lab members, Julian Leathart, Julia Patch, Elise Glen, Ahmad AL-Serri, Mohammad Alshabeeb and Thomas Chamberlain for giving their friendly help and technical support in the laboratory.
- My beloved family and friends, especially Terry Hong, Annie Hong, Elaine Hong, Kenneth Wood and Isobel Wood for their love, emotional and spiritual support that helped me press on in this journey.

The work described in this thesis, except where specifically stated otherwise, is entirely my own.

Ching Soon, Ng

Chapter 1. Introduction

1. Introduction

1.1 Adverse drug reactions

According to WHO, adverse drug reactions (ADRs) are defined as ‘a response to a medicine which is noxious and unintended, and which occurs at doses normally used in man for the prophylaxis, diagnosis, or therapy of disease, or for the modification of physiological function’ (WHO, 2002). ADRs are a significant cause of hospital admission, often lead to considerable morbidity and mortality and remain a challenging clinical issue faced by the healthcare professionals (Farcas and Bojita, 2009). A meta-analysis of 39 prospective studies reported by Lazarou et al. suggested that the total incidence of ADRs was 6.7% with an overall fatality rate of 0.32% of hospitalised patients and found that ADRs are listed as one of the top ten causes of death in the United States (Lazarou et al., 1998). A recent Swedish study has also implicated ADRs to be the seventh most common cause of death with an estimation of 6.4% for the incidence of fatalities in hospital caused by ADRs (Wester et al., 2008). In the UK, at least 1 in 7 hospital in-patient experienced an ADR, resulting in prolonged hospitalisation and considerable financial burden to National Health Service (NHS) (Davies et al., 2009). Warfarin, fibrinolytics, unfractionated heparin, loop diuretics and allopurinol were found to be the most frequently implicated drugs causing ADRs in the large-scale prospective study (Davies et al., 2009). That study estimated that ADRs cost the NHS around £637 million annually, or approximately £5000 per hospital bed per year. Non-steroidal anti-inflammatory drugs (NSAIDs) are one of the most widely prescribed drugs for their anti-inflammatory, anti-pyretic, anti-thrombotic and analgesic properties and causing serious gastrointestinal ADRs including bleeding and ulceration (Helin-Salmivaara et al., 2007). ADRs Over half of the ADRs are definitely or potentially avoidable, and strategies are needed to minimize the risk of preventable ADRs. Although medication errors can occasionally occur, not all ADRs are attributable to medication errors and therefore identification of risk factors contributing to ADRs is essential to reduce the event of preventable ADRs. Factor predisposing patients to ADRs are presented in **Table 1.1**. Patient with concomitant diseases such as renal, cardiac and hepatic impairment are at greater risk for developing an ADR. Incidence of ADR is increased in aged patients and patients receiving multiple medication or polypharmacy (Davies et al., 2009). Drug-drug interactions are also an important contributor to approximately 15% of ADRs involving altered bioavailability, distribution and clearance of certain drugs (Passarelli et al., 2005). Over the past few

decades, the association of genetic polymorphisms in drug metabolising enzymes with various ADRs have been extensively studied. Recent progress in pharmacogenetics research suggests that patients with specific genetic characteristics may be prone to specific ADRs and personalized drug therapy with pharmacogenetics can therefore lead to safer, more effective drugs and reduce ADRs. The detailed information of the current research progress on genetic polymorphisms in drug-metabolising enzymes and drug transporters is described in section 1.5. The evaluation of predisposing factors of ADRs may not fully prevent the occurrence of ADRs, but it can reduce the incidence and severity of ADRs, reduce the overall cost of healthcare and improve patient outcomes. The practice of pharmacovigilance by regulatory agencies, pharmaceutical companies, and individual health care providers is important in monitoring for ADRs. Pharmacovigilance is a science relating to the detection, assessment, understanding, and prevention of adverse effects, particularly long-term and short-term side effects of medicines (WHO, 2004). The involvement of all healthcare providers in pharmacovigilance practice and the participation of patients in ADRs reporting are vital to minimize the risk of ADRs as much as possible.

ADRs can be classified into Type A and B drug reactions (Patel et al., 2007). Type A reactions are predictable, dose related and account for the majority of ADRs. These common dose related ADRs are due to an increased in the effective concentration of the drug or its metabolite, resulting in either on-target or off-target toxic side effects. Unlike Type A, Type B ADRs are unpredictable, not dose related and do not resemble the known pharmacologic profile of the causative agent. Type B reactions are also referred to as idiosyncratic drug reactions and often involve a small subset of treated patients. Premarketing trials generally fail to identify potentially serious ADRs of this type due to their very low incidence and ADRs are usually observed only when the drugs are marketed for a period of time and given to large patient populations. Thus idiosyncratic ADRs are a major problem to the healthcare professionals, pharmaceutical industry and drug regulatory agencies such as the US Food and Drug Administration (FDA) and European Medicines Agency (EMA). They are the leading cause for drugs withdrawn from the market or receiving a black box warning. This often results in the abandonment of potentially effective drugs. Statin-induced myopathy, drug-induced long QT and drug-induced liver injury (DILI) are the major idiosyncratic ADRs. DILI, in particular, is a leading cause of acute liver failure and is described in more detail in section 1.2.

Table 1.1 Risk factors that contribute to the development of ADRs*

Risk factors for ADRs
Pharmacodynamics
Variation in drug response resulting from altered receptor sensitivity
Pharmacokinetics
Changes in drug absorption, distribution, metabolism and excretion
Presence of underlying or concurrent disease
Renal, cardiac and hepatic impairment
Drug-drug interactions
Concomitant administration of other drugs
Physiologic conditions
Age, pregnancy, obesity
Diet and lifestyle
Smoking, alcohol intake
Genetic polymorphisms
Variation in drug response traits
Adherence to regimen prescribed
Poor adherence to prescribed medication especially elderly patients who require continuous polypharmacy
Medication errors
Errors in medication prescribing, dispensing or use

* *Table adapted from Farcas et al: Adverse drug reactions in clinical Practice: A causality assessment of a case of drug-induced pancreatitis (Farcas and Bojita, 2009)*

1.2 Drug-induced liver injury

The liver is commonly affected by drugs because of its role as the central organ in drug metabolism and detoxification. Drug-induced liver injury (DILI) is the most common ADRs and accounts for more than 50% of acute liver failure cases (Ostapowicz et al., 2002). DILI or hepatotoxicity can be defined as liver injury caused by drugs used either in medical practice or herbal medicines resulting in persistent significant elevations in liver enzyme levels, abnormalities in liver test or liver dysfunction. Medications such as antibiotics, nonsteroidal anti-inflammatory drugs (NSAIDs) and analgesics are the most commonly prescribed drugs associated with DILI (Ibanez et al., 2002). Commonly used medications that have exhibited hepatotoxic effects are listed in **Table 1.2**. The effect of DILI leads to a large range of pathological conditions including chronic hepatocellular hepatitis, cholestasis, cirrhosis, steatosis, sinusoidal and hepatic artery or vein damage (Larrey, 2000). The idiosyncratic nature of such adverse drug reactions has drawn most attention because they are unpredictable and often occur unexpectedly (Boelsterli, 2003). Although DILI is infrequent, up to 10% of cases may develop acute liver failure (Kaplowitz, 2005) and it has been shown that 75% of cases of acute liver failure linked to DILI led to liver transplantation or death (Ostapowicz et al., 2002). This significant patient morbidity and mortality has caused DILI to be the key reason for drug withdrawals from the pharmaceutical market (Temple and Himmel, 2002). An examination of the *Physician's Desk Reference* (PDR) for all new chemical entities approved by the FDA within the past 25 years (1975-1999) by Lasser et al. had revealed that approximately 10% of a total of 548 new chemical entities acquired a new black box warning or were withdrawn from the market (Lasser et al., 2002). Four (25%) out of 16 drugs withdrawn from the market were associated with DILI. Unrecognised serious ADRs were usually emerged after FDA approval and the safety of the new drugs can only be established with complete certainty until the drugs are marketed for many years. Examples of drugs that have been received black box warnings for hepatotoxicity include bosentan, trovafloxacin, tolcapone, felbamate and isoniazid, while drugs withdrawn from the market because of idiosyncratic hepatotoxicity include nefazodone, rofecoxib, troglitazone and bromfenac.

DILI due to idiosyncratic reactions involves individual susceptibility related to environmental and/or genetic factors that remain poorly understood. Routine animal toxicology fails to identify the risk of subsequent problems in drug development as

idiosyncratic reactions are not reproduced in experimental animals and appear only after a latency period of weeks to years (Lee, 2003). Drug-induced idiosyncratic hepatotoxicity remains a major challenge for clinicians, the pharmaceutical industry and regulatory agencies including the Food and Drug Administration (FDA) because of the limited knowledge regarding its mechanism, identification of susceptible individuals and pre-clinical test systems. Clinical diagnosis and prediction of DILI remains complex due to confounding factors such as pre-existing liver disease, multiple drug usage and lack of reliable screening methods or diagnostic standards. Further advancement and better understanding of idiosyncratic drug hepatotoxicity is important to provide practical solutions instead of limiting the use of drugs associated with DILI through withdrawals from the pharmaceutical market.

Table 1.2 Commonly-used drugs associated with DILI

Indication/drug action	Drug
<i>Hepatocellular injury</i>	
Analgesic	Paracetamol
NSAIDs	Diclofenac, ibuprofen, naproxen
Antibiotics	Isoniazid, Pyrazinamide, minocycline, nitrofurantoin, trovafloxacin
Antifungal	Ketoconazole
Immunosuppressants	Azathioprine, cyclophosphamide
Anti-arrhythmia	Amiodarone
Anticonvulsant	Carbamazepine, phenytoin, felbamate, valproic acid
Pulmonary hypertension	Bosentan
Cholesterol-lowering	Niacin
Gout	Allopurinol
Antithyroid	Propylthiouracil
Anaesthetic	Halothane
Immunomodulator	Leflunomide
Acne	Isotretinoin
Anti-androgen	Flutamide
Alcoholism	Disulphiram
Muscle relaxant	Dantrolene
Diabetes	Acarbose
Antipsychotic	Nefazodone
Alzheimer's disease	Tacrine
Asthma	Zafirlukast, Zileutin
Parkinson's disease	Tolcapone
CNS stimulant	Pemoline
<i>Cholestatic injury</i>	
NSAIDs	Sulindac
Antibiotics	Rifampicin, ciprofloxacin, erythromycin, flucloxacillin, amoxicillin-clavulanic acid
Antifungal	Terbinafine
Antipsychotic	Phenothiazines, chlorpromazine
Depression	Tricyclic antidepressants
Hypertension	Angiotensin-converting enzyme inhibitors

* Table adapted from Kaplowitz (2005): *Idiosyncratic drug hepatotoxicity* (Kaplowitz, 2005)

1.2.1 The epidemiology of DILI

The epidemiology of DILI is poorly understood owing to the lack of prospective studies on its incidence (Bjornsson, 2010). The frequency of DILI among users of most drugs is extremely rare with the estimation of an occurrence rate from 1 in 10,000 to 1 in 100,000 or even lower in other drugs (Larrey, 2002). Most clinical drug trials recruit less than 10,000 patients, indicating that DILI is often not detected during clinical trial stages and it has been mostly discovered in the post-marketing phase. The highly variable and inconsistent findings in a small number of retrospective studies reflect the lack of internationally standards for its diagnosis, under-reporting and incomplete reporting of DILI events which lead to bias in the data collected (Bjornsson, 2010). Several retrospective studies have reported the incidences rate of DILI to be between 1.27 and 7.4 cases per 100,000 inhabitants, which is probably an underestimation (Hussaini et al., 2007; De Valle et al., 2006; Meier et al., 2005; de Abajo et al., 2004; Ibanez et al., 2002). Meier et al. have observed the incidence of DILI to be 1.4% with approximately 1 in 100 patients developing DILI during the course of hospitalisation (Meier et al., 2005) though most of the cases in this survey appeared to have suffered mild DILI with elevated levels of liver enzymes only just above the upper limit of normal. In retrospective studies from the UK, the reported crude incidence rate of DILI and drug-induced jaundice were 2.4 and 1.27 per 100,000 inhabitants per year respectively (Hussaini et al., 2007; de Abajo et al., 2004). In a recent study from Sweden, a crude incidence rate of 2.3 per 100,000 inhabitants was reported and DILI cases constituted 6.6% of patients in an out-patient hepatology clinic (De Valle et al., 2006). So far, only one population-based prospective study has been carried out in France but this is generally considered the best estimation so far of the true incidence of DILI (Sgro et al., 2002). The reported incidence rate of DILI was 13.9 per 100,000 inhabitants which would be 16 times greater than is being officially spontaneously acknowledged (Sgro et al., 2002). Determining DILI remains a major challenge in clinical practice because of the lack of reliable markers. Clinical scales such as the Councils for International Organisation of Medical Sciences/ Roussel Uclaf Causality Assessment Method (CIOMS/RUCAM) is considered the best method for assessing causality in DILI (Lucena et al., 2008b) and the details of this scoring system is discussed in section 1.3.1.

1.2.2 Types of DILI

DILI covers a wide variety of clinical and pathological expressions of liver damage (Zimmerman, 1981). Liver injury can result from direct damage to hepatocytes leading to hepatocellular necrosis and may interfere with bile flow by damaging the bile ducts or vascular structures (Lee, 2003). Total bilirubin (TBIL), alkaline phosphatase (ALP), alanine transaminase (ALT) and aspartate transaminase (AST) are the useful biochemical markers in the evaluation and detection of DILI. DILI can be characterised as hepatocellular, cholestatic, or mixed type injury (Lee, 2003). Although hepatocellular, cholestatic and mixed reactions are the general terms used to classified DILI, the other form of DILI phenotypes include granulomas, fibrosis, steatohepatitis, cirrhosis, vascular and neoplastic lesions (Verma and Kaplowitz, 2009). Hepatocellular hepatotoxicity is predominantly associated with the elevation of ALT whereas cholestatic injury is linked to an increase in ALP level, conjugated bilirubin, and γ -glutamyl transpeptidase (Holt and Ju, 2006). Mixed pattern or cholestatic hepatitis is manifested when both ALT and ALP are elevated. Even though biochemical markers are good predictors for the patterns of liver injury, observation of histological abnormality, clinical picture and the cell type involved are more accurate in characterisation of liver injury (Abboud and Kaplowitz, 2007).

1.2.2.1 *Hepatocellular injury*

Hepatocellular injury has been defined as an increase in serum transaminase with an ALT/ALP ratio greater than 5 (Benichou, 1990). Although manifestation of hepatocellular injury includes hepatocyte necrosis with or without steatosis, patients may present as asymptomatic or experience fatigue, right upper quadrant pain, jaundice or acute liver failure (Verma and Kaplowitz, 2009). Halothane, a widely used anaesthetic has been reported to cause serious hepatocellular injury and fatal jaundice with a high mortality rate (40 %) (Bjornsson and Olsson, 2005). Other common drugs associated with hepatocellular injury are disulfiram, isoniazid, nitrofurantoin, halothane, azathioprine, flutamide, omeprazole and ibuprofen (Bjornsson and Olsson, 2005). Reactive drug metabolites generated during the process of drug biotransformation have been postulated to be the important cause for hepatocellular injury. The interaction between these reactive metabolites and cellular macromolecules such as proteins, lipids, and nucleic acids will lead to protein dysfunction, lipid peroxidation, DNA damage, oxidative stress and cellular dysfunction (Holt and Ju, 2006). The accumulated

oxidative stress, loss of ionic gradients and altered cellular calcium homeostasis may result in the dysfunction of mitochondria and lead to the pathogenesis of necrotic and apoptotic cell death (Holt and Ju, 2006). Damage to hepatocytes may trigger activation and inflammatory responses of innate immune cells and result in the initiation of immunological reactions (Kaplowitz, 2005). The mechanism of immune-mediated DILI is further described in section 1.4.

1.2.2.2 Cholestatic injury

By contrast to hepatocellular injury, cholestatic injury is defined as the elevation of ALP or an increase in ALT/ALP ratio of less than 2. Cholestatic injury is manifested primarily by jaundice and pruritus, resulted from impairment of bile flow and retention of bile salts and bilirubin. Cholestatic injury due to progressive destruction of small bile ducts may also lead to vanishing bile duct syndrome (Reau and Jensen, 2008). Though it can be bland without any parenchymal inflammation or may show slight hepatocyte injury and mild portal inflammation, rare cases of cholestatic injury may progress to ductopenia and primary biliary cirrhosis (Reau and Jensen, 2008). Examples of drugs associated with cholestatic injury are rifampicin, estradiol, nafcillin, flucloxacillin, co-amoxiclav, chlorpromazine, erythromycin and trimethoprim-sulfamethoxazole (Lee, 2003). Cholestatic injury appears to be less serious than hepatocellular patterns of injury but a high mortality rate ranging from 5-14.3% has been reported in recent studies (Chalasani et al., 2008; Andrade et al., 2006; Bjornsson and Olsson, 2005). In patients with cholestatic injury, the liver test abnormalities often resolved over the course of several months longer compared to the hepatocellular type injury (Andrade et al., 2002; Andrade et al., 2001). The prolonged cholestatic injury could be due to the slower regeneration capacity of bile duct cells than the hepatocytes (Abboud and Kaplowitz, 2007).

1.2.2.3 Mixed pattern of liver injury

The mixed form of DILI is characterised by the combination of both hepatocellular and cholestatic injury. It is defined as the elevation of both ALT and ALP with an ALT/ALP ratio between 2 and 5. This pattern of liver injury has been associated with the lowest mortality rate (approximately 2%), comparing to hepatocellular and cholestatic type of DILI (Chalasani et al., 2008; Andrade et al., 2006; Bjornsson and Olsson, 2005). Drugs known to cause hepatocellular or cholestatic liver injury including flucloxacillin, erythromycin, diclofenac, amoxicillin-clavulanate and carbamazepine may also give rise

to this form of DILI in some patients (Bjornsson and Olsson, 2005). Though it is mainly drugs that are known to induce cholestatic injury that are most often implicated in mixed pattern DILI (Larrey, 2000), some drugs found to induce a hepatocellular pattern of damage may sometimes be associated with mixed injury (Andrade et al., 2004).

1.3 Causality assessment in DILI

The diagnosis of DILI and prediction of DILI occurrence remain challenging as DILI is a diagnosis of exclusion and the lack of an objective, valid and widely available screening method makes the causality assessment of DILI difficult. Identification of elements in the medical history, clinical presentation, laboratory results, as well as subsequent course is important in assigning causality in DILI. The assessment criteria such as the onset of DILI, course of the reaction, clinical features, risk factors for the reaction, the exclusion of other causes of liver damage, and previous information on the hepatotoxicity of the implicated agent were proposed to improve causality assessment. Information regarding the rechallenge of the administered drug could confirm the role of a drug in the development of DILI. A positive rechallenge is manifested by significant doubling of the ALT (hepatocellular injury) and ALP (cholestatic injury) values (Zimmerman, 1999). Nevertheless, it may not be feasible in some cases as false negative response to rechallenge may be seen in certain drugs such as isoniazid and some causative agents can evoke serious and potentially lethal hypersensitivity reactions upon rechallenge (Papay et al., 2009). Rechallenge is usually performed only if no other alternative medication available and the potential benefits of re-introducing the drug outweigh the potential risks to the patient (Lee, 2003). Evaluation of liver biopsy is essential for assigning causality in DILI although it is often not available. However, the timing in assessing histological features of DILI and also characterisation of the role of liver biopsy in improving the diagnosis and management of DILI are to be defined clearly (Fontana et al., 2010). The use of *in vitro* laboratory tests include the lymphocyte-stimulation or transformation test have been proposed to aid the diagnosis of immune-mediated drug reactions, particularly in patients exposed to more than one drug (Maria and Victorino, 1998). Though the studies of this test have been promising, standardisation, test sensitivity and reproducibility are needed in order to fully realise its potential benefits in the identification of causative drugs. Recently, several reports suggest that use of the CIOMS assessment method (see section 1.3.1) with some modification is the most appropriate approach for assessing DILI causality (Aithal,

2011; Takikawa et al., 2003; Lucena et al., 2001). This approach has the advantage that it is suitable for use by non-expert assessors (Aithal, 2011). However, there are also alternative recent recommendations requiring assessment of each case by expert hepatologists (Fontana et al., 2010) and these are considered in Section 1.3.2 below.

1.3.1 International Organisation of Medical Sciences (CIOMS) scale/ RUCAM

The first method developed at international consensus meetings for drug causality assessment in DILI was the International Organisation of Medical Sciences (CIOMS) method which is also referred to as the Roussel Uclaf Causality Assessment Method (RUCAM) (Danan and Benichou, 1993). It was established by an international panel of experts who aimed to develop a standardised scoring system for the diagnosis and determination of the severity of DILI. The parameters required for RUCAM scale were based on six components:

- Time to onset and clinical course of the reactions
- Risk factors (age, alcohol consumption, pregnancy)
- Assessing the role of concomitant therapies
- Screening for non-drug related causes
- Previous information on hepatotoxicity of the drug
- Validation of the reaction by positive rechallenge or in vitro assay

According to RUCAM, hepatocellular injury pattern is characterised by an increase in ALT $>2 \times$ ULN (upper limit of normal) or $R \geq 5$, where R is the ratio of serum activity of ALT to ALP. Cholestatic type is defined by ALP $>2 \times$ ULN or $R \leq 2$, whereas mixed injury pattern is defined by ALT $>2 \times$ ULN and $2 < R < 5$. The RUCAM scale provides a scoring system with the sum of points varied from -3 to +3 for each component. Based on the final scores ranges from -8 to +14, the degree of association between the causative agent and ADRs was translated as highly probable (score > 8), probable (score 6-8), possible (score 3-5), unlikely (score 1-2) and excluded (score ≤ 0).

Validation of the RUCAM using patients who had been positively rechallenged was originally assessed by (Benichou et al., 1993) The system had shown to be reliable with high levels of sensitivity (86%) and specificity (89%) in assessing causality for DILI prior to rechallenge or when concomitant drugs were included (Benichou et al., 1993). The RUCAM has the advantage of providing a subjective and definite diagnosis of DILI

with minimal required questions and also with newly marketed drugs or old drugs associated with unrecognised DILI previously (Andrade et al., 2007). Nevertheless, the RUCAM scale has its limitations, which include the complexity of its scoring system and the arbitrary weighting of factors such as age, alcohol consumption and pregnancy (Andrade et al., 2007). It was recently validated by three experts in the Drug-induced Liver Injury Network (DILIN) study and was found to be of mediocre reliability in assessing DILI events (Rochon et al., 2008). Though RUCAM appears to be superior to other causality assessment systems and proved useful to identify the event of ADRs, modifications are needed to improve its efficiency, reliability and reproducibility in DILI causality assessment. Detailed recommendations on how this can be achieved have now been assembled as part of a phenotype standardisation project for DILI (Aithal, 2011).

1.3.2 DILIN expert opinion

An attempt to standardise expert opinion for assessing causality was initiated by the Drug-Induced Liver Injury Network (DILIN) by reviewing a prospective registry of patients with DILI with the aims to develop and evaluate causality assessment instruments for used prescription and non-prescription drugs, as well as herbal products (Fontana et al., 2009). This methodology relies on the clinical judgment of three experienced hepatologists who were given clinical, laboratory and imaging data to assign a causality score independently ranging from 1 to 5 to minimise individual biases. Score 1 is assigned as definite when the percentage likelihood of causality used was $\geq 95\%$, and followed by score 2 (highly likely; 75-94% likelihood), score 3 (probable; 50-74% likelihood), score 4 (possible; 25-49% likelihood) and score 5 (unlikely; $<25\%$). The DILIN's expert opinion method has its strengths by providing a prospective evaluation of patients who met the minimal laboratory or histological criteria within 6 months of DILI onset. A long term follow up was also included to identify any other etiology in causing DILI and whether rechallenge occurred. Though expert opinion has been considered as the gold standard for diagnosis of DILI, it is limited by its lack of generalizability and the weighted kappa score for assessment of the level of agreement between all three hepatologists was low (0.23-0.38) (Fontana et al., 2010). Thus, continuous efforts to produce an authoritative, unbiased, reliable and user-friendly causality assessment instrument are needed to improve the diagnosis, management and prevention of DILI.

1.4 Mechanism of DILI

1.4.1 Overview of DILI mechanism

Though the liver is involved in detoxification of many drugs, drugs and their reactive metabolites can also potentially cause toxicity to the liver in various ways based on their mechanism of action. The exact mechanism of DILI remains largely unknown, but currently there have been at least six mechanisms involving hepatocytes proposed for liver injury (Lee, 2003) (**Figure 1.1**). Drugs and their reactive metabolites that interrupt the bile salt transport proteins such as basolateral bile salt efflux pump (BSEP), encoded by ABCB11 at the canalicular membrane, may disrupt bile excretion, allowing toxic bile acids to accumulate and causing injury to hepatocytes (Trauner et al., 1998). Biotransformation by CYP enzymes may lead to covalent binding of drugs to intracellular proteins, causing disruption of calcium homeostasis that results in the disassembly of actin fibrils at the cell surface, cell rupture and lysis (Kaplowitz, 2002). Formation of adducts through binding of drug metabolites to cellular proteins, DNA or other cellular molecules could result in hepatic cellular dysfunction that then initiates both adaptive and innate immune responses. Drug-protein adducts may migrate to the cell surface and induce adaptive immune responses that causes liver damage by direct cytotoxic T cell or antibody-mediated cytotoxic responses (Robin et al., 1997). Hepatocyte stress could trigger the inflammatory responses of the innate immune system by the activation of Kupffer cells (KC), natural killer (NK) cells and natural killer T (NKT) cells. Hepatocyte exposure to cytokines produced in immune-mediated injury may initiate apoptosis through ligand-receptor interactions of TNF- α and Fas ligand (FasL) that triggers a cascade of caspases activation leading to loss of viability (Reed, 2001). Another mechanism for liver injury involves drug induced mitochondrial damage by disrupting fatty acid oxidation and energy production (Pessayre et al., 1999). Hepatocellular and cholestatic/mixed patterns liver injury can be classified as immune- and non-immune-mediated reactions (Abboud and Kaplowitz, 2007). An immune-mediated reaction is characterised by the presence of clinical signs of drug hypersensitivity such as fever, rash, eosinophilia, formation of autoantibodies and the rapid onset on rechallenge. Conversely, non-immune-mediated reactions, also known as metabolic idiosyncratic reactions are characterised by the absence of such signs (Abboud and Kaplowitz, 2007; Zimmerman, 1999).

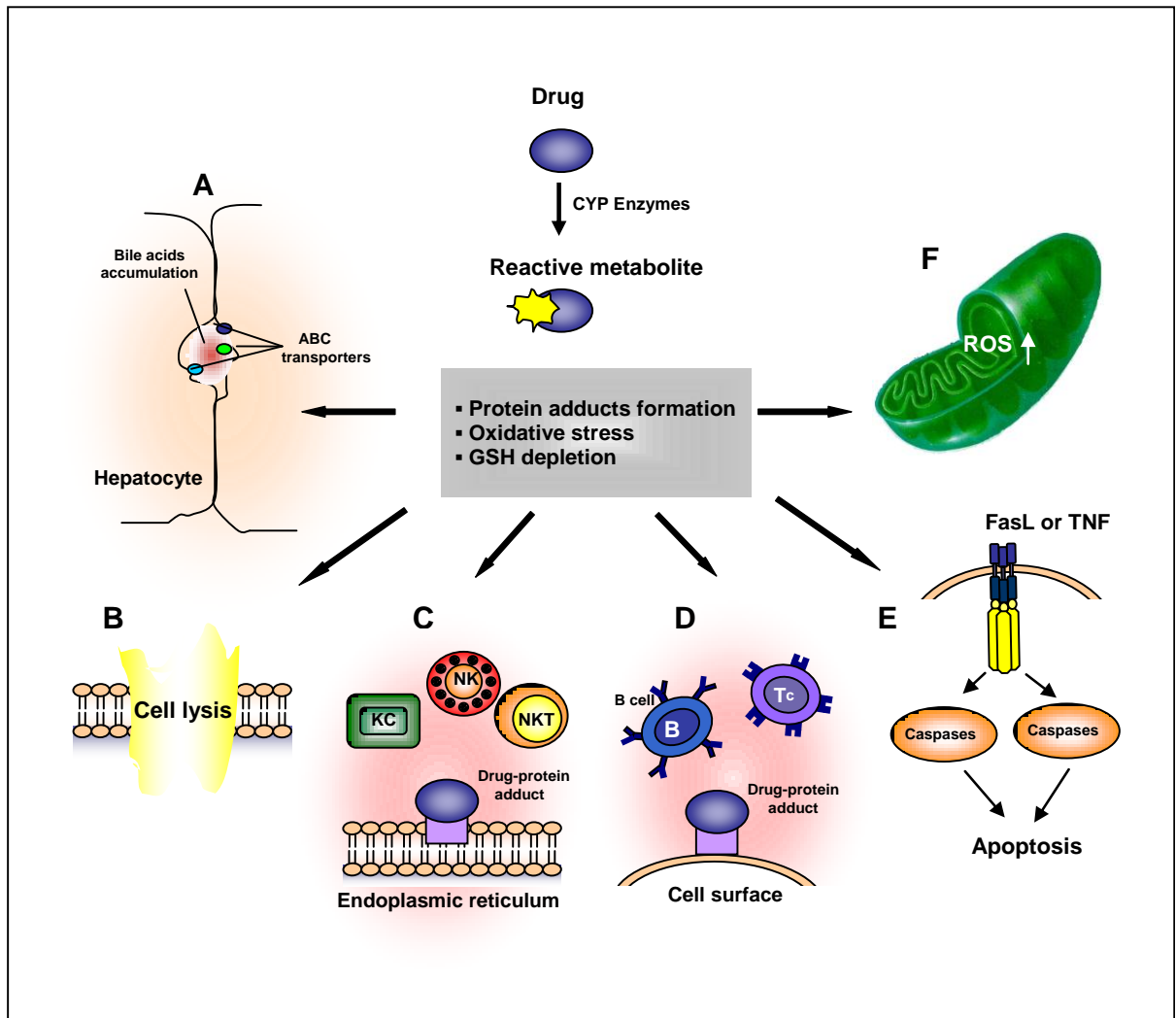


Figure 1.1 The six mechanisms of DILI

Drugs and its metabolites may affect the hepatocytes in six ways. (A) Drugs may interact with the bile salt transport proteins at the canalicular membrane hence, disrupting bile excretion and causing injury to hepatocytes as toxic bile acid accumulates. (B) Biotransformation of drugs cause disruption of calcium homeostasis that results in the disassembly of actin fibrils at the cell surface leading to cell lysis. (C) Drug-protein adduct formation may initiate the innate immune responses by activating the Kupffer cells (KC), natural killer (NK) cells and natural killer T (NKT) cells; or (D) induce the adaptive immune response causing liver damage by direct cytotoxic T cell (T_c) and antibody-mediated cytotoxic response. (E) Immune-mediated injury may initiate apoptosis through ligand-receptor interactions of $TNF-\alpha$ and FasL that triggers a cascade of caspases activation leading to the loss of viability. (F) Drugs may disable respiratory chain enzymes or mitochondrial DNA causing oxidative stress that lead to severe adverse effects in liver cells (Image adapted from Lee, 2003 (Lee, 2003)).

1.4.2 Immunological idiosyncratic reactions

1.4.2.1 The hapten hypothesis

Many DILI reactions appear to be immune-mediated rather than due to metabolic idiosyncrasy (Utrecht 2007). Though several hypotheses for DILI mechanisms have been proposed in the past, the hapten hypothesis is still considered as a dominant mechanistic hypothesis. The hapten hypothesis involves a chemically reactive drug or reactive metabolite acting as a hapten that covalently binds to cellular protein, DNA or other cellular molecule and lead to an adaptive immune response. It was first observed by Landsteiner et al. that immune reactions could not be triggered by small molecules unless they were chemically reactive and bound to protein (Landsteiner and Jacobs, 1935). Many drugs can be converted into a chemically reactive metabolite by drug metabolising enzymes such as the cytochrome P450 enzymes to form the hapten. For instance, halothane is oxidized by cytochrome P450 to trifluoroacetyl chloride (TFA), an electrophilic reactive intermediate which may bind covalently to hepatocyte macromolecules and phospholipids to form TFA-protein adducts (Eliasson et al., 1998). These TFA-protein adducts may be recognised as foreign by the immune system, resulting in the generation of autoantibodies (Eliasson and Kenna, 1996). It has been demonstrated that several different autoantibodies and TFA-protein adducts can be detected in the serum of patients with halothane-induced hepatitis (Spracklin et al., 1997). In addition, TFA can also bind to the CYP enzyme responsible for the generation of these electrophilic reactive intermediate and thus elevate the immunological reaction. It has been reported that a high levels of autoantibodies against TFA-modified CYP2E1 was identified in human and rats treated with halothane, indicating that the autoantibodies recognizing this autoantigen may evoke an immune response and play an important role in the pathogenesis of halothane hepatitis (Spracklin et al., 1997).

1.4.2.2 Danger hypothesis

The danger hypothesis of Matzinger proposes that an additional “danger signal” is required for the development of an immune-related idiosyncratic drug reaction as haptenized proteins alone might not be sufficient to trigger an immune reaction (Matzinger, 1994). Absence of a danger signal even though drug- and/or metabolite-specific antibodies were detected in some cases would be associated with immunologic tolerance (Utrecht, 2008). This tolerance prevents the body from initiating an immune response when the foreign antigens/hapten poses no threat or danger to the individual.

Thus, a second-stimulatory trigger, the danger signal is required alongside the presentation of the hapten to the APC for the development of a full immune response. Danger signals which include cytokines may be released as a result of oxidative stress and/or cellular damage.

1.4.2.3 Activation of the adaptive immune response

Formation of adducts through binding of drug metabolites to cellular proteins, DNA or other cellular molecules results in hepatic cellular dysfunction that may initiate both adaptive and innate immune responses. Drug-protein adducts may migrate to the cell surface and induce adaptive immune responses that cause liver damage by direct cytotoxic T cell or antibody-mediated cytotoxic responses (Robin et al., 1997). Major histocompatibility complex (MHC) class II proteins present on the surface of antigen presenting cells (APC) along with the release of co-stimulatory signals allow recognition by helper T cells, leading to a T cell response to the antigen. The cytotoxic T cells are then targeted against hepatocytes that express the protein adducts or with MHC class I present on the cell surface and this leads to the subsequent development of DILI (Kaplowitz, 2005). Activation of B cells by helper T cells causes production of antibody to protein adducts, promoting antibody-dependent hepatotoxicity.

1.4.2.4 Stimulation of innate immune response

Hepatocyte stress and/or cell damage could release the danger signals that trigger the inflammatory responses of the innate immune system by the activation of Kupffer cells (KC), natural killer (NK) cells and natural killer T (NKT) cells. These cells produce proinflammatory mediators including cytokines, chemokines and reactive oxygen species (ROS) that contribute to the progression of DILI. Inflammatory cytokines such as tumour necrosis factor alpha (TNF- α), interferon gamma (IFN- γ), Fas or Fas ligand (FasL) and interleukin-1 beta (IL-1 β) have been shown to be directly involved in causing tissue damage in the liver (Ishida et al., 2002; Blazka et al., 1996; Blazka et al., 1995). On the other hand, activated innate immune cells also release interleukin-10 (IL-10), interleukin-6 (IL-6) and other cytokines which play a hepatoprotective role of counteracting inflammatory responses and stimulating liver regeneration (Masubuchi et al., 2003; Bourdi et al., 2002; Ju et al., 2002). It has been shown that IL-10 and IL-6 null mice are more susceptible to paracetamol toxicity, suggesting the protective role of IL-10 and IL-6 against paracetamol-induced liver injury (Masubuchi et al., 2003; Bourdi et

al., 2002). Therefore, the balance of hepatotoxic and hepatoprotective mediators produced by activation of innate immune cells will determine an individual's susceptibility to DILI.

1.4.2.5 Autoimmunity

Drug-induced autoimmunity is associated with the apparent lack of immune reactions observed in immune-mediated hepatitis and often misclassified as metabolic or nonimmune-mediated DILI (Utrecht, 2008). Two drugs, nitrofurantoin and minocycline were reported to be the main causes of drug-induced autoimmune hepatitis (Bjornsson et al., 2010). The autoimmune reactions resulting in production of autoantibodies against self-antigens/haptenised proteins and the antigens are still present even after the causative drug is stopped. However, autoimmune DILI usually, although not always, resolves rapidly after administration of the offending drug has stopped. Therefore the continued administration of the responsible drug is required in an event of autoimmune DILI, possibly to provide the additional danger signal necessary to stimulate an immune response (Utrecht, 2008). When the drug is removed, the autoimmune T cells are consequently made anergic. Thus, the lack of a rapid onset on rechallenge seen in drug-induced autoimmunity could be due to the induction and maintenance of immune tolerance involving the autoimmune T cells. Many immune-mediated DILI cases could have been misclassified and autoimmunity is still remained a special problem when causality in DILI is being assessed.

1.4.3 Metabolic idiosyncratic reactions

1.4.3.1 Toxic metabolites

Metabolic idiosyncrasy is also referred as non-immune idiosyncratic reactions may be caused by aberrant drug metabolism or clearance, leading to the accumulation of toxic metabolites and causing toxicity to hepatocytes. For this reason, genetic variation affecting drug-metabolizing enzymes has been suggested to be a risk factor for DILI. The inter-individual differences in the ability to metabolize or detoxify certain drugs could increase susceptibility to DILI due to toxic metabolites accumulation. Polymorphisms in genes encoding drug metabolizing enzymes such as cytochromes P450 (CYP450), glutathione S-transferases (GST) and *N*-acetyltransferase 2 (NAT2), together with others encoding proteins such as superoxide dismutase 2 (SOD2) and

cytokines have been proposed to be associated with metabolic idiosyncrasy (Verma and Kaplowitz, 2009). Though P450-mediated metabolism usually biotransforms drugs into water-soluble metabolites which are easier to eliminate, in some cases it causes the activation of a drug to a hepatotoxic metabolite and increases drug toxicity. In the case of isoniazid, polymorphisms in metabolic enzymes such as NAT2 and CYP2E1 have been shown to be associated with isoniazid-induced liver injury due to the increased level of toxic metabolites of isoniazid. However, significance of *NAT2* and *CYP2E1* polymorphisms and their susceptibility to isoniazid-induced liver injury remains unclear and has not been confirmed in all studies, suggesting that additional factors may be required to explain the idiosyncratic nature of liver toxicity caused by isoniazid (Utrecht, 2008). Isoniazid-induced hepatotoxicity is discussed further in section 1.6. It is also possible that metabolic idiosyncrasy may be due to environmental or nutritional factors rather than genetic factors (Xu et al., 2005).

1.4.3.2 Disruption of intracellular calcium homeostasis

Drug and their reactive metabolites may cause hepatotoxicity which is usually predictable and dose-dependent. Paracetamol is a classic example of a known intrinsic or predictable hepatotoxin, however paracetamol overdoses can produce the reactive metabolite N-acetyl-p-benzoquinone imine (NAPQI), which depletes glutathione resulting in an excessive quantity of reactive metabolites. The resultant unconjugated reactive metabolites may bind covalently to cellular proteins and DNA, causing disruption of calcium homeostasis. Disruption of intracellular calcium homeostasis leads to the disassembly of actin fibrils at the cell surface of the hepatocyte which results in cell rupture and lysis (Kaplowitz, 2002).

1.4.3.3 Mitochondrial damage

Another mechanism for liver injury involves drug induced mitochondrial damage by disrupting fatty acid oxidation and energy production. Extensive formation of reactive metabolites that disable respiratory chain enzymes or mitochondrial DNA results in oxidative stress, defined as the exposure of the cell to extreme amount of oxidants commonly known as reactive oxygen species (ROS). ROS such as superoxide, hydrogen peroxide and hydroxyl radicals have been implicated in liver injury. When hepatocytes are exposed to excess ROS or there is lack of ROS elimination by antioxidants, oxidative stress occurs and can trigger the mitochondrial permeability

transition pore to open. The pore opening leads to an influx of protons from the intermembrane space into the mitochondrial matrix, culminating in mitochondrial depolarisation, major ATP depletion and cell necrosis (Boelsterli and Lim, 2007). Pore opening may also result in the entry of water into the mitochondrial matrix, causing the rupture of the outer membrane and release proapoptotic substances such as cytochrome c, which activate caspases and induce apoptosis (Haouzi et al., 2000). It has been suggested that progressive mitochondrial damage may produce a danger signal and initiate an innate and/or adaptive immune response (Utrecht, 2008).

1.5 Pharmacogenomics in DILI

1.5.1 Xenobiotic metabolism

Genetic factors determining susceptibility to drug-induced hepatotoxicity have recently gained much attention as the important risk factor for DILI. Genetic associations related to DILI are generally drug specific. Most of the susceptibility genes may relate to a range of different pathways, including those encoding drug-specific metabolising enzymes and drug transporters, immune reactions, mitochondrial function and apoptosis (Kaplowitz, 2005). The rarity of DILI and the wide range of drugs have contributed to the difficulty of recruiting a desired number of affected individuals for statistical power. However, some replicated associations for DILI susceptibility with particular genes due to specific drugs have been detected by using genome-wide association studies (GWAS) and candidate gene association studies (Daly, 2010).

Biotransformation of drugs usually involves several steps, including Phase I reactions including reduction, oxidation or hydrolysis, followed by Phase II metabolism which includes acetylation, methylation, conjugation to glucuronide, sulphate or glutathione that will produce hydrophilic products to be exported into plasma or bile and subsequently excreted by the kidney or the gastrointestinal tract. Inter-individual and inter-ethnic differences in gene encoding the drug metabolising enzymes result in variability to drug response. It may cause abolished, reduced, altered or increased enzyme activity and can either cause susceptibility or protection to DILI dependent upon whether the drug or its metabolite causes the adverse drug reactions.

1.5.2 Phase I metabolising enzymes

Human cytochrome P450 (CYP450) superfamily of phase I metabolising enzymes are often responsible for many idiosyncratic hepatotoxicity due to the formation of reactive metabolites of the drug. CYP450 enzymes are present primarily in drug-eliminating organs, including the liver, kidney and intestinal tract. So far, over 57 CYP450 genes have been identified. Within the same family, all CYP proteins share at least 40% sequence identity in their amino acid sequence and those within the same subfamily sharing greater than 55% identity (Nelson et al., 1996). Families CYP1, CYP2, and CYP3 are those most commonly involved in the metabolic clearance of the most xenobiotics/drugs and these genes are highly polymorphic resulting in interindividual variation in the rate of enzyme activity. There is some limited data suggesting associations between CYP polymorphisms and susceptibility to some forms of DILI. The main association reported is between INH-induced DILI and certain *CYP2E1* allelic variants. *CYP2E1* plays a major role in the metabolic activation of paracetamol, chlorzoxazone, and ethanol and it has been linked to paracetamol-induced DILI in humans though data on this is quite limited (Sinclair et al., 1998). The *CYP2E1**5 allele is common *CYP2E1* variant with polymorphisms in the 5'-flanking region which have been reported to cause an increase in the expression of the enzyme (Watanabe et al., 1994; Hayashi et al., 1991) and it has been linked to associated with an increased risk of developing hepatotoxicity due to anti-tuberculosis drugs including INH, though not all studies show this. Genetic polymorphism of *CYP2E1* and the risk of anti-tuberculosis medication are discussed further in section 1.7.

Another P450 named *CYP3A4*, may also have a more indirect involvement in some forms of DILI. It is believed that *CYP3A4* interindividual variability is mainly due to *CYP3A4* enzyme induction and inhibition rather than variations in the gene (Burk et al., 2004). *CYP3A4* is regulated by pregnane X receptor (*PXR*). It has been shown that *CYP3A4* contributes to the formation of reactive metabolites in troglitazone and flucoxacillin, though there is currently no evidence for the involvement of the reactive metabolite in the troglitazone or flucoxacillin induced hepatotoxicity (Masubuchi, 2006; Lakehal et al., 2001). However, in a recent study, an upstream polymorphism affecting levels of *PXR* expression was found to be associated with flucoxacillin-induced liver injury (Andrews et al., 2010). DILI cases due to this drug were more likely to have the allele associated with low *PXR* expression which may be associated with lower *CYP3A4* expression.

1.5.3 Phase II metabolising enzymes

Phase II reactions consist of glucuronidation, acetylation, methylation, sulphation, and glutathione conjugation. Associations between genetic polymorphisms of Phase II metabolising enzymes with DILI have been studied extensively. Polymorphism in the genes encoding arylamine N-acetyltransferase 2 (NAT2), glutathione transferases (GSTs) and UDP-glucuronosyltransferases (UGTs) have been reported to increase susceptibility to adverse drug reactions.

1.5.3.1 UDP-glucuronosyltransferases (UGTs)

The human UDP-glucuronyl transferase (UGT) superfamily has been classified into the UGT1A, 2A and 2B subfamilies which catalyse reactions of conjugation with glucuronic acid. UGTs are found in many of the major organs including the liver and responsible for the elimination of drugs and other xenobiotics and endogenous compounds such as bile acids, bilirubin hydroxyl-steroids and thyroid hormones (Kaivosaaari et al., 2011). UGT1A1 is the most abundant UGT isoform in the liver and individuals who carry the *UGT1A1**28 mutant allele can be more susceptible to irinotecan toxicity due to impaired UGT1A activity (Iyer et al., 2002). An association between UGT1A6-A528G polymorphism with tolcapone-induced hepatotoxicity was found by Acuna *et al.*, where the G allele was associated with decreased enzyme activity resulting in compromised drug clearance and drug toxicity (Acuna et al., 2002). Diclofenac-induced liver injury has also been associated to glucuronidation mechanism pathway, resulting in the production of reactive metabolite, diclofenac acyl glucuronide. The reactive diclofenac acyl glucuronide is capable of covalent modification of cellular proteins and resulting in immune-mediated destruction of hepatocytes (Kretz-Rommel and Boelsterli, 1995). The *UGT2B7* has been implicated in the diclofenac-induced DILI and the variant *UGT2B7**2 allele is associated with increased enzyme activity which in turn may result in the increased production of the toxic diclofenac acylglucuronide (Daly et al., 2007).

1.5.3.2 Arylamine N-acetyltransferase 2 (NAT2)

The human arylamine N-acetyltransferase 2 (*NAT2*) is involved in the acetylation of numerous xenobiotics and ary-lamine or hydrazine-containing drugs such as isoniazid (INH), sulfamethoxazole, hydralazine, dapsone and procainamide. Blum and colleagues

have first provided evidence that the gene encoding NAT2 is polymorphic through 'INH inactivation', thus causing interindividual variation in the NAT2 acetylation capacity and resulting in rapid or slow acetylator phenotypes (Blum et al., 1990). NAT1, on the other hand, is monomorphic and shows no variability in the N-acetylation of certain arylamine drugs such as p-aminosalicylic acid. Vatsis and colleagues were then confirmed that NAT2 corresponds to INH acetylator phenotypes (Vatsis et al., 1991). Determination of *NAT2* genotype and phenotype has been proposed to predict hepatotoxicity in patients with tuberculosis receiving INH or concomitant treatment of INH with other anti-tuberculosis medication such as rifampicin, pyrazinamide and ethambutol. It has been suggested that slow acetylators/poor metabolisers are prone to adverse drug reactions due to accumulation of toxic metabolites or low detoxification of drugs and/or their toxic metabolites. The role of *NAT2* in DILI caused by anti-tuberculosis medication is described in detail in section 1.7.

1.5.3.3 Glutathione S-transferases

The glutathione *S*-transferase enzymes (GSTs) play a major role against endogenous oxidative stress, as well as in the detoxification of exogenous potential toxins including toxic chemicals, carcinogens and drugs. They protect cells for direct toxicity by their detoxification effects through the conjugation of glutathione with harmful electrophiles generated during oxidative stress and lipid peroxidation. The mammalian cytosolic GSTs have been classified into eight classes including alpha, kappa, mu, omega, pi, sigma, theta and zeta (Pearson, 2005). Studies to date have been limited to the common deletion polymorphisms in the genes encoding the *GSTM1* and *GSTT1* resulting in the absence of enzyme. The presence of combined alleles *GSTM1* and *GSTT1* deficiencies has been associated with raised liver enzymes and increases susceptibility to DILI regardless of the type of causative agents (Lucena et al., 2008a). A more detailed role of GSTs in DILI caused by anti-tuberculosis medication is described in section 1.7.

1.5.4 Drug transporters

Member of the ATP binding cassette (ABC) transporter family such as P-glycoprotein (P-gp) and multidrug resistance-associated protein (MRP) play a vital role in the disposition of drugs in the body by providing a formidable barrier against drug penetration (Xu et al., 2005). Drugs and their metabolites can be effluxed from the

hepatocyte via these ABC transporters into the bile (**Figure 1.2**). Along with P-gp (MDR1; ABCB1), the bile salt efflux protein (BSEP; ABCB11) is a major bile acid efflux pump. The human MRP subfamily consists of at least nine members. MRP2, also known as ABCC2 is present on the canalicular membrane and involved in drug excretion into bile, especially of glucuronidated metabolites. Different from MRP2, MRP1 and MRP3 are found on the basolateral membrane of polarised cells which efflux drugs and metabolites into the bloodstream leading to increased excretion into the urine. Polymorphisms in some transporter genes have been shown to affect susceptibility to DILI caused by either specific drugs or a mix of drugs. A polymorphism in exon 13 of *BSEP* which has been linked with apparent decreased of hepatic BSEP expression was found to have an association with drug-induced cholestasis caused by various drugs (Lang et al., 2007). The C-24T *MRP2* polymorphism which has previously been associated with decreased functional expression of the transporter was shown to be associated with diclofenac-induced liver injury (Daly et al., 2007). Choi and colleagues have further studied a few variants in *MRP2* and found that a haplotype containing the C-24T variant was associated with hepatocellular type liver injury, and haplotype containing the -1774delG polymorphism was found with increased frequency in cholestatic and mixed liver injury caused by various causative drugs, specifically herbal remedies. The same study also looked at the functional significance of these variants including -1774delG, G-1549A and C-24T polymorphisms, and results revealed that these genetic variations in the promoter region of *MRP2* are associated with decreased promoter activity leading to the development of liver injury (Choi et al., 2007).

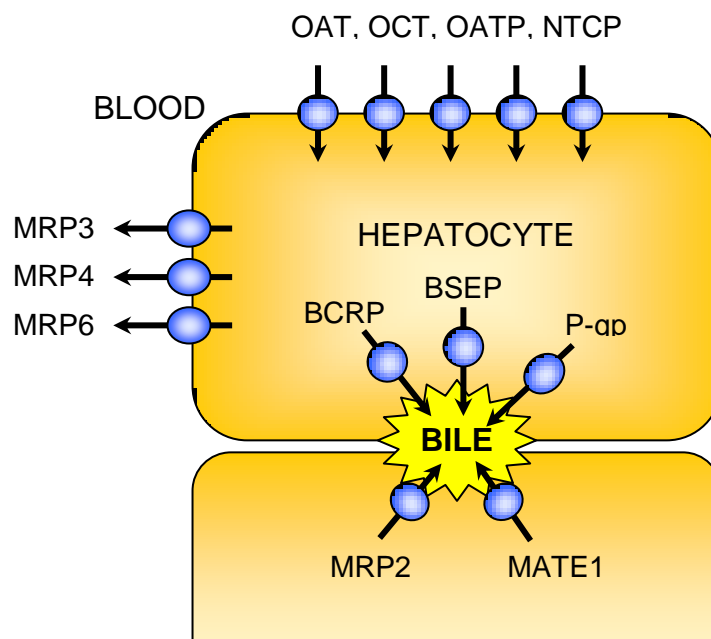


Figure 1.2 Transport proteins for drugs and endogenous substances in basolateral and apical membranes of hepatocytes.

Human hepatocyte uptake transporters in the basolateral (sinusoidal) membrane include the sodium/taurocholate co-transporting peptide (NTCP), organic anion transporting polypeptide (OATP), organic anion transporter (OAT) and organic cation transporter (OCT). Efflux pumps include several multidrug resistance proteins (MRP3, MRP4 and MRP6) are localised to the basolateral membrane and efflux chemicals. Apical (canalicular) efflux pumps of the hepatocyte comprise P-gp; bile-salt export pump (BSEP); breast cancer resistance protein (BCRP); and MRP2. In addition, multidrug and toxin extrusion protein 1 (MATE1) is located in the apical hepatocyte membrane for excretion of organic cations in the liver (Image adapted from Giacomini et al., 2010 (Giacomini et al., 2010)).

1.5.5 Oxidative stress

Reactive oxygen species (ROS) such as hydrogen peroxide, superoxide and hydroxyl radical are generated as a result of energy production from mitochondria, as well as detoxification reactions carried out by the CYP450 system. When the production of ROS exceeds the body's natural antioxidant defence mechanisms, oxidative stress occurs. Oxidative stress in liver can be induced by drugs and their reactive metabolites, ethanol and inflammatory stress, causing cell death and leading to the pathogenesis of liver injury. Genetic polymorphisms in ROS detoxification enzymes can contribute to individual susceptibility to DILI. These enzymes participate in a number of different reactions. Superoxide dismutases (SOD) convert superoxide to hydrogen peroxide whereas glutathione peroxidases (GPX) convert hydrogen peroxide to water in glutathione-dependent reactions. A polymorphism in mitochondrial enzyme manganese-dependent superoxide dismutase (SOD2), a major scavenger of mitochondrial superoxide is associated with DILI. This T to C allele substitution in exon 2 of the *SOD2* which results in a valine to alanine change (*SOD2* Val16Ala) in the leader sequence involved in import of the enzyme into mitochondria, was subsequently related to increased susceptibility to DILI caused by a combination of hepatotoxic drugs (Huang et al., 2007). Recently, Lucena and colleagues have found an association of *SOD2* Val16Ala polymorphism with the risk of developing DILI, particularly in patients with cholestatic/mixed hepatotoxicity (Lucena et al., 2010). In addition to *SOD2*, the group also studied the glutathione peroxidase I (*GPXI*) polymorphism, a proline to leucine substitution (*GPXI* Pro200Leu) which has previously been associated with reduced enzyme activity (Hamanishi et al., 2004). Patients homozygous for *GPXI* Leu allele were shown to be associated with a 5.1-fold increased risk for developing cholestatic type liver injury (Lucena et al., 2010). Another mitochondrial enzyme, DNA polymerase gamma (*POLG*) may also be relevant to risk of DILI. Rare mutations lead to decreased activity which may result in impaired ability to deal with oxidative stress. Patients exhibiting rare mutations in *POLG* were more likely to develop DILI caused by sodium valproate (VPA) (Stewart et al., 2010; McFarland et al., 2008).

1.5.6 Immune related genes

1.5.6.1 *Human leukocytes antigen (HLA)*

Genetic polymorphisms of the human leukocyte antigens (HLA) have been strongly associated with drug-induced hepatotoxicity, indicating the presence of an immune-mediated reaction (Daly, 2010). The HLA is the name of the human major histocompatibility complex (MHC) and can be classified into HLA class I and HLA class II whose gene products are predominantly involved in antigen presentation on the surface of cells. Genes of the HLA class I are grouped into A, B or C and the class II genes are grouped into DR, DP or DQ. All these genes are located in the MHC region of chromosome 6 in a region where there is strong linkage disequilibrium extending over a long distance.

A GWAS has revealed that the class I *HLA-B*5701* is strongly associated to flucloxacillin-induced liver injury with a significant odds ratio of approximately 80 when DILI cases were compared to flucloxacillin-tolerant controls (Daly et al., 2009). Abacavir-induced hypersensitivity reactions are found to be very significantly associated with the *HLA-B*5701* in another study (Mallal et al., 2002) though these reactions don't normally involve the liver and the reason why the flucloxacillin and abacavir reactions show a similar genetic association remains unclear. The HLA class II allele *DRB1*1501* has been previously associated with co-amoxiclav induced liver injury in two small cohort studies (O'Donohue et al., 2000; Hautekeete et al., 1999). Recently the association between *DRB1*1501* and DILI due to co-amoxiclav was replicated, suggesting that *DRB1*1501* allele may play a particularly important role in co-amoxiclav induced hepatotoxicity (Donaldson et al., 2010). Very recently, a GWAS on co-amoxiclav DILI has found that in addition to the *DRB1*1501* association, a HLA class I gene *A*0201* is also a risk factor for DILI (Lucena et al., 2011). It has also been suggested that ximelagatran-induced hepatotoxicity is related to immune-mediated DILI as it is found to be associated with a HLA class II haplotype *DRB1*0701-DQA1*0201* (Kindmark et al., 2008). A further HLA association has recently found to be associated with DILI caused by selective NSAID COX-2 inhibitor lumiracoxib (Singer et al., 2010). The GWAS study has identified a strong association to a common HLA haplotype *DRB1*1501-DQB1*0602-DRB5*0101-DQA1*0102* which may indicate a role of HLA class II alleles as a markers for NSAID-induced liver injury (Singer et al., 2010). A high incidence of ticlopidine-induced severe cholestatic hepatotoxicity was

observed in Japanese patients with *HLA-A*3303*, suggesting a role of HLA polymorphisms in ticlopidine-induced hepatotoxicity (Hirata et al., 2008). Sharma and colleagues have shown that patients with specific HLA alleles (the absence of *HLA-DQA1*0102* or the presence of *HLA-DQB1*0201* alleles were at increased risk of hepatotoxicity due to anti-tuberculosis medication (Sharma et al., 2002). However, in a genome-wide association study involving 28 European DILI cases linked to INH, no evidence for a HLA association was found (Urban et al., 2011). All these published studies have demonstrated associations between certain HLA genotypes with their relevant causative agents, thus suggesting that the immune mechanism in these specific examples of DILI could be caused by drug-specific factors rather than by the types of liver injury (Daly, 2010).

1.5.6.2 Cytokine genes

Associations between genetic polymorphisms in genes encoding cytokine-related proteins and susceptibility to DILI have been reported. Aithal and colleagues observed polymorphisms in IL-4 (C-590TA) and IL-10 (C-627A) resulting in low IL-10 and high IL-4 gene transcription were associated with diclofenac-induced hepatotoxicity (Aithal et al., 2004). Apart from IL-4 and IL-10, genetic polymorphisms of IL-6 (-597A, -572G, -174G and variable nucleotide tandem repeat-D alleles) were found to be associated with DILI caused by tacrine, an anticholinesterase inhibitor used for the treatment of Alzheimer's disease (Carr et al., 2007). Although some associations of cytokine polymorphisms have been associated with DILI, the associations are not as strong as that seen in HLA alleles, thus suggesting a minor role of cytokines in contributing to DILI.

1.6 Anti-tuberculosis drugs-induced liver injury

1.6.1 The burden of tuberculosis (TB)

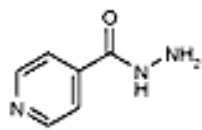
Tuberculosis (TB) is a deadly infectious disease caused by *Mycobacterium tuberculosis* (*M. tuberculosis*) and a major cause of disease burden worldwide. This disease is contracted through the exposure to *M. tuberculosis* in microscopic droplets expelled into the air from an infected person by coughing, speaking or sneezing. According to the World Health Organisation (WHO), over one-third of the world's population is currently infected with *M. tuberculosis* (WHO, 2010b) but not everyone who is infected develops the disease as asymptomatic latent TB infection is most common. However,

untreated latent infections will eventually progress to active TB. In 2009, the estimates of the global burden of disease caused by TB are as follows: 14 million latent TB cases (a prevalence rate of 203 cases per 100,000 population), 9.4 million active TB cases (an incidence rate of 139 cases per 100,000 population), 1.3 million deaths among human immunodeficiency virus (HIV) -negative people and 0.38 million deaths among HIV-positive people (WHO, 2010a). In the UK, a total of 8497 active TB cases were reported in 2006, a rate of 14.0 cases per 100,000 population (HPA, 2007). Increased risk factors for contracting TB have been identified as age, sex, HIV infection, smoking and family history of TB infection (Lienhardt et al., 2003). The disease is more common in countries with poverty, malnutrition and crowding as the risk of exposure to *M. tuberculosis*, consequently risk of infection is increased (Accorsi et al., 2005). According to the latest WHO annual report, most cases were in the South-East Asia (35%), African (30%) and western Pacific regions (20%) (WHO, 2010a). HIV-positive individuals who infected with *M. tuberculosis* are more susceptible to develop active TB due to their weak immune system. In Africa, HIV is the single most important factor contributing to the increase in the incidence of TB and accounted for approximately 80% of these cases (WHO, 2010a). It has also been noted that healthcare workers have higher risk of exposure and latent infection (Kayanja et al., 2005).

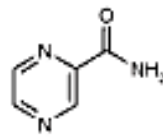
1.6.2 Anti-TB drugs (ATD)

First-line anti-TB drugs used for disease treatment and latent TB infection (LTBI) are isoniazid (INH), rifampicin (RMP), pyrazinamide (PZA), ethambutol and streptomycin (**Figure 1.3**). For the past 15 years, the gold-standard treatment for TB involves six months of daily treatment with RMP and INH, supplemented with PZA and either ethambutol or streptomycin in the initial two months (six-month, four-drug regimen) (HPA, 2007). The initial four-drug regimen is designed to diminish the bacterial population as rapidly as possible and also to prevent emergence of drug- and multidrug-resistant TB strains. The recommended daily oral dosages for the treatment of TB by the British National Formulary are 300mg for INH, 450-600mg for RMP, 1.5-2g for PZA and 15mg/kg for ethambutol (**Table 1.3**). Ethambutol is bacteriostatic against actively growing mycobacteriae by disrupting cell wall synthesis and is included in a treatment regimen when INH resistance is suspected. Streptomycin, a bactericidal aminoglycoside given at a dose of 15 mg/kg daily, is rarely used in the UK except for the initial phase of TB treatment if resistance to INH has been established. INH, also known as isonicotinyl

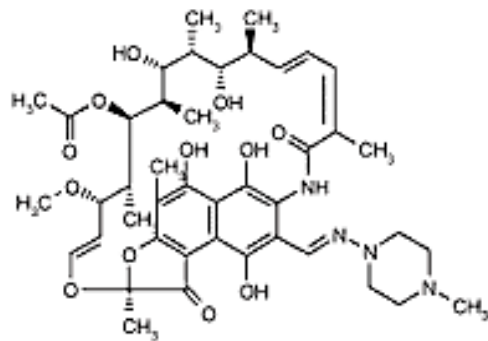
hydrazine, is cheap and highly effective, and commonly combined with RMP in treating TB. RMP belongs to the rifamycin group of antibiotics produced by *Streptomyces mediterranei* and covers a broad spectrum of antibacterial, antiviral and antineoplastic activity. It acts by binding to DNA-dependent RNA polymerase in bacterial cells, thus inhibiting transcription and subsequent translation of proteins. PZA is an effective TB drug that helps shorten the treatment regimen from 9 months to 6 months when used in combination with RMP and INH. It is a prodrug that needs to undergo metabolic activation catalysed by bacterial pyrazinamidase into its active derivative pyrazinoic acid for activity against *M. tuberculosis* (Konno et al., 1967). The emergence of drug-resistant TB is mainly caused by human errors, including inconsistent or incomplete treatment, wrong treatment regimens prescribed by doctors and health workers, and also unknown or unreliable source of quality drugs (WHO, 2010b). Multidrug-resistant TB (MDR-TB), a particularly dangerous form of drug-resistant TB is caused by mycobacterial strains resistant to the two most potent first-line anti-TB drugs, especially INH and RMP. Though MDR-TB is generally curable by extensive chemotherapy with second-line anti-TB drugs that takes up to two years, the treatments are more costly and cause more severe ADRs than the first-line drugs. These second-line agents include amikacin, capreomycin, cycloserine, azithromycin, clarithromycin and moxifloxacin.



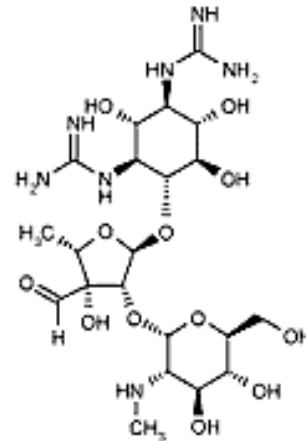
Isoniazid



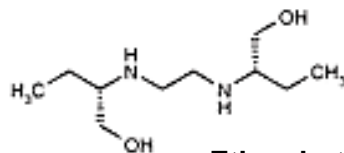
Pyrazinamide



Rifampicin



Streptomycin



Ethambutol

Figure 1.3 Schematic diagrams of molecular structures of isoniazid, rifampicin, pyrazinamide, streptomycin and ethambutol (Kumari and Ram, 2004).

Table 1.3 Recommended doses of first-line anti-tuberculosis drugs for adults

Drugs	Dose and range (mg/kg body weight)	Maximum dose
Isoniazid +	5 (4-6) mg/kg daily	300
Rifampicin +	10 (8-12) mg/kg daily	600
Pyrazinamide <i>together with</i>	25 (20-30) mg/kg daily	2000
Ethambutol or	15 (15-20) mg/kg daily	–
Streptomycin	15 (12-18) mg/kg daily	–

1.6.3 Metabolism of anti-TB drugs (ATD)

1.6.3.1 Isoniazid (INH)

INH is primarily cleared through acetylation by N-acetyltransferase 2 (NAT2) in the liver, resulting in acetylisoniazid which is then hydrolysed to isonicotinic acid and monoacetylhydrazine (MAH) (**Figure 1.4**). INH also undergoes hydrolysis catalysed by isoniazid hydrolase and forms hydrazine, which is then metabolised to MAH by NAT2. MAH can be acetylated to diacetylhydrazine which is non-toxic, or oxidised by cytochrome P4502E1 (CYP2E1) into hepatotoxic intermediates (Ryan et al., 1985). Acetylhydrazine can be hydrolysed to hydrazine which may further induce CYP2E1, increasing the production of toxic metabolites. Hydrazine, MAH and isonicotinic acid are potentially hepatotoxic metabolites of INH and accumulation of these reactive metabolites in patients may cause serious adverse drug reactions. The enzyme responsible for INH hydrolysis has still not been well characterised. It is usually described as an amidase but in a recent report (Tafazoli et al., 2008), it was found that hydrazine formation from INH in rat hepatocytes could be inhibited by treatment with bis-p-nitrophenylphosphate, which was originally described as a carboxylesterase inhibitor (Buch et al., 1969). There is increasing evidence that the hydrolysis of INH is catalyzed by a carboxylesterase but the precise isoform responsible is still unclear (Yamada et al., 2009). In human liver, two carboxylesterase isoforms CES1A1 and

CES2 are expressed at detectable levels and show different substrate specificities (Yang et al., 2009).

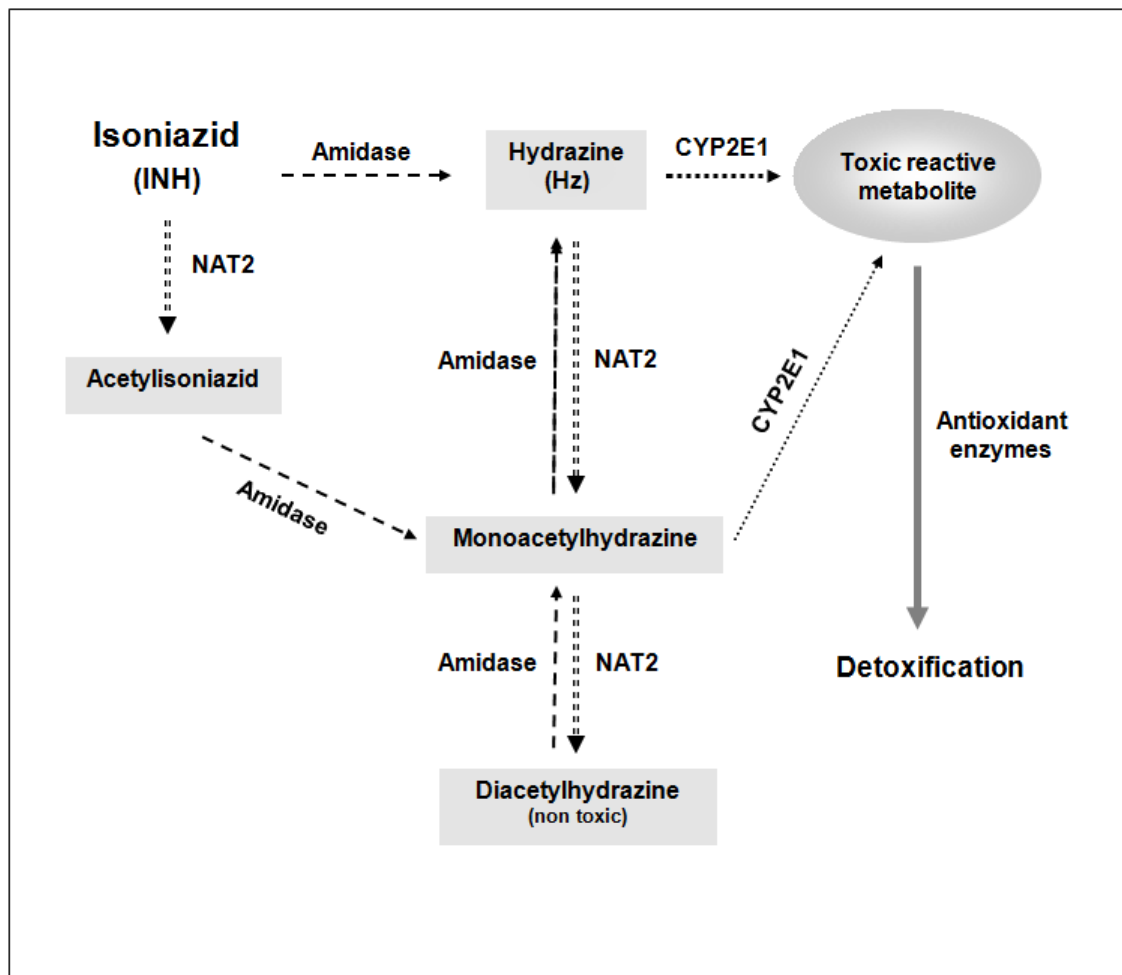


Figure 1.4 Isoniazid metabolic pathways

1.6.3.2 Rifampicin (RMP)

The metabolic pathways for RMP are deacetylation and non-enzymatic hydrolysis (Venkatesan, 1989). In the liver, RMP is deacetylated to 25-desacetyl rifampicin, a major metabolite that possesses potent bactericidal activity against *M. tuberculosis*. RMP is also hydrolysed to form 3-formylrifampicin SV and 3-formyl desacetyl rifampicin. It is known as a very potent inducer of drug metabolism, including its own metabolism. This is due to it being a potent agonist for the nuclear pregnane X receptor (PXR) which upregulates expression of a number of enzymes important in drug

metabolism. It promotes the upregulation of phase I CYP450 enzymes, particularly CYP3A4 which catalyse the metabolism of 50-60% of clinically prescribed drugs (Kolars et al., 1994; Shimada et al., 1994). In addition to CYP3A4, RMP has shown to induce drug transporters such as multidrug resistance 1 (MDR1), mediated through *PXR* activation (Rae et al., 2001). It promotes the clearance of potentially toxic xenobiotics or their reactive metabolites from the liver and intestine, and has also been shown to interplay with CYP3A4 in RMP inducing drug-drug interactions (Cummins et al., 2003). Studies have indicated that RMP administration may induce the production of hepatotoxic hydrazine metabolites by accelerating the INH hydrolase activity in the non-acetylating hydrolysis metabolic pathway particularly in individual with slow acetylator phenotype (Fukino et al., 2008; Askgaard et al., 1995; Sarma et al., 1986).

1.6.3.3 Pyrazinamide (PZA)

PZA is an effective sterilising drug and subjected to metabolism by hepatic microsomal deamidase and xanthine oxidase (XO) (Yamamoto et al., 1989). PZA, a prodrug is hydrolysed to the active metabolite pyrazinoic acid by a liver microsomal deamidase (**Figure 1.5**). This reaction can also be performed by the mycobacterial enzyme pyrazinamidase. Pyrazinoic acid is further hydroxylated to 5-hydroxypyrazinoic acid by XO. PZA is also directly oxidised to 5-hydroxypyrazinamide by XO. As with INH conversion to hydrazine (section 1.6.3.1), the microsomal deamidase involved in pyrazinamide hydrolysis is probably a carboxylesterase but the isoform responsible has not been identified. These three PZA metabolites are mainly excreted in urine (Lacroix et al., 1989; Weiner and Tinker, 1972). Pyrazinoic acid may be converted to pyrazinuric acid through a minor pathway by its conjugation with glycine.

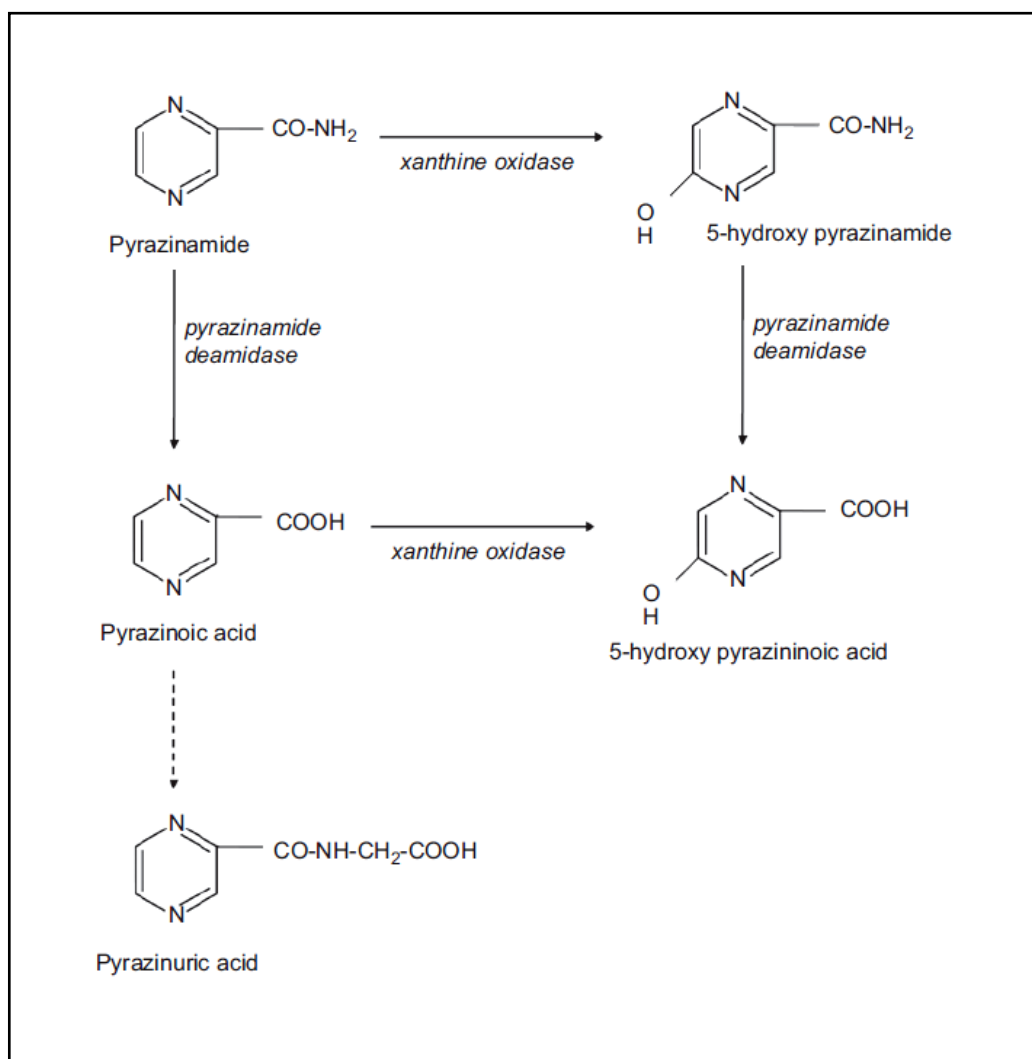


Figure 1.5 Pyrazinamide metabolic pathways (Tostmann et al., 2010).

1.6.4 Anti-TB drugs-induced liver injury (ATD-DILI)

The three key drugs for this treatment, RMP, INH and PZA are potential causes of hepatotoxicity and may lead to serious adverse effects including hepatitis, cutaneous reactions, gastrointestinal intolerance, haematological reactions and renal failure (Forget and Menzies, 2006). The frequency of anti-TB drugs hepatotoxicity increases greatly when they are used simultaneously (van Hest et al., 2004). It has been reported that the frequency of overt clinical hepatitis caused by INH and RMP coadministration was 2.6%, but only 1.1% with rifampicin alone and 1.6% with INH alone (Steele et al., 1991). ATD-DILI varies widely in severity, ranging from asymptomatic elevation of liver transaminases to acute liver failure (Kumar et al., 2010; Reuben et al., 2010).

Factors that increase the risk of anti-TB drug-induced hepatotoxicity include HIV infection, chronic viral hepatitis B and C infections, old age, malnutrition and alcoholism (Tostmann et al., 2008; Dworkin et al., 2005; Fernandez-Villar et al., 2004; Ungo et al., 1998; Krishnaswamy et al., 1991).

In 1969, INH received a black box warning from the US Food and Drug Administration due to its association with high incidence of adverse drug reactions, particularly hepatocyte injury (Black et al., 1975). Various metabolites of INH have been suggested as hepatotoxic, including hydrazine, monoacetyl hydrazine (MAH), acetylisoniazid and isonicotinic acid (Mitchell et al., 1976). Administration of acetylhydrazine or acetylisoniazid in rats leads to the production of reactive alkylating species and covalent binding to liver proteins, causing hepatocyte injury (Timbrell et al., 1980). NAT2, the major known enzyme involved in the metabolic pathway of INH and metabolites is suggested to play an important role in INH-induced hepatotoxicity, particularly the NAT2 slow acetylator genotypes/phenotypes. A more detailed of the association between NAT2 genetic polymorphisms and ATD-DILI is found in section 1.7. RMP has also been reported to affect metabolism of other drugs by inducing CYPs and UGT activities (Burk et al., 2004; Schuetz et al., 1996), which may complicate the analyses of ATD-DILI due to potential overlapping toxicities and drug-drug interactions following the concomitant administration of RMP and some first-line ATD. It has also been suggested that RMP may increase hepatotoxicity by inducing CYP3A4 metabolic activity in combination treatment with INH (Li et al., 1997). It is also shown to enhance idiosyncratic hepatocellular reactions by inducing formation of hydrazine from INH particularly in NAT2 slow acetylators (Sarma et al., 1986). Several studies have shown that serious liver injury by RMP alone is rare but this apparent low rate of hepatotoxicity awaits confirmation in larger prospective studies (Page et al., 2006; Menzies et al., 2004).

PZA may exhibit both dose-dependent and idiosyncratic hepatotoxicity. The incidence of PZA-induced liver injury has been reported to be higher when supplemented with other first-line anti-TB drugs (Chang et al., 2007; Yee et al., 2003; Parthasarathy et al., 1986; Association, 1981). A retrospective cohort study involving 3,007 patients has shown that the risk of hepatotoxicity for PZA-containing regimens relative to standard regimens that do not contain PZA was 2.6, suggesting that incorporation of PZA to INH and RMP increases the risk of DILI. In a separate study, seven out of 12 patients (58%)

treated for latent TB with ethambutol and PZA developed transaminase elevation of more than four times the upper limit of normal (Younossian et al., 2005). Because ethambutol alone is not hepatotoxic, PZA was likely to be the offending agent. The two months regimen of RMP and PZA for latent infection has reported serious hepatotoxicity and therefore it is no longer recommended to patients (CDC, 2003). RMP may occasionally cause interference with bilirubin excretion by inhibiting the major bile salt exporter pump, resulting in transient hyperbilirubinaemia (Byrne et al., 2002). It is probably that co-administration of RMP affects the activities of drug transporters of some first-line ATD (INH, PZA and ethambutol) and leads to a more severe ATD-DILI.

Hepatotoxicity has also been reported in simultaneous administration of the anti-TB drugs with other hepatotoxic drugs including paracetamol, methotrexate, sulfasalazine, carbamazepine and allopurinol (Vanhoof et al., 2003; Berkowitz et al., 1998; Crippin, 1993; Lacroix et al., 1988). For example, increased paracetamol metabolism as a consequence of CYP induction by INH causes the formation of toxic metabolites, depletion of GSH stores and subsequent hepatotoxicity (Crippin, 1993). Accumulation of pyrazinoic acid induced by allopurinol will decrease its clearance and cause toxicity in the liver (Lacroix et al., 1988). Anti-TB DILI occurs with high frequency and severity in patients demonstrating hepatotoxicity risk factors (Fernandez-Villar et al., 2004) and complications could be reduced by monitoring patients at risk through frequent laboratory testing of liver function.

1.7 Candidate genes for ATD-DILI

Metabolism of ATD is a very complex process, involving both activation and detoxification processes catalysed by a variety of enzymes. Genetic polymorphisms in the genes that encode ATD-metabolising enzymes have been hypothesised to contribute to the development of ATD-DILI. Genetic variants in these genes can result in differences in protein expression and catalytic activity, thus resulting in individuals, groups or population variability in the efficacy and toxicity of ATD. Reactive toxic metabolites generated by ATD-metabolising enzymes may cause more hepatotoxicity than the parent drug itself and could be converted to immunogens by covalently binding to endogenous proteins to initiate an immune response. Thus, identification and analysis of single nucleotide polymorphisms (SNPs) in the ATD-metabolising enzymes can

potentially unveil the underlying genetic mechanism of ATD-DILI. The relationship between particular genes and susceptibility to ATD-DILI has been identified and some of these reported associations such as *NAT2*, *CYP2E1* and *GSTM1* have now been replicated.

1.7.1 N-acetyltransferase 2 (NAT2)

Polymorphism in *NAT2* gene causes different biotransformation rates of substrate drugs and individual INH *N*-acetylation capacity is used to classify rapid or slow acetylators phenotypes (Blum et al., 1991). Besides INH, other substrates such as sulfamethazine, sulfonamides, procainamide, hydralazine, dapsone, and caffeine were used to determine the *NAT2* acetylator phenotype (Blum et al., 1991). The *NAT2* phenotype variation is due to SNPs in the 870bp *NAT2* protein coding sequence. Rapid acetylators are homozygous or heterozygous for wild-type allele (*NAT2*4*) while slow acetylators are homozygous for mutant alleles (*NAT2*5*, *NAT2*6* and *NAT2*7*) associated with amino acid substitutions which appear to abolish enzyme activity. The frequency of slow acetylators varies widely among different ethnic groups, ranging from 90% in North Africans, 50% in Caucasians and South Asians and 10% in East Asians (Daly, 2003). A number of studies have examined the association between INH-induced DILI and *NAT2* acetylator status. It was initially suggested that rapid acetylator individuals were more susceptible to hepatic injury because they generate more acetyl isoniazid, which further metabolise to the toxic intermediate, MAH (Yamamoto et al., 1986; Mitchell et al., 1975). However, both rapid and slow acetylators were observed to excrete similar proportions of MAH, suggesting that rapid acetylators also convert MAH into non-toxic diacetyl hydrazine more rapidly and decrease MAH hepatotoxin accumulation (Ellard et al., 1978). Another *NAT2* phenotyping study has shown that the slow acetylator phenotype lacking functional *NAT2* catalytic activity is associated with an increased risk of INH-induced DILI (Dickinson et al., 1981). Several confirmation studies involving genotyping analyses (**Table 1.4**) have been performed during the past decade, indicating that slow acetylator instead of rapid acetylator status predisposes to ATD-DILI. Among these, five studies on East Asian populations (Japan, Korea and Taiwan) which have a lower prevalence of *NAT2* slow acetylator genotypes (approximately 10%) have reported a significant increased frequencies of ATD-DILI in slow acetylators (Lee et al., 2010; Kim et al., 2009; Cho et al., 2007; Huang et al., 2002; Ohno et al., 2000). Another three studies based in Brazil, Turkey and Northern India where a higher

prevalence of the slow acetylation genotypes is found have also confirmed the findings in Asia (Bose et al., 2011; Bozok Cetintas et al., 2008; Possuelo et al., 2008).

Nonetheless, no association of risk with acetylator status was observed in two studies based in Europe and Canada with mixed ethnicity (Yamada et al., 2009; Vuilleumier et al., 2006). Recently a polymorphism in the *NAT2* promoter region (-9796T>A) was found to be associated with decreased expression of *NAT2* with individuals carrying the variant -9796 A allele were predisposed to ATD-DILI (Kim et al., 2009). Generally, the role for *NAT2* in susceptibility to ATD-DILI is evident and has been highlighted in majority of published studies, however its overall impact on DILI severity is not well understood and requires further investigation.

Table 1.4 Previous published genotyping studies of *NAT2* acetylator status and their association with ATD-DILI

Ethnicity	Number of cases	Increased risk of DILI	Odds ratio	Reference
Japanese	14	slow acetylator	4.0 (1.9-6.1) and 28 (26-30)	(Ohno et al., 2000)
Taiwanese	33	slow acetylator	3.66 (1.58-8.49); P=0.003	(Huang et al., 2002)
Korean	18	slow acetylator	5.4 (1.8–16.6); P=0.005;	(Cho et al., 2007)
Turkish	30	slow acetylator	8.8 (3.3-23.9); P<0.0001	(Bozok Cetintas et al., 2008)
Brazilian	14	slow acetylator	5.4 (1.57 – 19.4); P=0.003	(Possuelo et al., 2008)
Korean	67	slow acetylator	2.33 (1.45-3.78) for <i>NAT2*6</i> possession	(Kim et al., 2009)
Taiwanese	45	slow acetylator	3.15 (1.47-6.48); P=0.0026	(Lee et al., 2010)
Northern India		slow acetylator	2.99 (1.4-6.2); P=0.0045	(Bose et al., 2011)
Mixed	34	No association	Not significant	(Vuilleumier et al., 2006)
Mixed	23	No association	Not significant	(Yamada et al., 2009)

1.7.2 *CYP2E1*

CYP2E1 is constitutively expressed primarily in the human liver and involved in the metabolic activation of many toxicants including paracetamol and ethanol. Several polymorphic sites in the *CYP2E1* at the 5'-regulatory or intron as well as in exon regions have been identified. To date, 13 different *CYP2E1* alleles have been described from the Human Cytochrome P450 Allele Nomenclature Committee (<http://www.cypalleles.ki.se/cyp2e1.htm>). In the 5'-flanking region, a tandem repeat polymorphism namely *CYP2E1*1D* is associated with greater *CYP2E1* transcriptional activity and has been shown to promote metabolic activity in patients with chronic alcoholism and obesity (Nomura et al., 2003; McCarver et al., 1998). Three nonsynonymous polymorphisms have been identified but only one allele namely *CYP2E1*2* (Arg to His substitution) is associated with decreased enzyme synthesis and catalytic activity (Hu et al., 1997). This variant allele occurs at a low frequency (2.6%) and has only been identified in Chinese population but not other ethnic groups (Hu et al., 1997). *CYP2E1*5* and *CYP2E1*6* polymorphisms in the 5'-flanking region are the most studied variants. The *CYP2E1*5B* allele is identified by loss of a *RsaI* restriction site and designated c2 whereas the wild-type allele with the restriction site is designated c1. The *CYP2E1*6* allele is identified by a *DraI* restriction fragment length polymorphism (RFLP). A common allele *CYP2E1*5A* is designated when both the *RsaI* variant and *DraI* variant are present, as is usually the case. The *RsaI* polymorphism has been evaluated in association with DILI due to anti-tuberculosis drugs including INH. *CYP2E1* is involved in the metabolism of INH, catalyses oxidation of MAH and forms hepatotoxic intermediates (Ryan et al., 1985). Huang and colleagues have reported that the wild-type *CYP2E1* c1/c1 genotype shows higher *CYP2E1* activity and therefore may lead to increased production of hepatotoxins (Huang et al., 2003). They have further demonstrated an increased risk of ATD-DILI from 3.94 for *NAT2* rapid acetylators with *CYP2E1* c1/c1 genotype to 7.43 for slow acetylators with the *CYP2E1* c1/c1 genotype (Huang et al., 2003). Another two independent studies based in China (Wang et al., 2010) and Taiwan (Lee et al., 2010) have also reported a significant association between ATD-DILI and the *CYP2E1* c1/c1 genotype. Bose and colleagues have recently found an association between the mutant C allele of *CYP2E1 DraI* polymorphism (*CYP2E1*5A* and **6* alleles) with the risk of ATD-DILI (Bose et al., 2011). Combined analysis of acetylator status and variants for the *CYP2E1 DraI* polymorphism was further performed and it was shown that slow acetylators and

carriers of the variant allele were predisposed to develop ATD-DILI (Bose et al., 2011). However, controversial results have been reported in some studies with no association found between *CYP2E1* and susceptibility to ATD-DILI in Koreans (Kim et al., 2009; Cho et al., 2007) and in the British Columbian population of Canada (Yamada et al., 2009).

1.7.3 Glutathione S-transferase enzymes (GSTs)

Oxidative stress has been suggested as the important factor that accelerates the progression of ATD-DILI. Increased oxidative stress and raised levels of reactive oxygen species (ROS) due to generation of reactive ATD metabolites are closely associated with decreased glutathione levels. The glutathione S-transferase enzymes (GST) may play a major role against liver injury by its detoxification effects through the conjugation of glutathione with harmful electrophiles generated during oxidative stress and lipid peroxidation. However there is limited information about genetic polymorphism of these detoxification enzymes and their association with DILI as previous published studies appear to be restricted to *GSTM1* and *GSTT1*. *GSTM1* and *GSTT1* deficiencies, caused by a homozygous deletion of the gene (null genotype) are common. Though the prevalence of *GSTM1* and *GSTT1* null genotypes varies between different ethnic groups, it was reported that the frequency of *GSTM1* null genotype ranges from 13.1% to 54.5% in Caucasians, from 41.7% to 55.5% in Asians, 46.7% in African-Americans, and 26.9% in Africans (Mo et al., 2009). For the *GSTT1* null genotype, the reported prevalence rates were 11.1-28.6% in Caucasians, 41.9-52% in Asians, 26.7% in African-Americans, and 36.6% in Africans (Mo et al., 2009). Individuals with homozygous null mutations of these genes have no enzymatic activity for the particular enzyme and therefore are likely to be more susceptible to carcinogens and drug-related toxicities. The presence of combined alleles *GSTM1* and *GSTT1* deficiencies has been associated with raised liver enzymes and increases susceptibility to tacrine-induced hepatotoxicity in Alzheimer's disease patients (Simon et al., 2000). Lucena and colleagues have shown an 8.8-fold increased risk of developing NSAID-induced hepatotoxicity in carriers of double *GSTM1* and *GSTT1* deletion (Lucena et al., 2008a). They have also reported the individuals of double *GSTM1/GSTT1* null genotypes had an overall of 2.7-fold increased risk of developing DILI regardless of the type of causative agents, indicating the possible role of both *GSTT1/GSTM1* null genotypes as the non drug-specific biomarkers of DILI susceptibility (Lucena et al.,

2008a). Individuals homozygous null for both *GSTM1* and *GSTT1* have also been associated with an increased risk of DILI relating to troglitazone, co-amoxiclav and carbamazepine (Lucena et al., 2008a; Ueda et al., 2007; Watanabe et al., 2003). It has been shown that homozygosity for the *GSTM1* or *GSTT1* null allele was associated with ATD-DILI in three independent studies. Two studies based in India and Taiwan reported an association with the *GSTM1* null genotype but no association was found between cases and controls for *GSTT1* null genotype (Huang et al., 2007; Roy et al., 2001), whereas another study involving the Caucasian population showed an a higher frequency of *GSTT1* null genotype in cases compared with controls but no difference was found for *GSTM1* null genotype (Leiro et al., 2008). In addition, the gene encoding the manganese superoxide dismutase (MnSOD) which is known as SOD2, an anti-oxidative stress gene important in detoxifying mitochondrial ROS was also found to be associated with increased susceptibility to DILI, especially to ATD-DILI (Huang et al., 2007).

1.8 Aims of the study

The primary aim of this study was to identify specific genes conferring susceptibility to hepatotoxicity due to anti-tuberculosis drugs (ATD). To identify novel genetic associations, polymorphisms in genes involved in relevant ATD metabolic pathways were evaluated by a case-control study approach. The examined predictors of ATD-DILI were chosen based on previously published studies or biological relevance and include *NAT2*, *CYP2E1*, *GSTM1*, *GSTT1* and *SOD2*, as well as *PXR*, *GSTA1*, *GSTA4* and *NAT1* which may be potential genetic predictors for ATD associated hepatotoxicity. The functional significance of *NAT2* acetylation phenotypes will also be examined using an *in vitro* overexpression approach to characterise *NAT2* acetylation phenotypes and their relevance to the development of isoniazid-induced hepatotoxicity. In addition, the protective role of glutathione *S*-transferase (GSTs) and their association with isoniazid-induced DILI will be assessed by using *in vitro* overexpression and siRNA knockdown approaches.

Chapter 2. General Materials and Methods

2 General Materials and Methods

2.1 General Laboratory Practice

All experiments were performed to university standards for safe working with chemicals substances in laboratories, which comply with the Control of Substances Hazardous to Health Regulations 2002 (COSHH, 2002). Routinely used chemicals of analytical and molecular biology grade were obtained from the named suppliers as listed (**Table 2.1**). Water for all experiments was purified by a Nanopure water purification system (Thermo Scientific). Where necessary, sterilisation of water, biological and chemical reagents, plastics, glassware and other equipment was achieved by autoclaving at 120°C, 15 pounds per inch (PSI) pressure for 20 min. In addition solutions for tissue culture work were filter-sterilised using 0.2 µm filters (Millipore). For PCR work and primer dilution pre-purchased sterile water was used (Fresenius Kabi Limited). For all RNA work, diethyl pyrocarbonate (DEPC) treated, nuclease free water (Fisher Scientific) was used in the preparation of solutions.

2.2 Chemical Reagents

Unless otherwise stated, all routine chemical reagents were purchased from Sigma-Aldrich.

Table 2.1 List of suppliers and addresses

Supplier	Address
Bioline	London, UK
Bio-Rad	Hemel Hempstead, UK
Eurofin MWG Operon	London, UK
Fermentas	York, UK
Fisher Scientific	Loughborough, UK
GE Healthcare	Little Chalfont, UK
Greiner Bio-ONE	Stonehouse, UK
Gibco-Invitrogen	Paisley, UK
Macherey-Nagel (MN)	Surrey, UK
Merck Biosciences	Nottingham, UK
Milipore	Watford, UK
Molecular Devices	Widdersley, UK
New England Biolabs (NEB)	Hitchin, UK
PAA Laboratories GMBH	Austria
PE Applied Biosystems	Warrington, UK
Promega	Southampton, UK
QIAGEN	Crawley, UK
Sarstedt	Leicester, UK
Scientific Laboratory Supplies	Newcastle, UK
Sigma Aldrich	Gillingham, UK
Stuart Scientific	Essex, UK
Thermo Scientific	Barnstead, UK
VH Bio	Gateshead, UK

2.3 Mammalian Cell culture

2.3.1 General Materials

Unless stated otherwise, all disposable tissue culture plastic ware was from Greiner Bio-One and cell culture reagents from PAA Laboratories.

2.3.2 Routine Passage

Cell culture was performed under aseptic conditions in a Class II laminar flow microbiological safety cabinet. LS180 colon cancer cells, HepG2 hepatoblastoma cells, Huh7.5 hepatocellular carcinoma and Caco-2 colon cancer cells were cultured as adherent monolayers in T75 flask at 37°C, 5% CO₂ in humidified air. Routine culture was performed in complete growth medium (GM). LS180, HepG2 and Caco-2 cells were cultured in Eagle's Minimum Essential Medium (EMEM) and Huh7.5 cells were cultured in high glucose Dulbecco's modified Eagle's medium (DMEM). Both Media were supplemented with 10% foetal calf serum (FCS), Penicillin-Streptomycin (0.1 mg/ml), 2 mM L-glutamine and 0.1 mM non essential amino acid (NEAA). Cells exposed to drugs were cultured in drug-containing maintenance media (MM) supplemented with 2% FCS, Penicillin-Streptomycin (0.1 mg/ml) and 2 mM L-glutamine. All media were stored at 4°C and warmed to 37°C prior to use.

2.3.3 Cell line maintenance

Cultures displaying 70-80% confluence were passaged within 3-5 days. Medium was aspirated, the cell monolayer rinsed with sterile 1x Dulbecco's phosphate buffered saline (PBS) (PAA Laboratories) followed by 0.25% trypsin-EDTA (ethylenediaminetetraacetic acid) (Gibco-Invitrogen). After removing trypsin-EDTA, the monolayer was then incubated at 37°C for 5 min until the cells dissociated. Detached cells were resuspended in GM, and passaged at a ratio of 1:3-6.

2.3.4 Cell line storage

Cell stocks were accumulated early and frozen at -80°C allowing experiments to be performed using stores of low passage number cells. Logarithmically growing cell cultures were pelleted then resuspended in freezing medium composed of FCS

supplemented with 10% dimethylsulphoxide (DMSO). 1 ml aliquots of 5×10^6 were frozen in 1.8 ml cryogenic vials (Corning). To revive the cells, frozen stocks were rapidly thawed at 37°C, resuspended in GM and centrifuged at 1000 rpm for 5 min. The supernatant was discarded, the cell pellet was resuspended in GM, and plated in tissue culture flasks.

2.3.5 Microscopy and cell counting

Cell pellets were resuspended in complete medium and 10 µl of single cell suspension was then transferred to a haemocytometer counting chamber. The number of cells overlying the ruled grid was counted using low power magnification (x10) on an inverted microscope (Olympus) and the number of cells per ml was calculated. The suspension was then appropriately diluted, and the correct cell number seeded out for each experiment.

2.3.6 Cell lines

The LS180 colon cancer cell line, purchased from the European Collection of Cell Cultures (ECACC) (Porton Down, UK), was derived from a 58 year old female Caucasian with Dukes type B adenocarcinoma of the colon. Caco-2, HepG2 and Huh7.5 cell lines were given by Professor Geoffrey Toms. Caco-2 is derived from a human colon adenocarcinoma, while HepG2 and Huh7.5 are derived from human hepatoblastoma and hepatocellular carcinoma respectively.

2.4 Genomic DNA preparation and analysis

2.4.1 DNA extraction

Cells were pelleted by centrifugation (Sigma 3-16PK centrifuge) at 3000 g for 10 min at 4°C and resuspended with 2 ml of nuclear lysis buffer (400 mM tris-HCl pH 8.0, 60 mM EDTA, 150 mM sodium chloride and 1% (w/v) sodium dodecyl sulphate). The mixture was then transferred into a 15 ml polypropylene centrifuge tube and 0.5 ml of 5 M sodium perchlorate was added. The samples were then rotary mixed at room temperature for 15 min (Stuart Scientific) and incubated at 65°C for 30 min. The samples were combined with 2.5 ml chloroform and rotary mixed for 10 min at room temperature to form a homogenous emulsion before centrifugation at 3000 g for 10 min

at 4°C. The top aqueous layer containing DNA was removed and dispersed into a new 15 ml polypropylene centrifuge tube. Ethanol (5 ml) was added and mixed by rapid inversion of the tube several times. The precipitated DNA was spooled using a sterile disposable plastic loop and allowed to air-dried for 10 min at room temperature. The DNA was then dissolved overnight at 60°C in 200 µl 5 mM tris -HCl, pH 8.0 in a sterile 1.5 ml screw-cap microcentrifuge tube.

2.4.2 Determinants of DNA yield and purity

The amount and purity of the DNA samples were examined by Nanodrop spectrophotometer ND-1000 (Thermo Scientific). An absorbance unit of 1 at 260 nm is equivalent to 50 µg/ml double stranded DNA. The absorbance at 260 and 280 nm is used to assess the purity of DNA and a 260/280 nm ratio of 1.8 – 2.0 indicates pure DNA. A secondary measure of DNA purity can be assessed by measuring the absorbance at 260 and 230 nm. The 260/230 nm ratio of 1.8-2.2 indicates pure DNA. If the ratio is appreciably lower, it may indicate the presence of protein, phenol or other contaminants.

2.4.3 DNA sample storage

The quantified DNA samples were diluted to 50 ng/µl and aliquoted into 1.5 ml sterile screw-cap microfuge tubes. Working stocks were kept at 4°C and the remaining aliquotes were stored at -80°C.

2.4.4 Polymerase Chain Reaction (PCR)

2.4.4.1 Primers

Primer sets were designed using PerlPrimer v1.1.3 software, unless otherwise stated. Nucleotide blast search (NCBI, www.ncbi.nlm.nih.gov/blast) was performed to ensure sequence specificity. Primers were purchased from Eurofin MWG Operon in a lyophilized state. All primers were dissolved in sterile water to a stock concentration of 200 µM and stored at -20°C.

2.4.4.2 PCR procedure

The PCR reaction was carried out in 25 µl solution consisting of 0.25 µM specific primer (Eurofin MWG Operon), 0.1 mM dNTPs (VH Bio), 0.1 µg of genomic DNA as template, and 0.625U Taq polymerase (NEB) in 50 mM potassium chloride, 10 mM tris-HCl pH 9.0, 0.1% (v/v) triton X-100, 1.5 mM MgCl₂. The PCR program consisted of initial denaturation at 95°C for 5 min and 35 cycles of denaturation at 94°C for 1 min, annealing at a specified temperature for 1 min, extension at 72°C for 1 min, and a final extension at 72°C for 7 min. Amplifications were performed in an Applied Biosystems 2720 Thermo Cycler (PE Applied Biosystems). PCR products were visualized by ethidium bromide staining on 2% agarose gel (see section 2.6).

2.4.5 Electrophoresis and visualisation of DNA fragments

2.4.5.1 Agarose gel electrophoresis

Two percent agarose gels were made using DNase and RNase free agarose powder (Bioline) in 1x tris-borate-EDTA (TBE) buffer (0.09 M tris-base, 0.09 M boric acid and 2 mM EDTA), containing ethidium bromide (0.5 µg/ml). One micro litre of 6 X gel loading buffer (0.25 % bromophenol blue, 0.25 % xylene cyanol, 30% glycerol) was mixed with 5 µl DNA sample and applied to the gel. The DNA fragment sizes were estimated by comparison to a 100 bp DNA ladder (NEB). Electrophoresis was performed at constant voltage of 80V for 30-45 min in 1 X TBE buffer.

2.4.5.2 Polyacrylamide gel electrophoresis (PAGE)

Polyacrylamide gel solution (10%) containing 30% acrylamide-bis acrylamide 29:1 (Fisher Scientific) in 1X TBE buffer, 0.4 mg/ml ammonium persulphate (APS) and 0.1% TEMED was prepared. The gel was cast between two 200 mm x 200 mm glass plates separated by 0.8 mm spacers and allowed to polymerize at room temperature for 30 min. Three micro litres of 6 X gel loading was mixed with 15 µl of DNA samples and applied to the gel. The DNA fragment sizes were estimated by comparison to a 100bp DNA ladder (NEB). Electrophoresis was performed at constant voltage of 150V for 4-6 h in 1 X TBE buffer and the gels were stained for 30 min in 0.5 µg/ml ethidium bromide in 1 X TBE buffer. Gels were then destained for 10 min in distilled water before viewing.

2.4.5.3 Gel visualisation

Visualization of the DNA fragments was done using the Flour-S MultiImager system (Bio-Rad Laboratories) and Quantity One analysis software (Bio-Rad Laboratories).

2.4.6 DNA purification and sequencing

PCR products and plasmid DNA were electrophoresed in 1% agarose gel along with a 100 bp DNA ladder. DNA fragments were then excised from the agarose gel and purified using the QIAquick gel extraction kit (QIAGEN) according to the manufacturer's protocol. Both purified PCR products (5 ng/ μ l) and plasmid DNA (100 ng/ μ l) were transferred into 1.5 ml microfuge tubes in a minimum volume of 15 μ l. Primers used for PCR products sequencing were diluted to 2 ng/ μ l and transferred into 1.5 ml microfuge tubes in a minimum volume of 15 μ l. Both purified PCR products and plasmid DNA together with their specific primers used for sequencing were sent to Eurofin MWG. DNA sequencing was performed by Eurofin MWG and the sequences were then compared using BLAST alignment tool.

2.5 Recombinant cell line construction

2.5.1 Insertion of PCR product into plasmid vector

PCR product was purified and ligated into a pTARGET mammalian expression vector (Promega) according to the manufacturer's instructions. The pTARGET vector contains a 3' terminal thymidine at both ends which improve the efficiency of ligation with the A-tailing of PCR product into the vector. **Figure 2.1** shows the map of the pTARGET vector. Briefly, a 10 μ l reaction mixture was set up with 10 ng mammalian expression vector pTARGET (Promega), 5 μ l of ligation buffer (2x), 1 μ l T4 DNA ligase (1U), and 3 μ l of 300 ng of insert DNA fragment. The ligation reaction mixture was incubated at 4°C for 16 h prior to transformation.

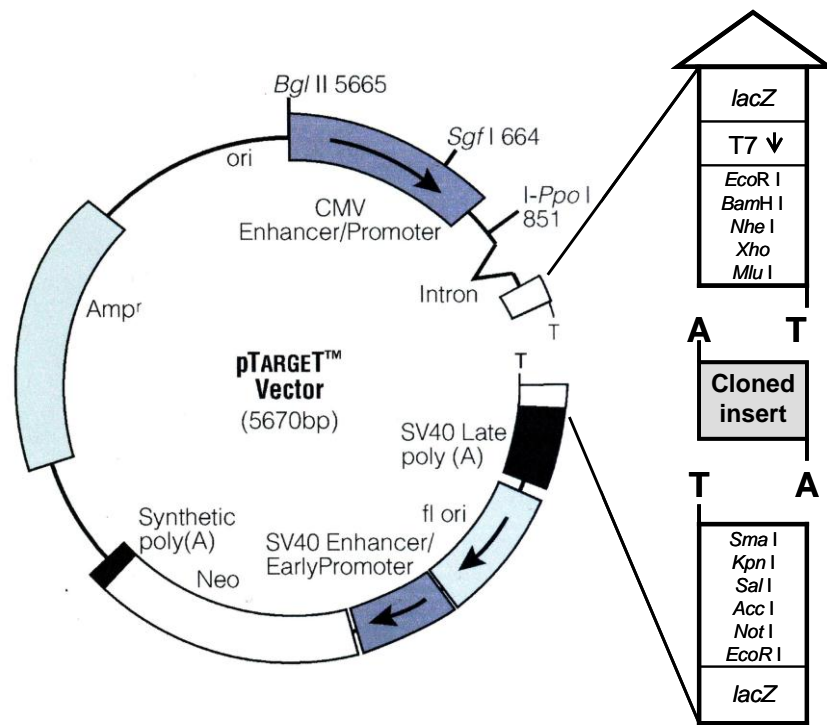


Figure 2.1 Map of the pTARGET mammalian expression vector

The pTARGET mammalian expression vector contains a 3' terminal thymidine at both ends which improve the efficiency of ligation with the A-tailing of PCR product into the plasmid. The vector contains a modified version of coding sequence of the α -peptide of β -galactosidase, allowing blue/white recombinant screening. The vector carries the human cytomegalovirus (CMV) immediate-early enhancer/promoter region to promote constitutive expressions of cloned DNA inserts in mammalian cells. This vector also contains the neomycin phosphotransferase gene, a selectable marker for mammalian cells. Expression of the neomycin phosphotransferase gene in the pTARGET vector confers resistance to the antibiotic G-418 and allows the selection of stably transfected cells.

2.5.2 Transformation

Competent *Escherichia coli* (*E. coli*) JM109 cells (50 μ l) were mixed with 2 μ l of ligation reaction mixture in a sterile 15 ml polypropylene tube and transformed by placing on ice for 20 min. The *E. coli* cells were heat shocked by incubating the reaction tube in a water bath at 42°C for 1 min. After heat shock, the tube was immediately transferred to ice and incubated for 2 min. SOC medium (950 μ l) (10 mM NaCl, 2.5 mM KCl, 10 mM MgSO₄, 10 mM MgCl₂, 20 mM glucose, 0.5% yeast extract and 2 % tryptone) was added into the cells. The tube was then incubated in an orbital incubator at 150rpm at 37°C for 1.5 h. Subsequently, *E. coli* cells (100 μ l) were plated onto a 1.5% Luria-Bertani (LB) agar plate containing 100 μ g/ml ampicillin, 20 mg of 5-bromo-4-chloro-3-indolyl- β -D-galactopyranoside, and 200 mg/ml of isopropyl- β -D-thiogalactopyranoside (IPTG). The plate was incubated overnight at 37°C.

2.5.3 Isolating recombinant plasmid DNA

The pTARGET vector contains a modified version of coding sequence of the α -peptide of β -galactosidase, allowing blue/white recombinant screening. The transformants (white colonies) were inoculated individually using a sterile pipette tip and transferred into LB broth (5 ml) containing 100 μ g/ml ampicillin. Transformants were allowed to grow for 16 h at 37°C and harvested by centrifugation at 1500rpm at 4°C for 10 min. Plasmids were then extracted using the QIAGEN mini-prep plasmid extraction kit. The presence of the recombinant construct was confirmed by digesting the plasmid DNA (3 μ l) with *Eco*RI restriction enzyme. Plasmids containing the desired insert were further confirmed by sequencing in both forward and reverse strands (see section 2.4.6).

2.5.4 Transfection and generation of stable cell lines

Exponentially growing cells were seeded at a density of 3×10^5 cells per ml using 2 ml of antibiotic-free culture medium into 6-well plates. After 24 h, cells were transiently transfected using GeneJuice transfection reagent (Novagen, Merck Biosciences). Briefly, GeneJuice (3 μ l) was premixed with 250 μ l of EMEM (serum-free, non-antibiotics) in a sterile 15 ml polyethylene tube and incubated for 5 min at room temperature. Plasmid DNA (1 μ g) was then added into the mixture and incubated further at room temperature for 10 min. The complex mixture was then added into the

cells and incubated for 24 h. At 24 h after transient transfection, cells were transferred into 100 mm culture dish and stable cell lines were generated by selection with 500 µg/ml G-418 antibiotic (Sigma) for 2-5 weeks. The pTARGET vector contains the neomycin phosphotransferase gene, which confers resistance to G-418. Death of cells not expressing neomycin phosphotransferase was detected after 10-14 days following addition of G-418. The medium were changed every 2-3 days until the drug-resistant clones appear. The cell clones were observed after PBS washing and the larger single cell clones were separated with sterile tip, cultured in 500 µg/ml G-418 selective culture medium for another 2 weeks. The stable transfected cell lines were obtained after passage by 2-3 generations and maintained in 250 µg/ml G-418 selective culture medium.

2.6 RNA isolation and analysis

2.6.1 RNA isolation and quantification

Monolayer cell cultures were washed twice with ice-cold PBS, scraped off into PBS and pelleted by centrifugation for 5 min at 1000 rpm. Total RNA was extracted using NucleoSpin RNA II extraction kit (Macherey-Nagel, MN) according to the manufacturer's instructions. RNA concentrations were then quantified using a NanoDrop 1000 spectrophotometer (Thermo Scientific).

2.6.2 Synthesis of cDNA

One microgram of RNA was reverse transcribed in 1 X RT buffer + 2.5 U/µl reverse transcriptase (NEB), 5 mM deoxynucleotide (dNTP) mixture (Fermentas), 20 ng/µl random hexamers (QIAGEN), and 1 U/µl RNase inhibitor (NEB). RNA with random hexamers were incubated at 65°C for 10 min and immediately put on ice. Reverse transcription was carried out at 42°C for 30 min, 50°C for 30 min, 70°C for 10 min, then incubated at 4°C. The cDNA was then stored at -20°C prior to analysis.

2.6.3 Semiquantitative reverse transcription-PCR (Semiquantitative RT-PCR)

Amplification of cDNA was performed using PCR (see section 2.4.4). The PCR conditions for the target gene were 35 cycles at 95°C for 15 s, annealing at a specified temperature for 30 s, and 72°C for 45 s except for Beta-actin (β -actin) and Glyceraldehyde-3-phosphate (GAPDH). β -actin and GAPDH are housekeeping genes which used as internal control to evaluate the gene expression analysis. The PCR conditions for β -actin and GAPDH were 30 cycles at 95°C for 15 s, 52°C for 30 s, and 72°C for 45 s. PCR products were then visualized by ethidium bromide staining on a 2% agarose gel. The primer sequences and PCR conditions used for semiquantitative RT-PCR analysis are summarized in **Table 2.2**.

Table 2.2 Semiquantitative RT-PCR primer sequences and conditions

Gene name	Short name	Primer sequences	Expected size	Annealing Temperature
Glyceraldehyde-3-phosphate	<i>GAPDH</i>	5'-GACAACTTTGGTATCGTGGAAGGA-3' 5'-ACCAGGAAATGAGCTTGAC-3'	445 bp	52°C
Beta-actin	<i>β-actin</i>	5'-GTTGCCAATAGTGATGACCT-3' 5'-GACCTGACAGACTACCTCA-3'	207 bp	52°C
N-acetyltransferase 2	<i>NAT2</i>	5'-ACGTCTCCAACATCTTCATTTATAACC-3' 5'-TCAACCTCTTCCTCAGTGAGAGTTTTA-3'	161 bp	51°C
Glutathione S-transferase alpha 4	<i>GSTA4</i>	5'-CAAGTTGCAGGATGGTAACC-3' 5'-ACATGTCAATCAGGGTTCTC-3'	158 bp	53°C

2.6.4 Quantitative real-time PCR (Quantitative RT-PCR)

Real-time PCR is the continuous collection of fluorescent signal from polymerase chain reactions over a range of cycles. Quantitative real-time PCR, on the other hand, allows the conversion of the fluorescent signals from each PCR reaction into a numerical value for each sample (Dorak, 2006). It is based on the detection of the fluorescence signals produced by a reporter molecule which increases, as each cycle of the PCR amplification proceeds. By monitoring and recording the intensity of the fluorescence emission during each PCR cycle, it is possible to identify the exponential phase of the PCR reaction and from this to determine the initial amount of target template (Dorak, 2006). The amount of target template present corresponds to the level of fluorescence. Thus, the higher the starting copy number of the target template, the fewer the amplification cycles needed before a significant increase in fluorescence is observed. During the initial cycles of PCR, the background signal prior to the significant accumulation of the target amplicon is used to determine the baseline fluorescence across the entire reaction. When the target amplification is sufficiently above the baseline value and within the exponential part of the amplification curve, a fixed fluorescence threshold is set. The threshold cycle (Ct) reveals the cycle number at which the fluorescence emission crosses the fixed threshold. It reflects the statistically significant point above the baseline during a reaction at which a sufficient number of amplicons have accumulated. Thus, the higher the initial amount of target template, the faster accumulated PCR product is detected, and the lower the Ct value.

The commonly used fluorescent reporter molecules include intercalating fluorescent dyes such as SYBR Green I and sequence specific probes. Sequence specific probes, such as TaqMan probes are oligonucleotides longer than the primers (20-30 bases long) that contain a fluorescent reporter (FAM- and VIC-labelled) and a quencher (usually TAMRA or a non-fluorescent quencher) at their 5' and 3' ends, respectively (**Figure 2.2**). A passive reference dye such as 6-carboxyl-x-rhodamine (ROX) is primarily used to normalise for non-PCR-related fluctuations in fluorescence signal. When the probe binds to an internal region of a PCR product, the 5' exonuclease activity of the DNA polymerase cleaves the reporter dye from the probe. This separates the reporter dye from quencher dye, ends the activity of the quencher and thus allows the fluorescence emitted by the reporter. The increased in the reporter fluorescence signal is correlated to

the amount of the PCR product generated in each reaction. The resulting fluorescence is only detectable if the cleavage occurs when the probe hybridizes to its target sequences. Therefore the detected fluorescence is specific amplification and little optimization is required for a well-designed TaqMan probe. However, compared to SYBR Green, TaqMan probes are relatively expensive and a different probe has to be synthesized for each specific target.

SYBR Green I dye is an intercalating agent that binds to all double-stranded DNA or PCR products. During DNA denaturation, SYBR Green I dye is released and the fluorescence signal is drastically reduced. When PCR amplification is complete, SYBR Green I dye binds to the double stranded products, resulting in an increase in fluorescence (**Figure 2.2**). The advantage of using SYBR Green I dye is the relative simplicity of this assay system where no probes are required, thus reduces assay setup and running cost. However, the primary disadvantage is that it may generate false positive signals by binding to any double-stranded DNA including primer dimers, contaminating DNA, and PCR product from mis-annealed primer. Extensive optimization is therefore required for assay setup. **Figure 2.3** shows a typical amplification plot on NAT2 expression obtained during this project. Melting point or dissociation curve analysis can be generated following a reaction to verify whether only one product is being amplified. As shown in **Figure 2.4a**, once the final PCR amplification cycle is completed, a maximum amount of SYBR Green I is bound to double-stranded DNA and a high level of fluorescence signals is generated. However, DNA product melts or dissociates with increasing temperature ($>80^{\circ}\text{C}$), releasing SYBR Green and decreasing the fluorescent signal. The melting point is defined as the inflection point of the melting curve which is shown as a peak in the derivative melt curve plot (**Figure 2.4b**). A single peak indicates a single product whereas multiple peaks indicate the presence of non-specific priming including primer dimers and genomic DNA contamination. The predicted size of single peak can be verified by agarose gel electrophoresis.

The expression level of a target gene can be measured by relative quantitative in relation to the level of a control gene. An ideal control generally demonstrates gene expression that is highly abundant and relatively constant across tissues and cell types. By using an invariant control, quantitation of an mRNA target can be normalised for differences in

the amount of total RNA added to each reaction. Commonly used internal control genes such as Glyceraldehyde-3-phosphate (GAPDH), β -actin and 18S ribosomal RNA (18S rRNA) are constitutively expressed housekeeping proteins, however, they may not always be the most ideal or appropriate candidates for normalisation in RT-PCR. For instance, GAPDH expression may be upregulated in proliferating cells, and β -actin is a better active reference for these cells instead of GAPDH (Suzuki et al., 2000). GAPDH is also not recommended for cancer studies due to its high expression in aggressive cancer cells (Goidin et al., 2001). Additional caution should be taken when 18S rRNA is used as a control especially if the expression level of the target gene is low (Dorak, 2006). The strategy of using a combination of multiple controls as normaliser may be useful for relative expression studies by quantitative RT-PCR. More details and a typical calculation are shown in section 4.3.2.1. A Taqman probe-based RT-PCR assay (allelic discrimination assay) can also be used to perform genotyping studies with any possible SNP by using two allele-specific probes. Use of a Taqman SNP genotyping assay is described in detail in section 3.2.7.

The SYBR green-based RT-PCR assay used in our present study is SYBR Green I JumpStart Taq ReadyMix, obtained from Sigma-Aldrich. The hot-start mediated Taq polymerase (JumpStart Taq) enhances the efficiency and increases the specificity and yields of the desired sequence by eliminating polymerase activity at temperatures below 70°C. Briefly, quantitative RT-PCR was performed utilizing 0.2 μ l cDNA per reaction in triplicate in a 13 μ l volume on a ABI Prism 7000 Sequence Detection System. PCR amplification conditions were as follows: 50°C, 2 min, followed by 95°C, 10 min, then 40 cycles at 95°C, 15 s; and 40 cycles at 60°C, 1 min. Amplification of GAPDH or β -actin was performed using the same conditions as the genes being tested but in separate tubes. A “no template” control for each gene was performed, replacing cDNA with water. Data analysis was performed using SDS 2.2 software (PE Applied Biosystems). At the end of the PCR, dissociation curves were generated and analysed to identify the possibility of non-specific PCR products. Standard curves were assessed by r^2 value, with a minimum of 0.98 required for successful PCR analysis. Quantitation of the target cDNAs in all samples was normalized to GAPDH or β -actin ($\text{GAPDH}; C_{t_{\text{target}}} - C_{t_{\text{GAPDH}}} = \Delta C_t$), and the effects of each compound on the target cDNA was expressed relative to the amount in the vehicle control sample ($\Delta C_{t_{\text{compound}}} - \Delta C_{t_{\text{vehicle}}} = \Delta \Delta C_t$). Relative fold changes in target gene expression were determined by taking 2 to the power of the $\Delta \Delta C_t$

value ($2^{-\Delta\Delta C_t}$) as per the user bulletin (PE Applied Biosystems) (Livak and Schmittgen, 2001). The primer sequences used for Q-RT-PCR analysis are summarized in **Table 2.3**.

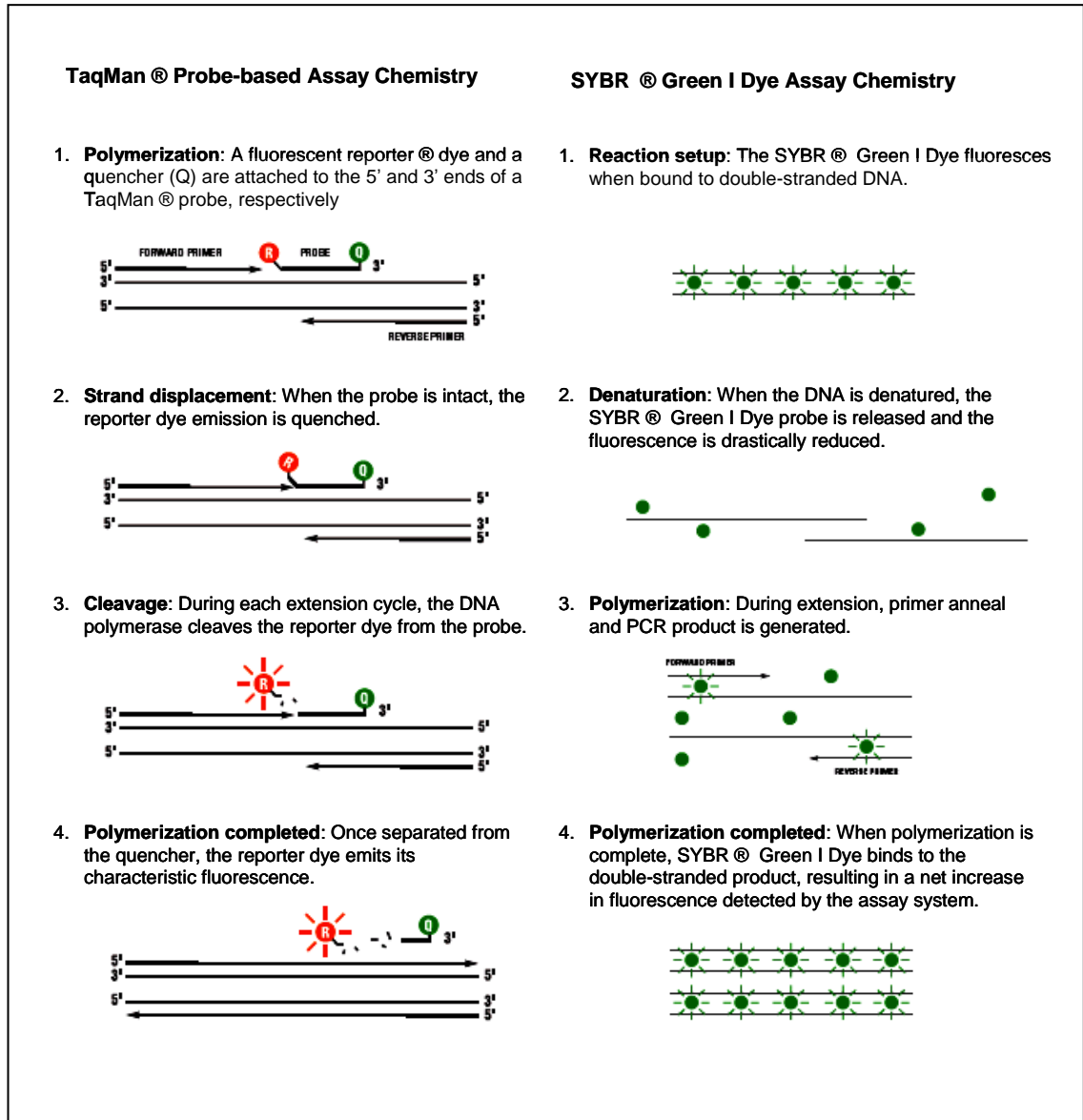


Figure 2.2 Comparison of Taqman®- and SYBR®-Green based detection (Image obtained from Applied Biosystems website (<http://www.appliedbiosystems.com>))

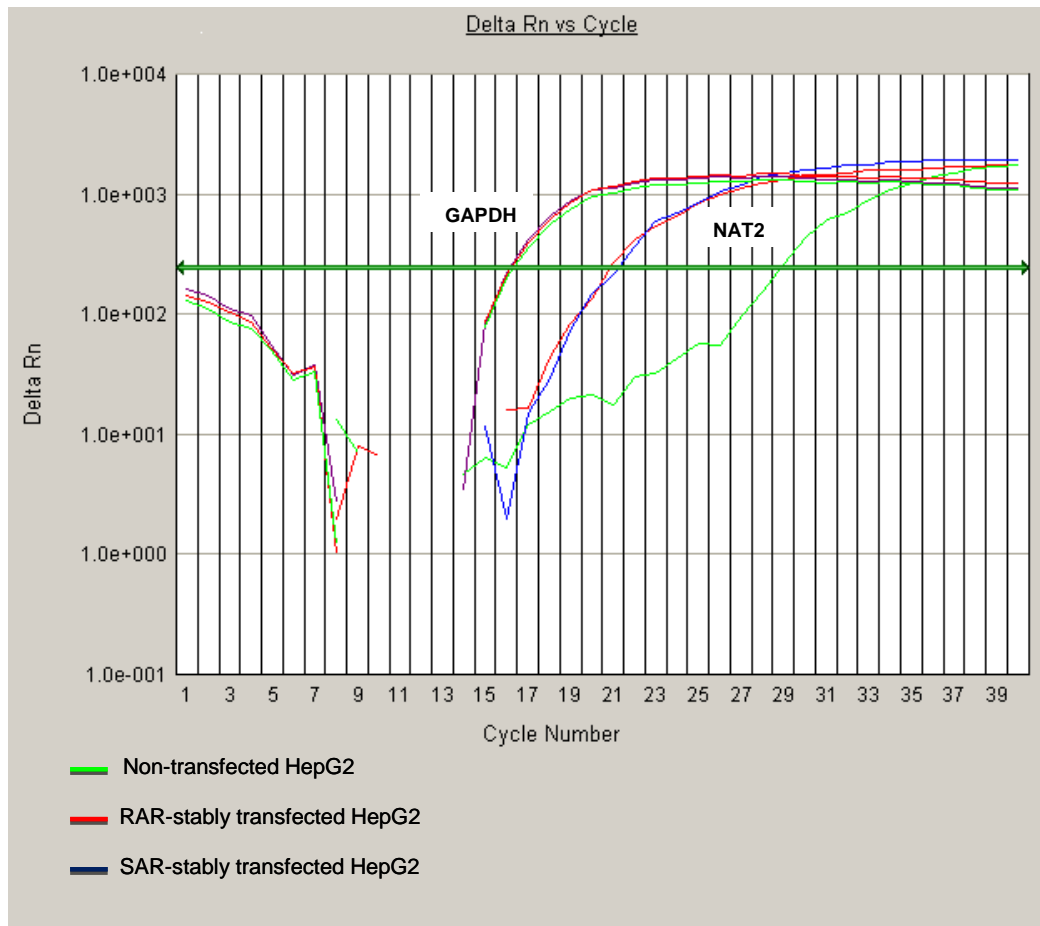


Figure 2.3 Representative amplification plot quantitative RT-PCR using SYBR Green I detection dye

Figure shows the amplification plots of target gene (NAT2) and control (GAPDH) in non-transfected, RAR- and SAR stably transfected HepG2 cells. NAT2 expressions in RAR- and SAR-stably transfected cells are higher than the non-transfected cells as a much lower Ct values (20-21) was detected in those cells compares to the non-transfected cells (Ct values \approx 30). The Ct values for GAPDH are quite consistent in all three types of cells with Ct values around 17.

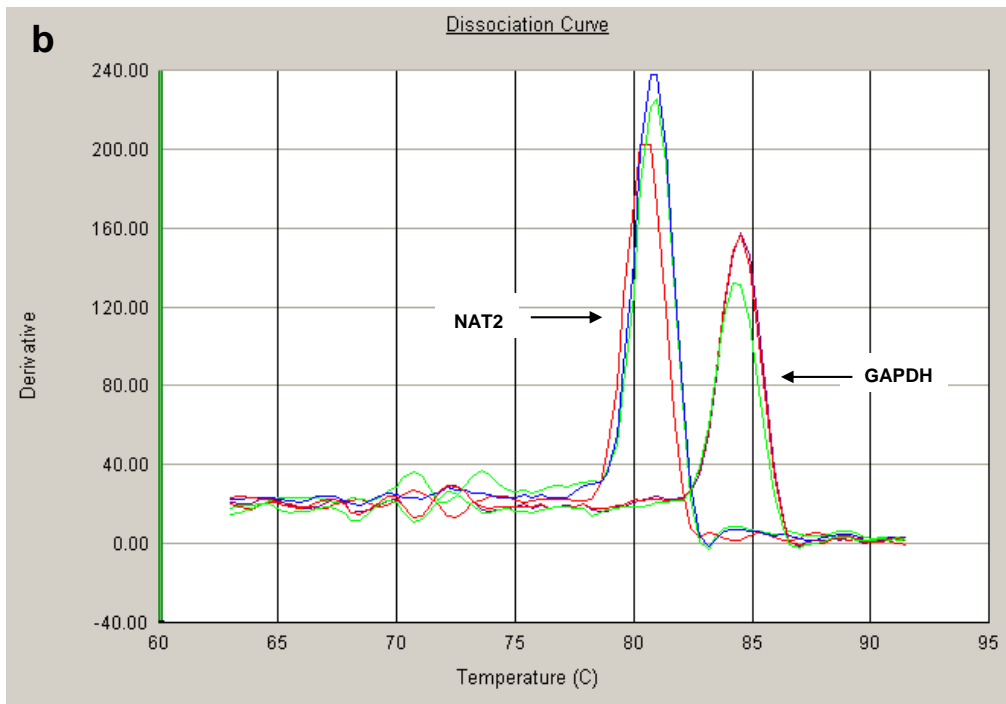
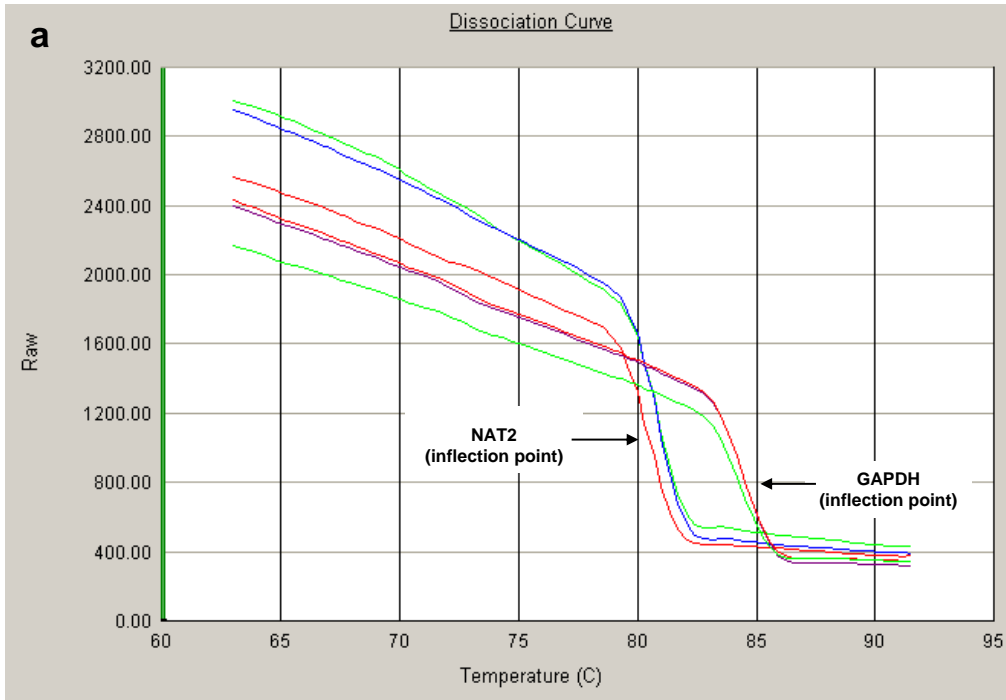


Figure 2.4 Melting curve (a) and derivative melting curve (b) analyses for the reactions shown in Figure 2.3

Table 2.3 Quantitative RT-PCR primer sequences

Gene name	Short name	Primer sequences
Glyceraldehyde-3-phosphate	<i>GAPDH</i>	5'-GGGTGTGAACCATGAGAAGTATGA-3' 5'-CATGAGTCCTTCCACGATACCAA -3'
Beta-actin	<i>β-actin</i>	5'-GTTGCCAATAGTGATGACCT-3' 5'-GACCTGACAGACTACCTCA-3'
Cytochrome P450 3A4	<i>CYP3A4</i>	5'-TGTCCTACCATAAGGGCTTTTGTA-3' 5'-TTCCTAGCACTGTTTTGATCATG-3'
Carboxylesterase 2	<i>CES2</i>	5'-AACCTGTCTGCCTGTGACCAAGT-3' 5'-ACATCAGCAGCGTTAACATTTTCTG-3'
Cytochrome P450 2E1	<i>CYP2E1</i>	5'-ACCTGCCCCATGAAGCAACC-3' 5'-GAAACAACCTCCATGCGAGCC-3'
N-acetyltransferase 2	<i>NAT2</i>	5'-ACGTCTCCAACATCTTCATTTATAACC-3' 5'-TCAACCTCTTCCTCAGTGAGAGTTTTA-3'
Glutathione S-transferase alpha 4	<i>GSTA4</i>	5'-CCGGATGGAGTCCGTGAGATGG-3' 5'-CCATGGGCACTTGTTGGAACAGC-3'
Glutathione S-transferase alpha 1	<i>GSTA1</i>	5'-AAGGAGAGAGCCCTGATTGATATGT-3' 5'-GTCTTGTCCATGGCTCTTTAAGACT-3'

2.7 Protein analysis

2.7.1 Protein extraction and quantification

Protein was extracted from harvested cells using RIPA buffer (Fisher Scientific) containing 25 mM tris-HCl pH 7.6, 150 mM NaCl, 1% NP-40, 1% sodium deoxycholate, 0.1% SDS and a protease inhibitor cocktail (Sigma). Cell lysates were homogenised using a syringe and quantified using BioRad DC Protein Assay. A standard dilution of Bovine Serum Albumin (BSA) (Bio-Rad) was prepared ranging from 0.125 – 4 mg/ml in RIPA buffer. Absorbance was read at 750nm using Spectramax M5e and protein concentrations were calculated using the Softmax Pro5.2 software.

2.7.2 SDS polyacrylamide Gel Electrophoresis (SDS-PAGE)

Protein preparations were analysed by SDS-polyacrylamide gel electrophoresis (PAGE) according to Laemmli et. al. (Laemmli, 1970). Polyacrylamide gels were cast and run using Mini PROTEAN II equipment (Bio-Rad). A 12% SDS-polyacrylamide resolving gel was cast under a 4% stacking gel. The resolving gel contained 16 ml acrylamide/bis solution, 20 ml resolving gel buffer (0.75 M tris-HCl, pH 8.8 and 0.2% (w/v) SDS), 400 µl APS, 160 µl TEMED and 4 ml H₂O. The stacking gel contained 2 ml acrylamide/bis solution with 5 ml stacking gel buffer (0.25 M tris-HCl, pH 6.8 and 0.2% (w/v) SDS), 100 µl APS, 40 µl TEMED and 3 ml H₂O. The resolving gel was first cast between two 200 mm x 200 mm glass plates and the gel surface was overlaid with 2-butanol to avoid any formation of air bubbles. The resolving gel was allowed to polymerize at room temperature for 30 min and rinsed with water after polymerisation. Subsequently the stacking gel solution was added on top of the resolving gel and a comb was placed between the gel plates. The stacking gel was then allowed to polymerize for 30 min before removing the comb. Fifty micrograms of protein was mixed with SDS sample loading buffer (5 M urea, 2.5% SDS, 0.5 M tris-HCl pH 6.8, 3.5% β-mercaptoethanol and 0.02% bromophenol blue) in the ratio of 1:1 and heated at 95°C for 5 min. Protein samples and molecular weight marker (PageRuler Prestained Protein Ladder, Fermentas) were applied to a SDS-PAGE gel and separated at 175V for 2 h in running buffer (25 mM tris-HCl pH 8.3, 192 mM glycine and 0.1% SDS). Proteins were then transferred onto a nitrocellulose membrane (Amersham Hybond-C, GE Healthcare) in transfer buffer (25 mM tris base, 0.15 M glycine, 10% methanol) at 60V for 2 h. After

transfer, proteins were visualised by staining the nitrocellulose membrane with Ponceau S solution and scanned before immunoblotting to ensure equal loading. Membranes were then rinsed with PBS to remove remaining Ponceau S stain.

2.7.3 Western Blotting

The nitrocellulose membrane containing transferred proteins was blocked for non-specific binding with 10% milk in 1x phosphate buffered saline (PBS, pH 7.4) (120 mM NaCl, 9 mM Na₂HPO₄, 3.7 mM NaH₂PO₄ and 2.7 mM KCl) for 1 h at room temperature on a shaker. Primary antibodies were diluted in 1% milk made in PBS according to their optimised concentration and added onto the membrane for an overnight incubation at 4°C on a shaker. Membranes were washed three times in PBS for 10 min before incubated in appropriate horseradish peroxidase (HRP) labelled secondary antibodies for 1 h at room temperature on a shaker. After incubation, the membranes were washed three times in PBS for 10 min and the proteins were detected using chemiluminescence system by Amersham ECL Western Blotting Detection Reagents (GE Healthcare). The membrane was then exposed on Amersham Hyperfilm (GE Healthcare) and developed manually through a 1 min rinse each in GBx developing and fixing solution. Membranes were then stripped by incubation at room temperature with gentle shaking for 10 min in 100% acetonitrile. The acetonitrile was removed from the membrane before their incubation at 56 °C in 150 ml stripping buffer for 30 min with gentle rocking. Membranes were then washed four times for 15 min in PBS on shaker and six times for 15 min in deionised water. They were either dried at room temperature and store between sheets of whatmann paper at -20 °C or used immediately for immunostaining. The list of antibodies used was shown in **Table 2.4**.

Table 2.4 Antibodies used for Western blotting

Primary antibodies	Source	Company	Dilution
Anti-GAPDH polyclonal	Rabbit	Sigma	1:1000
Anti- β -actin polyclonal	Rabbit	Sigma	1:1000
Anti-NAT2 polyclonal	Mouse	Abnova	1:500
Anti-GSTA4 polyclonal	Mouse	Abnova	1:1000
Anti-GSTA1 monoclonal	Mouse	Abnova	1:1000
Secondary antibodies			
HRP-labelled anti-mouse	Goat	DAKO	1:3000
HRP-labelled anti-rabbit	Goat	DAKO	1 :3000

2.7.4 Quantitation of protein bands

Quantitation of the protein bands was done by using ImageJ software (Wayne Rasband, INH). A scanned image of the immunoblot was saved as a TIFF file and the intensity of the protein bands were quantified according the procedure detailed.

(<http://rsb.info.nih.gov/ij/>).

2.8 Assessment of cell viability

A cell viability test was performed using the 3-(4,5-dimethylthiazol-2-yl)-2,5-diphenyltetrazolium bromide (MTT) assay in a 6-well plate. Cells were seeded overnight at a density of 1×10^6 cells per ml and exposed to drug treatment for designated period of time. On the day of assay, medium was removed, cells were washed with PBS, and 900 μ l of fresh medium together with 100 μ l MTT solution in PBS (5mg/ml) was added into each well at 37°C for 3 h. The media containing MTT solution was removed and 100 μ l of isopropanol containing 0.04 M HCl was added to each well. The plates were shaken to solubilise the blue formazan produced for 30 min at 4°C and absorbance was measured at a wavelength of 570nm with background

subtraction at 690nm in a plate reader. Assays were performed in duplicate from three independent experiments. Data of the MTT assays were analyzed using two-way analysis of variance (ANOVA) to identify specific differences between selected groups. In all cases, $P < 0.05$ was required for significance to identify specific differences. The fifty-percent effective concentration (EC_{50}), representing the concentration of drug causing 50% cell death compared with control cells, was determined by non-linear regression using GraphPad Prism 5.0 (California, USA).

2.9 Determination of intracellular glutathione content

The amount of reduced glutathione (GSH) and oxidized glutathione (GSSG) in mammalian cells were determined using the enzymatic recycling method adapted to microplate reader according to Baker et al. (Baker et al., 1990). The total intracellular GSH was determined by the colorimetric reaction of 5,5'-dithiobis(2-nitrobenzoic acid) (DTNB) with GSH to form the coloured product 5-thio-2-nitrobenzoic acid (TNB). GSSG is then reduced by glutathione reductase (GR) to form GSH, using the reduced β -nicotinamide adenine dinucleotide phosphate (NADPH) as a cofactor. The rate of formation of TNB, which is proportional to the total GSH content (GSH + GSSG), was measured spectrophotometrically at 405nm. Briefly, cells were seeded overnight on a 6-well plate at a density of 1×10^6 cells/ml and subjected to drug treatment for designated time period in duplicate. A positive control was included in the assay by treating the cells with 0.5 mM diethyl maleate (DEM) which reduce GSH levels when compared to the media control (no drug treatment). Cells were then washed with room temperature PBS and lysed by scraping them in 100 μ l ice-cold 5% 5-sulfosalicylic acid (SSA). Lysed cells were transferred to 0.5 ml microfuge tubes, incubated for 10 min on ice and centrifuged at 8000 x g for 5 min. To assay for total GSH, cell lysates were first diluted 1:2 with 5% SSA, and further diluted to 1:2 with 400 mM sodium carbonate, then further diluted 1:8 with phosphate-EDTA dilution buffer (100 mM sodium phosphate, 1 mM EDTA, pH 7.4) (total dilution of 1:32). Standards containing from 0-8 μ M of GSSG were prepared by diluting the 5% SSA-diluted GSSG stock (16 μ M) with 200 mM sodium carbonate and 2.5% SSA. The samples and standards were kept on ice until being loaded in the 96-wells microtiter plate. To measure the GSSG, the GSH in the samples was treated with 2-vinylpyridine (2VP) to conjugate GSH before assay of residual GSSG (Griffith, 1980). Equal volume of the optimized concentration of 2VP, 200 mM final, was added into the samples and the samples were further diluted 1:2 with

400 mM sodium carbonate (total dilution 1:4). GSSG assay samples were incubated at room temperature for an hour to allow the conjugation of GSH with 2VP. The microtitre plate was prepared by pipetting 20 µl of standards, 2VP-treated and untreated samples and blank per well. Subsequently, 180 µl of freshly prepared assay reaction mixture containing 0.4 mM NADPH, 0.3 mM DTNB, and 1.9 units/ml of GR in phosphate-EDTA dilution buffer was added into the wells and the plate was incubated in the dark on an orbital shaker. The absorbance in the wells at 405nm after 25 min was measured using a plate reader. The GSH and GSSG content were determined from the GSH standard curves by using the following formula:

$$\text{GSH} = \frac{(\text{Absorbance at } 405\text{nm}) - (\text{Y-intercept})}{\text{Slope}} \times \text{sample dilution}$$

$$\text{GSSG} = \frac{(\text{Absorbance at } 405\text{nm}) - (\text{Y-intercept})}{\text{Slope}} \times (\text{sample dilution})/2$$

The dilution factor for GSSG content was corrected for the conversion of GSH to GSSG as GR reduces the GSSG formed into 2GSH. Protein concentration of each cell extract was quantified using BioRad DC Protein Assay (see section 2.9.1). The total glutathione (GSH+GSSG, µM/mg) and GSH/GSSG ratio data in each sample were analyzed. A two-way ANOVA was performed to identify specific differences between selected groups using GraphPad Prism 5.0. In all cases, $P < 0.05$ was required for significance to identify specific differences. **Figure 2.2** shows the GSH standard curve ranging in concentration from 0.2-8.0 µM. Data presented are means ± S.D. of duplicates.

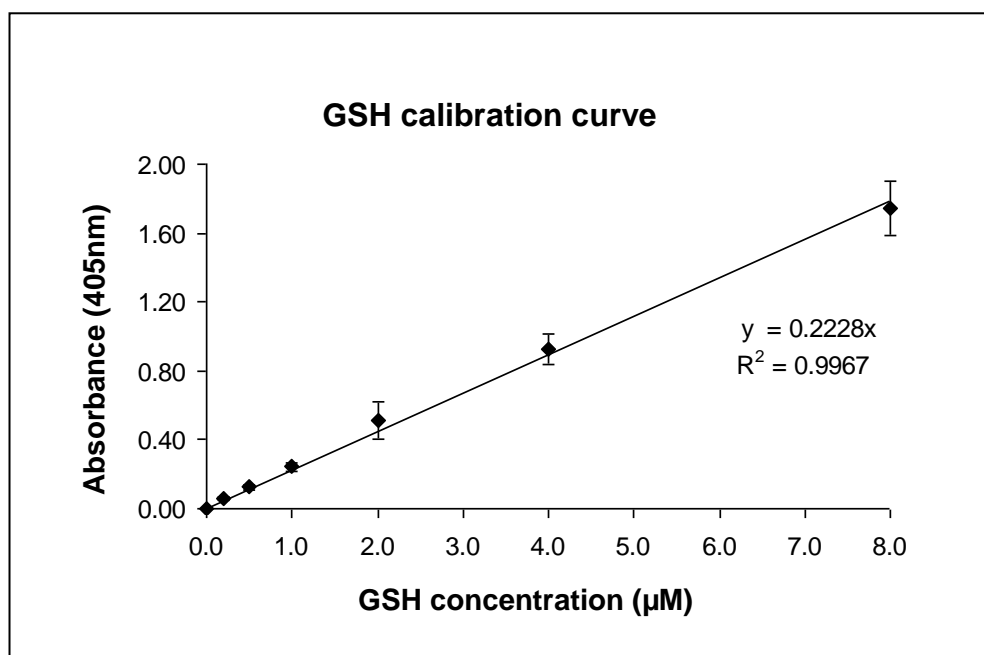
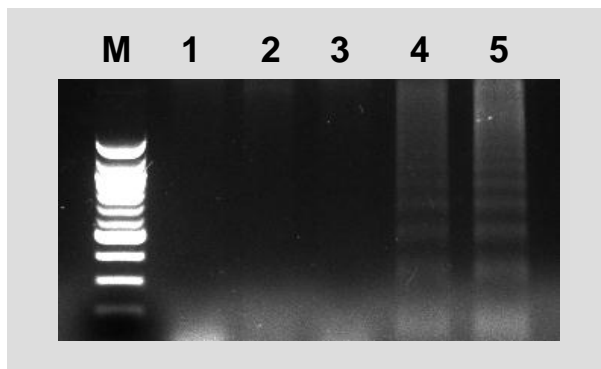


Figure 2.5 GSH calibration curve as absorbance values versus glutathione concentrations

GSH calibration curve was prepared from serial dilution of GSH ranging from 0.2-8.0 µM plotted versus their absorbance values. Data presented are means \pm S.D. of duplicates. The change in absorbance at 405 nm is a linear function of the GSH concentration with $r^2 > 0.99$.

2.10 DNA fragmentation assay

DNA fragmentation was assessed by Apoptotic DNA Ladder Extraction Kit (Biovision). Briefly, approximately 1×10^7 cells were harvested, washed with PBS, and pelleted by centrifugation for 5 min at $500 \times g$. The supernatant was removed and the cell pellet was resuspended in 50 μ l DNA Ladder Extraction Buffer. The mixture was then mixed by gentle pipetting for 10 seconds and centrifuged for 5 min at $1600 \times g$. The supernatant was transferred to a new 1.5 ml microfuge tube and the cell pellet was extracted again with 50 μ l DNA Ladder Extraction Buffer. The supernatants were combined and 5 μ l Enzyme A solution was added into the supernatant. The solution was mixed by gentle vortexing and incubated at 37°C for 10 min. Enzyme B solution (5 μ l) were then added into the mixture and further incubated overnight at 50°C . The following day, 5 μ l of ammonium acetate solution was added to the sample and mixed well. Isopropanol (100 μ l) was then added and the solution was mixed well and kept at -20°C for 20 min. DNA pellet was obtained by centrifugation at $13,000 \times g$ for 10 min followed by washing twice with 75% ethanol. The pellet was air-dried for 5 min and resuspended in 30 μ l DNA Suspension Buffer. Samples were loaded on to a 1.2% agarose gel and subjected to electrophoresis at 50 V for 1 h in 1 X TBE buffer. Gels were then stained with ethidium bromide and observed under UV light and photographed. For each experiment, a negative control was prepared by incubating the cells with medium only (no drug treatment). A positive control for apoptosis was also included each time when the assay was performed by treating the cells with 5 μM camptothecin. **Figure 2.3** reveals a characteristic ladder pattern of low molecular weight DNA fragments from apoptotic cells induced by camptothecin for 24 h.



Lane M : DNA molecular mass marker (100-bp ladder)
Lane 1 : No treatment (control)
Lane 2 : 1 μM camptothecin
Lane 3 : 2.5 μM camptothecin
Lane 4 : 5 μM camptothecin
Lane 5 : 10 μM camptothecin

Figure 2.6 Camptothecin induces apoptotic DNA fragmentation in HepG2 cells

The apoptotic DNA laddering patterns was observed in HepG2 cells treated with 5 and 10 μM camptothecin for 24 h. No DNA fragmentation was detected in cells treated with 0-2.5 μM camptothecin.

2.11 Caspase-3 activity assay

Caspase-3 activity in cell extracts was measured using Sigma Caspase-3 Fluorometric Assay Kit. The detection of caspase activity is based on the hydrolysis of the peptide substrate acetyl-Asp-Glu-Val-Asp-7-amido-4-methylcoumarin (Ac-DEVD-AMC) by caspase-3, resulting in the release of the fluorescent 7-amino-4-methylcoumarin (AMC) moiety. Cells were seeded in T75 flasks at a density of 1×10^7 cells/ml and exposed to inducing agent for designated period of time, pelleted and washed twice with PBS. A negative control was prepared by incubating the cells in the absence of inducing agent. Cells were then lysed by adding 100 μ l of lysis buffer (50 mM HEPES pH7.4, 5 mM 3-[(3-cholamidopropyl) dimethylammonio]-propanesulfonate (CHAPS), and 5 mM dithiothreitol (DTT)) and incubated on ice for 30 min. The lysed cells were centrifuged at 4500 rpm for 10 min at 4°C. Five micro litres of cell lysates or caspase 3 positive controls were transferred into a black 96-well view plates. These are black plates designed for optimal measurement of fluorescence. Assays were performed in the presence and absence of 2 μ l of caspase 3 inhibitor, Acetyl-Asp-Glu-Val-Asp-al (Ac-DEVD-CHO) to exclude nonspecific background in the enzymatic reaction. A blank control containing assay buffer (20 mM HEPES pH 7.4, 0.1% CHAPS, 5 mM DTT and 2 mM EDTA) was included to determine the background fluorescence of the substrate. The reaction was carried out by adding 200 μ l of Ac-DEVD-AMC containing reaction mixture into each sample and plates were further incubated for 2 h in the dark. The reaction scheme was summarized in **Table 2.5**. The fluorescence intensity (relative fluorescence units, Δ FU) was then measured at excitation 360nm and emission 460nm in the Spectramax M5e plate reader (Molecular Devices). Protein concentration of each cell extract was quantified using BioRad DC Protein Assay (see section 2.6.1). A standard curve was prepared by 10 mM AMC with assay buffer to yield AMC solutions ranging in concentration from 200-4000 pmol (**Figure 2.4**). Data presented are means \pm S.D. of triplicates. The enzyme specific activity for each sample was calculated using the formula below.

X = pmol AMC liberated per h in the absence of inhibitor

Y = pmol AMC liberated per h in the presence of inhibitor

Caspase activity = $\frac{(X-Y)}{\text{protein (mg)}}$ pmol AMC liberated/ h/ mg

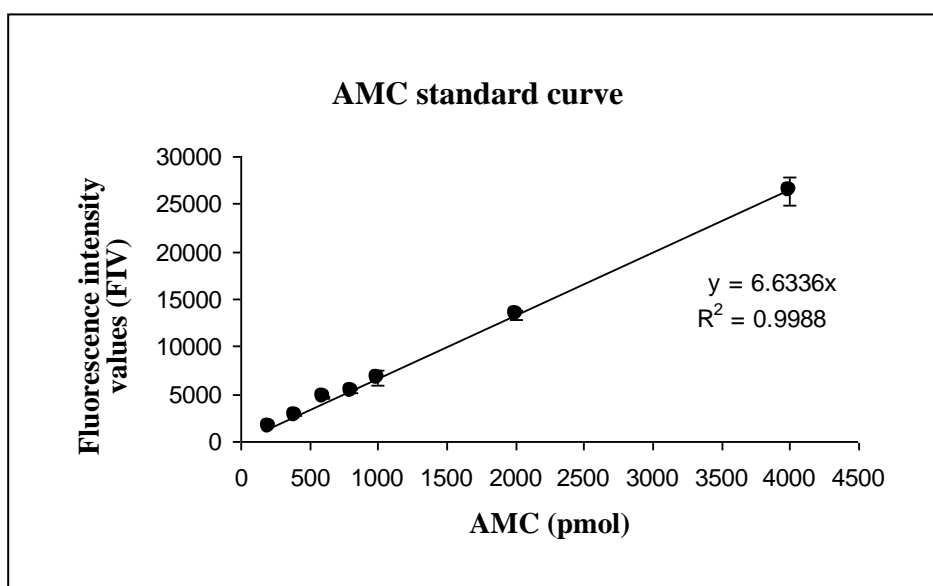


Figure 2.7 AMC reference standard calibration curve

A 7-amino-4-methylcoumarin (AMC) fluorescent reference standard was plotted as FIV (fluorescence intensity value) versus AMC concentration in the range of 200-4000 pmol. Data presented are means \pm S.D. of triplicates.

Table 2.5 Reaction scheme for caspase 3 assay

	1 x Assay Buffer	Caspase 3 (0.5µg/ml)	Cell lysate	Caspase 3 inhibitor Ac-DEVD-CHO (200 µM)	Reaction Mixture
Reagent Blank	5 µl	–	–	–	200 µl
Caspase 3 positive control	–	5 µl	–	–	200 µl
Caspase 3 positive control + inhibitor	–	5 µl	–	2 µl	200 µl
Non-induced cells	–	–	5 µl	–	200 µl
Non-induced cells + inhibitor	–	–	5 µl	2 µl	200 µl
Induced cells	–	–	5 µl	–	200 µl
Induced cells + inhibitor	–	–	5 µl	2 µl	200 µl

**Chapter 3. Genetic Polymorphisms of Anti-tuberculosis
Drugs Metabolizing Enzymes**

3 Genetic polymorphisms of anti-tuberculosis drugs metabolizing enzymes

3.1 Introduction

As described in section 1.7, there have been a number of previous studies relating genotype to susceptibility to DILI due to anti-TB drugs (ATD), though the overall findings are still unclear. *NAT2* remains the best studied genotype, especially since there is a clear rationale for an association since it has been demonstrated the levels of *NAT2* will affect isoniazid metabolite levels and patterns of metabolites (Lauterburg et al., 1985; Timbrell et al., 1980). Polymorphisms in *CYP2E1*, *GSTM1*, *GSTT1* and *SOD2* have also been investigated previously though the contribution of the gene products to anti-TB drug metabolism is less direct. The main aim of the work presented in this chapter was to investigate the association between *NAT2* genotype and ATD-DILI. It was also decided to study *CYP2E1*, *GSTM1*, *GSTT1* and *SOD2* polymorphisms in view of the previous contradictory data linking these polymorphisms to ATD-DILI. In addition, it was decided to study selected polymorphisms in *GSTA1*, *GSTA4*, *NAT1* and *PXR* as more novel candidates. *GSTA1* and *GSTA4* were chosen because of their role in the detoxification of products of oxidative stress (section 1.5.3.3) including 4-hydroxynonenal (Gardner et al., 2003; Hartley and Petersen, 1997). *NAT1* was studied because of unpublished data that became available from a collaborating laboratory pointing to a novel association with ATD-DILI (Shen Y and Daly AK, unpublished). *PXR* is of general relevance to both drug metabolism and metabolism of endogenous compounds relevant to liver injury such as bile acids, with rifampicin being a potent agonist (section 1.6.3.2).

3.2 Materials and Methods

3.2.1 Patient recruitment

The DILIGEN study seeks to identify susceptibility genes for DILI by collecting DNA samples from patients diagnosed with DILI either in the past or at the time of sample collection from hospitals throughout the UK (Daly et al., 2009). In particular, patients who have suffered DILI linked to anti-TB drugs, co-amoxiclav and flucloxacillin are being studied. When the study was initiated in 2004, the aim was to collect samples from 300 cases of DILI linked to anti-TB drugs. However, up to September 2009, only 28 cases linked to anti-TB drugs had been enrolled which is poor compared with approximately 150 cases linked to flucloxacillin, co-amoxiclav and, more recently, other prescribed drugs. Among these 28 cases, a number of different ethnicities were represented, including 14 white European, 3 Chinese, 2 African and 9 from the Indian subcontinent. The patients were taking a number of different drug combinations for their TB, but for all except for one patient of European origin, this included INH. An additional 4 cases of Bangladeshi origin were recruited by Dr Abul Hasnat, University of Dhaka, Bangladesh. All had been exposed to isoniazid. All cases met one of the following biochemical criteria for enrolment into this study: (a) alanine aminotransferase (ALT) > 5 x the upper limit of normal (ULN), (b) alkaline phosphatase (ALP) > 2 x ULN and bilirubin > ULN, or (c) clinical jaundice or bilirubin > 40µmol/l. For the DILIGEN cases, causality assessment was based on the biochemical markers and Roussel Uclaf Causality Assessment Method (RUCAM) (Danan and Benichou, 1993). The causality assessment was performed using the international consensus criteria (ICC) with ICC scoring graded as unlikely, possible, probable and highly probable (see section 3.3.1). Only cases assessed as highly probable, probable or possible were enrolled in the study. For the Dhaka samples, causality assessment was not possible but other causes of liver damage such as hepatitis A or B infection were excluded. Ethical approval for the DILIGEN study was provided by the Leeds East Research Ethics committee with ethical approval in Bangladesh provided by the University of Dhaka.

It was decided to study the 13 white European cases exposed to isoniazid, the 9 DILIGEN cases from the Indian subcontinent and the 4 Bangladeshi cases in a case-control study on NAT2 and other genotypes. As controls, 50 controls of European ancestry were supplied by Dr Pete Donaldson (Velaga et al., 2004) together with 81

ATD-tolerant controls and 40 controls without TB from the Indian subcontinent. **Table 3.1** summarises clinical information on the cases from the Indian subcontinent and of European ethnic origin. The African and Chinese cases were not studied in the case control study but sequencing studies were performed on one African patient who underwent a liver transplant.

Table 3.1 Clinical and biochemical parameters of DILI patients exposed to INH

	European cohort	South Asian cohort	
	DILIGEN (n=13)	DILIGEN (n=9)	BANGLADESH (n=4)
Sex (F/M)	8/5	7/2	1/3
Age of onset (years)	58.8 ± 12.5	39.3 ± 14.3	46 ± 4.5
Time to onset (days)	32.4 ± 37.4	52.75 ± 61.8 *	Data not available
Total days on drug	38.8 ± 35.9	60.25 ± 74.0 *	Data not available
Histology patterns			
Cholestatic	3 (23.08%)	6	Data not available
Hepatocellular	10 (76.92%)	2	
ICC scoring			
3-5 (possible)	5 (38.46)		
6-8 (probable)	5 (38.46)		Data not available
>8 (highly probable)	3 (23.08)		
Peak Bilirubin (µmol/l)	130 ± 110.0	179 ± 252.7 *	83.4 ± 19.5
Peak ALT (U/l)	937 ± 1001.0	793 ± 488.8 *	Data not available
Peak ALP (U/l)	219 ± 98.0	225 ± 146.0 *	Data not available
Liver transplant	2 (15.38%)	3 (33.33%)	0

* Average of the values from 8 samples as the clinical data of 1 patient was not available for this study

3.2.2 PCR-restriction fragment length polymorphism (PCR-RFLP)

PCR reactions were carried out according to section 2.4.4. RFLP analyses were developed for a range of polymorphisms by using specific restriction endonuclease enzymes (New England Biolabs) and the restriction fragments were separated by electrophoresis on either 2% agarose gels or 10% polyacrylamide gels as described in section 2.4.5.

3.2.3 Genotyping of *NAT2*

The amplification of *NAT2* fragment in the region of exon 2 was performed by PCR with 2 previously reported primers (Kocabas et al., 2004). The sequences of the primers were 5'-GACATTGAAGCATATTTTGAAAG-3' and 5'-GATGAAAGTATTTGATGTTAGG-3'. The PCR program consisted of initial denaturation at 94°C for 5 min and 35 cycles of denaturation at 94°C for 1 min, annealing at 50°C for 1.5 min, extension at 72°C for 2 min, and a final extension at 72°C for 7 min. The 999bp PCR product was digested with KpnI, TaqI, and BamHI for the detection of mutations 481C>T (rs1799929), 590G>A (rs1799930), and 857G>A (rs1799931) respectively (**Figure 3.1-3.3**). The wild-type *NAT2**4 allele is designated when none of the mutant alleles are present. *NAT2**5, *NAT**6 and *NAT**7 variant alleles were identified by KpnI, TaqI and BamHI digestions respectively. The presence of any 2 variant alleles defines the slow-acetylator phenotype, whereas rapid acetylators have 1 or 2 wild-type *NAT2**4 alleles. In addition, a genetic variant in the promoter region of *NAT2* (-9796T>A; rs4646244) which has shown a significant lower luciferase activity in reporter gene assays was included in the current study (Kim et al., 2009). Amplification of the -9796T>A promoter region was performed using the primers 5'-AATCCCAGTAGACAACACCAG-3' and 5'-AATAGGTTTTGAGGGCCATG-3'. PCR was subjected to initial denaturation at 94°C for 5 min and 35 cycles of denaturation at 94°C for 1 min, annealing at 54°C for 1 min, extension at 72°C for 1 min, and a final extension at 72°C for 7 min. The 469bp PCR product was then digested with restriction enzyme MboI resulting in fragments of 277bp and 192bp (A allele; cut) or 467bp (T allele; uncut). **Figure 3.4** shows the detection of the MboI restriction fragments of *NAT2* -9796T>A on a 2% agarose gel. For selected samples, the *NAT2* coding region was sequenced. The same PCR reaction used for genotyping was performed with sequencing carried out as described in section 2.4.5.

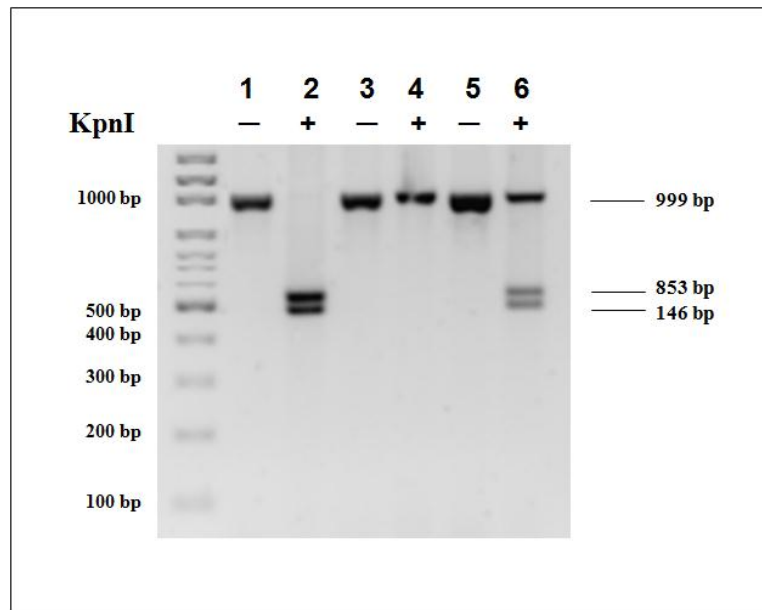


Figure 3.1 PCR-RFLP analysis of NAT2*5 (481C>T) polymorphism

*Restriction analysis for NAT2*5 (481C>T) gene fragment after digestion with KpnI on a 2% agarose gel; lane 1 and 2 [without (–) and with (+) KpnI digestion] display homozygous CC; lane 3 and 4 [without (–) and with (+) KpnI digestion] are homozygous TT; lane 5 and 6 [without (–) and with (+) KpnI digestion] are heterozygous CT*

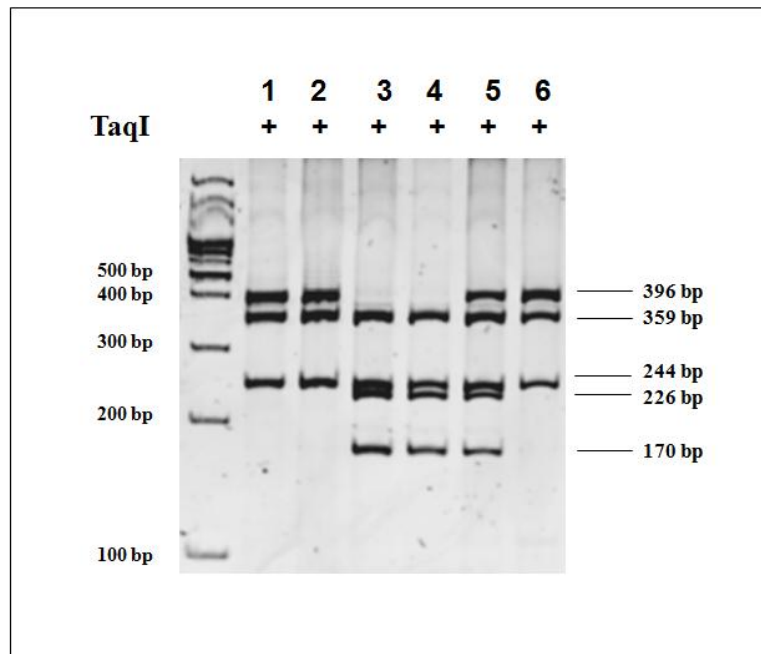


Figure 3.2 PCR-RFLP analysis of NAT2*6 (590G>A) polymorphism

*Restriction analysis for NAT2*6 (590G>A) gene fragment after digestion with TaqI on a 10% Polyacrylamide gel; lane 1, 2 and 6 display homozygous AA; lane 3 and 4 are homozygous GG; lane 5 are heterozygous GA*

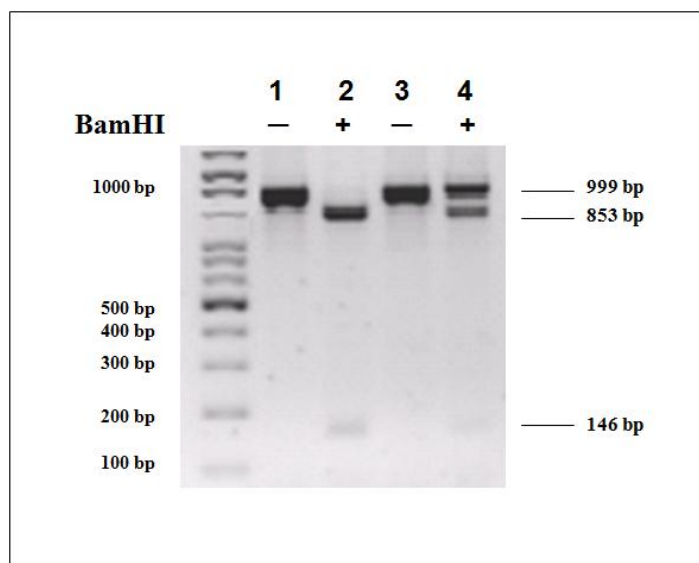


Figure 3.3 PCR-RFLP analysis of *NAT27(857G>A) polymorphism**

*Restriction analysis for *NAT2**7(857G>A) gene fragment after digestion with *Bam*HI on a 2% agarose gel; lane 1 and 2 [without (–) and with (+) *Bam*HI digestion] display homozygous GG; lane 3 and 4 [without (–) and with (+) *Bam*HI digestion] are heterozygous GA*

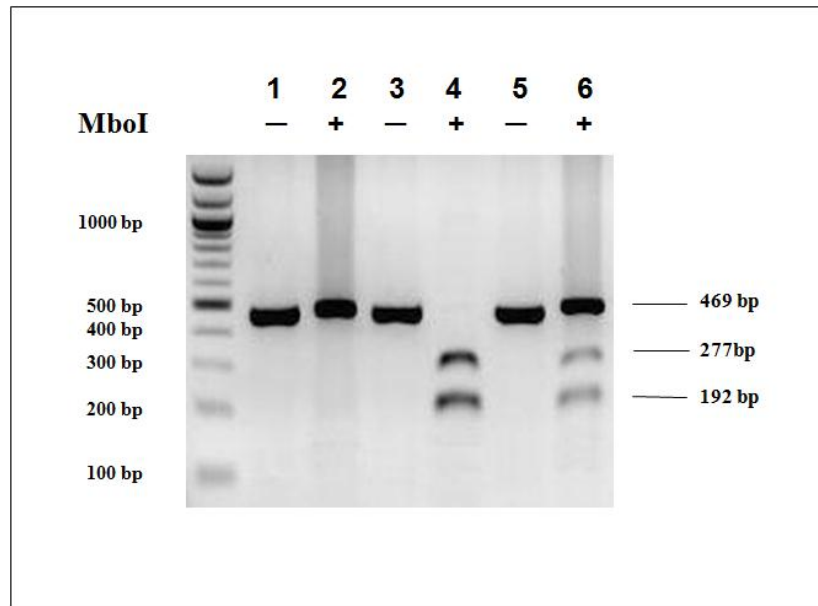


Figure 3.4 PCR-RFLP analysis of NAT2 (rs4646244)

Restriction analysis for NAT2 (rs4646244) gene fragment after digestion with MboI on a 2% agarose gel; lane 1 and 2 [without (-) and with (+) MboI digestion] display homozygous TT; lane 3 and 4 [without (-) and with (+) MboI digestion] are homozygous AA; lane 5 and 6 [without (-) and with (+) MboI digestion] are heterozygous TA

3.2.4 Genotyping of *CYP2E1*

For *CYP2E1* genotyping, 3 SNPs from the promoter region -1293G>C (CYP2E1*5B), -1053C>T (CYP2E1*5B) and -71G>T (CYP2E1*7B), and 1 SNP from the intron 7 9896C>G (CYP2E1*1B) were **genotyped using the** PCR-RFLP method (see section 3.2.3). **Figure 3.5** and **Table 3.2** show the position of the 4 SNPs on the positive strand of the gene and also their respective PCR-RFLP conditions. For -1293G>C (CYP2E1*5B) genotyping, PCR product was digested with *Pst*I resulting in fragments of 413bp (G allele; uncut) or 295bp and 118bp (C allele; cut) (**Figure 3.6**). For -1053C>T (CYP2E1*5B) analysis, PCR product was digested with *Rsa*I to differentiate the C→T polymorphism. The wild type C allele produced two fragments of 352bp and 61bp, whilst T alleles yielded one single fragment of 413bp (**Figure 3.7**). Analysis of -71G>T (CYP2E1*7B) polymorphism was performed by digesting the PCR product with *Dde*I. Fragments of 212bp and 163bp (G allele; cut) or 375bp (T allele; uncut) were identified following gel electrophoresis analysis (**Figure 3.8**). For 9896C>G (CYP2E1*1B) analysis, a 444bp PCR product was amplified and digested with *Taq*I. The common C allele was identified from its two fragments on 273bp and 171bp, whilst G allele remains uncut (**Figure 3.9**).

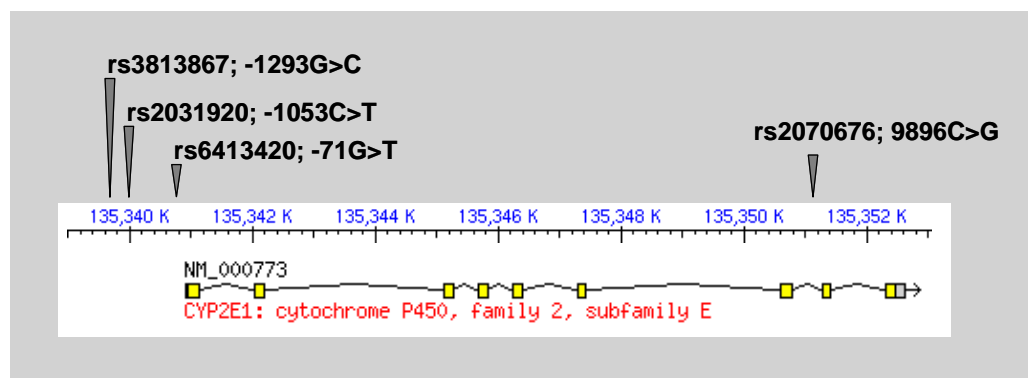


Figure 3.5 The position of four studied SNPs in *CYP2E1*

Table 3.2 Description of *CYP2E1* alleles and their PCR-RFLP conditions

Alleles	Location	Nucleotide change	Rs identifier	Primer sequences	Expected size	Annealing Temperature	Restriction enzyme
CYP2E1*5B	Promoter	-1293G>C	rs3813867	5' CCAGTCGAGTCTACATTGTCA 3' 5' TTCATTCTGTCTTCTAACTGG 3'	413 bp	51 °C	<i>Pst</i> I
CYP2E1*5B	Promoter	-1053C>T	rs2031920	5' CCAGTCGAGTCTACATTGTCA 3' 5' TTCATTCTGTCTTCTAACTGG 3'	413 bp	51 °C	<i>Rsa</i> I
CYP2E1*7B	Promoter	-71G>T	rs6413420	5' CACAGTCCAACCTCCATCCTC 3' 5' GAAGAGGTTCCCGATGATGG 3'	375 bp	57 °C	<i>Dde</i> I
CYP2E1*1B	Intron 7	9896C>G	rs2070676	5' AAGAGCCTCAGCAGATAGTG 3' 5' TGATCTTTCTCACCTGTGGA 3'	444 bp	51 °C	<i>Taq</i> I

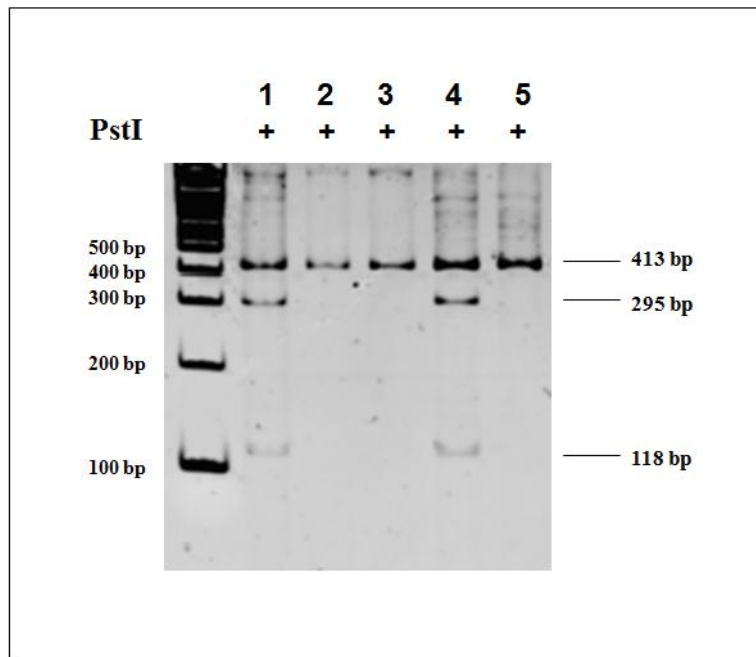


Figure 3.6 PCR-RFLP analysis of *CYP2E1* -1293G>C (rs3813867)

Restriction analysis for CYP2E1 -1293G>C (rs3813867) gene fragment after digestion with PstI on a 10% Polyacrylamide gel; lane 2, 3 and 5 display homozygous GG; lane 1 and 4 are heterozygous GC

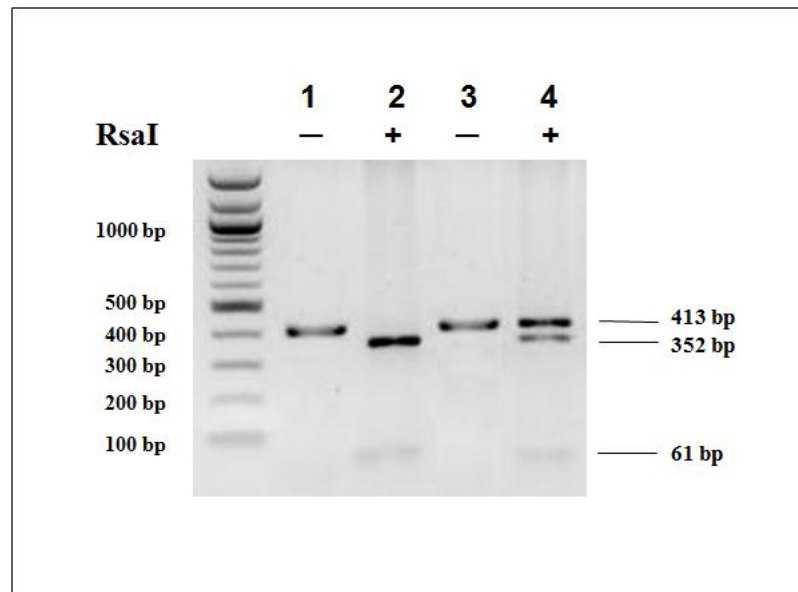


Figure 3.7 PCR-RFLP analysis of *CYP2E1* (rs2031920)

Restriction analysis for CYP2E1 (rs2031920) gene fragment after digestion with RsaI on a 2% agarose gel; lane 1 and 2 [without (–) and with (+) RsaI digestion] display homozygous CC; lane 3 and 4 [without (–) and with (+) RsaI digestion] are heterozygous CT

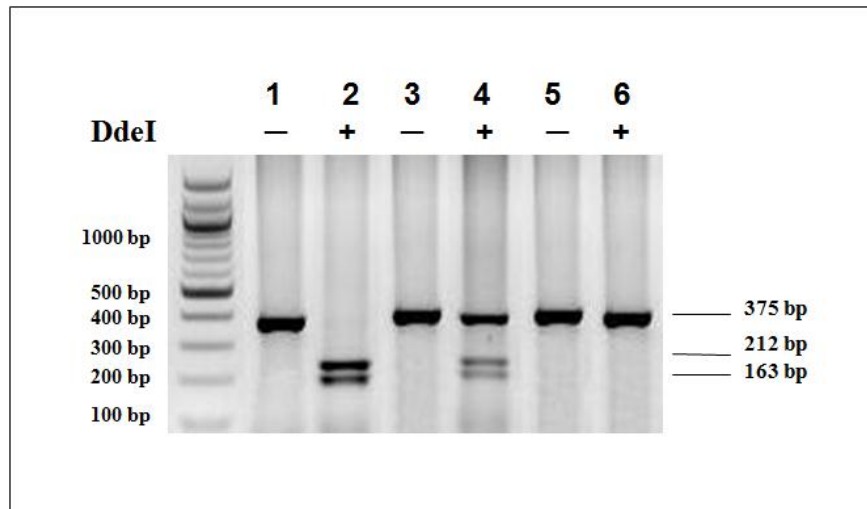


Figure 3.8 PCR-RFLP analysis of *CYP2E1* (rs6413420)

Restriction analysis for CYP2E1 (rs6413420) gene fragment after digestion with DdeI on a 2% agarose gel; lane 1 and 2 [without (–) and with (+) DdeI digestion] display homozygous GG; lane 3 and 4 [without (–) and with (+) DdeI digestion] are heterozygous GT; lane 5 and 6 [without (–) and with (+) DdeI digestion] are homozygous TT

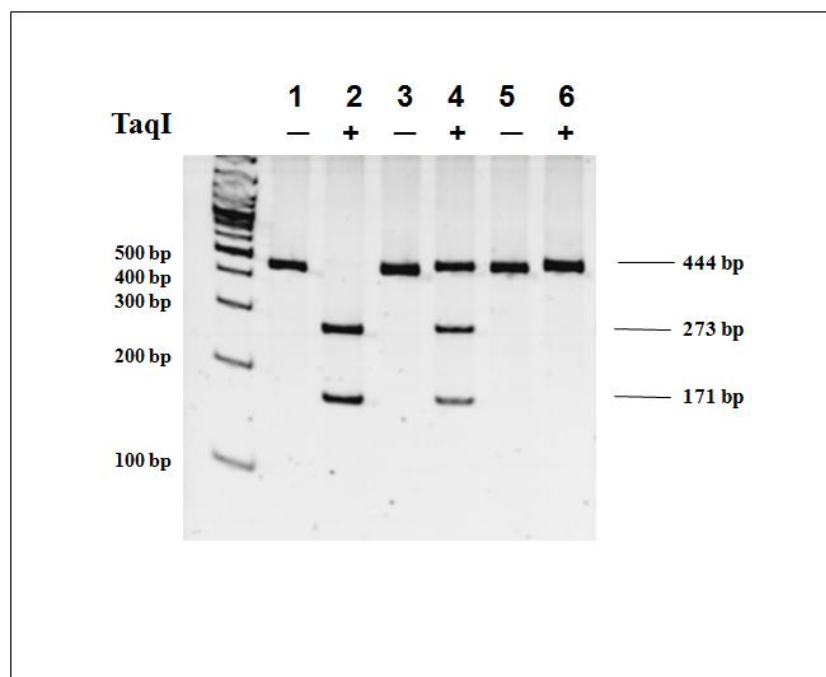


Figure 3.9 PCR-RFLP analysis of *CYP2E1* (rs2070676)

Restriction analysis for Cyp2E1 (rs2070676) gene fragment after digestion with TaqI on a 10% Polyacrylamide gel; lane 1 and 2 [without (–) and with (+) TaqI digestion] display homozygous CC; lane 3 and 4 [without (–) and with (+) TaqI digestion] are heterozygous CG; lane 5 and 6 [without (–) and with (+) TaqI digestion] are homozygous GG

3.2.5 *PXR* -25385 SNP genotyping

Analysis of *PXR* -25385C>T polymorphism (rs3814055) was performed by the approach of primer-engineered RFLP detection described in Andrews et al. (Andrews et al.). The sequences of the forward and the reverse primers used for PCR amplification were 5'-TTTTTTGGCAATCCCAGGAT-3' and 5'-CGAATGTGGTGGATACCAG-3'. An *Mbo*I restriction site was engineered by a nucleotide substitution (T→A) in the forward primer to allow RFLP analysis. PCR was subjected to initial denaturation at 94°C for 5 min and 35 cycles of denaturation at 94°C for 1 min, annealing at 51°C for 1 min, extension at 72°C for 1 min, and a final extension at 72°C for 7 min. PCR product was digested with *Mbo*I resulting in fragments of 220bp (T allele; uncut) or 200bp and 16bp (C allele; cut). **Figure 3.10** shows the 10% polyacrylamide gel electrophoresis of the *Mbo*I digestion products.

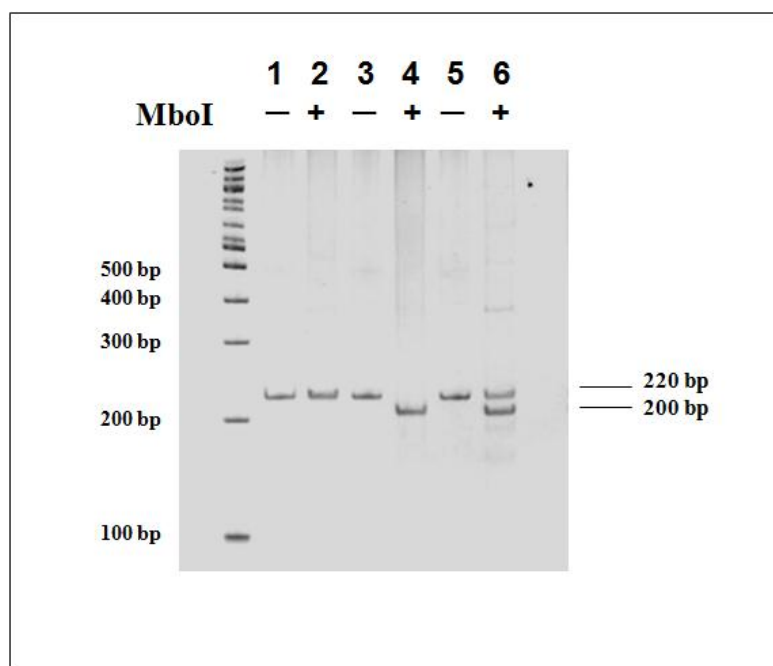


Figure 3.10 PCR-RFLP analysis of PXR-25385 C/T (rs3814055)

Restriction analysis for PXR-25385 C/T (rs3814055) gene fragment after digestion with MboI on a 10% Polyacrylamide gel; lane 1 and 2 [without (−) and with (+) MboI digestion] display homozygous TT; lane 3 and 4 [without (−) and with (+) MboI digestion] are homozygous CC; lane 5 and 6 [without (−) and with (+) MboI digestion] are heterozygous CT

3.2.6.2 *GSTA4*

Tag SNPs in the *GSTA4* gene region were chosen using the Hapmap database (<http://www.hapmap.org>) and Haploview (<http://www.broad.mit.edu/mpg/haploview>). Haploview was used to generate the linkage disequilibrium (LD) plot patterns as shown in **Figure 3.12**, and the tag SNPs were selected using Tagger with a pairwise tagging algorithm with a minor allele frequency (MAF) ≥ 0.08 and an $r^2 \geq 0.8$. Five tag SNPs, rs316141, rs4147618, rs316128, rs3756980 and rs13207376, which cover most of the genetic variation in the *GSTA4* were selected and **genotyped using the** PCR-RFLP method (see section 3.2.3). The position of the SNPs and their PCR-RFLP assay conditions are summarised in **Table 3.3**. For rs316141 genotyping, a 329bp PCR product was digested with restriction enzyme Msp1 resulting in fragments of 164bp and 165bp (C allele; cut), or 329bp (T allele; uncut) (**Figure 3.13**). RFLP analysis of a T→A polymorphism in rs4147618 was performed by digesting the PCR product with HinfI. Fragments of 216bp and 74bp (T allele; cut) or 290bp (A allele; uncut) were identified following gel electrophoresis analysis (**Figure 3.14**). For rs316128 genotyping, PCR product was digested with Bpu10I. The wild type A allele yielded one single fragment of 268bp, whilst C allele produced two fragments of 177bp and 91bp (**Figure 3.15**). Genotyping of rs3756980 was done by digesting the 218bp PCR product with HpyCH4III resulting in fragments of 218bp (A allele; uncut) or 183bp and 35bp (G allele; cut). **Figure 3.16** shows the restriction enzyme digestion products on 10% Polyacrylamide gel. Analysis of rs13207376 was performed by digesting the PCR product with HpyCH4IV. Fragments of 122bp and 119bp (G allele; cut) or 241bp (A allele; uncut) were identified following agarose gel electrophoresis analysis (**Figure 3.17**).

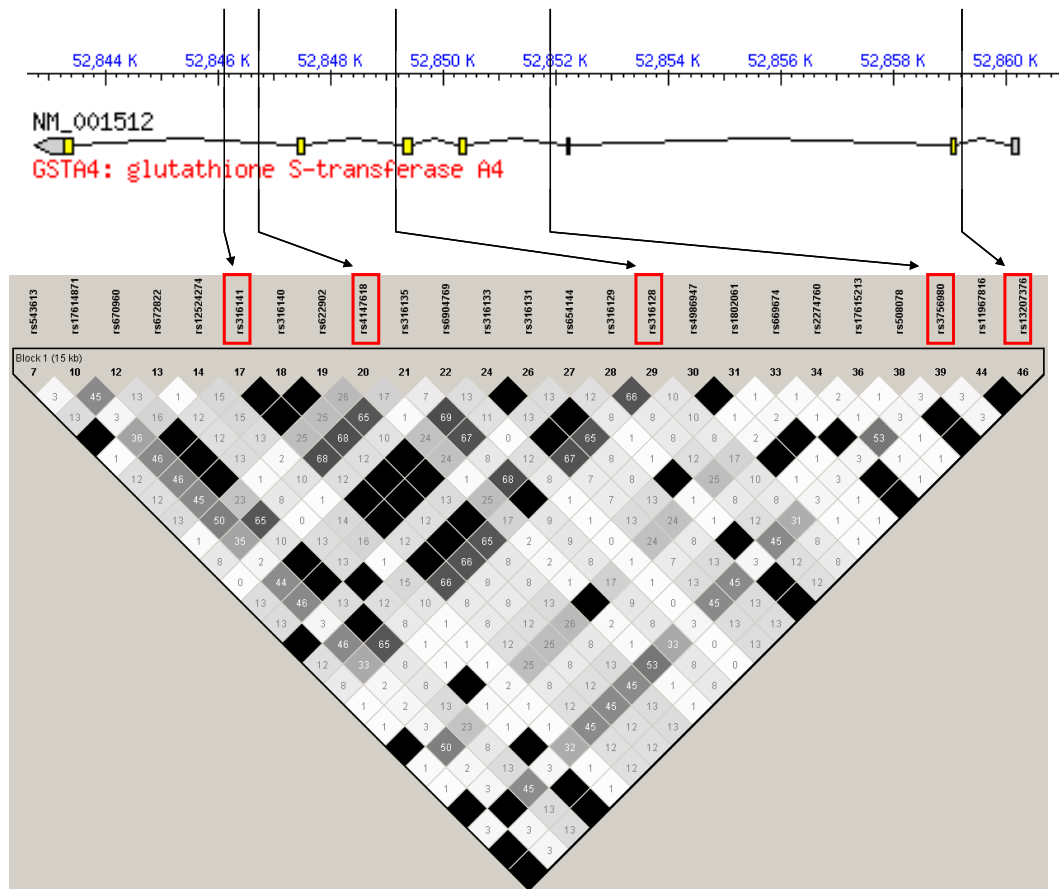


Figure 3.12 LD plot of *GSTA4* tag SNPs and their position in the gene

GSTA4 tag SNPs are displayed according to their position on the positive strand of the gene. The r^2 pairwise LD plot and its values were generated using Haploview 4.2 software with its standard R-squared colour scheme. The intensity of the colour is proportional to the strength of the LD. Five tag SNPs ($r^2 \geq 0.8$; $MAF \geq 0.08$) out of a total of 25 reference SNPs, rs316141, rs4147618, rs316128, rs3756980, and rs13207376, which cover most of the genetic variation in the *GSTA4* were selected for analysis.

Table 3.3 PCR-RFLP primer sequences and conditions of *GSTA4* tag SNPs

Rs identifier	Location	Chromosome position	Alleles	Primer sequences	Expected size	Annealing Temperature	Restriction enzyme
rs316141	Intron 1	52846158	C/T	5'-CATTGGTACAAAGCCATGC-3' 5'-TGTACTIONATTGAACTGGTGG-3'	329 bp	56 °C	<i>MspI</i>
rs4147618	Intron 1	52846742	T/A	5'- AAGTTAGGAAATTCTAAGCC-3' 5'-AAACTCAAGCATCCACTGCC-3'	292 bp	51 °C	<i>HinfI</i>
rs316128	Intron 2	52849146	A/C	5'-GGAAGTGGTTAACATGGCCC-3' 5'-CTGAATCATGTGGTCCTAGC-3'	269 bp	57 °C	<i>Bpu10I</i>
rs3756980	Intron 4	52851979	A/G	5'- GTTGAAATTGCCAGGAAATCAC-3' 5'-CCAGGATGCCTCAGATAGTG-3'	218 bp	55 °C	<i>HpyCH4III</i>
rs13207376	Intron 6	52859230	A/G	5'-GTCTTCAACCCAGTGCTCA-3' 5'-ATTTGTGAAATCCCGTACTG-3'	241 bp	56 °C	<i>HpyCH4IV</i>

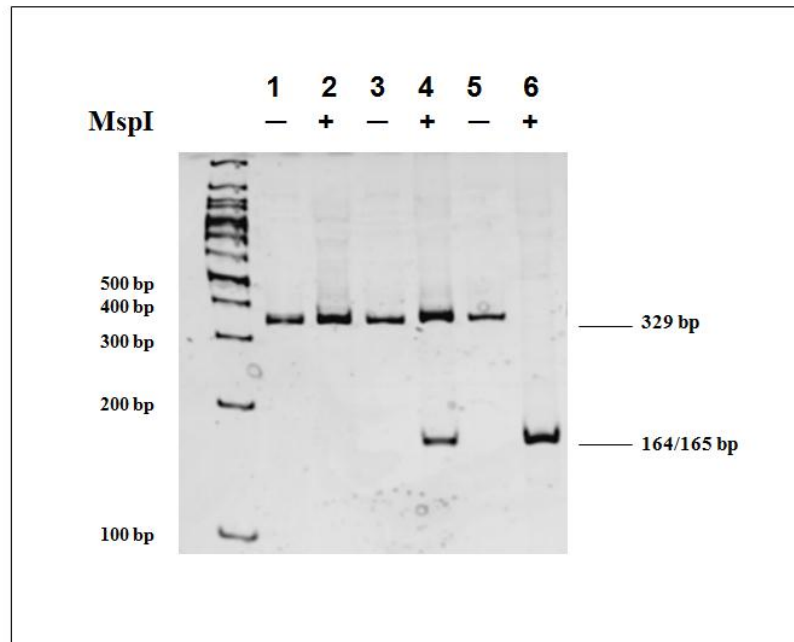


Figure 3.13 PCR-RFLP analysis of GSTA4 (rs316141)

Restriction analysis for GSTA4 (rs316141) gene fragment after digestion with MspI on a 10% Polyacrylamide gel; lane 1 and 2 [without (–) and with (+) MspI digestion] display homozygous TT; lane 3 and 4 [without (–) and with (+) MspI digestion] are heterozygous CT; lane 5 and 6 [without (–) and with (+) MspI digestion] are homozygous CC

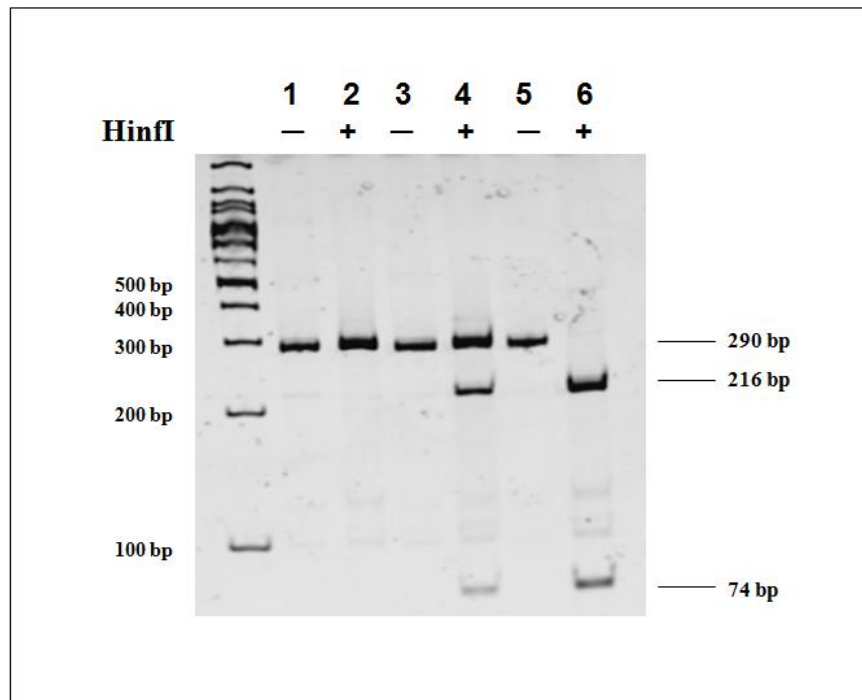


Figure 3.14 PCR-RFLP analysis of GSTA4 (rs4147618)

Restriction analysis for GSTA4 (rs4147618) gene fragment after digestion with HinfI on a 10% Polyacrylamide gel; lane 1 and 2 [without (-) and with (+) HinfI digestion] display homozygous AA; lane 3 and 4 [without (-) and with (+) HinfI digestion] are heterozygous TA; lane 5 and 6 [without (-) and with (+) HinfI digestion] are homozygous TT

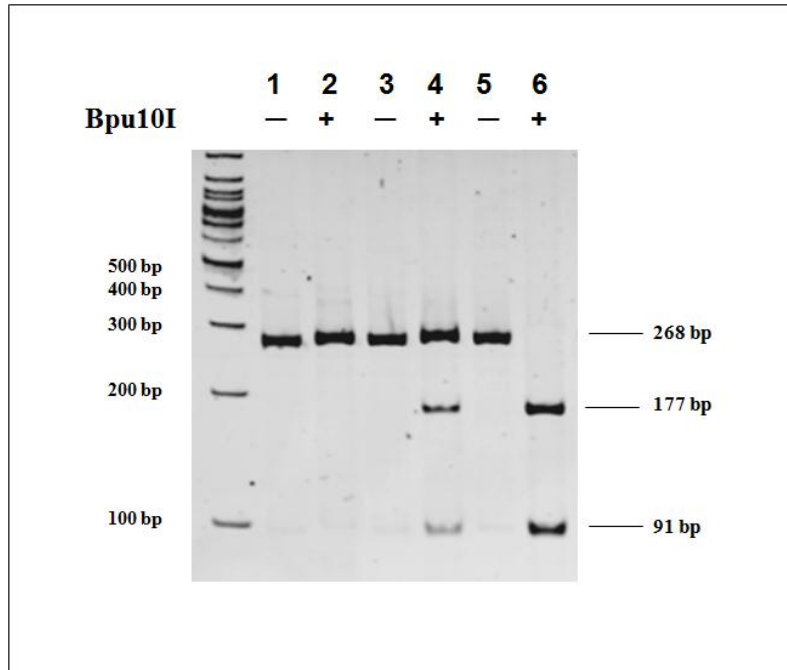


Figure 3.15 PCR-RFLP analysis of GSTA4 (rs316128)

Restriction analysis for GSTA4 (rs316128) gene fragment after digestion with Bpu10I on a 10% Polyacrylamide gel; lane 1 and 2 [without (−) and with (+) Bpu10I digestion] display homozygous AA; lane 3 and 4 [without (−) and with (+) Bpu10I digestion] are heterozygous AC; lane 5 and 6 [without (−) and with (+) Bpu10I digestion] are homozygous CC.

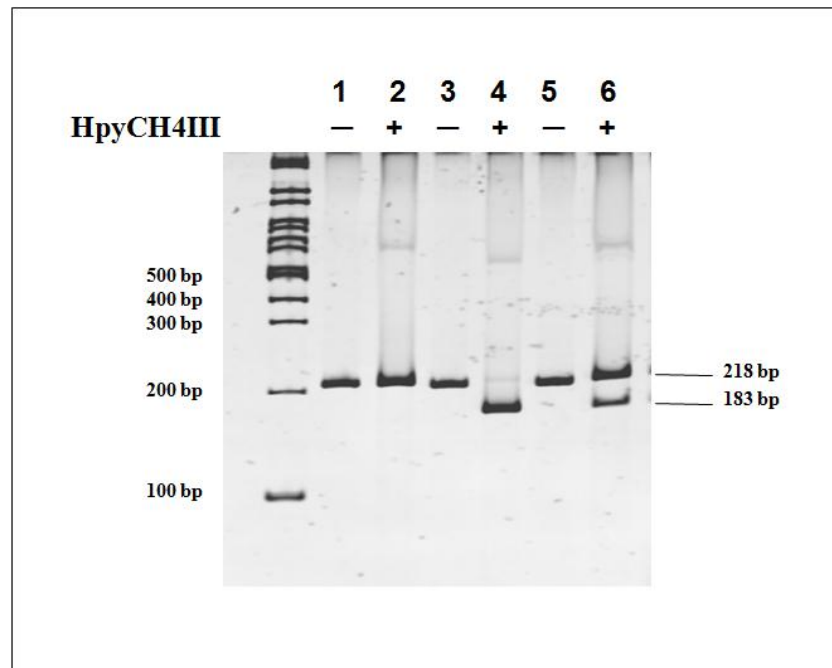


Figure 3.16 PCR-RFLP analysis of GSTA4 (rs3756980)

Restriction analysis for GSTA4 (rs3756980) gene fragment after digestion with HpyCH4III on a 10% Polyacrylamide gel; lane 1 and 2 [without (–) and with (+) HpyCH4III digestion] display homozygous AA; lane 3 and 4 [without (–) and with (+) HpyCH4III digestion] are homozygous GG; lane 5 and 6 [without (–) and with (+) HpyCH4III digestion] are heterozygous AG.

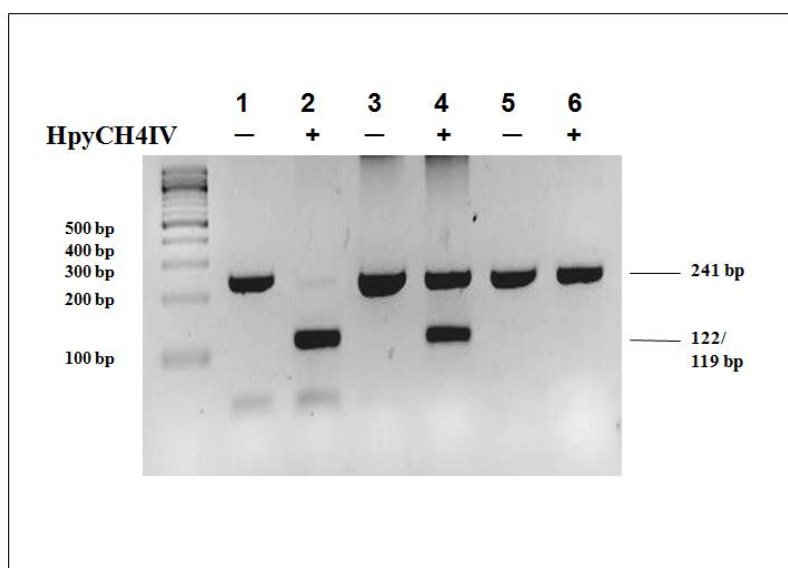


Figure 3.17 PCR-RFLP analysis of GSTA4 (rs13207376)

Restriction analysis for GSTA4 (rs13207376) gene fragment after digestion with HpyCH4IV on a 2% agarose gel; lane 1 and 2 [without (–) and with (+) HpyCH4IV digestion] display homozygous GG; lane 3 and 4 [without (–) and with (+) HpyCH4IV digestion] are heterozygous AG; lane 5 and 6 [without (–) and with (+) HpyCH4IV digestion] are homozygous AA

3.2.6.3 *GSTT1*

Analysis of *GSTT1* gene polymorphism was performed by PCR described in Abdel-Rahman et al. using primers 5'-TTCCTTACTGGTCCTCACATCTC-3' and 5'-TCACCGGATCATGGCCAGCA-3' (Abdel-Rahman et al., 1998). The promoter region of gene encoding tumour necrosis factor-alpha (*TNF- α*) was co-amplified and used as an internal control with the primers 5'-ATCTGGAGGAAGCGGTAGTG-3' and 5'-AATAGGTT TTGAGGGCCATG-3'. PCR was subjected to initial denaturation at 94°C for 5 min and 35 cycles of denaturation at 94°C for 1 min, annealing at 50°C for 1 min, extension at 72°C for 1 min, and a final extension at 72°C for 7 min. *GSTT1* null genotypes were detected by the absence of 430bp DNA fragment, while the internal positive control (*TNF- α*) yielded a band of 222bp (**Figure 3.18**).

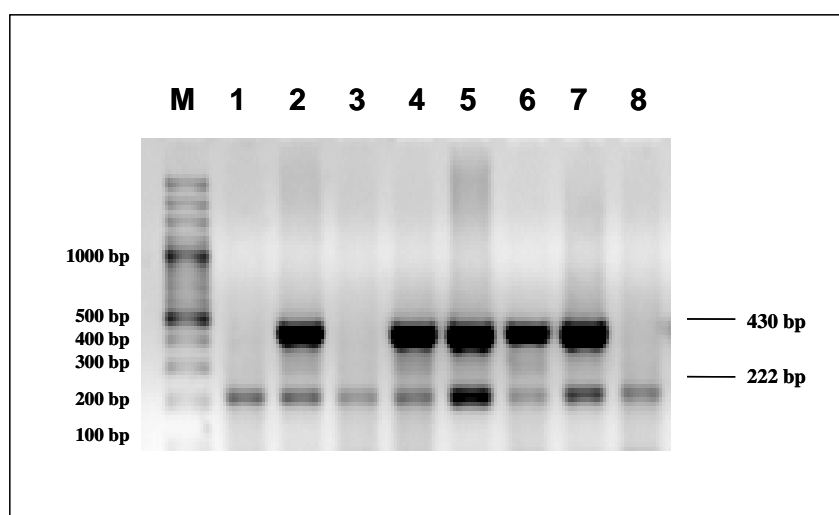


Figure 3.18 PCR analysis of *GSTT1* genotype

*The presence of *GSTT1* gene was detected by the presence of a 430bp PCR fragment (lane 2, 4, 5, 6, and 7). Lane 1, 3 and 8 show the *GSTT1* null genotype (the absence of the 430bp fragment). Fragments of 222bp indicate the internal controls for *TNF- α* .*

3.2.6.4 *GSTM1*

Analysis of *GSTM1* gene polymorphism was performed by PCR described in Zhong *et al.* using primers 5'-CGCCATCTTGTGCTACATTGCCCG-3' and 5'-TTCTGGATTGTAGCAGATCA-3' (Zhong *et al.*, 1993). For an internal control, *GSTM4* gene fragment was co-amplified using the primers 5'-CGCCATCTTGTGCTACATTGCCCG-3' and 5'-ATCTTCTCCTCTTCTGTCTC-3'. PCR was subjected to initial denaturation at 94°C for 5 min and 35 cycles of denaturation at 94°C for 1 min, annealing at 53°C for 1 min, extension at 72°C for 1 min, and a final extension at 72°C for 7 min. *GSTM1* null genotypes were detected by the absence of 230bp DNA fragment, while the internal positive control (*GSTM1*) yielded a band of 157bp (**Figure 3.19**).

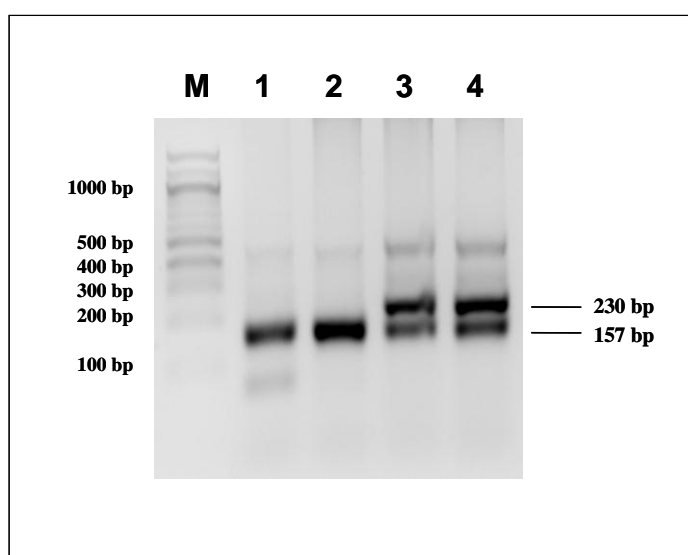


Figure 3.19 PCR analysis of *GSTM1* genotype

The presence of GSTM1 gene was detected by the presence of a 230bp PCR fragment (lane 3 and 4). Lane 1 and 2 show the GSTM1 null genotype (the absence of the 230bp fragment). Fragments of 157bp indicate the internal controls for GSTM1.

3.2.6.5 *SOD2*

Tag SNPs in *SOD2* ($r^2 \geq 0.8$; $MAF \geq 0.08$) were selected from HapMap CEU population and the Linkage disequilibrium (LD) calculation was performed by the Haploview software (**Figure 3.20**). Two tag SNPs, rs4880 and rs**5746136** **which encompass the majority of the genetic variation in SOD2 were identified and genotyped using the PCR-RFLP method.** PCR for rs4880 was performed using the primers 5'-CAGCCCAGCCTGCGTAGACGG-3' and 5'-GCGTTGATGTGAGGTTCCAG-3'. A 172bp PCR product was then digested with restriction enzyme *BsaW1* to identify the common T→C polymorphism resulting in an amino acid substitution (Valine to Alanine). The T allele (Val) resulted in fragments of 89bp and 83bp, whilst the C allele (Ala) remain uncut, which is 172bp (**Figure 3.21**). For rs5746136, a 534bp PCR product was amplified using the primers 5'-AGTAAGCTGCTCTATTGTAGC-3' and 5'-TTTGCTGTTGAAGTTTGCCT-3', followed by restriction digestion with *TaqI* resulting in fragments of 534bp (A allele; uncut) or 364bp and 170bp (G allele; cut). **Figure 3.22** shows the agarose gel electrophoresis of the restriction enzyme digestion products.

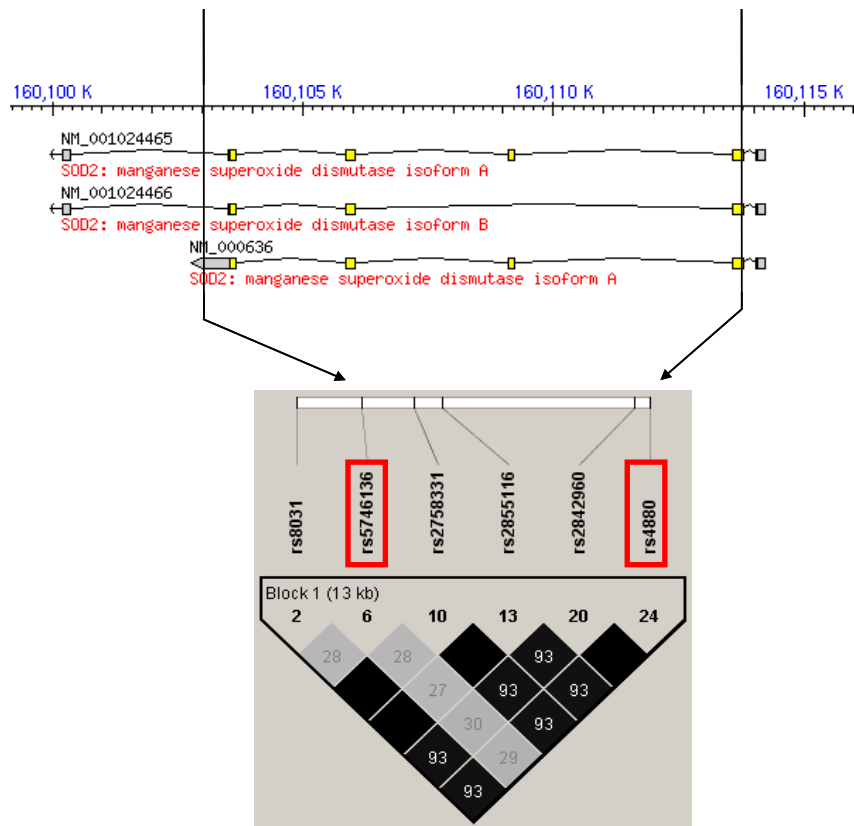


Figure 3.20 LD plot of SOD2 tag SNPs and their position in the gene

SOD2 tag SNPs are displayed according to their position on the positive strand of the gene. The r^2 pairwise LD plot and its values were generated using Haploview 4.2 software with its standard R-squared colour scheme. Two SNPs out of a total of 6 reference SNPs, rs4880 and rs5746136, which encompass the majority of the genetic variation in the SOD2 were selected for analysis.

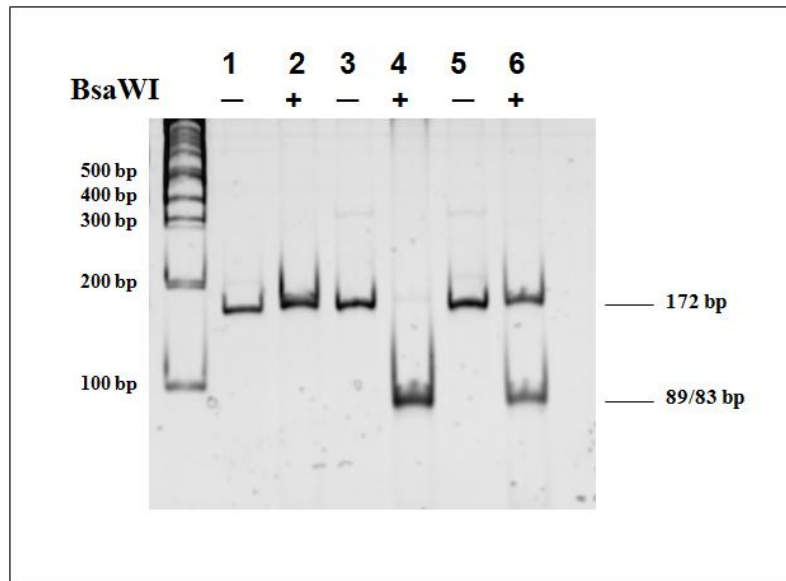


Figure 3.21 PCR-RFLP analysis of *SOD2* V16A (rs4880)

Restriction analysis for SOD2 V16A (rs4880) gene fragment after digestion with BsaWI on a 10% Polyacrylamide gel; lane 1 and 2 [without (–) and with (+) BsaWI digestion] display homozygous Ala/Ala (CC); lane 3 and 4 [without (–) and with (+) BsaWI digestion] are homozygous Val/Val (TT); lane 5 and 6 [without (–) and with (+) BsaWI digestion] are heterozygous Val/Ala (TC)

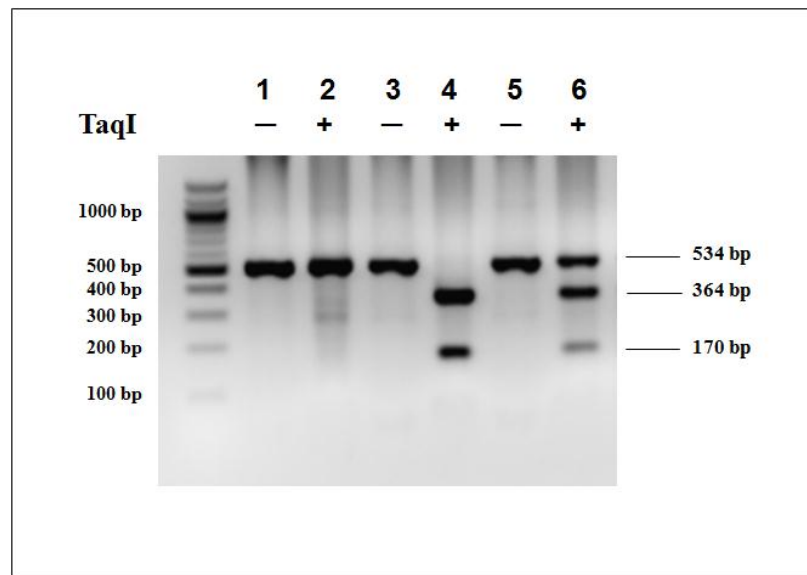


Figure 3.22 PCR-RFLP analysis of *SOD2* (rs5746136)

Restriction analysis for SOD2 (rs5746136) gene fragment after digestion with TaqI on a 2% agarose gel; lane 1 and 2 [without (–) and with (+) TaqI digestion] display homozygous AA; lane 3 and 4 [without (–) and with (+) TaqI digestion] are homozygous GG; lane 5 and 6 [without (–) and with (+) TaqI digestion] are heterozygous GA

3.2.7 Taqman SNP genotyping assay for NAT1 (rs2739685)

Genotyping for a C/T polymorphism in rs2739685 was carried out using the validated Taqman SNP genotyping assay method (assay ID: C__15930238_10, PE Applied Biosystems). The assay contains two probes, one for each allele in a two-allele system. Each probe consists of oligonucleotides for amplifying the specific sequence with a 5'-end fluorescence reporter dye. Specifically, the VIC fluorescence reporter dye is linked to the allele 1 probe for the detection of allele C. FAM, another fluorescence reporter dye, is linked to the allele 2 probe for the detection of allele T. The reactions were prepared in duplicate by using 2x Taqman Universal Master Mix, 40x SNP Genotyping Assay Mix, DNase-free water, and 10ng genomic DNA in a final volume of 20µl per reaction. Positive controls and a no template control were included in each assay as a quality control measure. The positive controls consist of three different genotypes were validated by sequencing (**Figure 3.23**). The PCR amplification was done using the ABI Prism 7000 Sequence Detection System machine under the following thermocycler conditions: 10 min at 95°C to activate the AmpliTaq Gold polymerase followed by 40 cycles of denaturation at 95 °C for 15s and annealing/extension at 60 °C for 1 min. The allelic discrimination results were determined using the SDS 2.2 software after the amplification by performing an end-point read.

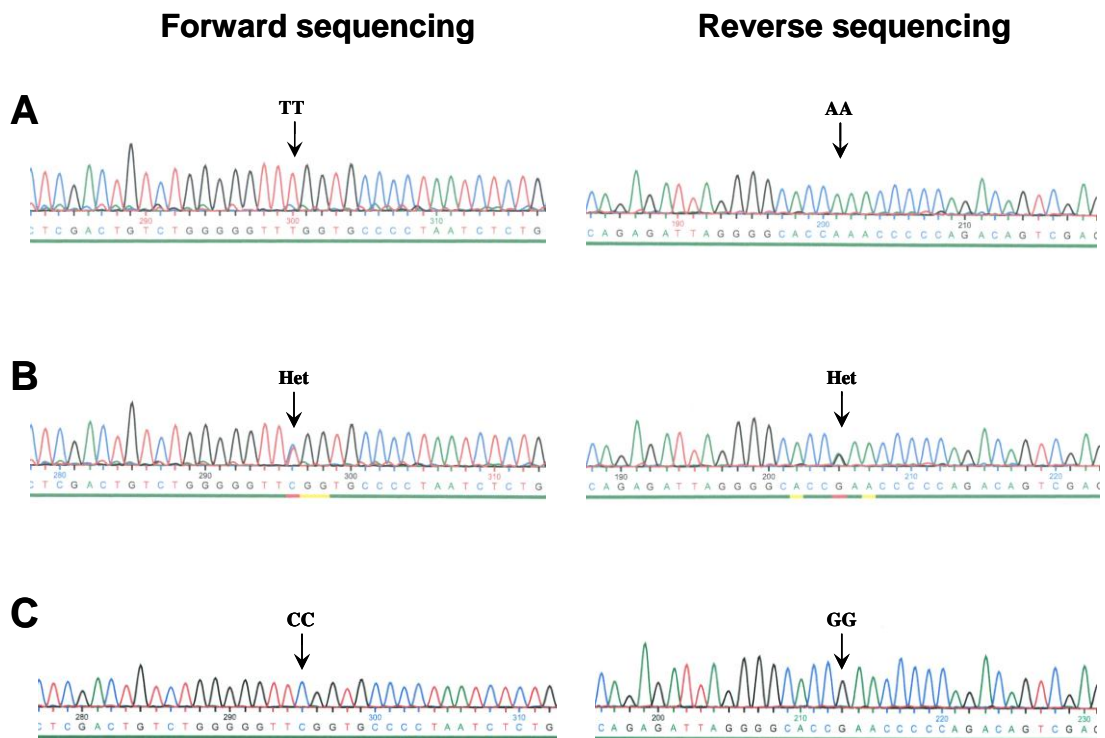


Figure 3.23 Sequence electropherogram of the forward and reverse sequence traces from a C/T polymorphism in SNP rs2739685 in *NAT1*

Sequencing trace for SNP rs2739685 TT homozygote, TC heterozygote and CC homozygote positive controls are shown in A, B, C respectively in both forward and reverse sequence orientations.

3.2.8 Statistical analysis

3.2.8.1 Power Calculations

Using an online statistical power calculator (<http://statpages.org/proppowr.html>), a power calculation was performed for the NAT2 polymorphism based on the number of samples available before the genotyping studies were initiated. The use of 26 cases and 90 controls provided a statistical power of 80% to detect a change in the proportion of slow acetylators from 50% to 80% (Odds ratio 3.33 approx) at a significance level of $p=0.05$.

3.2.8.2 Hardy-Weinberg Equilibrium

In the early twentieth century, through mathematical modelling, both G.H. Hardy and W. Weinberg separately concluded that allelic frequencies in a gene pool are inherently stable, however evolution should be expected in all populations at all times (Weinberg, 1963; Hardy, 1908). The model has become known as the Hardy-Weinberg equilibrium (HWE) based on the principle for a hypothetical situation in which there is no change of the frequencies of alleles in the gene pool and therefore no mechanisms of evolution are acting on a population. In order for equilibrium to remain in effect from generation to generation, a few basic assumptions need to be met; first, the population has to be infinitely large with no random shifts in the frequency of the individual alleles in the gene pool. Spontaneous mutations are negligible and there is no migration into or emigration out of the population. Individuals are mating randomly and natural selection is not occurring in the population. In addition, all individuals in the population are able to breed and produce the same number of offspring. When all these assumptions are valid and being met, both allele and genotype frequencies in a population will remain constant over generations, and the population is said to be in HWE. However, evolution is a common occurrence in nature due to natural selection and hence it is virtually impossible to meet all these assumptions in the HWE model. Hence, Hardy-Weinberg model plays an important role in the field of population genetics and provides a theoretical basis for the measurement of evolutionary change. It enables the comparison of the predicted or “expected” genotype frequencies with the actual or “observed” frequencies in a population and allows scientists to determine whether the population is in HWE. If the genotype frequencies deviate from values expected from HWE, it can be

assumed that evolution occurs where one or more of the model's assumptions are being violated.

The Hardy-Weinberg model consists of two equations that allow the calculation of allele and genotype frequencies respectively. Both equations will sum up to one since frequency is involved. In the simplest case of a single locus with two alleles of a diploid organism, the dominant allele is denoted A and the recessive allele is denoted a. If p represents the frequency of A, $f(A)=p$ and q represents the frequency of a, $f(a)=q$, the equation for allele frequency is $p+q=1$. Three possible genotypes, AA, Aa and aa can be derived from these two allelic forms using a Punnett square (**Table 3.4**). The Punnett square depicts the probabilities of generating all possible genotypes at a diallelic locus in a population that conforms to Hardy-Weinberg assumptions. The final three expected genotypic frequencies in the offspring become $f(AA)=p^2$, $f(Aa)=2pq$ and $f(aa)=q^2$ and the equation for genotype frequencies is $(p^2) + (2pq) + (q^2) = 1$. The genotypic frequency distribution will not change from generation to generation once a population is in HWE. Nevertheless, populations in their natural environment are unable to meet all the assumptions required to achieve HWE. Genetic drift or allelic drift happens when the allele frequencies in a population change across generations. To test whether observed genotypes of a population conform to Hardy-Weinberg expectations, a simple chi-square goodness-of-fit test can be performed. Under the null hypothesis of HWE, the observed genotype frequencies are not significantly different from those predicted for a population in equilibrium. A probability value, or P value is used to evaluate the significance of a chi-square by setting a cutoff point of 0.05 (5%) for significance. For example, a P value of less than or equal to 0.05 indicates a significant difference between the observed and expected genotype frequencies, the null hypothesis is rejected and the population is therefore not in HWE. For large-scale genomic studies especially those involve the evaluation of thousands of loci segregating for multiple alleles, a more robust and powerful exact test is needed for HWE testing to reduce the risk of a type I error (Wigginton et al., 2005).

Table 3.4 Punnett square for Hardy-Weinberg equilibrium

		Females	
		A (p)	a (q)
Males	A (p)	AA (p^2)	Aa (pq)
	a (q)	Aa (pq)	aa (q^2)

Deviation from Hardy-Weinberg expectations denotes the evolution of a population due to the violation of the assumptions of HWE model. Factors that cause violation include non-random mating, mutations, selection, limited population size, random genetic drift, gene flow and meiotic drive. In a small population, inbreeding or mating between close relatives is more likely to occur rather than random mating. Inbreeding changes genotype proportions by decreasing the frequency of heterozygotes and increasing the frequency of homozygotes. This effect of inbreeding resulting from the inheritance of a copy of the same recessive allele from both parents may increase the homozygous recessive diseases susceptibility in an individual or a population. Assortative mating is another cause of deviation from the HWE. Assortative mating occurs when individuals select mates non-randomly from within their population which causes an increase in homozygosity for the genes involved in the trait. Small population size may lead to a random change in allele frequency. This is due to a sampling effect, also known as genetic drift which causes greater chance of deviation of a population from Hardy-Weinberg expectations during random mating. These sampling effects may result from the processes of genetic drift, founder events and population bottlenecks in natural populations. All these sampling errors can cause a rapid loss of genetic variation through the loss of rare alleles, leading to decreased heterozygosity and an increased degree of inbreeding and adaptation impairment (Shama et al., 2011; Nei, 1975). Mutation and natural selection can cause the change in allele frequencies. Natural selection leads to differential rates of survival and reproduction where individuals with some favouring traits are able to adapt to their environment better than individuals with other traits. While directional selection leads to decrease over time in the frequency of an unfavoured allele, balancing selection, in the contrast to the directional selection,

maintains genetic polymorphism in populations (Andrews, 2010). Balancing selection leads to equilibrium population with Hardy-Weinberg proportions even though it violates the assumption in Hardy-Weinberg principles.

Deviations of the observed genotype frequencies with those expected by Hardy-Weinberg may suggest violation of HWE assumptions, but may also indicate genotyping errors due to selection bias in sample enrolment or laboratory error. These genotyping errors could lead to false conclusions and decrease the power of certain statistical test for linkage and/or association studies. Thus, the used of HWE testing for data quality control is important to limit and detect genotyping error within population-based data sets. Checking for HWE deviation is a standard practice when performing genome wide association studies with markers which fail at test of HWE generally discarded. However, deviation can also be due to disease association when this is present in a disease group though the controls should still be in HWE. It is also suggested that copy number variation (CNV), an event in which a large DNA fragment (range from 1,000 base pairs to 5 megabases) is duplicated or deleted could play an important factor of HWE violation (Lee et al., 2008). Therefore the study of these SNP markers that lies within CNV regions may show an apparent deviation from HWE.

3.2.8.3 *Genotype analysis*

Statistical analysis was performed using GraphPad Prism 3.0 (California, USA). Genotype frequencies between groups were compared using Fisher's exact test, where p-values <0.05 were considered to be statistically significant. Odd ratios (OR) and 95% confidence intervals (CI) were also calculated to estimate the risk of ATD-DILI associated with each polymorphism.

3.2.8.4 *Haplotype analysis*

Haplotypes were constructed from genotype data and assigned to each of the case-control subjects. Haplotype frequencies of the case and control groups for *GSTA4* were analysed using PHASE v2.1.1. Odd ratios and 95% confidence intervals were calculated using the GraphPad Prism 3.0 software. The p-value was determined by fisher's exact

test to assess the significance of differences in haplotype frequencies between the case-control groups.

3.2.8.5 Multiple testing

The null hypothesis H_0 is a hypothesis which a researcher seeks to disprove, reject or nullify. The acceptance or rejection of the null hypothesis is based on an appropriate statistical test (Wackerly D., 2008). Type I errors happen when the null hypothesis H_0 is rejected although the hypothesis is in fact true. On the other hand, Type II error occurs when the null hypothesis H_0 is accepted although the hypothesis is false. The probability of making a Type I error is denoted by α (alpha), and the probability of making a Type II error is denoted by β (beta). A cut-off point of the α level is commonly set at 0.05, which means one in twenty statistical tests will incorrectly reject the null hypothesis H_0 and give rise to a false positive finding (**Table 3.5**). The chance of Type I error could be reduced by using a more stringent cut-off value such as 1% (1 in 100) or 0.1% (1 in 1000) to increase specificity. However, as shown in Table 3.1, when there is a decrease in the probability of a Type I error, there is an increase in the probability of a Type II error occurring (false negative rate). Therefore, it is important to estimate and optimise the balance between Type I and Type II errors.

Table 3.5 Contingency table showing Type I and Type II errors (Rao D. C., 2008)

	Null is true	Alternative is true
Reject null	False positive (Type I error)	True positive
Accept null	True negative	False negative (Type II error)

With recent advances in single nucleotide polymorphism (SNP) genotyping technologies, candidate gene approaches and also genome-wide associations studies (GWAS) have gained much popularity in identifying gene with common variants that influence susceptibility to complex diseases. The simultaneous testing of hundreds of thousands or even millions of SNP markers was made possible, however, this has also led to challenges in multiple comparison testing. Failure to adjust for multiple comparisons appropriately will yield the rate of Type I errors and decrease the power to detect association between genetic markers and a disease phenotype. When a large

number of SNPs are tested, the Type I error rate is more inflated as the magnitude of increase in type I error rate depends on the sample size (Marquard et al., 2009; Moskvina et al., 2006). Generally, the nominal significance level which is also the probability of making type I error (α) is adjusted downwards to reduce the likelihood of false positive results. Several methods have been proposed to overcome this problem. The effects of multiple testing could be minimised through the adjustment of the number of tests by limiting the number of association tests performed (Lunetta, 2008). For instance, when the associations of a single phenotype and numerous SNPs are examined, one could limit the number of tests by performing a single test per SNP by selecting the most closely associated SNP with the phenotype. Another option to limit the number of tests includes the use of haplotype or multilocus genotypes, rather than single SNPs alone to strengthen the power to detect associations. A multivariate test is useful for large scale association studies involving different phenotypes and numerous SNPs. Associations between individual genetic markers (SNPs) and each phenotype will be tested to find out which phenotype or subset of phenotypes is associated with the marker (Lunetta, 2008).

Bonferroni correction is a simple and widely used method to correct for multiple testing. The adjustment of Bonferroni correction is made by multiplying the nominal P values by the total number of tests performed. The adjustment controls the family-wise error rate (FWER), which is the probability of making one or more Type I errors. For example, if one sets the experiment-wide error rate at 0.05 over 50 independent tests, then the Bonferroni-adjusted P values must be <0.001 to be considered significant, and the probability of observing at least 1 such result in the entire experiment is ≤ 0.001 . By assuming analyses involve independent markers and phenotypes, Bonferroni correction is considered as the most stringent and highly conservative method for multiple comparisons. Several less conservative multiple test corrections have been proposed, such as the step-down correction of Holm (Holm, 1979), the Westfall and Young permutation method (Westfall and Young, 1993), and the Benjamini and Hochberg false discovery rate (Benjamini and Hochberg, 1995).

The step-down correction of Holm is reasonably similar to the Bonferroni, but slightly less conservative. By using a stepwise procedure to assess the ordered set of null hypotheses, the test with the lowest probability is tested first with a Bonferroni

correction involving all tests. The second test is tested with a Bonferroni correction involving one less test and so on for the remaining tests until it fails to reject a null hypothesis. This sequential Bonferroni correction procedure of Holm is thus less conservative and generally more powerful than the corresponding single-step procedure while still maintaining the FWER.

The Westfall and Young permutation method is an alternative way to correct for large numbers of tests in typical association studies (Westfall and Young, 1993). It integrates the correlation between phenotypes and genotypes and is far less stringent than that used in a standard Bonferroni adjustment. To rearrange the apparent relationship between phenotypes and genotypes, observed phenotypes are permuted with their respective genotypes while the correlation among phenotypes is preserved, and the relationship between genotypes (linkage disequilibrium patterns between SNPs) is retained within an individual. The entire process is performed by random rearrangement and repeated many times until all possible permutations are generated. The association between test statistics and corresponding P values of each permuted data set is computed similarly to the non-permuted data set. The new minimum P values from the permuted data sets are compared to the original P value of the non-permuted data set. The adjusted P value is defined when the permuted-based minimum P values is less than the original P values. Although permutation testing is complex and computationally expensive, it is considered the gold standard for multiple testing correction in GWAS by providing unbiased type I error control and high power (Pahl and Schafer, 2010).

The false discovery rate (FDR), first proposed by Benjamini and Hochberg, is the least stringent form of adjustment compared to other multiple comparison procedures described earlier on. The FDR aims at controlling the expected proportion of falsely rejected hypotheses (type I errors), unlike other multiple comparisons procedures that control the FWER. When all the null hypotheses are true, the FWER and FDR are equivalent; otherwise, the FDR is less than the FWER. The FDR approach tolerates more false positives while allowing considerably fewer type II errors, and therefore provides a sensible alternative with good balance between discovery of statistically significant genes and limitation of type I errors. FDR plays an important role in the analysis of high-throughput data, such as the discovery of differential expression in

microarray and SNP biomarker selection by offering a less conservative with greater ability or power to find truly significant results. Nevertheless, careful selection of multiple testing comparison procedure is important in limiting type I errors and also to prevent erroneous study conclusions. In this chapter, because the total number of genotyping tests performed was relatively small, it was decided to correct for multiple testing using the Bonferroni correction method above. The primary hypothesis that overall *NAT2* genotype predicts susceptibility was first investigated without correction.

3.3 Results

3.3.1 NAT2

3.3.1.1 Investigation of a possible association between NAT2 genotype and susceptibility to ATD-DILI

To investigate our primary hypothesis that *NAT2* slow acetylators were more susceptible to ATD-DILI, a total of 26 DILI cases and 90 community controls together with 81 controls from the Indian subcontinent who were treated with similar anti-TB drugs without developing DILI were genotyped for three SNPs in the *NAT2* exons (481C>T, 590G>A and 857G>A). Since a SNP in the promoter region of *NAT2*-9796T>A (rs4646244) has recently been suggested to be associated with an increased risk of DILI (Kim et al., 2009), samples were also genotyped for this SNP. The *NAT2* genotyping results for the combined dataset and for the European and Asian cohorts separately are shown in **Table 3.6**, **Table 3.7** and **Table 3.8** respectively. All polymorphisms were in Hardy-Weinberg equilibrium. The odds ratios and *p*-value for the overall genotypes for the entire cohort as well as for the Europeans and South Asians considered separately shown. We observed no significant association between the case and control groups either in the combined dataset or in the Asian cohorts alone ($p>0.05$). However, in the European cohort alone, the AA genotype of 590G>A polymorphism was found to be associated with ATD-DILI with a *p*-value of 0.028 (OR=6.96; 95% CI=1.33-36.57). For -9796T>A, the combined European-South Asian cohort showed no evidence for an association of this variant with the risk of ATD-DILI ($p=0.35$) and there was also no significance in the Asian subjects. In the European cohort alone, the frequency of the homozygous AA genotype was significantly higher in cases compared to control subjects (OR=6.96; 95% CI=1.33-36.57) with a *p*-value of 0.028.

Table 3.6 Association of NAT2 genotypes and the risk of ATD-DILI in combined European and South Asian cohorts

NAT2

SNP	Genotype	Cases (n=26)	Community controls (n=90)	Cases vs Controls	
				P-value	OR (95% CI)
481C>T (rs1799929)	CC	10 (0.38)	41 (0.46)	0.37	1.78 (0.6-5.26)
	CT	10 (0.38)	36 (0.40)		
	TT	6 (0.24)	13 (0.14)		
590G>A (rs1799930)	GG	8 (0.31)	39 (0.43)	0.27	1.72 (0.68-4.37)
	GA	13 (0.50)	41 (0.46)		
	AA	5 (0.19)	10 (0.11)		
857G>A (rs1799931)	GG	23 (0.88)	79 (0.88)	1.00	1.07 (0.27-4.15)
	GA	3 (0.12)	11 (0.12)		
-9796T>A (rs4646244)	TT	11 (0.42)	38 (0.42)	0.16	2.44 (0.72-8.23)
	TA	10 (0.39)	44 (0.49)		
	AA	5 (0.19)	8 (0.09)		

P-value for comparison of genotypes frequencies possession of one or two variant alleles between cases vs controls using Fisher's exact 2 tailed test; OR, odds ratios; CI, confidence interval

Table 3.7 Association of NAT2 genotypes and the risk of ATD-DILI in European cohort

NAT2

SNP	Genotype	Cases (n=13)	Community controls (n=50)	Cases vs Controls	
				P-value	OR (95% CI)
481C>T (rs1799929)	CC	6 (0.46)	18 (0.36)	0.14	2.85 (0.75-10.77)
	CT	2 (0.15)	23 (0.46)		
	TT	5 (0.39)	9 (0.18)		
590G>A (rs1799930)	GG	6 (0.46)	26 (0.52)	0.028	6.96 (1.33-36.57)
	GA	3 (0.23)	21 (0.42)		
	AA	4 (0.31)	3 (0.06)		
857G>A (rs1799931)	GG	13 (1.00)	48 (0.96)	1.00	1.39 (0.06-30.78)
	GA	0 (0.00)	2 (0.04)		
-9796T>A (rs4646244)	TT	7 (0.54)	25 (0.50)	0.028	6.96 (1.33-36.57)
	TA	2 (0.15)	22 (0.44)		
	AA	4 (0.31)	3 (0.06)		

P-value for comparison of genotypes frequencies possession of one or two variant alleles between cases vs controls using Fisher's exact 2 tailed test; OR, odds ratios; CI, confidence interval

Table 3.8 Association of NAT2 genotypes and the risk of ATD-DILI in South Asian subjects

NAT2

481C>T (rs1799929)	CC	CT	TT	P-value	OR (95% CI)
Cases (n=13)	4 (0.31)	8 (0.61)	1 (0.08)		
ATD-tolerant controls (n=81)	47 (0.58)	30 (0.37)	4 (0.05)	0.08	3.11 (0.88-10.94)
Community controls (n=40)	23 (0.57)	13 (0.33)	4 (0.10)	0.12	3.04 (0.80-11.56)
590G>A (rs1799930)	GG	GA	AA	P-value	OR (95% CI)
Cases (n=13)	2 (0.15)	10 (0.77)	1 (0.08)		
ATD-tolerant controls (n=81)	34 (0.42)	37 (0.46)	10 (0.12)	0.12	3.98 (0.83-19.13)
Community controls (n=40)	13 (0.33)	20 (0.50)	7 (0.17)	0.31	2.65 (0.51-13.73)
857G>A (rs1799931)	GG	GA	AA	P-value	OR (95% CI)
Cases (n=13)	10 (0.77)	3 (0.23)	0 (0.00)		
ATD-tolerant controls (n=81)	64 (0.79)	17 (0.21)	0 (0.00)	1.00	1.13 (0.28-4.57)
Community controls (n=40)	31 (0.78)	9 (0.22)	0 (0.00)	1.00	1.03 (0.23-4.58)
-9796T>A (rs4646244)	TT	TA	AA	P-value	OR (95% CI)
Cases (n=13)	4 (0.31)	8 (0.62)	1 (0.08)		
ATD-tolerant controls (n=81)	34 (0.42)	37 (0.46)	10 (0.12)	0.55	1.63 (0.46-5.73)
Community controls (n=40)	13 (0.33)	22 (0.55)	5 (0.12)	1.00	1.71 (0.18-16.19)

P-value for comparison of genotypes frequencies possession of one or two variant alleles between cases vs controls using Fisher's exact 2 tailed test; OR, odds ratios; CI, confidence interval

The three SNPs in the exons were further assigned into alleles *NAT2**5 (481C>T), *NAT2**6 (590G>A), *NAT2**7 (857G>A) and *NAT2**4 (apparent wild-type). The presence of any two mutant alleles defines the slow acetylator phenotype (genotypes *NAT2**5*5, *NAT2**5*6, *NAT2**5*7, *NAT2**6*6, *NAT2**6*7 and *NAT2**7*7), whereas rapid acetylators had no more than one mutant allele (genotypes *NAT2**4*4, *NAT2**4*5, *NAT2**4*6 and *NAT2**4*7). The overall genotype results obtained are summarised in **Table 3.9**. The odds ratios and *p*-value for the overall phenotypes for the entire cohort as well as for the Europeans and South Asians considered separately shown in **Table 3.10**. In the combined European-South Asian cohort, the slow acetylator phenotype was found to be associated with the risk of ATD-DILI (OR=4.60; 95% CI=1.47-14.44) (*p*-value=0.006) when compared with the community controls with 80% of cases being slow acetylators. In the European cohort alone, an apparent increased frequency of the slow acetylator phenotype was observed in the cases but this was not statistically significantly different (OR=3.33; 95% CI=0.82-13.58; *p*=0.12). However, for the South-Asian cohort, slow acetylator status was found to be associated with an increased susceptibility to ATD-DILI with the *p*-value of 0.002 (OR=13.58; 95% CI=1.69-109.4) when compared to the ATD-tolerant controls. A borderline significant difference was also observed in these cases when compared to the community controls with a *p*-value of 0.041 (OR=8.00; 95% CI=0.94-67.67).

The relationship between -9796T>A and the other *NAT2* polymorphisms studied was also investigated. As summarised in **Table 3.11**, many subjects positive for -9796T>A were also positive for *NAT2**6. In particular, among the community controls, all 8 individuals with a AA genotype for the -9796 SNP had a *NAT2**6*6 genotype while for the cases this was true for 5 of the 6 individuals. Analysis by Fisher's exact test comparing *6 genotypes in those carrying one or more A-9796 alleles (**Table 3.12**) showed a highly significant association for both cases (*p*=0.0008) and controls (*p*<0.0001) suggesting that the 590G>A and -9796T>A SNPs were in strong linkage disequilibrium.

Table 3.9 Association of *NAT2* genotypes and the risk of ATD-DILI

NAT2

Combined European-South Asian cohort			
<i>NAT2</i> Allele	Cases (n=26)	Community controls (n=90)	
Rapid acetylator			
<i>NAT2</i> *4*4	2 (0.08)	6 (0.07)	
<i>NAT2</i> *4*5	0 (0.00)	14 (0.16)	
<i>NAT2</i> *4*6	2 (0.08)	16 (0.18)	
<i>NAT2</i> *4*7	0 (0.00)	5 (0.06)	
Slow acetylator			
<i>NAT2</i> *5*5	6 (0.23)	13 (0.14)	
<i>NAT2</i> *5*6	8 (0.31)	20 (0.22)	
<i>NAT2</i> *5*7	1 (0.04)	2 (0.02)	
<i>NAT2</i> *6*6	5 (0.19)	10 (0.11)	
<i>NAT2</i> *6*7	2 (0.08)	4 (0.04)	
European cohort			
<i>NAT2</i> Allele	Cases (n=13)	Community controls (n=50)	
Rapid acetylator			
<i>NAT2</i> *4*4	2 (0.15)	4 (0.08)	
<i>NAT2</i> *4*5	0 (0.00)	12 (0.24)	
<i>NAT2</i> *4*6	1 (0.08)	9 (0.18)	
<i>NAT2</i> *4*7	0 (0.00)	0 (0.00)	
Slow acetylator			
<i>NAT2</i> *5*5	5 (0.38)	9 (0.18)	
<i>NAT2</i> *5*6	1 (0.08)	11 (0.22)	
<i>NAT2</i> *5*7	0 (0.00)	1 (0.02)	
<i>NAT2</i> *6*6	4 (0.31)	3 (0.06)	
<i>NAT2</i> *6*7	0 (0.00)	1 (0.02)	
South Asian cohort			
<i>NAT2</i> Allele	Cases (n=13)	ATD-Tolerant controls (n=81)	Community controls (n=40)
Rapid acetylator			
<i>NAT2</i> *4*4	0 (0.00)	7 (0.09)	2 (0.05)
<i>NAT2</i> *4*5	0 (0.00)	10 (0.12)	2 (0.05)
<i>NAT2</i> *4*6	1 (0.08)	17 (0.21)	7 (0.18)
<i>NAT2</i> *4*7	0 (0.00)	9 (0.11)	5 (0.13)
Slow acetylator			
<i>NAT2</i> *5*5	1 (0.08)	4 (0.05)	4 (0.10)
<i>NAT2</i> *5*6	7 (0.54)	16 (0.20)	9 (0.23)
<i>NAT2</i> *5*7	1 (0.08)	4 (0.05)	1 (0.03)
<i>NAT2</i> *6*6	1 (0.08)	10 (0.12)	7 (0.18)
<i>NAT2</i> *6*7	2 (0.15)	4 (0.05)	3 (0.08)

Table 3.10 Predicted NAT2 acetylator phenotype and the risk of ATD-DILI

NAT2

	Acetylator Phenotype		P-value	OR (95% CI)
	Rapid	Slow		
Combined European and South Asian cohort				
Cases (n=26)	4 (0.15)	22 (0.85)	0.006	4.60 (1.47-14.44)
Community controls (n=90)	41 (0.46)	49 (0.54)		
European cohort				
Cases (n=13)	3 (0.23)	10 (0.77)	0.120	3.33 (0.82-13.58)
Community controls (n=50)	25 (0.50)	25 (0.50)		
South Asian cohort				
Cases (n=13)	1 (0.08)	12 (0.92)	0.002	13.58 (1.69-109.40)
ATD-tolerant controls (n=81)	43 (0.53)	38 (0.47)		
Community controls (n=40)	16 (0.40)	24 (0.60)	0.041	8.00 (0.94-67.67)

P-value for comparison of acetylator phenotype frequencies between cases vs controls using Fisher's exact 2 tailed test; OR, odds ratios; CI, confidence interval

Table 3.11 The relationship between 9796T>A and the other NAT2 polymorphisms

Combined European-South Asian cohort						
NAT2 Allele	Genotype -9796T>A (rs4646244)					
	Cases (n=26)			Community controls (n=90)		
	TT	TA	AA	TT	TA	AA
Rapid acetylator						
NAT2*4*4	2 (0.08)	-	-	4 (0.04)	2 (0.02)	-
NAT2*4*5	-	-	-	12 (0.13)	2 (0.02)	-
NAT2*4*6	1 (0.04)	1 (0.04)	-	1 (0.01)	15 (0.17)	-
NAT2*4*7	-	-	-	3 (0.03)	2 (0.02)	-
Slow acetylator						
NAT2*5*5	5 (0.19)	1 (0.04)	-	13 (0.14)	-	-
NAT2*5*6	1 (0.04)	7 (0.27)	-	3 (0.03)	17 (0.19)	-
NAT2*5*7	1 (0.07)	-	-	2 (0.02)	-	-
NAT2*6*6	-	1 (0.04)	5 (0.19)	-	2 (0.02)	8 (0.09)
NAT2*6*7	1 (0.07)	-	-	-	4 (0.04)	-

Table 3.12 Statistical analysis of the association between -9796T>A and other NAT2 alleles

	Genotype -9796T>A (rs4646244)		P-value	OR (95% CI)
	TT	TA/AA		
Cases				
NAT2*6 positive	3 (0.12)	14 (0.54)	0.008	37.33 (3.3-421.8)
NAT2*6 negative	8 (0.31)	1 (0.04)		
Controls				
NAT2*6 positive	4 (0.04)	46 (0.51)	<0.0001	65.2 (17.1-249.1)
NAT2*6 negative	34 (0.38)	6 (0.07)		

*P-value for comparison of NAT2-9796T>A genotypes frequencies between NAT2*6 positive vs NAT2*6 negative using Fisher's exact 2 tailed test; OR, odds ratios; CI, confidence interval*

A total of 6 patients who underwent liver transplant following liver failure due to ATD-DILI were studied in detail. Five of these were cases in the main study but a sixth case was of African ethnic origin and was not included in the main study. As shown in **Table 3.13**, genotyping for NAT2*5, *6 and *7 suggested that 50% of these cases were fast acetylators including two, of European ethnic origin and African ethnic origin respectively, who were homozygous for NAT2*4 and therefore predicted to be very rapid acetylators. To investigate the possibility that some of these cases of severe DILI might be positive for additional NAT2 mutations, the complete coding sequence in all 6 cases was determined. For the African case, the sequencing showed that this individual was heterozygous for NAT2*14A because a G>A base change at position 191 (Arg to Glu) was detected (**Figure 3.24**). This individual was still classed as a rapid acetylator as the final genotype was NAT2*4*14A.

Table 3.13 NAT2 genotypes (for *5, *6 and *7) and predicted phenotypes in 6 liver-transplanted patients

Patient	Ethnic origin	NAT2 Genotypes	NAT2 Phenotype
1	African*	NAT2*4*4	Rapid acetylator
2	Bangladeshi	NAT2*4*6	Rapid acetylator
3	European	NAT2*4*4	Rapid acetylator
4	European	NAT2*5*5	Slow acetylator
5	Pakistani	NAT2*5*6	Slow acetylator
6	Indian	NAT2*5*6	Slow acetylator

* Later found by sequencing to have the genotype NAT2*4*14A

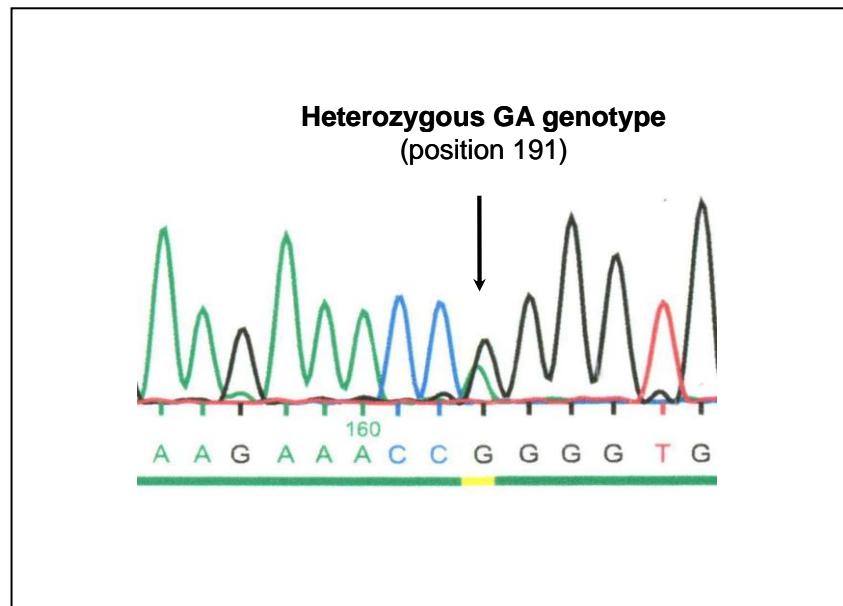


Figure 3.24 Detection of the NAT2 191G>A nucleotide change in a liver transplant patient from African origin

*Sequencing traces showed that this individual possessed the GA genotype and therefore was heterozygous for NAT2*14A.*

3.3.1.2 Sensitivity analysis on NAT2 genotype as a predictor of anti-TB DILI

Using the data shown in Table 3.8 for the combined European and South Asian cohort, analysis of the value of NAT2 genotype for predicting DILI due to anti-TB drugs was determined. Sensitivity, specificity, negative predictive value and positive predictive value were each calculated using standard methods (www.hpa-midas.org.uk/sensitivity_calculator.asp). The incidence of DILI due to anti-TB drugs was assumed to be 2% for the predictive value calculations. The results obtained are shown in **Table 3.14**.

Table 3.14 Sensitivity analysis for NAT2 genotyping

	Sensitivity	Specificity	Predictive value*	
			Positive	Negative
NAT2 genotyping	84.6%	45.6%	0.03	0.99

* Predictive values are expressed as a proportion or probability, with a range of 0 to 1

3.3.2 Genotyping for additional candidate genes for ATD-DILI

3.3.2.1 Genes chosen for study

To assess the possible contribution of other genes relevant to either ATD metabolism or to protection against oxidative stress, it was decided to study the candidate genes and SNPs listed in **Table 3.15**. In the case of *PXR*, *GSTA1*, *GSTT1* and *GSTA1*, it was decided to study specific polymorphisms which had previously been demonstrated to show functional significance. For *CYP2E1*, the SNPs chosen for study were based on previous studies on disease association but for *GSTA4* because of the absence of previous data, we selected SNPs that tagged the most common haplotypes based on information from the Hapmap. For *SOD2*, we chose to study one SNP previously suggested to be functionally significant and relevant to DILI but also selected a second SNP so that the common haplotypes were tagged. A total of 14 different polymorphisms were chosen for study. All SNPs studied were successfully genotyped and we found no deviation from the Hardy-Weinberg equilibrium in all controls except for -1053C>T in

CYP2E1. The minor allele frequency of -1053C>T in *CYP2E1* is closed to zero which results in a deficiency of heterozygotes relative to Hardy-Weinberg expectations. For *GSTT1* and *GSTM1*, the Hardy-Weinberg equilibrium analysis was excluded for these genes as the data presented (presence versus the absence of the *GSTT1/GSTM1* polymorphism) cannot be used to assess Hardy-Weinberg equilibrium. Considering that a total of 15 genotyping assays were evaluated in our study, the adjusted significant *P* value is 0.0033 after Bonferroni correction for multiple testing.

Table 3.15 Additional candidate genes chosen for study

Gene	Position	SNP	Reference SNP ID
<i>CYP2E1</i>	Promoter	-1053C>T	rs2031920
	Promoter	-71G>T	rs6413420
	Intron 7	9896C>G	rs2070676
<i>PXR</i>	Promoter	-25385C>T	rs3814055
<i>GSTA1</i>	Promoter	-69C>T	rs3957357
<i>GSTA4</i>	Intron 1	–	rs316141
	Intron 1	–	rs4147618
	Intron 2	–	rs316128
	Intron 4	–	rs3756980
	Intron 6	–	rs13207376
<i>GSTT1</i>		Null allele	
<i>GSTM1</i>		Null allele	
<i>SOD2</i>	Exon 2	–	rs4880
	3'UTR	–	rs5746136

3.3.2.2 *CYP2E1*

Four SNPs in *CYP2E1* (-1293G>C, -1053C>T, -71G>T and 9896C>G) were selected and genotyped. The -1293G>C and -1053C>T genotypes were in complete linkage disequilibrium and therefore the genotype data for the -1293G>C was excluded in this study. The genotyping results for -1053C>T, -71G>T and 9896C>G polymorphisms for the combined European-South Asian cohorts are shown in **Table 3.16**. As shown in **Table 3.16**, an apparent increased frequency of the -1053CT genotype was observed in ATD-DILI cases compared to the community controls, however, the difference was not significant (OR=7.42; 95% CI=0.65-85.35; p=0.13). We also observed no significant differences between the groups in the analysis of -71G>T and 9896C>G polymorphisms. In the European cohorts, an increased frequency of the -1053CT genotype was found in ATD-DILI cases compared to the community controls (OR=21.96; 95% CI=0.99-489.3) with a p-value of 0.04. The result is however not reliable as the genotype frequencies in the community controls for the SNP -1053C>T did not fit with the Hardy-Weinberg equation (**Table 3.17**). If Bonferroni correction for multiple testing is performed to reflect the fact that genotyping for 15 different polymorphisms has been performed and the level of significance is set at 0.0033, the *p*-values here are not significant. Genotyping for -71G>T and 9896C>G polymorphisms in the cases and controls also showed no significant difference in frequency between the groups (p=0.69-0.30). As shown in **Table 3.17**, there was an increased frequency of wild-type CC (9896C>G) in cases compared to ATD-tolerant controls (OR=3.68; 95% CI=0.45-23.48) and community controls (OR=4.55; 95% CI=0.53-39.29); however it showed no statistical difference in the South Asian cohorts. For the -1053C>T and -71G>T polymorphisms, there were no differences between the cases and ATD-tolerant controls, nor in the community controls (p=1.00).

Table 3.16 Association of CYP2E1 genotypes and the risk of ATD-DILI in combined European-South Asian cohorts

<i>CYP2E1</i>		Cases (n=26)	Controls (n=90)	Cases vs Controls	
Genotypes	P-value			OR (95% CI)	
-1053C>T (rs2031920)	CC	24 (0.92)	89 (0.99)	0.13	7.42 (0.65-85.35)
	CT	2 (0.08)	1 (0.01)		
	TT	0 (0.00)	0 (0.00)		
	CC vs CT+TT				
-71G>T (rs6413420)	GG	22 (0.85)	79 (0.88)	0.74	1.31 (0.38-4.51)
	GT	4 (0.15)	11 (0.12)		
	TT	0 (0.00)	0 (0.00)		
	GG vs GT+TT				
9896C>G (rs2070676)	CC	21 (0.81)	68 (0.76)	0.76	1.35 (0.43-4.27)
	CG	5 (0.19)	11 (0.12)		
	GG	0 (0.00)	1 (0.01)		
	CC vs CG+GG				

P-value for comparison of genotypes frequencies possession of one or two variant alleles between cases vs controls using Fisher's exact 2 tailed test; OR, odds ratios; CI, confidence interval

Table 3.17 Association of CYP2E1 genotypes and the risk of ATD-DILI in European cohorts

<i>CYP2E1</i>		Cases (n=13)	Controls (n=50)	Cases vs Controls	
Genotypes	P-value			OR (95% CI)	
-1053C>T (rs2031920)	CC	11 (0.85)	50 (1.00)	0.04	21.96 (0.99-489.3)
	CT	2 (0.15)	0 (0.00)		
	TT	0 (0.00)	0 (0.00)		
	CC vs CT+TT				
-71G>T (rs6413420)	GG	10 (0.77)	43 (0.86)	0.42	1.84 (0.40-8.41)
	GT	3 (0.23)	7 (0.14)		
	TT	0 (0.00)	0 (0.00)		
	GG vs GT+TT				
9896C>G (rs2070676)	CC	9 (0.69)	39 (0.78)	0.49	1.58 (0.41-6.11)
	CG	4 (0.31)	11 (0.22)		
	GG	0 (0.00)	0 (0.00)		
	CC vs CG+GG				

P-value for comparison of genotypes frequencies possession of one or two variant alleles between cases vs controls using Fisher's exact 2 tailed test; OR, odds ratios; CI, confidence interval

Table 3.18 Association of CYP2E1 genotypes and the risk of ATD-DILI in South Asian subjects

CYP2E1

-1053C>T (rs2031920)					
	CC	CT	TT	P-value	OR (95% CI)
Cases (n=13)	13 (1.00)	0 (0.00)	0 (0.00)		
ATD-tolerant controls (n=81)	76 (0.94)	5 (0.06)	0 (0.00)	1.00	1.94 (0.10-37.20)
Community controls (n=40)	39 (0.97)	1 (0.03)	0 (0.00)	1.00	1.03 (0.04-26.72)
-71G>T (rs6413420)					
	GG	GT	TT	P-value	OR (95% CI)
Cases (n=13)	12 (0.92)	1 (0.08)	0 (0.00)		
ATD-tolerant controls (n=81)	74 (0.91)	6 (0.08)	1 (0.01)	1.00	1.14 (0.13-10.07)
Community controls (n=40)	36 (0.90)	4 (0.10)	0 (0.00)	1.00	1.33 (0.14-13.13)
9896C>G (rs2070676)					
	CC	CG	GG	P-value	OR (95% CI)
Cases (n=13)	12 (0.92)	1 (0.08)	0 (0.00)		
ATD-tolerant controls (n=81)	62 (0.77)	18 (0.22)	1 (0.01)	0.29	3.68 (0.45-23.48)
Community controls (n=40)	29 (0.73)	10 (0.25)	1 (0.02)	0.25	4.55 (0.53-39.29)

P-value for comparison of genotypes frequencies possession of one or two variant alleles between cases vs controls using Fisher's exact 2 tailed test; OR, odds ratios; CI, confidence interval

3.3.2.3 PXR

The genotyping results for *PXR* -25385C>T polymorphism in the European and South Asian cohorts are shown in **Table 3.19**. In the combined European-South Asian cohorts, an increased frequency for the carriage of a wild-type C allele was observed in the cases compared with the community controls, yet the difference was not significant (OR=3.00; 95% CI=0.65-13.89; p=0.24). In the European cohort, no association was observed between the cases and the community controls (p=0.54). However, in the South Asian cohort, a slight increase for the carriage of a wild-type C allele was found in the cases compared with the community controls, however the difference was not significant (OR=6.05; 95% CI=0.32-113.50; p=0.17). There was also no association found between the ATD-tolerant controls with ATD-DILI cases (p=1.00).

Table 3.19 Association of *PXR* genotypes and the risk of ATD-DILI

<i>PXR</i>					
-25385C>T (rs3814055)	TT	CT	CC	P-value	OR (95% CI)
Combined European-South Asian cohorts					
Cases (n=26)	2 (0.08)	15 (0.58)	9 (0.35)		
Community controls (n=90)	18 (0.20)	33 (0.37)	39 (0.43)	0.24	3.00 (0.65-13.89)
European cohorts					
Cases (n=13)	2 (0.15)	8 (0.62)	3 (0.23)		
Community controls (n=50)	11 (0.22)	21 (0.42)	18 (0.36)	0.72	1.55 (0.30-8.07)
South Asian cohorts					
Cases (n=13)	0 (0.00)	7 (0.54)	6 (0.46)		
ATD-tolerant controls (n=81)	4 (0.05)	42 (0.52)	35 (0.43)	1.00	1.57 (0.08-30.84)
Community controls (n=40)	7 (0.18)	12 (0.30)	21 (0.53)	0.17	6.05 (0.32-113.5)

P-value for comparison of genotypes frequencies possession of one or two variant alleles between cases vs controls using Fisher's exact 2 tailed test; OR, odds ratios; CI, confidence interval

3.3.2.4 *GSTAI*

The genotyping results of -69C>T in the European and South Asian cohorts are shown in **Table 3.20**. We found no association of *GSTAI* genotypes and the risk of ATD-DILI in Europeans, South Asians and both cohorts combined. The relative frequency of the TT genotype among the community control groups varied from 21% in Europeans to 5% in South Asians. An increased frequency of TT genotype was observed in the cases compared to the community controls in the South Asian cohort, however it showed no statistical difference in each group (OR=3.46; 95% CI=0.44-27.44; p=0.25).

Table 3.20 Association of *GSTA1* genotypes and the risk of ATD-DILI

<i>GSTA1</i>					
-69C>T (rs3957357)	TT	CT	CC	P-value	OR (95% CI)
Combined European-South Asian cohorts					
Cases (n=26)	6 (0.23)	9 (0.35)	11 (0.42)		
Community controls (n=90)	14 (0.16)	41 (0.46)	35 (0.39)	0.38	1.63 (0.56-4.78)
European cohorts					
Cases (n=13)	4 (0.31)	5 (0.38)	4 (0.31)		
Community controls (n=50)	12 (0.24)	23 (0.46)	15 (0.30)	0.72	0.71 (0.19-2.73)
South Asian cohorts					
Cases (n=13)	2 (0.15)	4 (0.31)	7 (0.54)		
ATD-tolerant controls (n=81)	7 (0.09)	33 (0.41)	41 (0.51)	0.61	1.92 (0.35-10.47)
Community controls (n=40)	2 (0.05)	18 (0.45)	20 (0.50)	0.25	3.46 (0.44-27.44)

P-value for comparison of genotypes frequencies possession of one or two variant alleles between cases vs controls using Fisher's exact 2 tailed test; OR, odds ratios; CI, confidence interval

3.3.2.5 *GSTA4*

The association of five SNPs in *GSTA4* and the risk of ATD-DILI in the combined dataset and for the European and South Asian cohorts separately are shown in **Table 3.21**, **Table 3.22** and **Table 3.23** respectively. In the combined European-South Asian cohorts, we observed an apparently significant association ($p < 0.05$) in rs316128 and rs3756980 with the risk of ATD-DILI (**Table 3.21**). For rs316128, the proportion of A allele carriers was significantly higher in the cases compared to the controls (OR=7.14; 95% CI=0.91-56.05) with a p -value of 0.041. Patients with AA genotype (rs3756980) were associated with a higher risk of developing hepatotoxicity due to anti-TB drugs (OR=3.67; 95% CI=1.02-13.24) with a p -value of 0.046. However, the p -values here are not significant after correction for multiple testing ($p > 0.0033$). In the South Asian cohorts, lack of association was observed between *GSTA4* polymorphisms and the risk of ATD-DILI ($p = 0.45-1.00$). In the European cohort, carriage of a wild-type A allele in rs316128 was found to be associated with increased susceptibility to ATD-induced DILI with a p -value of 0.027 (OR=11.79; 95% CI=0.7-211.2). An apparent differences of the homozygous AA genotype in rs3756980 was also found in the cases compared to the controls but this was not significant (OR=8.00; 95% CI=1.0-66.5; p -value=0.045). For

rs316141, the frequency of the homozygous CC genotype was higher in the cases than the controls; again the difference was not significantly different (OR=3.00; 95% CI=0.86-10.51; p=0.103).

Further analysis was performed by reconstructing haplotypes and estimating their frequencies using PHASE v2.1.1. The results are summarised in **Table 3.24** and **Table 3.25**. In the combined European-South Asian dataset, no association was found between the ATD-DILI susceptibility with a particular haplotypes. However, in the European cohort, a greater frequency of the CTAAA haplotype in the case group (69%) compared to the controls (44%) was detected. This gave an odds ratio of 2.86 (95% CI=1.14-7.2) with a *p*-value of 0.028 (**Table 3.24**).

Table 3.21 Association of GSTA4 genotypes and the risk of ATD-DILI in combined European-South Asian cohorts

<i>GSTA4</i>		Genotypes	Cases (n=26)	Controls (n=90)	Cases vs Controls	
					<i>P</i> -value	OR (95% CI)
rs316141	TT		2 (0.08)	17 (0.19)	0.240	2.80 (0.6-12.99)
	CT		12 (0.46)	40 (0.44)		
	CC		12 (0.46)	33 (0.37)		
	CC+CT vs TT					
rs4147618	TT		23 (0.88)	75 (0.83)	0.760	1.53 (0.41-5.77)
	TA		3 (0.12)	15 (0.17)		
	TT vs TA					
rs316128	AA		9 (0.34)	30 (0.33)	0.041	7.14 (0.91-56.05)
	AC		16 (0.62)	40 (0.45)		
	CC		1 (0.04)	20 (0.22)		
	AA+AC vs CC					
rs3756980	AA		22 (0.85)	60 (0.67)	0.046	3.67 (1.02-13.24)
	AG		3 (0.12)	27 (0.30)		
	GG		0 (0.00)	3 (0.03)		
	AA vs AG+GG					
rs13207376	AA		23 (0.88)	84 (0.93)	0.420	1.83 (0.42-7.87)
	AG		2 (0.08)	2 (0.02)		
	GG		1 (0.04)	4 (0.05)		
	AA vs AG+GG					

P-value for comparison of genotypes frequencies possession of one or two variant alleles between cases vs controls using Fisher's exact 2 tailed test; OR, odds ratios; CI, confidence interval

Table 3.22 Association of GSTA4 genotypes and the risk of ATD-DILI in European cohorts

GSTA4

	Genotypes	Cases (n=13)	Controls (n=50)	Cases vs Controls	
				P-value	OR (95% CI)
rs316141	CC	7 (0.54)	14 (0.28)	0.103	3.00 (0.86-10.51)
	CT	6 (0.46)	24 (0.48)		
	TT	0 (0.00)	12 (0.24)		
	CC vs CT+TT				
rs4147618	TT	12 (0.92)	40 (0.80)	0.433	3.00 (0.4-25.9)
	TA	1 (0.08)	10 (0.20)		
	TT vs TA				
rs316128	CC	0 (0.00)	15 (0.30)	0.027	11.79 (0.7-211.2)
	CA	8 (0.62)	22 (0.44)		
	AA	5 (0.38)	13 (0.26)		
	AA+CA vs CC				
rs3756980	AA	12 (0.92)	30 (0.60)	0.045	8.00 (1.0-66.5)
	AG	1 (0.08)	18 (0.36)		
	GG	0 (0.00)	2 (0.04)		
	AA vs AG+GG				
rs13207376	AA	11 (0.85)	47 (0.94)	0.273	0.35 (0.1-2.4)
	AG	2 (0.15)	2 (0.04)		
	GG	0 (0.00)	1 (0.02)		
	AA vs AG+GG				

P-value for comparison of genotypes frequencies possession of one or two variant alleles between cases vs controls using Fisher's exact 2 tailed test; OR, odds ratios; CI, confidence interval

Table 3.23 Association of *GSTA4* genotypes and the risk of ATD-DILI in South Asian subjects

GSTA4

rs316141	TT	CT	CC	P-value	OR (95% CI)
Cases (n=13)	2 (0.15)	6 (0.46)	5 (0.39)		
ATD-tolerant controls (n=81)	11 (0.14)	36 (0.44)	34 (0.42)	1.00	1.16 (0.35-3.85)
Community controls (n=40)	5 (0.13)	16 (0.40)	19 (0.47)	0.75	1.45 (0.40-5.20)
rs4147618	TT	TA	AA	P-value	OR (95% CI)
Cases (n=13)	11 (0.85)	2 (0.15)	0 (0.00)		
ATD-tolerant controls (n=81)	73 (0.90)	7 (0.09)	1 (0.01)	0.63	0.60 (0.11-3.22)
Community controls (n=40)	35 (0.88)	5 (0.12)	0 (0.00)	1.00	0.79 (0.13-4.64)
rs316128	AA	AC	CC	P-value	OR (95% CI)
Cases (n=13)	4 (0.31)	8 (0.61)	1 (0.08)		
ATD-tolerant controls (n=81)	31 (0.38)	39 (0.48)	11 (0.14)	0.76	1.40 (0.40-4.92)
Community controls (n=40)	17 (0.42)	18 (0.45)	5 (0.13)	0.53	1.66 (0.44-6.32)
rs3756980	AA	AG	GG	P-value	OR (95% CI)
Cases (n=13)	10 (0.77)	2 (0.15)	1 (0.08)		
ATD-tolerant controls (n=81)	59 (0.73)	21 (0.26)	1 (0.01)	1.00	1.24 (0.31-4.94)
Community controls (n=40)	30 (0.75)	9 (0.22)	1 (0.03)	1.00	1.11 (0.25-4.86)
rs13207376	AA	AG	GG	P-value	OR (95% CI)
Cases (n=13)	12 (0.92)	0 (0.00)	1 (0.08)		
ATD-tolerant controls (n=81)	78 (0.96)	0 (0.00)	3 (0.04)	0.45	0.46 (0.04-4.81)
Community controls (n=40)	37 (0.92)	0 (0.00)	3 (0.08)	1.00	0.97 (0.09-10.26)

P-value for comparison of genotypes frequencies possession of one or two variant alleles between cases vs controls using Fisher's exact 2 tailed test; OR, odds ratios; CI, confidence interval

Table 3.24 Association of the most common *GSTA4* haplotypes and the risk of ATD-DILI in combined European-South Asian cohorts

GSTA4

Haplotype	Haplotype frequency		Frequency of other haplotype		P-value	OR (95% CI)
	Cases n=52	Controls n=180	Cases n=52	Controls n=180		
CTAAA	28 (0.54)	95 (0.53)	24 (0.31)	85 (0.47)	1.00	1.04 (0.56-1.94)
TTCAA	10 (0.19)	33 (0.18)	42 (0.88)	147 (0.82)	0.84	1.06 (0.48-2.33)
TTCGA	1 (0.02)	18 (0.10)	51 (0.96)	162 (0.90)	0.08	5.67 (0.74-43.52)

P-value for comparison of genotypes frequencies between groups using Fisher's exact 2 tailed test; OR, odds ratios; CI, confidence interval

Table 3.25 Association of the most common *GSTA4* haplotypes and the risk of ATD-DILI in European cohorts

GSTA4

Haplotype	Haplotype frequency		Frequency of other haplotype		P-value	OR (95% CI)
	Cases n=26	Controls n=100	Cases n=26	Controls n=100		
CTAAA	18 (0.69)	44 (0.44)	8 (0.31)	56 (0.51)	0.028	2.86 (1.14-7.2)
TTCAA	3 (0.12)	20 (0.20)	23 (0.88)	80 (0.88)	0.404	1.92 (0.52-7.03)
TTCGA	1 (0.04)	12 (0.12)	25 (0.96)	88 (0.88)	0.300	3.41 (0.42-27.5)

P-value for comparison of genotypes frequencies between groups using Fisher's exact 2 tailed test; OR, odds ratios; CI, confidence intervals

3.3.2.6 *GSTT1*

The relative frequency of the *GSTT1* null genotype among community control groups varies from 27% in the Europeans and 10% in the South Asians (**Table 3.26**). No *GSTT1* null mutation was detected in the South Asian cases and only 2 cases (15%) with *GSTT1* null mutation was observed in the European cohorts. We observed no association between *GSTT1* null genotype and ATD-DILI in combined dataset and also the European and South Asian cohorts separately, thus suggesting that *GSTT1* null mutation is unlikely to be associated with the risk of ATD-DILI in our studied cohorts.

Table 3.26 Statistical analysis of *GSTT1* ‘null’ polymorphism and the risk of ATD-DILI

	<i>GSTT1</i>		<i>P</i> -value	OR (95% CI)
	Present	Absent		
Combined European and South Asian cohorts				
Cases (n=26)	2 (0.08)	24 (0.92)	0.24	3.00 (0.65-13.89)
Community controls (n=90)	18 (0.20)	72 (0.80)		
European cohorts				
Cases (n=13)	2 (0.15)	11 (0.85)	0.49	2.14 (0.42-10.90)
Community controls (n=50)	14 (0.28)	36 (0.72)		
South Asian cohorts				
Cases (n=13)	0 (0.00)	13 (1.00)	0.12	6.29 (0.35-111.8)
ATD-tolerant controls (n=81)	15 (0.19)	66 (0.81)		
Community controls (n=40)	4 (0.10)	36 (0.90)		

P-value for comparison of genotypes frequencies between cases vs controls using Fisher’s exact 2 tailed test; OR, odds ratios; CI, confidence intervals

3.3.2.7 *GSTM1*

The association of *GSTM1* null polymorphism and the risk of ATD-DILI in Europeans, South Asians and both cohorts combined are shown in **Table 3.27**. All samples, except one from the South Asian cases, were successfully genotyped. In the European cohort, frequency of the *GSTM1* null genotype was higher in the cases than the controls but this was not statistically significant (OR=2.44; 95% CI=0.66-8.98; p=0.221). In the South Asian cohorts, an apparent increased frequency of the *GSTM1* null genotype was observed in the cases, however it was not statistically significant when compared to the ATD-tolerant controls (OR=3.40; 95% CI=0.94-12.26; p=0.064) and the community controls (OR=3.71; 95% CI=0.95-14.54; p=0.094). In the combined dataset, we observed an apparently significant increase in the *GSTM1* null mutation in the cases (68%) compared to the controls (42%) with a *p*-value of 0.026 (OR=2.91; 95% CI=1.14-7.43). The *p*-value here however is not significant after correction for multiple testing (p>0.0033). The association of the combined effect of *NAT2* and *GSTM1* polymorphisms with the risk of ATD-DILI was further examined (**Table 3.28**). In the combined European-South Asian cohorts, the *NAT2* slow acetylator phenotype and *GSTM1* null genotype together showed highest distribution in the cases (56%) compared to the controls (26%) with a *p*-value of 0.007 (OR=3.71; 95% CI=1.48-9.31). In contrast, the *NAT2* rapid acetylator and *GSTM1* null genotype combination was higher in the controls with a *p*-value of 0.008 (OR=9.75; 95% CI=1.25-75.87). This suggests that *NAT2* slow acetylator and *GSTM1* null genotype combination correlated significantly with susceptibility to ATD-DILI.

Table 3.27 Statistical analysis of GSTM1 ‘null’ polymorphism and the risk of ATD-DILI

	<i>GSTM1</i>		<i>P</i> -value	OR (95% CI)
	Present	Absent		
Combined European-South Asian cohorts				
Cases (n=25)	17 (0.68)	8 (0.32)	0.026	2.91 (1.14-7.43)
Community controls (n=90)	38 (0.42)	52 (0.58)		
European cohorts				
Cases (n=13)	9 (0.69)	4 (0.31)	0.221	2.44 (0.66-8.96)
Community controls (n=50)	24 (0.48)	26 (0.52)		
South Asian cohorts				
Cases (n=12)	8 (0.67)	4 (0.33)	0.064	3.40 (0.94-12.26)
ATD-tolerant controls (n=81)	30 (0.37)	51 (0.63)		
Community controls (n=40)	14 (0.35)	26 (0.65)	0.094	3.71 (0.95-14.54)

P-value for comparison of genotypes frequencies between cases vs controls using Fisher’s exact 2 tailed test; OR, odds ratios; CI, confidence interval

Table 3.28 Statistical analysis of combined effect of NAT2 acetylator status and GSTM1 ‘null’ polymorphism in ATD-DILI

Combined European-South Asian cohorts	Case (n=25)	Control (n=90)	P-value	OR (95% CI)
Slow acetylator + <i>GSTM1</i> null	14 (0.56)	23 (0.26)	0.007	3.71 (1.48-9.31)
Slow acetylator + <i>GSTM1</i> present	7 (0.28)	26 (0.29)	1.000	1.04 (0.39-2.80)
Rapid acetylator + <i>GSTM1</i> null	3 (0.12)	15 (0.17)	0.760	1.47 (0.39-5.53)
Rapid acetylator + <i>GSTM1</i> present	1 (0.04)	26 (0.29)	0.008	9.75 (1.25-75.87)
European cohorts	Case (n=13)	Control (n=50)	P-value	OR (95% CI)
Slow acetylator + <i>GSTM1</i> null	7 (0.54)	13 (0.26)	0.092	3.32 (0.94-11.71)
Slow acetylator + <i>GSTM1</i> present	3 (0.23)	12 (0.24)	1.000	1.05 (0.25-4.46)
Rapid acetylator + <i>GSTM1</i> null	2 (0.15)	11 (0.22)	0.729	1.55 (0.30-8.07)
Rapid acetylator + <i>GSTM1</i> present	1 (0.08)	14 (0.28)	0.162	4.67 (0.55-39.32)
South Asian cohorts	Case (n=12)	Control (n=40)	P-value	OR (95% CI)
Slow acetylator + <i>GSTM1</i> null	7 (0.58)	10 (0.25)	0.042	4.20 (1.09-16.24)
Slow acetylator + <i>GSTM1</i> present	4 (0.33)	14 (0.35)	1.000	1.08 (0.28-4.22)
Rapid acetylator + <i>GSTM1</i> null	1 (0.08)	4 (0.10)	1.000	1.22 (0.12-12.11)
Rapid acetylator + <i>GSTM1</i> present	0 (0.00)	12 (0.30)	0.047	5.14 (0.60-44.12)
South Asian cohorts	Case (n=12)	ATD-tolerant control (n=81)	P-value	OR (95% CI)
Slow acetylator + <i>GSTM1</i> null	7 (0.58)	17 (0.21)	0.147	2.69 (0.76-9.54)
Slow acetylator + <i>GSTM1</i> present	4 (0.33)	21 (0.26)	0.728	1.43 (0.39-5.24)
Rapid acetylator + <i>GSTM1</i> null	1 (0.08)	13 (0.16)	0.685	2.10 (0.25-17.72)
Rapid acetylator + <i>GSTM1</i> present	0 (0.00)	30 (0.37)	0.054	7.06 (0.87-57.03)

P-value for comparison of genotypes frequencies between cases vs controls using Fisher's exact 2 tailed test; OR, odds ratios; CI, confidence interval

3.3.2.8 SOD2

The association of *SOD2* polymorphisms and their risk with ATD-DILI in the combined dataset and the European and South Asian cohorts separately are shown in **Table 3.29**, **Table 3.30** and **Table 3.31** respectively. Two SNPs in *SOD2* (rs4880 and rs5746136) were selected and genotyped. No significant association was found between the case and control groups either in the combined dataset or in the European and South Asian cohorts separately ($p>0.05$).

Table 3.29 Association of *SOD2* genotypes and the risk of ATD-DILI in combined European-South Asian cohorts

		<i>SOD2</i>			
	Genotypes	Cases (n=26)	Controls (n=90)	Cases vs Controls	
				<i>P</i> -value	OR (95% CI)
rs4880	TT	7 (0.27)	20 (0.22)		
	TC	12 (0.46)	45 (0.50)		
	CC	7 (0.27)	25 (0.28)		
	CC+TC vs TT			0.61	1.29 (0.47-3.50)
rs5746136	GG	8 (0.31)	42 (0.47)		
	GA	16 (0.61)	39 (0.43)		
	AA	2 (0.08)	9 (0.10)		
	GA+AA vs GG			0.18	1.97 (0.78-4.99)

P-value for comparison of genotypes frequencies possession of one or two variant alleles between cases vs controls using Fisher's exact 2 tailed test; OR, odds ratios; CI, confidence interval

Table 3.30 Association of SOD2 genotypes and the risk of ATD-DILI in European cohorts

		<i>SOD2</i>			
	Genotypes	Cases (n=13)	Controls (n=50)	Cases vs Controls	
				P-value	OR (95% CI)
rs4880	TT	3 (0.23)	11 (0.22)	0.74	1.57 (0.38-6.50)
	TC	7 (0.54)	23 (0.46)		
	CC	3 (0.23)	16 (0.32)		
	CC+TC vs TT				
rs5746136	GG	4 (0.31)	25 (0.50)	0.35	2.25 (0.61-8.27)
	GA	9 (0.69)	21 (0.42)		
	AA		4 (0.08)		
	GA+AA vs GG				

P-value for comparison of genotypes frequencies possession of one or two variant alleles between cases vs controls using Fisher's exact 2 tailed test; OR, odds ratios; CI, confidence interval

Table 3.31 Association of SOD2 genotypes and the risk of ATD-DILI in South Asian subjects

		<i>SOD2</i>				
	Genotypes	Cases (n=13)	ATD-tolerant controls (n=81)	Community controls (n=40)	P-value	OR (95% CI)
	TT	4 (0.31)	11 (0.14)	9 (0.23)	0.21	2.83 (0.74-10.79)
	TC	5 (0.38)	36 (0.44)	22 (0.55)		
	CC	4 (0.31)	34 (0.42)	9 (0.23)		
	CC+TC vs TT				0.71	1.53 (0.38-6.16)
rs5746136	GG	4 (0.31)	40 (0.49)	17 (0.42)	0.25	2.20 (0.63-7.71)
	GA	7 (0.54)	34 (0.42)	18 (0.45)		
	AA	2 (0.15)	7 (0.09)	5 (0.13)		
	GA+AA vs GG					

P-value for comparison of genotypes frequencies possession of one or two variant alleles between cases vs controls using Fisher's exact 2 tailed test; OR, odds ratios; CI, confidence interval

3.3.3 *NATI*

As preliminary evidence from a genome-wide association study on the European ATD-DILI cases suggested that rs2739685 showed borderline significance for a genome-wide association using a different control group (Daly and Shen, unpublished), it was decided to genotype all the ATD-DILI cases and the controls for this SNP. A Taqman SNP genotyping assay used in this study produced a satisfactory allelic discrimination for rs2739685 SNP in all the DNA samples. **Figure 3.25** shows three distinct genotype clusters from the intensity plot of an allelic discrimination assay using VIC and FAM dyes. The generation of the fluorescent signals from VIC and FAM probes only occur in the presence of the complementary target sequence to indicate the specific allele. The allelic distribution was in Hardy Weinberg equilibrium in both European ($p=0.335$) and South Asian cohorts ($p=0.997$). As shown in **Table 3.32**, the frequency of allele C was significantly higher in the European cases than controls (OR=7.13; 95% CI=1.86-27.34). Fisher's exact test revealed a significant association between the variant allele (C) and the risk of ATD-DILI ($p=0.006$), suggesting its role of conferring increased risk of the development of ATD-DILI. If correction for multiple testing is performed which for a total of 15 genotyping assays results in the level of significance set at 0.0033, the association observed here is not statistically significant. In the South Asian cohorts, an increased frequency of the carriage of T allele was found in the cases but it was not statistically significant when compared to the ATD-tolerant controls (OR=2.68; 95% CI=0.76-9.40; $p=0.14$) and community controls (OR=3.75; 95% CI=0.98-14.33; $p=0.06$). In the combined dataset, no significant association was detected between *NATI* genotypes and ATD-DILI. The lack of association in the combined dataset could be due to the allelic heterogeneity between the two populations. The minor allele frequencies (MAF) and its 95% confidence interval (CI) values of our present community control data sets were analysed and compared against genotypes data from population based controls. Using the publicly available data from the British 1985 Birth Cohort (<http://www.b58cgene.squl.ac.uk/>), the MAF from 1398 population controls was 15% (95%CI=13-16%). In our present European community controls data set, the MAF was 12% (95%CI=7-17%), similar to that in the population control group. On the other hand, genome data of Gujarati Indians in Houston ($n=88$) obtained from Ensembl genome viewer (<http://www.ensembl.org/index.html>) was used as the ethnically matched control to compared with our South Asian cohort. The published MAF of Gujarati Indians was

34% (95%CI=29-39%) which is similar to our South Asian cohort (MAF=32% (95%CI=24-39%).

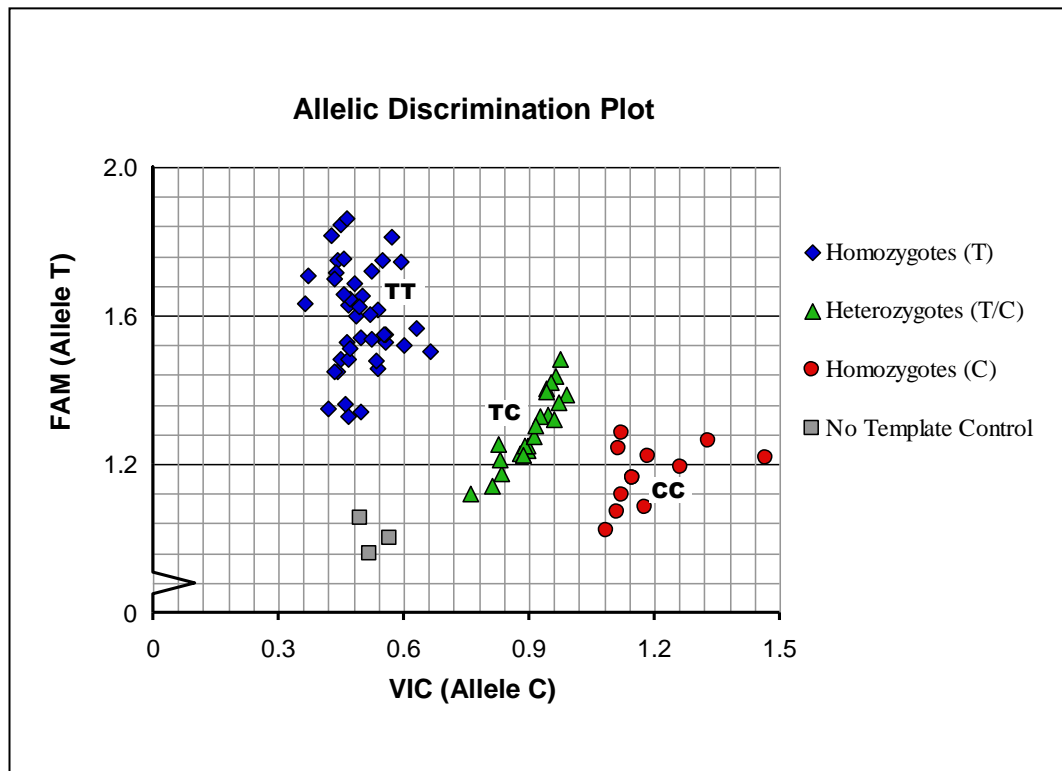


Figure 3.25 Allelic discrimination plot of the DNA samples

Vertical axis represents relative fluorescence for FAM label (marker of T-major allele); horizontal axis represents relative fluorescence for VIC label (marker of C- minor allele). Cluster colored blue is homozygous TT genotype. Green colored cluster is heterozygous TC genotype while red cluster is homozygous CC genotype. Grey colored cluster denotes the no template control (containing distilled water).

Table 3.32 Association of NAT1 genotypes and the risk of ATD-DILI

<i>NAT1</i>					
rs2739685	TT	TC	CC	P-value	OR (95% CI)
Combined European-South Asian cohorts					
Cases (n=26)	13 (0.50)	10 (0.38)	3 (0.12)		
Community controls (n=90)	53 (0.59)	31 (0.34)	6 (0.07)	0.50	1.43 (0.60-3.44)
European cohorts					
Cases (n=13)	4 (0.31)	6 (0.46)	3 (0.23)		
Community controls (n=50)	38 (0.76)	12 (0.24)	0 (0.00)	0.006	7.13 (1.86-27.34)
MAF=12% (95% CI=7-17%)					
South Asian cohorts					
Cases (n=13)	9 (0.69)	4 (0.31)	0 (0.00)		
ATD-tolerant controls (n=81)	37 (0.46)	33 (0.41)	11 (0.14)	0.14	2.68 (0.76-9.40)
Community controls (n=40)	15 (0.38)	19 (0.48)	6 (0.15)	0.06	3.75 (0.98-14.33)
MAF=32% (95%CI=24-39%)					

P-value for comparison of genotypes frequencies between cases vs controls using Fisher's exact 2 tailed test; OR, odds ratios; CI, confidence interval; MAF, minor allele frequency

3.4 Discussion

The *NAT2* polymorphism has been shown as a major susceptibility risk factor for ATD-DILI; variants associated with slow acetylation showed an increased risk of ATD-DILI and this clear association has been confirmed in several studies (Bose et al., 2011; Lee et al., 2010; Kim et al., 2009; Bozok Cetintas et al., 2008; Possuelo et al., 2008; Cho et al., 2007; Huang et al., 2002; Ohno et al., 2000) including our present findings. The frequency of the slow acetylator genotypes in the present study is significantly higher in cases (85%) compared to the community controls (54%) with a *p*-value of 0.006 (OR=4.60; 95% CI=1.47-14.44) in the combined European-South Asian cohorts. When the data from this combined analysis was used for sensitivity analysis, it was found that though sensitivity and negative predictive values were high at 85% and 0.99 respectively, specificity was relatively low at 46% and the positive predictive value was only 0.03. This means that if genotyping for *NAT2* was performed before prescribing isoniazid and slow acetylators were not given this drug, only 3 cases of anti-TB DILI would be prevented for every 100 cases tested with many patients being deprived of

beneficial isoniazid treatment unnecessarily and possibly prescribed more toxic drugs instead.

When the cohorts were studied separately, slow acetylator status in the South Asian cohort was found to be associated with an increased susceptibility to ATD-DILI with the *p*-value of 0.002 (OR=13.58; 95% CI=1.69-109.4) when compared to the ATD-tolerant controls. Similar observations were found in India which showed a statistically significant increased frequency of the slow acetylator genotypes in cases (71%) compared to the ATD-tolerant controls (45%) with a *p*-value of 0.005 (OR=2.99; 95% CI=1.4-6.2) (Bose et al., 2011). However the differences of the slow acetylator frequencies were not significant between cases and controls in the European cohort (*p*-value=0.12) which may be a consequence of having insufficient statistical power due to small sample sizes (n=13). When the variants of *NAT2* in the exon region (481C>T, 590G>A and 857G>A) were examined separately, 590G>A polymorphism or *NAT2**6 allele was the only SNPs found to be associated to ATD-DILI in the European cohort alone with a *p*-value of 0.028 (OR=6.96; 95% CI=1.33-36.57). The lack of significant association of *NAT2**6 allele with ATD-DILI susceptibility observed in cases of the South Asian cohorts could be due to their high frequency of *NAT2**6 allele (42%) in the controls compared to the European controls (27%). The prevalence of *NAT2**6 allele is low in East Asians with approximately 20% reported in Korean and Taiwan (Lee et al., 2010; Kim et al., 2009; Huang et al., 2002). Nevertheless, Kim and colleagues have reported that *NAT2**6 allele was significantly associated with ATD-DILI susceptibility (*p*-value=0.0016) in the Korean population (Kim et al., 2009). Similar observations were found by Huang and colleagues where a higher frequency of *NAT2**6 allele was detected in DILI cases compared to the ATD-tolerant controls (*P*<0.05) among the Taiwanese (Huang et al., 2002). It is however another study based in Taiwan which reported neither *NAT2**6 nor *NAT2**5 (481C>T) alleles were associated with the risk of ATD-DILI. Instead, a significant association between *NAT2**7 (857G>A) allele and the risk of ATD-DILI was found (Lee et al., 2010). In our current study, *NAT2**5 allele was highly prevalent (42%) among the South Asians which is in agreement with a previous study based in India (Bose et al., 2011) indicating that this allele is very common in the Indian/South Asian population. *NAT2**5 allele was rare among the East Asians with a low frequency of 7%, whereas the *NAT2**6 and *NAT2**7 alleles were predominant (47% and 25% respectively) in Taiwanese population (Lee et al., 2010; Huang et al., 2002).

*NAT2**7 allele was rare among the Europeans (2%) compared to that in South Asians (11%) as shown in our current study. When the three alleles were further assigned into slow and rapid acetylator phenotypes, both European and South Asian cohorts showed a similar frequency of slow acetylator distribution (50-60%), higher than those reported in East Asian cohorts (10%). A meta-analysis showed a stronger significant association of slow acetylator status with ATD-DILI when the analysis was limited to Asian populations (OR=2.52; 95%CI=1.49-4.26) compared to the results from a combination of various ethnicity (OR= 1.93; 95%CI 0.81-4.62) (Sun et al., 2008), indicating heterogeneity between and within populations could account for the lack of association of *NAT2* slow acetylator status with ATD-DILI susceptibility. This ethnic heterogeneity for the *NAT2* effect was observed in two studies based in Europe and Canada with mixed ethnicity where no association of risk with acetylator status was found (Yamada et al., 2009; Vuilleumier et al., 2006). A polymorphism (-9796T>A) in the *NAT2* promoter region was found to be associated with decreased expression of *NAT2* and individuals carrying the variant -9796 A allele and *NAT2**6 allele were predisposed to ATD-DILI (p=0.0004) (Kim et al., 2009). In the present study, a strong linkage disequilibrium between -9796 A allele and *NAT2**6 allele was observed in both cases (p=0.0008) and controls (p<0.0001). Both alleles were also found to be associated to ATD-DILI in the European cohort with a *p*-value of 0.028 (OR=6.96; 95% CI=1.33-36.57), indicating that these variants in the promoter and exons of *NAT2* increase the risk of ATD-DILI by decreasing the expression of *NAT2* thus confer slow acetylator status. As well as numbers of cases being small and of more than one ethnic origin, an additional limitation of the present study is that the majority of the patients studied had been treated with additional ATD to INH. Though generally causality had been demonstrated between exposure to ATD and onset of DILI, it is not possible to determine which drug caused DILI and the numbers studied are too small to look at separate drug groups. It remains possible that some of the observed DILI was caused by pyrazinamide exposure, but DILI due to this drug is unlikely to relate to *NAT2* genotype.

Besides *NAT2*, association between *CYP2E1* and ATD-DILI have been reported. Huang and colleagues have reported that the *CYP2E1* c1/c1 genotype which is associated with the *CYP2E1**5B allele shows higher *CYP2E1* activity and therefore may lead to a greater production of hepatotoxic intermediates by the increased oxidation of

acetylhydrazine (Huang et al., 2003). Another two independent studies based in China (Wang et al., 2010) and Taiwan (Lee et al., 2010) have also reported a significant association between ATD-DILI and *CYP2E1* c1/c1 genotype. The *CYP2E1**5B (c2 allele) occurs in approximately 24% of the East Asian population (Lee et al., 2010; Wang et al., 2010; Huang et al., 2003), but was rarely found in our present study cohorts (<2%). The lack of significant association observed in our present study cohorts might be explained by the substantially lower statistical power caused by the lower prevalence of *CYP2E1* c2 allele. However the high frequency of the c1 allele (>98%) may indicate a high prevalence of ATD-DILI susceptibility in the South Asian and European cohorts. Controversial results have been reported in some studies with no association found between *CYP2E1**5B and susceptibility to ATD-DILI in Korean (Kim et al., 2009; Cho et al., 2007) and British Columbian population of Canada (Yamada et al., 2009). This may indicate that the role of *CYP2E1* in determining ATD-DILI may be less important compared to *NAT2*. However the combined risk for ATD-DILI associated with *CYP2E1* genotype and acetylator status may be essential to predict the risk of ATD-DILI. Huang and colleagues have demonstrated an increased risk of ATD-DILI in patients with combined slow acetylator status with *CYP2E1* c1/c1 genotype (OR=7.43; 95% CI=2.42-22.79) compared to patients possess *NAT2* rapid status and *CYP2E1* c1/c1 genotype (OR=3.94; 95% CI=1.45-10.67) (Huang et al., 2003). Bose and colleagues have also shown that slow acetylators carrying the *CYP2E1* mutant CD or CC genotype were predisposed to develop ATD-DILI (OR=4.76; 95% CI=2.19-10.48) compared to rapid acetylators with *CYP2E1* mutant CD or CC genotype (Bose et al., 2011).

In present study, some evidence for associations between polymorphisms in the glutathione S-transferase genes, particularly *GSTM1* and *GSTA4* and ATD-DILI was found, suggesting a protective role of these enzymes in preventing ATD-DILI. However, these associations were not significant after correction for multiple testing. *GSTA4* plays a major role against liver injury by its detoxifying effects through the conjugation of glutathione with harmful electrophiles generated during oxidative stress and lipid peroxidation (Zimniak et al., 1994). In particular, *GSTA4* has been reported to conjugate with 4-hydroxynonenal, a mutagenic compound produced during oxidative stress and lipid peroxidation (Esterbauer et al., 1991). Though polymorphisms in *GSTA4* have not been extensively studied, associations between *GSTA4* variants with Alzheimer's disease and Parkinson's disease have been suggested, which may both be

linked to ROS exposure (Coppede et al., 2005). The result produced by this study suggests that the *GSTA4* haplotype [C-T-A-A-A] carrying A allele at rs316128 and rs3756980 (OR=2.86; 95% CI=1.14-7.2) is associated with increased risk of ATD-DILI but loses significance after correction for multiple testing. For *GSTM1* genotyping analysis, we observed an increased incidence of *GSTM1* null mutation in the cases (68%) compared to the controls (42%) with a *p*-value of 0.026 (OR=2.91; 95% CI=1.14-7.43) in the combined European-South Asian cohorts. This result is consistent with two other studies involved Indian (OR=2.13; 95% CI=1.25-3.50) and Taiwanese populations (OR= OR=2.23; 95% CI=1.07-4.67) (Huang et al., 2007; Roy et al., 2001). However, when our studied cohorts were analysed separately, frequency of the *GSTM1* null genotype was higher in the cases than the controls but this was not statistically significant in neither European nor South Asian cohorts ($p>0.05$). This could be possibly due to an inadequate sample size of the European ($n=13$) and South Asian ($n=12$) to achieve adequate power. A similar observation was made in a Taiwanese population where the frequency of *GSTM1* null genotype was higher in the cases (60.6%) than the controls (48.6%) but this was not statistically significant (OR=1.62; 95% CI=0.94-2.79). Another two studies involving Indian and Caucasians have however reported no difference of *GSTM1* null genotype between cases and controls (Chatterjee et al., 2010; Leiro et al., 2008). It was reported that the frequency of *GSTM1* null genotype ranges from 20% to 79% in the Indian population (Naveen et al., 2004). India has a heterogeneous population with subjects from the southern part differing significant from those of the northern and eastern regions, thus require careful consideration for subject recruitment. Our current South-Asian cohort has shown a frequency of 35% of *GSTM1* null genotype in the community controls which was in agreement with a previous report based on South India population (30.4%) (Naveen et al., 2004). As for the European cohort, we have observed a frequency of 48% of *GSTM1* null genotype among the controls which is similar to studies based in Taiwan (46%), China (48.6%) and Spain (41.7%) (Wang et al., 2010; Leiro et al., 2008; Huang et al., 2007). of 48% 13.1% to 54.5% in Caucasians, from 41.7% to 55.5% in Asians, 46.7% in African-Americans, and 26.9% in Africans (Mo et al., 2009). In our present study, the risk of ATD-DILI susceptibility was significantly increased in subjects with combined *NAT2* slow acetylator phenotype and *GSTM1* null genotype (OR=3.71; 95% CI=1.48-9.31). In contrast, the *NAT2* rapid acetylator and *GSTM1* null genotype combination was higher in the controls (OR=9.75; 95% CI=1.25-75.87). This finding

was in agreement to a study reported by Fukino and colleagues which involved Japanese populations (Fukino et al., 2008). In their study, the genotypes of genes coding for drug-metabolising enzymes involved in INH metabolism including *NAT2*, *CYP2E1*, *GSTT1* and *GSTM1*, and their relationship with serum concentrations of INH and its metabolites were examined in 129 tuberculosis patients. It was found that serum concentration of hydrazine was significantly higher in subjects with *NAT2* slow acetylator phenotypes, high concentration of serum RMP, and *GSTM1* null genotype. Hydrazine, a major INH toxic metabolite can be formed both directly by amidase-catalysed hydrolysis of INH or indirectly by amidase-catalysed hydrolysis of acetyl isoniazid. Studies have indicated that hydrazine plays an important role in the mechanism of INH-induced hepatotoxicity in animals and human (Sarich et al., 1999; Woo et al., 1992). It has also been demonstrated that RMP enhance idiosyncratic hepatocellular reactions by inducing formation of hydrazine from isoniazid particularly in slow acetylators (Sarma et al., 1986). Thus, GST enzymes could play an important role to limit or prevent ATD-DILI by reducing INH toxic metabolites or neutralising toxic products of oxidative stress such as 4-hydroxynonenal, particularly in slow acetylators.

PXR genotype was studied because RMP treatment may lead to the increased expression of certain genes including various CYPs and carboxyesterases that may be relevant to INH metabolism. The SNP studied had been shown to be functionally significant and a risk factor for flucloxacillin-induced DILI (Andrews et al., 2010) but had not been studied previously in ATD-DILI. No association was detected but as with the other genes studied, the possibility of a small effect not detectable because of lack of statistical power cannot be ruled out.

A significant association was detected between a *NAT1* SNP (rs2739685) and ATD-DILI in European cohort (OR=7.13; 95% CI=1.86-27.34). This result confirmed the preliminary evidence from a genome-wide association study on the European ATD-DILI cases (Daly and Shen, unpublished). However no association was found in South Asian cohort and also currently there is no clear role of this gene in the metabolism of anti-tuberculosis medications. Further studies are required to elucidate a possible role for *NAT1* in ATD-DILI. In our present study, we found no association of ATD-DILI susceptibility with *GSTA1*, *GSTT1*, *SOD2*, *CYP2E1* and *PXR*. We could not confirm the

previous findings that the risk of ATD-DILI is higher in subjects with *GSTT1* null genotype (OR=2.60; 95%CI=1.08-6.24) (Leiro et al., 2008), the C variant allele of *SOD2* (OR=2.47; 95%CI=1.13-5.39) (Huang et al., 2007) or *CYP2E1* alleles (Bose et al., 2011; Lee et al., 2010; Wang et al., 2010; Vuilleumier et al., 2006; Huang et al., 2003). In addition, genotyping for an additional *SOD2* SNP so that the main haplotypes were tagged did not indicate any further *SOD2* association. *SOD2* is an attractive candidate gene for susceptibility to DILI induced by a variety of drugs because of its major role in protecting against oxidative stress. An association has been reported with *SOD2* C homozygotes suggested to be more prone to suffer DILI from drugs that are hazardous to mitochondria or produce reactive intermediates (Lucena et al., 2010). Though INH is a drug which may be in this category, the studies performed here did not confirm this association with C homozygotes.

HLA genotypes are also important genetic risk factors for DILI due to certain drugs (Daly, 2010). Though the present study did not consider *HLA* genotypes in ATD-DILI, the absence of *HLA-DQA1*0102* (OR=4.0), and the presence of *HLA-DQB1*0201* alleles (OR=1.9) (Sharma et al., 2002) have been suggested to be risk factors previously. However, recent GWAS analysis of the European ATD-DILI cases did not find any evidence that *HLA* genotype was a predictor for this form of DILI (Daly and Shen, unpublished). Nevertheless, the previously reported *HLA* class II gene association may indicate the possibility of some cases of ATD-DILI involving an adaptive immune mechanism. It has been previously shown that INH can induce other immune responses, in particular autoimmunity similar to lupus (Salazar-Paramo et al., 1992).

**Chapter 4. *In Vitro* Hepatotoxicity and
Interactions between Anti-tuberculosis Drugs**

4 *In vitro* hepatotoxicity and interactions between anti-tuberculosis drugs

4.1 Introduction

Rifampicin (RMP) is an effective antibiotic and prescribed along with isoniazid (INH) for the treatment of TB. It has been reported that the concurrent use of RMP and INH has resulted in increased incidence of hepatotoxicity (2.6%), greater than when these drugs were administered separately (1.6% with INH and 1.1% with RMP alone) (Steele et al., 1991). Though RMP combined with pyrazinamide (PZA) has been used previously for treating latent TB, a two months regimen of PZA and RMP is no longer recommended as severe and fatal cases of hepatotoxicity were observed among patients receiving the RMP plus PZA regimen (CDC, 2003; Lee et al., 2002). The additive or synergistic adverse effects of RMP with other anti-TB drugs could be due to its potent inducing or suppressing effect on drug-metabolising enzymes, which can result in clinically relevant drug-drug interactions (Grange et al., 1994). Studies have indicated that RMP administration may induce the formation of hepatotoxic hydrazine metabolites by stimulating the INH hydrolase activity in the non-acetylating hydrolysis metabolic pathway (see section 1.6) particularly in individuals with the slow acetylator phenotype (Fukino et al., 2008; Askgaard et al., 1995; Sarma et al., 1986). A previous *in vivo* study in rats suggested that hydrazine induced the cytochrome P4502E1 (CYP2E1) and increased the hepatotoxicity of INH (Yue et al., 2004). CYP2E1 is a major contributor of reactive oxygen species (ROS) and has been associated with lipid peroxidation stimulation which plays an important role in the development of INH-induced hepatotoxicity (Caro and Cederbaum, 2004). Recently, it has been proposed that RMP enhanced INH-induced toxicity via induction of CYP2E1 in primary human hepatocytes *in vitro* (Shen et al., 2008). However, there is controversy about the CYP2E1-inducing effect of RMP seeing that the levels of CYP2E1 mRNA and protein were not increased by RMP in human hepatocytes *in vitro* as well as rat liver *in vivo* (Yue et al., 2009; Raucy et al., 2004; Yue et al., 2004; Rae et al., 2001). On the contrary, it appears that RMP suppresses the expression of CYP2E1 in rats and thus reduces the risk of INH-induced oxidative stress through hepatic CYP2E1 (Yue et al., 2009; Yue et al., 2004). Previous studies in mice also demonstrated that RMP protects against carbon tetrachloride-induced hepatotoxicity by suppressing CYP2E1 expression and therefore reduced the formation of free radicals (Takeda et al., 2000; Huang et al.,

1995). It has also been suggested that another drug-metabolising enzyme rather than *CYP2E1* could be involved in the adverse effects of RMP in INH-induced hepatotoxicity (Shen et al., 2008).

RMP binds to nuclear pregnane X receptor (PXR) resulting in the activation of target genes that involved in xenobiotic detoxification and excretion. It promotes the upregulation of phase I CYP450 enzymes such as CYP2B6, CYP2C8, CYP2C9 and CYP3A4 (Song et al., 2004; Kliewer et al., 2002). CYP3A4, the most abundant CYP450 isoform, comprises approximately 50% and 60% of total P450 expressed in human liver and small intestine respectively (Kolars et al., 1994; Shimada et al., 1994). CYP3A4 is more efficiently induced than other CYP450 enzymes and catalyses the metabolism of 50-60% of clinically prescribed drugs subject to P450 metabolism (Desai et al., 2002; Gibson et al., 2002). Variations in its catalytic activity occur in humans resulting in individual differences in the oral bioavailability of CYP3A4 substrates (Evans and McLeod, 2003; Guengerich, 1999; Shimada et al., 1994). These differences may be of clinical significance and affect the disposition of drugs and their metabolites which in turn increase drug toxicity due to toxic metabolites accumulation and CYP3A4-mediated drug-drug interactions (Martinez-Jimenez et al., 2007). In addition to CYP3A4, RMP has been shown to induced the expression of carboxylesterase 2 (CES2) in cultured human and rat hepatocytes (Yang and Yan, 2007; Zhu et al., 2000). CES2, highly expressed in the human small intestine and liver, plays an important role in the metabolism and detoxification of drugs/prodrugs by increasing their bioavailability and aqueous solubility (Sato et al., 2002). It is possible that the induced expression of CES2 by RMP stimulates the INH hydrolysis pathway and increases the formation of toxic metabolite hydrazine. Furthermore, INH-induced toxicity was greatly reduced following *in vivo* administration of carboxylesterase inhibitor, bis-*p*-nitrophenyl phosphate (Tafazoli et al., 2008; Mitchell et al., 1975).

In the present study, we investigated the role of RMP in regulation of CYP2E1, CYP3A4 and CES2 expression in LS180 cells and also in human hepatocytes. LS180 is a well characterized human intestinal colon carcinoma cell line and appears to be responsive to RMP, in contrast to other cell lines such as HepG2, thus making it a suitable model for intestinal drug absorption studies. Human hepatocytes cultured *in vitro* are excellent hepatic model system in predicting enzyme induction *in vivo* and valuable for evaluating the effects of xenobiotics on drug-metabolizing enzyme

induction, particularly of the CYP450 family. The aim was to examine the expression of these genes in the presence or absence of RMP and the response of the cells to INH and PZA treatment in the presence or absence of RMP.

4.2 Materials and Methods

4.2.1 Cell culture of human hepatocytes

Fresh human primary hepatocytes from three donors were purchased from Gibco-Invitrogen Corporation (UK) in a 24-well plate with a density of 3×10^5 cells per well. Immediately upon arrival, the medium of the hepatocytes were replaced with Williams' medium E (WME) supplemented with $1 \mu\text{g/ml}$ insulin (Sigma), $50 \mu\text{g/ml}$ gentamicin (Sigma), 100U/ml Penicillin (PAA), 10mg/ml Streptomycin (PAA) and 2 mM Glutamine (PAA). The cells were allowed to settle overnight prior to any treatment.

4.2.2 Cell proliferation effects of RMP combined with INH and PZA

4.2.2.1 *LS180 cells*

The effects of RMP combined with INH and PZA on cell proliferation were assessed by performing the MTT assay according to section 2.8. The intestinal human colon adenocarcinoma cell line LS180 (passage number 56-62) was cultured according to section 2.3 and seeded overnight in a 6-well plate at 1×10^6 cells per well. To examine the effects of RMP on cell viability, LS180 cells were either pre-treated with $50 \mu\text{M}$ RMP for 72 h before adding INH or pre-treated with 0.5% DMSO for 72 h followed by simultaneous treatment of RMP and INH for 48 h. A control without RMP treatment was included by pre-treating the cells with 0.5% DMSO for 72 h followed by 0, 40, 50, 60, 70 and 80 mM INH for 48 h. In addition, the effect of RMP on PZA response was examined by exposing the cells with 0, 25, 50 and 75 mM of PZA for 24 h with or without 72 h RMP pre-treatment. Assays were performed in duplicate from three independent experiments.

4.2.2.2 *Human hepatocytes*

The cytotoxic effects of RMP on INH in human primary hepatocytes were determined by the MTT assay (see section 2.8). To examine the effects of RMP in cell proliferation,

hepatocytes were treated with 50 μ M RMP or vehicle control (0.5% DMSO) for 72 h before proceeding to INH treatment for 48 h. Assays were performed in duplicate from three independent experiments, derived from three donors.

4.2.3 Effects of Rifampicin on mRNA expression profile

4.2.3.1 *LS180 cells*

LS180 cells were cultured according to section 2.3 and seeded overnight in a 6-well plate at 1×10^6 cells per well. To determine the effect of RMP in the mRNA expressions of CES2, CYP2E1 and CYP3A4, LS180 cells were treated with 50 μ M RMP or vehicle control (0.5% DMSO) for 48 or 72 h. Medium was replaced daily under the same condition of drug treatment. Cells were then harvested using a sterile plastic scraper and RNA was immediately extracted and reverse-transcribed into cDNA prior to analysis (see section 2.6). The Q-RT-PCR was performed in triplicate from three independent experiments using specific primers listed in **Table 2.3**.

4.2.3.2 *Human hepatocytes*

Human hepatocytes derived from three donors were treated with 50 μ M RMP or vehicle control (0.5% DMSO) for 72 h. Medium was replaced daily under the same condition of drug treatment. Cells were then harvested using a sterile plastic scraper and RNA was immediately extracted and reverse-transcribed into cDNA. The transcript levels of CYP3A4, CYP2E1 and CES2 in these cells were then determined by quantitative RT-PCR using specific primers listed in **Table 2.3**.

4.2.4 NAT2 genotyping

To investigate whether NAT2 acetylator genotypes affect the cytotoxic effect of INH, NAT2 genotyping was performed on human hepatocytes derived from three donors and LS180 cells (see section 3.2.4). Briefly, cells were harvested using a sterile plastic scraper and genomic DNA was immediately prepared (see section 2.4). Amplification of NAT2 fragment was performed by PCR and RFLP analyses were carried out by digesting the PCR product with *KpnI*, *TaqI* and *BamHI* to detect the NAT2*5, NAT*6 and NAT2*7 mutant alleles respectively. The wild-type NAT2*4 allele is designated when none of the mutant alleles are present. The presence of any 2 mutant alleles

defines the slow-acetylator phenotype, whereas rapid acetylators have 1 or 2 wild-type *NAT2*4* alleles.

4.3 Results

4.3.1 Cell proliferation effects of RMP combined with other anti-TB medications

4.3.1.1 LS180 cells

The effect of 50 μ M RMP exposure on INH cytotoxicity was assessed in LS180 cells by MTT assay. As shown in **Figure 4.1**, cells receiving 40 mM INH and RMP concurrently are inclined to cell death ($P < 0.05$) compared to RMP pre-treated and no pre-treatment control cells. However, a significant INH-induced cell death at 40, 50, 60, 70 and 80 mM was observed in cells with RMP pre-treatment and concurrent administration of RMP and INH compared to the control cells. The EC_{50} values for cells with RMP pre-treatment (49.05 mM) and cells treated with INH and RMP simultaneously (48.04 mM) were lower than the control cells (60.33 mM). These findings suggest that concurrent or pre-administration of RMP amplifies the effect of INH on cell proliferation in LS180 cells. The effect of RMP on PZA response was also examined by exposing the cells with 0, 25, 50 and 75 mM of PZA for 24 h with or without 72 h RMP pre-treatment. **Figure 4.2** reveals that RMP pre-treated cells were more susceptible to PZA-induced inhibition of proliferation with a significant difference at 60 and 75 mM INH ($P < 0.001$). A lower EC_{50} (64.86 mM) was also observed in RMP pre-treated cells compared to the no pre-treatment cells (78.51 mM), suggesting administration of RMP increases the inhibitory effect of PZA on the proliferation of LS180 cells.

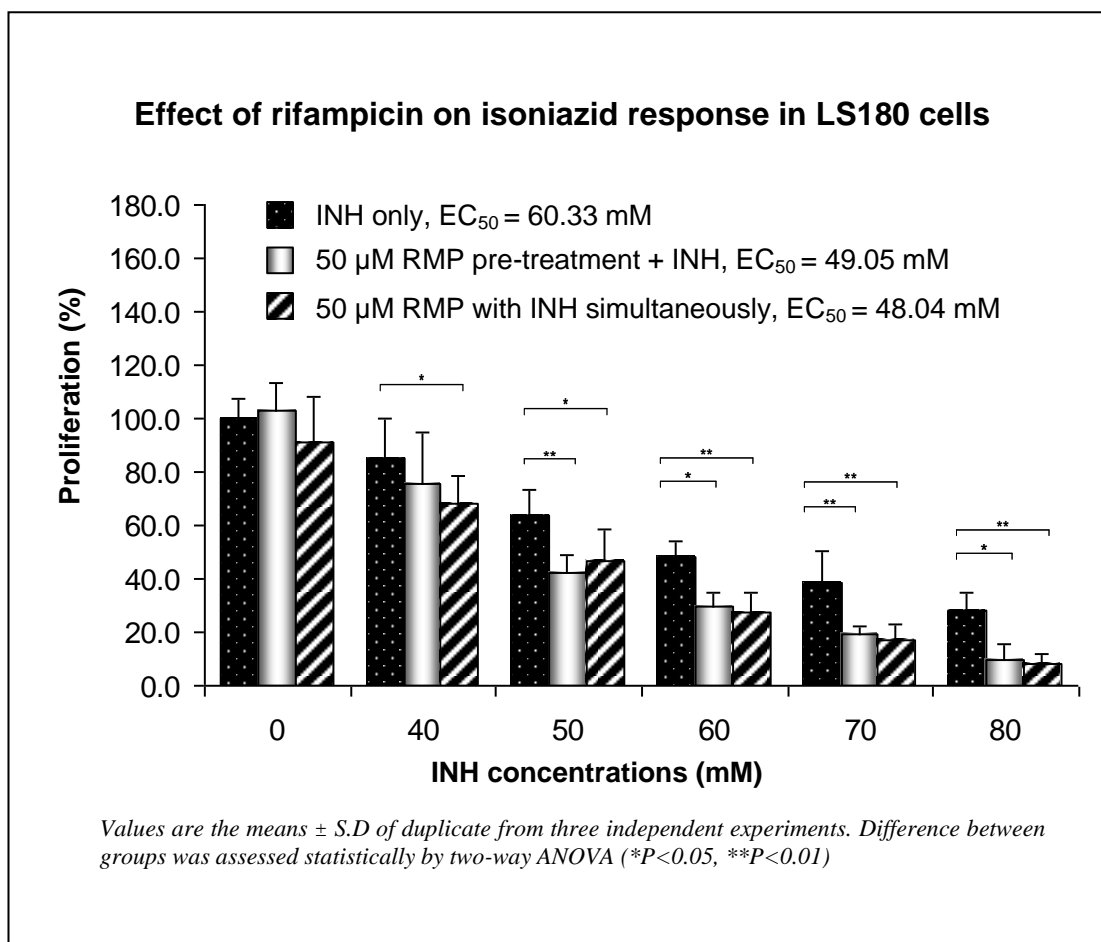


Figure 4.1 The influence of rifampicin co-administration on INH-induced decreased cell proliferation in LS180 cells

To examine the effects of RMP on cell proliferation, LS180 cells were either pre-treated with 50 μ M RMP for 72 h before INH treatment or pre-treated with 0.5% DMSO (vehicle control) for 72 h followed by concurrent administration of RMP and INH for 48 h. The inhibitory effect of INH alone on cell proliferation was also determined by pre-treating the LS180 cells with 0.5% DMSO for 72 h and followed by 48 h INH treatment at 0, 40, 50, 60, 70 and 80 mM. Proliferation was assessed immediately after 96 h of INH/RMP treatment using the MTT colorimetric assay. Treatment with INH causes a dose-dependent inhibition of LS180 cell proliferations. The EC₅₀ values of RMP pre-treated cells (49.05 mM) and concurrent administration of RMP with INH (48.04 mM) were lower than the no treatment control cells (60.33 mM). Concurrent or pre-administration of RMP has significantly inhibited cell proliferation in LS180 when treated with 40, 50, 60, 70 and 80 mM INH ($P < 0.05$) which indicates that RMP increases the inhibitory effect of INH on the proliferation of LS180 cells.

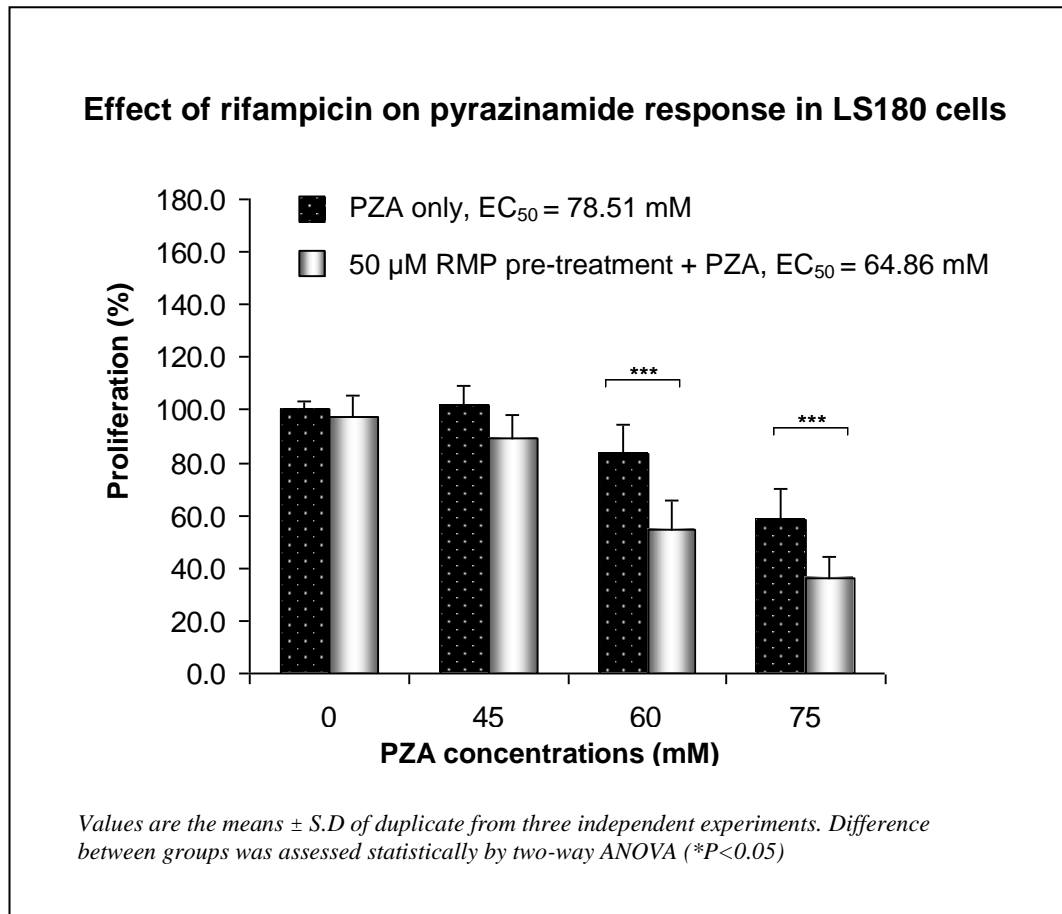


Figure 4.2 The influence of rifampicin co-administration on PZA-induced decreased cell proliferation in LS180 cells.

The effect of RMP on PZA response in LS180 cells was examined by exposing the cells with 0, 25, 50 and 75 mM of PZA for 24 h with or without 72 h RMP pre-treatment. Cells proliferation was assessed immediately after 96 h of PZA/RMP treatment using the MTT colorimetric assay. A dose-dependent inhibition on LS180 cell proliferation was observed following PZA treatment (0-75 mM). The EC₅₀ value of RMP pre-treated cells (64.86 mM) was lower than the no treatment control cells (78.51 mM). RMP pre-treatment has significantly decreased cell proliferation compared to the control cells when treated with 45, 60 and 75 mM PZA ($P < 0.001$), suggesting that RMP increases the inhibitory effect of PZA on the proliferation of LS180 cells.

4.3.1.2 *Human primary hepatocytes*

To evaluate the effect of RMP exposure on cell proliferation, human hepatocytes were treated with 50 μ M RMP or vehicle control (0.5% DMSO) for 48 h before proceeding to INH treatment for 48 h. **Figure 4.3** shows the results of MTT assay performed in duplicate from three donors. Hepatocytes from Donor 1 were pre-treated with or without RMP followed by INH treatment in the range from 0-10 mM INH. RMP pre-treatment has reduced cell proliferation compared with cells with no pre-treatment (**Figure 4.3 (A)**). However, no significant differences were found in these cells. It was also observed that no inhibitory effect of INH on cell proliferation in this range of concentration and therefore a higher concentration of INH (0-50 mM) was applied to Donor 2 and 3. As shown in **Figure 4.3 (B)**, reduced cell proliferation caused by RMP pre-treatment was observed compare to the control cells. The EC_{50} value of the RMP pre-treated cells was higher (29.89 mM) than the control cells (9.7 mM) with a significant increased at 10 mM INH treatment ($P < 0.05$). Conversely, these phenomena did not occur in hepatocytes obtained from Donor 3 as RMP pre-treated cells were more susceptible to the inhibition of cell proliferation compared to the control cells (**Figure 4.3 (C)**). The EC_{50} value of the RMP pre-treated cells (16.93 mM) was lower than the control cells (38.42 mM) with a significant decrease at 10 mM INH treatment ($P < 0.05$).

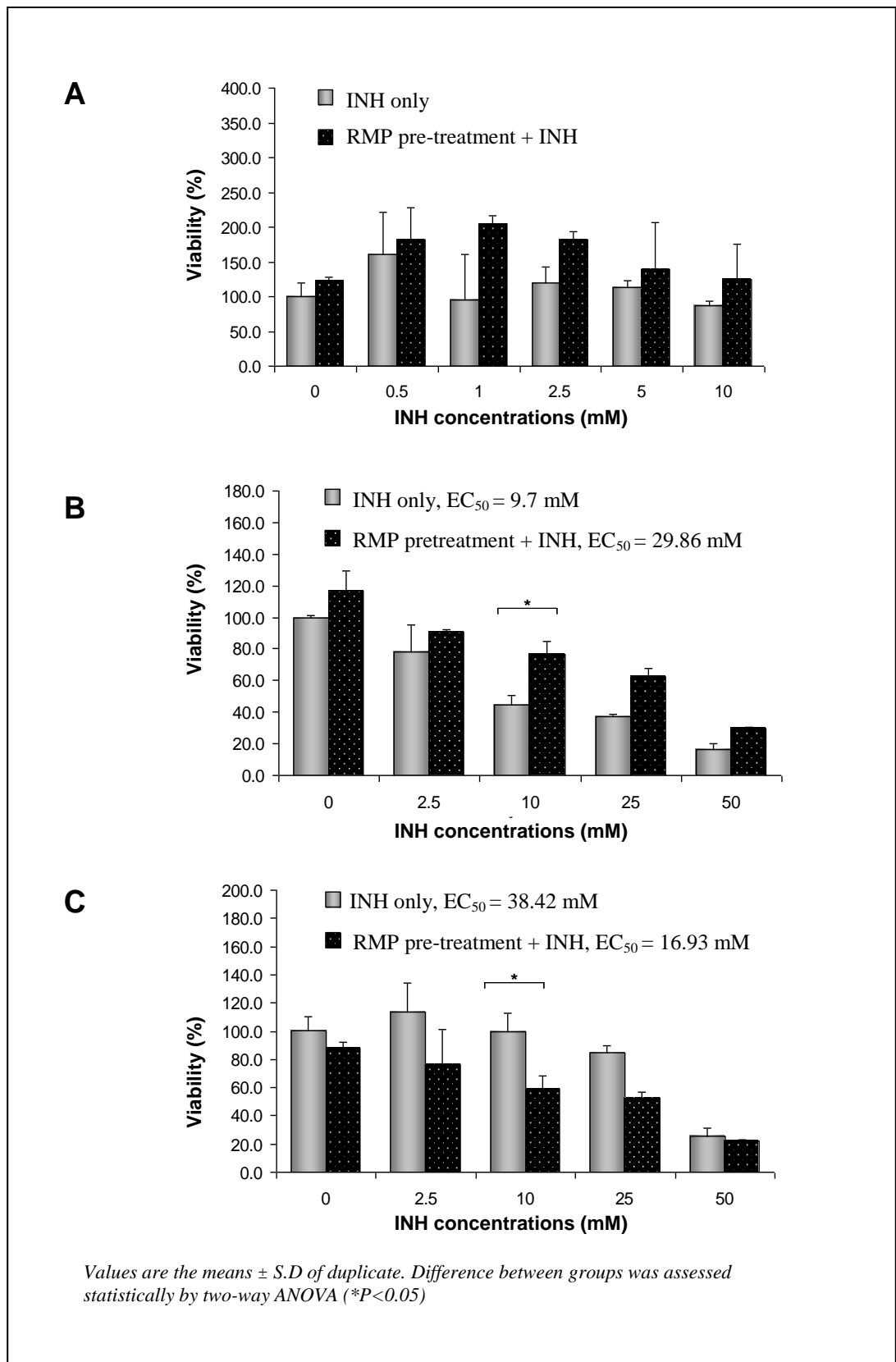


Figure 4.3 Effect of Rifampicin pre-treatment in hepatocytes derived from (A) Donor 1, (B) Donor 2 and (C) Donor 3, evaluated by the MTT assay

4.3.2 Effects of Rifampicin on mRNA expression profile

4.3.2.1 LS180 cells

The effect of RMP exposure on mRNA expression of CYP3A4, CYP2E1 and CES2 was further evaluated in LS180 cells by quantitative RT-PCR. A typical calculation of the relative expression study by using the $\Delta\Delta Ct$ method is shown in **Table 4.1**. **Figure 4.4** shows the average fold change found in LS180 cells in response to 50 μM RMP treatment to corresponding levels in vehicle controls (set as 1), normalized with respect to GAPDH mRNA levels. Following exposure to 72 h RMP, CYP3A4 and CES2 mRNA levels were significantly ($p < 0.001$) increased with 11- and 4-fold induction respectively, but the apparent elevation of these mRNA levels seen at 48 h was not statistically significant. At 48 h of exposure to RMP, CYP2E1 mRNA level was reduced by 30% compared with controls but this was not statistically significant. A longer RMP exposure time (72 h) showed no change in CYP2E1 mRNA level in LS180 cells.

Table 4.1 A sample calculation for the fold change expression of CYP3A4 after RMP treatment by using the $\Delta\Delta Ct$ method

Sample	CYP3A4 Average Ct	GAPDH Average Ct	ΔCt	$\Delta\Delta Ct$	$2^{-\Delta\Delta Ct}$
Vehicle control (0.5% DMSO)	28.51 \pm 0.40	17.34 \pm 0.17	11.16	0.00 \pm 0.54	1.0 \pm 0.35
50 μM RMP treatment (48 h)	26.47 \pm 0.21	16.99 \pm 0.12	9.49	-1.68 \pm 0.32	3.3 \pm 0.66

Data presented are means \pm S.D. of triplicates from an independent experiments of the fold increase of CYP3A4 mRNA expression levels in LS180 cells to corresponding levels in vehicle control (0.5% DMSO), normalized with respect to GAPDH mRNA levels. ΔCt values are calculated ($\Delta Ct = Ct_{CYP3A4} - Ct_{GAPDH}$), and the effects of RMP on the target cDNA was expressed relative to the amount in the vehicle control sample ($\Delta\Delta Ct = \Delta Ct_{compound} - \Delta Ct_{vehicle}$). Relative fold changes in target gene expression were determined by taking 2 to the power of the $\Delta\Delta Ct$ value ($2^{-\Delta\Delta Ct}$).

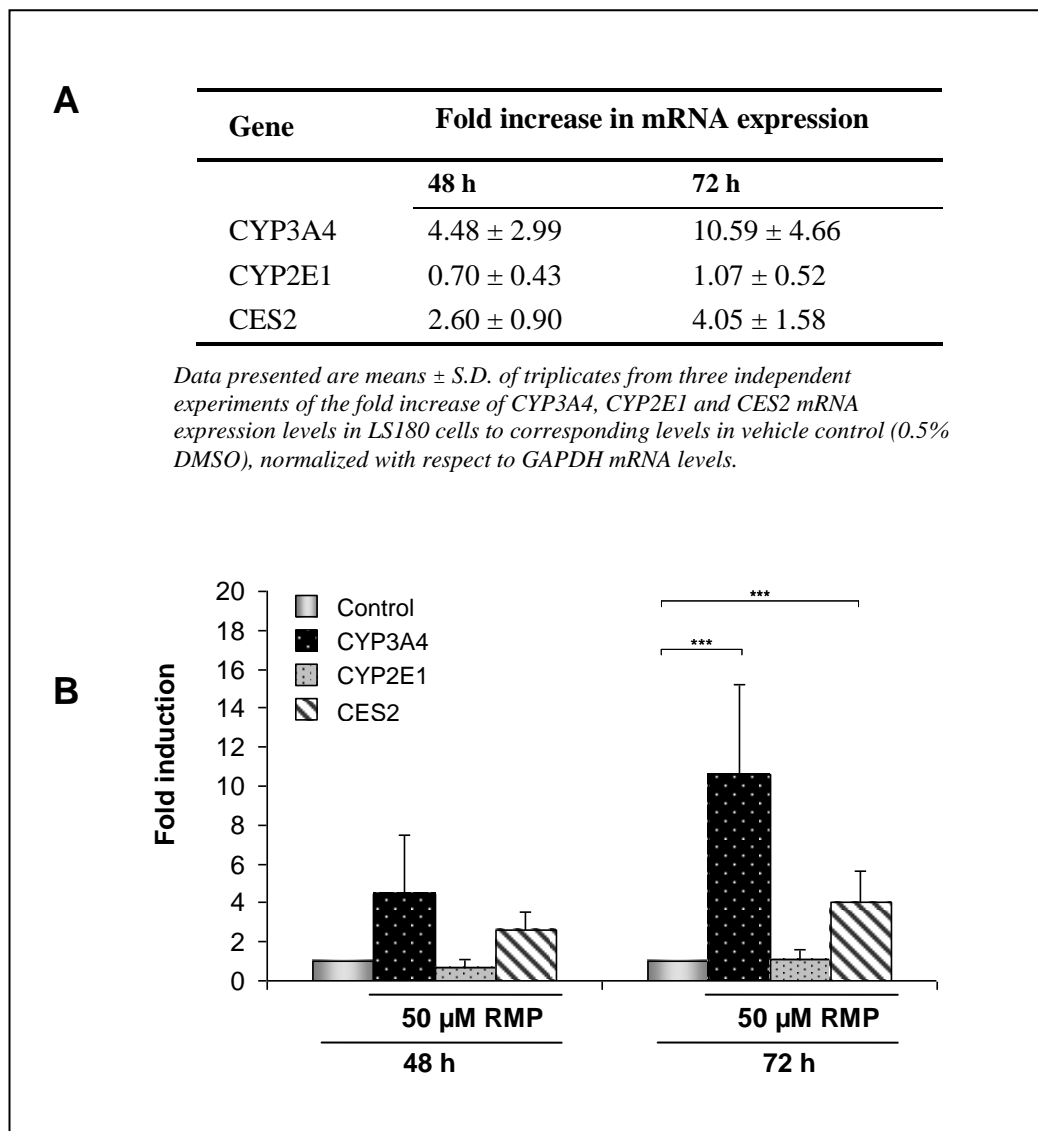


Figure 4.4 Quantitative RT-PCR analysis of the effect of 50 μ M of RMP on CYP3A4, CYP2E1 and CES2 mRNA expression level in LS180 cells.

LS180 cells were treated with 50 μ M RMP or 0.5% DMSO (control) for 48 or 72 h prior to quantitative RT-PCR analysis. (A) Table shown is the average fold change found in LS180 cells in response to 50 μ M RMP treatment to corresponding levels in controls (set as 1), normalized with respect to GAPDH mRNA. A chart (B) was then plotted and difference between groups was assessed statistically by two-way ANOVA (P <0.05, ** P <0.01, *** P <0.001).*

4.3.2.2 Human primary hepatocytes

The effect of RMP in the mRNA expression of CYP3A4, CYP2E1 and CES2 in human primary hepatocytes was evaluated by quantitative RT-PCR (**Figure 4.5**). Following exposure to 50 μ M RMP, approximately a 20-fold (Donor 1 and 2) and 10-fold (Donor 3) increase in CYP3A4 expression was observed. The CYP2E1 mRNA level in Donor 1 was not altered by RMP treatment. Conversely, a significant decrease of CYP2E1 level was found in Donor 3 ($P<0.01$) and a marginal significant decrease was observed in Donor 2 ($P=0.054$). The substantial decrease in CYP2E1 expression in Donor 2 and 3 may be associated with a rapid loss of CYP2E1 expression in these cells. RMP treatment caused significant differences in CES2 expression in all donors. Interestingly, CES2 expression was elevated in Donor 1 and 2 ($P<0.01$) but decreased in Donor 3 by 23% ($P<0.05$).

4.3.3 Determination of NAT2 genotype

Among the three donors of the human hepatocytes, Donor 1 ($NAT2^*5/NAT2^*4$) was a rapid acetylator and Donor 2 ($NAT2^*5/NAT2^*7$) and Donor 3 ($NAT2^*6/NAT2^*6$) were found to be slow acetylators. LS180 cells possessed the $NAT2^*5/NAT2^*6$ genotype and therefore was classified as slow acetylator.

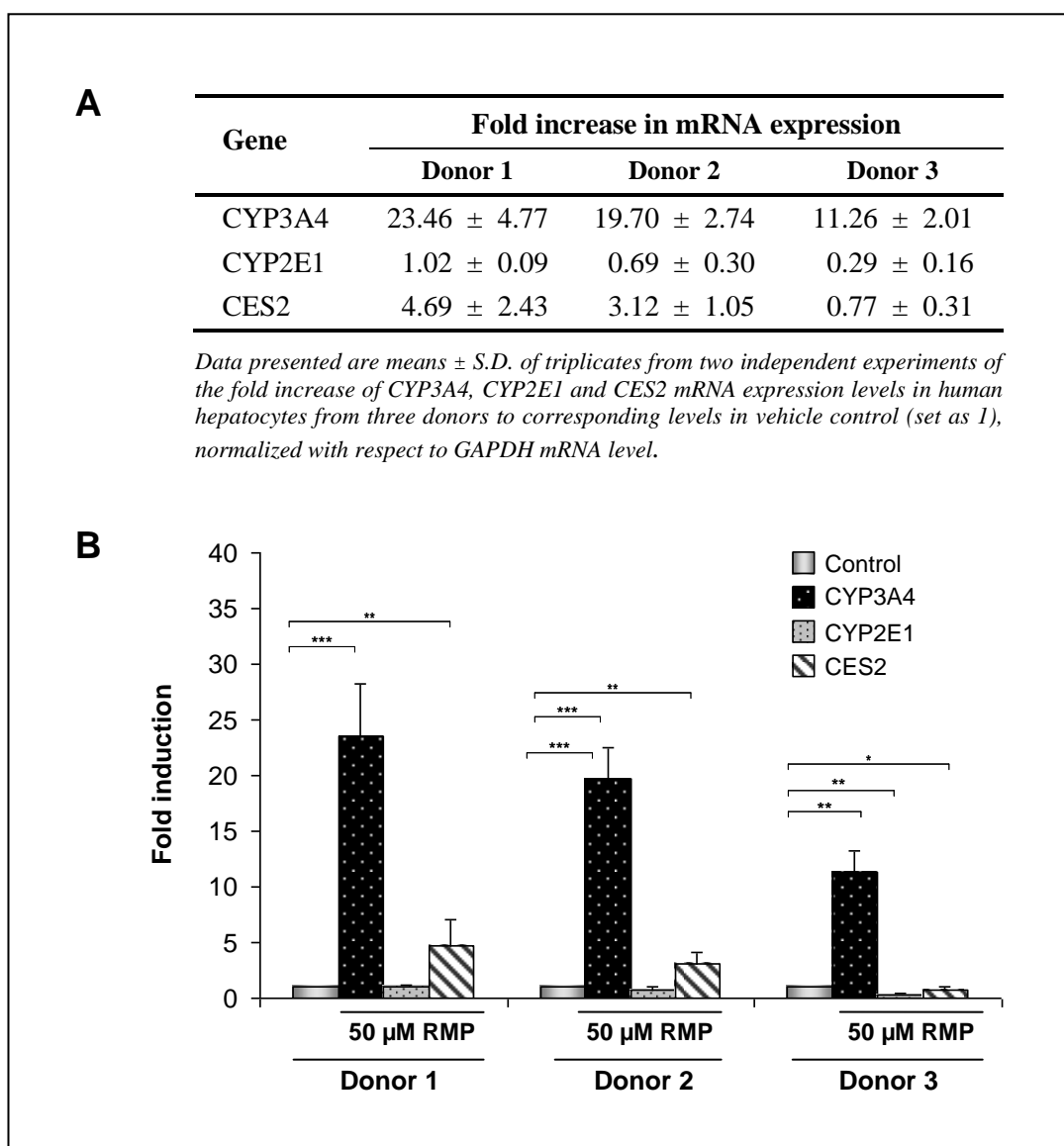


Figure 4.5 Quantitative RT-PCR of CYP3A4, CYP2E1 and CES2 transcript level in human hepatocytes exposed to rifampicin (50 μ M)

Human hepatocytes from 3 donors were treated with 50 μ M RMP or 0.5% DMSO (control) for 72 h prior to quantitative RT-PCR analysis. (A) Table shown is the average fold change of mRNA expression levels in response to 50 μ M RMP treatment to corresponding levels in controls (set as 1), normalized with respect to GAPDH mRNA. A chart (B) was then plotted and difference between groups was assessed statistically by student's t-test (P <0.05, ** P <0.01, *** P <0.001).*

4.4 Discussion

In the present study, the *in vitro* INH and PZA toxicity in LS180 was increased following pre-treatment or concurrent administration of a non-toxic concentration of RMP (50 μ M) (Figure 4.1 and 4.2). However, in the human hepatocyte samples, differential effect of RMP on INH toxicity was demonstrated by the results that RMP enhanced INH-induced cytotoxicity in Donor 3 but not in Donor 1 and 2 (**Figure 4.3**). Conversely, RMP pre-treatment was shown to provide some protection against INH-induced cytotoxicity in Donor 1 and 2. These results suggest the intriguing possibility that the altered expression or activity of drug-metabolising enzymes by RMP might have a protective role against INH toxicity. The lack of induction of CYP2E1 mRNA by RMP in both LS180 and human hepatocytes may indicate that CYP2E1 is unlikely to magnify INH toxicity caused by RMP pre-treatment. Furthermore, INH itself is an inducer of CYP2E1 (Skakun and Shman'ko, 1985) and therefore free radical generation through CYP2E1 induction could be from INH administration. It has been proposed that hepatic CYP2E1 induction by hydrazine contributes to INH-induced hepatotoxicity in rats through free radical generation (Yue et al., 2004). Rats, as well as rabbits appear more susceptible to INH-induced hepatotoxicity compared to the human due to a higher amidase activity, which catalyses the hydrolysis of INH to hydrazine, enhances CYP2E1 and therefore generates more free radicals. In our present study, RMP has shown to elevate the CES2 mRNA level in LS180 cells (approximately 2 to 4-fold) suggesting that CES2 elevation by RMP may increase the hydrolysis of INH which in turn generates more hydrazine. Therefore, it is possible that RMP can elevate CYP2E1 when RMP is given concomitantly with INH by an indirect mechanism involving CES2 induction and cause more toxicity to the cells through hydrazine formation. However, the moderate induction of CES2 did not demonstrate any obvious toxic effect in our current donor 1 and 2 hepatocyte cultures. In addition, a lack of CES2 expression was detected in Donor 3, thus suggesting that *CES2* may not play a major role in the aggravation of INH toxicity by RMP in human hepatocytes. It was recently revealed that RMP co-administration significantly reduced INH-induced CYP2E1 activity and increased the levels of the glutathione S-transferase mu isoform (GST mu) activity in rat liver (Yue et al., 2009). Previous studies in mice also demonstrated that RMP reduced the formation of free radicals by suppressing the CYP2E1 expression and may play an essential role against carbon tetrachloride-induced hepatotoxicity (Takeda et al., 2000;

Huang et al., 1995). Shen et al. presented data showing that RMP exacerbated INH toxicity in human hepatocytes possibly through CYP2E1 induction (Shen et al., 2008). In that study, hepatocytes from five patients were harvested where Donors 1-3 were used to demonstrate the effect of RMP on INH toxicity and CYP2E1 metabolic activity; Donors 3-5 were used to evaluate toxicity caused by INH only, and Donor 5 was used for CYP2E1 mRNA expression assay. The reliability of the results presented was questionable and inconclusive as the hepatocytes from different donors were used for separate experiments involving different treatments. According to Yue et al. (Yue and Peng, 2009), 4-nitrophenol hydroxylase (4-NPH) activity was the only probe used in the paper to demonstrate the increased CYP2E1 activity by RMP but CYP3A was also previously found to make a significant contribution to 4-NP activity in human and rat hepatocytes. The increase in 4-NPH activity could be due to the induction of CYP3A as RMP is a strong inducer of human CYP3A. Semi-quantitative RT-PCR but not quantitative RT-PCR was performed on Donor 5 only. The finding of Shen et al. that RMP exacerbates INH toxicity in human hepatocytes through increased CYP2E1 mRNA expression and metabolic activity is therefore questionable and needs confirmation by others. In the current study, as expected, RMP has greatly induced CYP3A4 and caused a 10 to 20-fold induction of CYP3A4 mRNA expression in LS180 and human hepatocytes. Previous observations in cultured human hepatocytes and small intestinal enterocytes revealed a marked inter-individual difference in CYP3A4 mRNA expression caused by RMP induction (Kolars et al., 1992; Watkins et al., 1989). These differences affect the oral bioavailability of CYP3A4 substrates and lead to variations in drug efficacy and/or toxicity. In the present study, we observed an approximately 10-fold CYP3A4 induction in LS180 and the hepatocytes from donor 3 after 72 h of RMP treatment. Both samples demonstrated a significant increased of INH toxicity caused by RMP. On the other hand, we observed a 20-fold CYP3A4 induction in hepatocytes from donors 1 and 2 and these observations correlated with an inhibitory effect of RMP in the development of INH toxicity. Nevertheless, it was previously reported that CYP3A4 contributed to INH toxicity in HepG2 cells by increasing the INH toxic metabolites (Vignati et al., 2005). Vignati et al. demonstrated that CYP3A4-overexpressing HepG2 cells exhibit higher INH toxicity and co-incubation with the CYP3A4 inhibitor ketoconazole prevented the INH toxicity by reducing the formation of toxic metabolites (Vignati et al., 2005). RMP did not increase the INH toxicity in rat and mouse (Yue et al., 2009; Takeda et al., 2000; Huang et al., 1995) possibly due to the lack of CYP3A

inducibility by RMP in rat and mouse because of differences in the PXR in these species (Martignoni et al., 2006). Hence, another drug-metabolizing enzyme rather than CYP3A4 could be involved in the reduced INH toxicity by RMP in hepatocytes from donors 1 and 2 in our current studies. *NAT2* acetylator status of the hepatocyte donors did not seem to be the likely factor that leads to RMP-induced INH toxicity as Donor 2 who possesses the *NAT2* slow acetylator genotype was also shown to have a reduced INH cytotoxic effect by RMP.

In addition to CYP3A4, RMP has shown to induce UDP-glucuronosyltransferase 1A (UGT1A), some glutathione-S-transferases (GSTs) and multidrug resistance 1 (MDR1) (Soars et al., 2004; Rae et al., 2001; Greiner et al., 1999). The upregulation of UGT1A by RMP through PXR and CAR promotes UGT glucuronidation of steroids and xenobiotics and thus increases the clearance of steroids and potentially toxic xenobiotics or their reactive metabolites (Soars et al., 2004; Xie et al., 2003). GSTs play an important role in the detoxification by catalysing the conjugation of reactive electrophilic alkylating agent of the xenobiotics with reduced glutathione. P-glycoprotein, a well characterised ATP-binding cassette (ABC) superfamily of transport proteins encoded by the *ABCB1* gene, is found primarily in the epithelia of drug-eliminating organs (intestine, liver and kidney) (Fromm, 2003). It is responsible for the efflux of toxins and xenobiotics from cells and has also been shown to interplay with CYP3A4 in RMP inducing drug-drug interactions (Cummins et al., 2003). RMP did not aggravate INH toxicity after 72 h treatment in Donor 1 and 2, which could be due to the general upregulation of PXR-mediated detoxification genes (UGT1A, GSTs and p-glycoprotein) by RMP which enhanced the excretion of both INH and its toxic metabolites from hepatocytes. Further work is needed to elucidate the potential role of RMP in INH-mediated hepatotoxicity.

The present results using primary human hepatocytes were slightly more sensitive to INH toxicity compared to the LS180 cell lines. Primary human hepatocytes appear to retain major drug metabolising activities including inducible cytochrome P450 enzymes, thus making it the most suitable *in vitro* model for use in drug metabolism and toxicity studies. An alternative to our current individual gene expression analysis is using the microarray approach which allows a more comprehensive evaluation of the effects of drugs by interrogating thousands of genes at once. It is an excellent tool for

gene expression studies especially in limited samples such as the primary human hepatocytes and provides useful information on the mechanism of drug toxicity. However, there are limitations in the use of human primary hepatocytes. One of the major limitations is the availability of the healthy human hepatocytes for primary culture, which makes it difficult to obtain a reproducible data. The rapid loss of specific drug metabolising enzymes especially the P450 enzymes due to dedifferentiation is a common problem with primary cultured cells (Elaut et al., 2006). It is notable that the human hepatocytes exhibit substantial interindividual variability in response to enzyme inducers such as that observed in our study. Recently a hepatoma cell line HepaRG was found to retain important hepatic functions for several weeks, including expression of the major CYP450 isoforms. It has also been shown to differentiate at levels comparable with those found in primary human hepatocytes (Andersson, 2010; Aninat et al., 2006). HepaRG cells could therefore provide an alternative to human hepatocytes for prediction of drug-induced hepatotoxicity.

In summary, these experiments indicated a modulatory effect by RMP on inhibition of cell proliferation by INH though this was rather inconsistent. The ability of RMP to induce CES2 expression at the RNA level was confirmed. Hepatocytes showing induction of CES2 by RMP treatment showed decreased INH toxicity suggesting that the hydrolysis pathway involving hydrazine formation from INH might not be an important contributor to overall toxicity.

**Chapter 5. *In Vitro* Effects of NAT2 Allelic Variants on
Isoniazid Toxicity**

5 *In vitro* effects of *NAT2* allelic variants on isoniazid toxicity

5.1 Introduction

The gene encoding *NAT2* is polymorphic, thus resulting in rapid and slow acetylator phenotype. As described previously in section 1.6, the predominant pathway of isoniazid (INH) is acetylation by the hepatic enzyme *NAT2*. Early *NAT2* phenotyping study has shown that the fast acetylator phenotype with detectable *NAT2* is associated with an increased risk of INH-induced DILI (Mitchell et al., 1975). However, later studies have revealed that individuals with the slow acetylator phenotype lacking functional *NAT2* catalytic activity are more susceptible to developing INH-induced DILI due to accumulation of the toxic metabolite acetylhydrazine (Lauterburg et al., 1985; Dickinson et al., 1981; Timbrell et al., 1980). Approximately 50% of Caucasians in Europe are of slow acetylator phenotype and are less efficient than rapid acetylators in the metabolism of INH (Blum et al., 1991). The slow acetylator phenotype results from nonsynonymous SNPs in the *NAT2* coding region. These SNPs have been identified and characterized for their functional and structural effects (**Table 5.1**) (Walraven et al., 2008).

Previous studies have investigated the relationship between *NAT2* genotype and acetylator phenotype through recombinant expression of *NAT2* alleles or haplotypes and individual SNPs using bacteria (Hein et al., 1995; Hein et al., 1994), yeast (Fretland et al., 2001) and mammalian (Zang et al., 2007a; Zang et al., 2004; Blum et al., 1991) cell systems. Some of these *NAT2* alleles including *NAT2**5 (341T>C), *NAT2**6 (590G>A) and *NAT2**7 (857G>A) showed reduced levels of *NAT2* protein and also decreased *NAT2* catalytic activity when compared with *NAT2**4 (Zang et al., 2007b; Blum et al., 1991). *NAT2**5 and *NAT2**6 alleles account for more than 90% of slow acetylator alleles of the European Caucasians (Blum et al., 1991). Our present study on *NAT2* genotyping has revealed that among the European control subjects, *NAT2**5 and *NAT2**6 alleles account for 60% and 36% of the slow acetylator alleles respectively. A strong linkage disequilibrium was reported among the 341T>C, 481C>T and 803A>G polymorphisms in European Caucasians as well as North Indian population (Batra et al., 2006).

The aim of this chapter is to examine the functional significance of *NAT2* acetylation phenotypes using an *in vitro* overexpression approach to characterise *NAT2* acetylation phenotypes and their relevance to the development of isoniazid-induced hepatotoxicity. Two recombinant plasmids contained the *NAT2**4 and *NAT2**5 (possessing 341T>C and 481C>T variants) alleles were constructed to represent the rapid and slow acetylation phenotype respectively.

Table 5.1 Non-synonymous SNPs in human *NAT2* function and structure*

SNP	rs identifier	Amino acid change	<i>NAT2</i> allele/haplotype	Functional effect(s)	Structural Effect(s)
190C>T	1805158	R64W	<i>NAT2*19</i>	Decreased stability	Loss of electrostatic interactions
191G>A	1801279	R64Q	<i>NAT2*14</i> cluster & others	Decreased stability	Loss of electrostatic interactions
341C>T	1801280	I114T	<i>NAT2*5</i> cluster	Increased protein degradation	Conformational change
364G>A	4986996	D112N	<i>NAT2*12D</i>	Decreased protein	Catalytic triad disruption
411A>T	4986997	L137F	<i>NAT2*5I</i>	Decreased protein	Conformational change
434A>C	-	Q145P	<i>NAT2*17</i>	Decreased protein	Conformational change
499G>A	-	E167K	<i>NAT2*10</i>	Decreased protein	Conformational change
590G>A	1799930	R197Q	<i>NAT2*6</i> cluster & others	Decreased stability	Loss of electrostatic interactions
803A>G	1208	K268R	<i>NAT2*12</i> cluster & others	No effect	None expected
845A>C	56054745	K282T	<i>NAT2*18</i>	Slight decreased stability	Loss of electrostatic interactions
857G>A	1799931	G286E	<i>NAT2*7</i> cluster	Decreased protein	Altered active site size/shape

* Table is adapted from (Walraven et al., 2008)

5.2 Materials and Methods

5.2.1 Choice of Cell line

To determine the best choice of cell line for NAT2 overexpression study, HepG2, LS180 and Huh 7.5 cell lines were genotyped for common *NAT2* alleles using the PCR-RFLP method (see section 3.4). The cell line with the slow acetylator phenotype was used for NAT2 overexpression studies.

5.2.2 Construction of NAT2 recombinant stable cells

Two 879 bp *NAT2* open reading frame DNA fragments representing the wild-type *NAT2*4* and *NAT2*5* (possessing 341T>C and 481C>T variants) alleles were amplified by PCR from DNA samples of known *NAT2* genotype. Comparison of both DNA inserts containing the *NAT2*4* and *NAT2*5* alleles are shown in **Figure 5.1**. The PCR parameters were 35 cycles at 95°C for 1 min, 55°C for 1.5 min, and 72°C for 1.5 min; forward primer: 5'-GCCACCATGGACATTGAAGCAT-3' and reverse primer: 5'-CTAAATAGTAA GGGATCCATCACC -3'. The PCR products were separated on a 2% agarose gel and purified using QIAGEN Gel Extraction Kit. The amplified product was cloned in the mammalian expression vector pTARGET (Promega) to generate a rapid acetylator recombinant (RAR) containing the *NAT2*4* allele and a slow acetylator recombinant (SAR) containing the *NAT2*5* allele (see section 2.5). The presence of the recombinant construct was confirmed by digesting the plasmid DNA (3 µl) with *EcoRI* restriction enzyme. **Figure 5.2** shows the presence of DNA inserts after *EcoRI* digestion of pTARGET plasmids. The sequences of both RAR and SAR plasmids were confirmed by sequencing (see section 2.4.6). The plasmids were then stably transfected into HepG2 cells and the cells were selected with 500 µg/ml G418 antibiotic for 3-4 weeks until the G418-resistant clones were established (see section 2.5.4). The stably transfected cells were then maintained in 250 µg/ml G418.

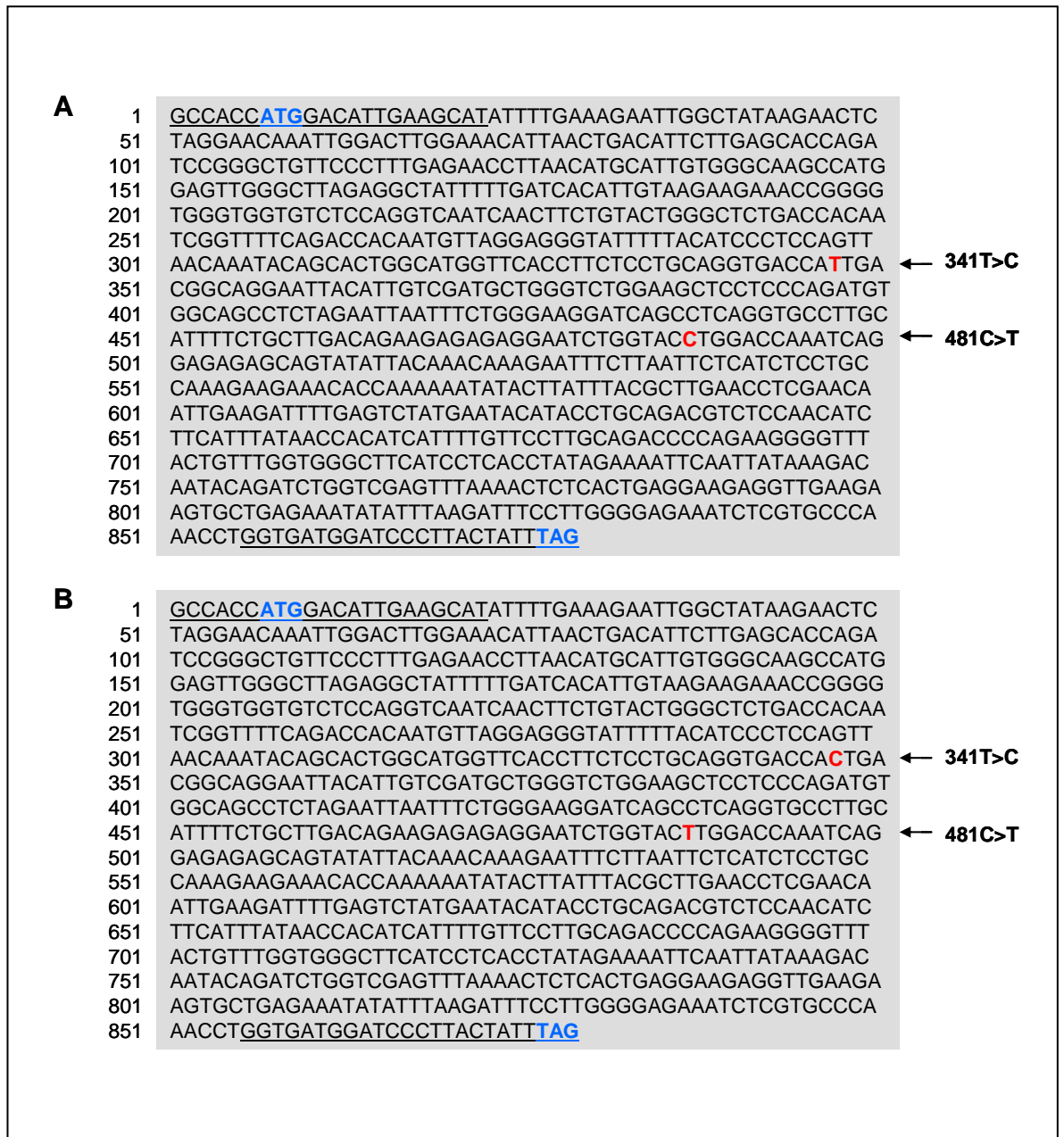


Figure 5.1 Comparison of DNA sequences of rapid acetylator recombinant (RAR) and slow acetylator recombinant (SAR) plasmids.

*The DNA sequences of NAT2 coding region of RAR (NAT2*4 allele) and SAR (NAT2*5) plasmids are shown in (A) and (B) respectively. Primers used to amplify the DNA fragments of NAT2*4 and NAT2*5 alleles are shown in underline; the start codon (ATG) and stop codon (TAG) are shown in blue bold letters; the 341T>C and 418C>T single nucleotide polymorphisms (SNPs) are highlighted in red bold letters.*

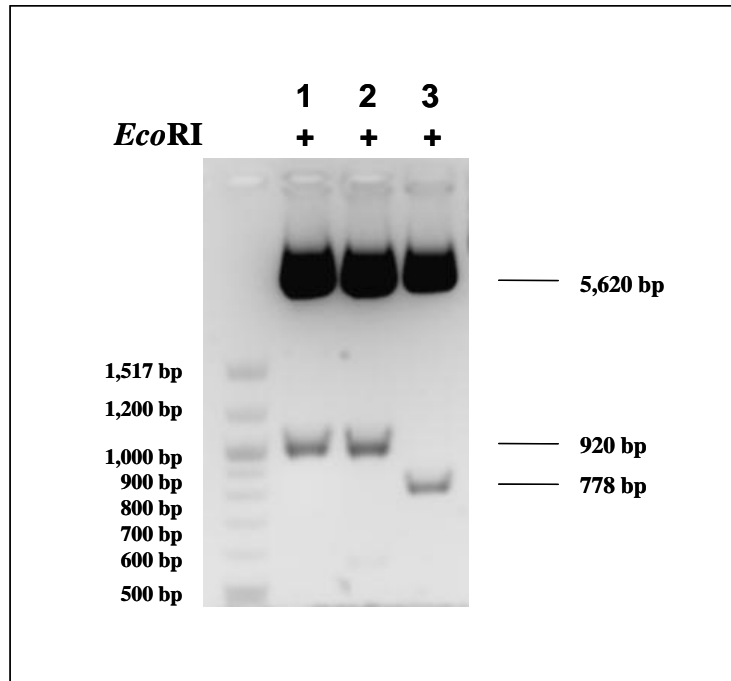


Figure 5.2 Ethidium bromide-stained agarose gel pattern showing digested pTARGET plasmids

*The presence of desired DNA fragments after EcoRI digestion demonstrates the successful cloning of insert DNA into the pTARGET plasmids. The upper bands (approximately 5,620 bp) of lane 1, 2 and 3 are the linearised pTARGET plasmids after EcoRI digestion. The lower bands of lane 1 and 2 are DNA fragments of NAT2*4 and NAT2*5A alleles respectively while the lower band of lane 3 is the cDNA fragment of GSTA4.*

5.2.3 Recombinant expression of NAT2 alleles

The NAT2 overexpression efficacy of rapid acetylator recombinant (RAR) and slow acetylator recombinant (SAR) were assessed by RT-PCR and immunoblotting. The non-transfected cells were used as a control. Immunoblotting and RT-PCR were performed as described in Section 2.6 and 2.7. For the immunoblot, quantification of the protein bands was done by uploading a scanned image of the blot saved as a GIF file into the program ImageJ and following the procedure for analysis described for this program (<http://rsb.info.nih.gov/ij/>).

5.2.4 N-acetyltransferase-2 enzyme assay

The NAT2 enzyme activity in RAR, SAR and non-transfected cells were measured by the bioluminescent NAT2 enzyme assay (Promega) using a novel luciferin derivative, Luciferin-NAT2 as a specific substrate. The Luciferin-NAT2 is prosubstrate for the light-generating reaction of firefly luciferase. As shown in **Figure 5.3**, Luciferin-NAT2 is substantially converted to a more active luciferin substrate by NAT2 enzyme that is detected in a second reaction with luciferin detection reagent (LDR). LDR containing firefly luciferase reacts with active luciferin to produce light. The amount of light generated is proportional to NAT2 enzyme activity. Briefly, cells were harvested and disrupted by sonication in buffer (66 mM NaH₂PO₄, pH 7.2, 1 mM EDTA, and 2 mM DTT). The cell lysates were centrifuged at 12,000g for 10 min at 4°C and the supernatants were immediately assayed. Protein concentration was determined using BioRad DC Protein Assay (see section 2.9.1). A stock solution of Luciferin-NAT2 (1 mM) was prepared in a solution of water and methanol (1:1) containing 2 mM HCl. The assay was performed by mixing 25 µl of 80 µM Luciferin-NAT2 solution in assay buffer (100 mM HEPES, pH 8) with 23 µl of cell lysate (1:10 dilution with assay buffer) and 2 µl of 10 mM acetyl coenzyme A (Acetyl-CoA). The final concentrations of Luciferin-NAT2 and Acetyl-CoA were 40 µM and 400 µM respectively. A no-enzyme background control for each sample was prepared by replacing acetyl-CoA with distilled water. The mixture was then incubated for 0-12 h prior to the addition of LDR (50 µl). The luminescence was measured 20 min later using a Modulus luminometer (Turner Biosystems). NAT2 enzyme activity for each sample was calculated by subtracting the background control and expressed in relative luminescent units per mg

of sample per h (RLU/mg/h). A positive control consisting of rat liver lysate was included each time when the assay was performed. Preparation of rat liver lysate is described in section 5.2.5. **Figure 5.4** shows the increased NAT2 activity of rat liver lysate using various concentration of Luciferin-NAT2 in assay buffer (2.5-80 μ M).

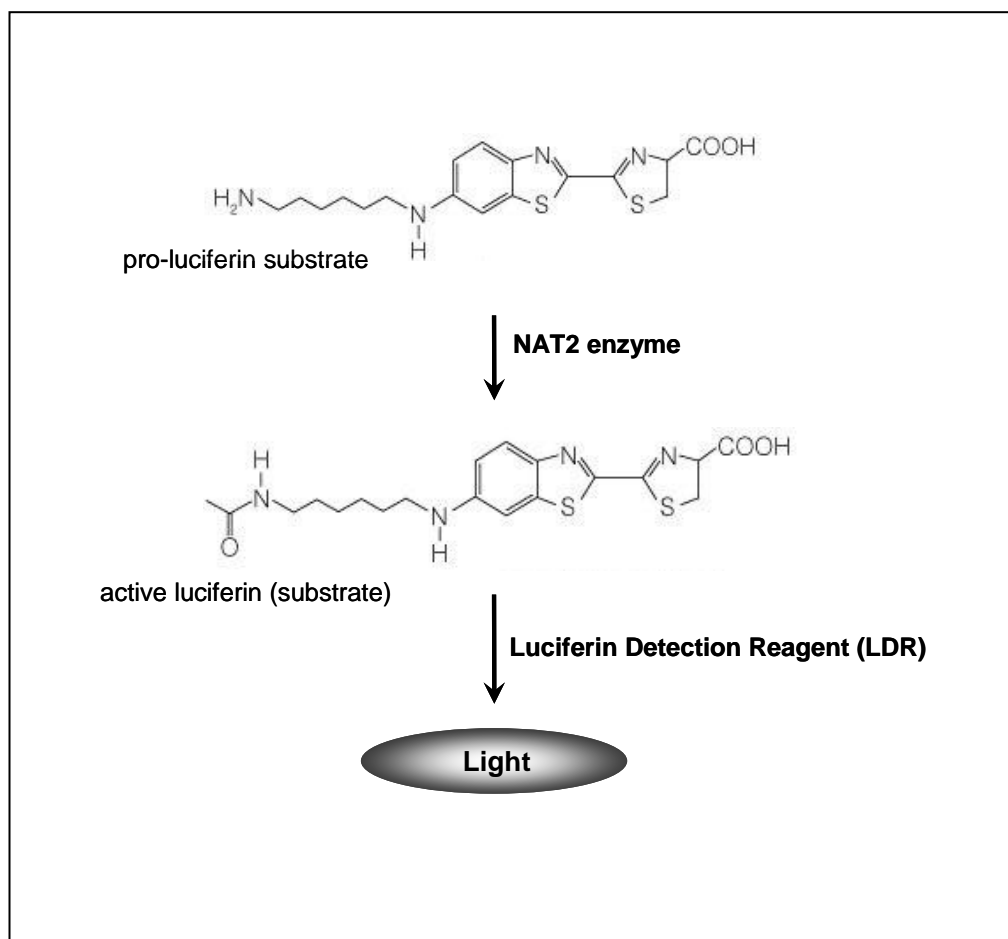


Figure 5.3 Detection of NAT2 enzyme activity using Luciferin-NAT2

The Luciferin-NAT2, a novel luciferin derivative, is a prosubstrate for the light-generating reaction of firefly luciferase. Acetylation of Luciferin-NAT2 by NAT2 enzyme produces a more active luciferin substrate for the light-generating enzyme in the luciferin detection reagent (LDR). LDR generates light in the proportion to the activity of the NAT2.

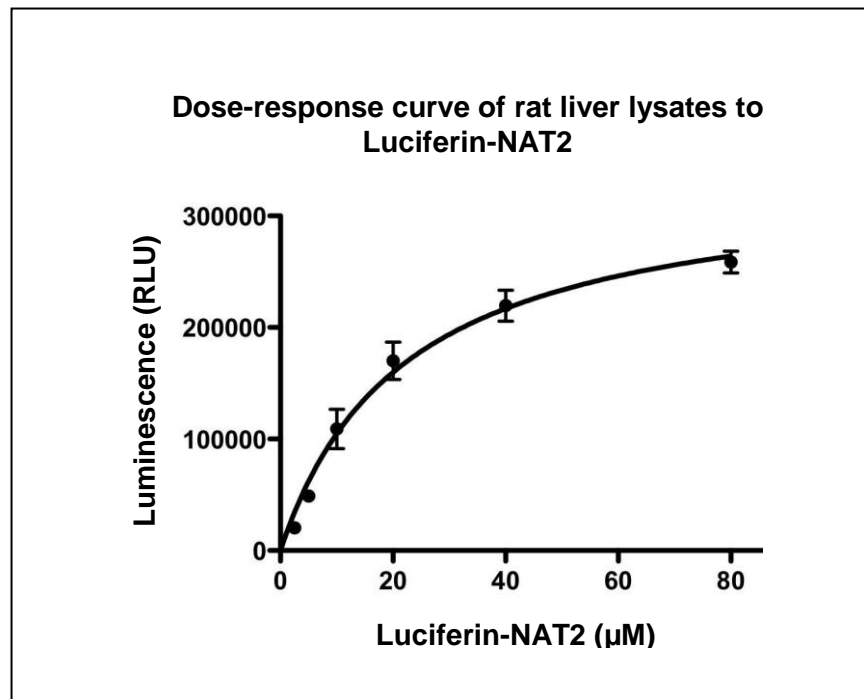


Figure 5.4: NAT2 activity in rat liver lysate using Luciferin-NAT2

The K_m of Luciferin-NAT2 with rat liver lysate is $22.2 \pm 4.0 \mu\text{M}$. Rat liver lysate were incubated with various concentration of Luciferin-NAT2 in assay buffer for 1 h before the addition of Luciferin Detection Reagent. Values presented are means \pm SD, $n=3$.

5.2.5 Rat liver lysate preparation

Rat liver (2 g) was washed repeatedly using homogenisation buffer (0.25 M sucrose in 10 mM Tris-HCl, pH 7.4 containing 1 mM EDTA), transferred into a pre-cooled beaker and minced into small pieces. Homogenisation buffer (10 ml) was then added into the beaker and the entire contents of the beaker were then transferred into a pre-cooled Potter-Elvehjem homogeniser tube. Homogenisation of the liver was done by five passes of a Teflon pestle. All steps were carried out at 4°C to reduce proteolysis. The homogenate was then transferred into a Beckman centrifuge tube and centrifuged at 1000 g for 10 min at 4°C. The supernatant was removed into a new centrifuge tube and subjected to centrifugation at 12,500 g at 4°C for 15 min. The supernatant was analysed on proteins and stored at -80°C.

5.2.6 Functional characterisation of NAT2 acetylation phenotypes

To test whether NAT2 acetylation phenotypes affect isoniazid toxicity, RAR, SAR and non-transfected HepG2 cells were subjected to MTT test, GSH assay, DNA fragmentation assay and Caspase-3 activity assay (see section 2.8-2.11). A two-way ANOVA analysis was performed to identify specific differences between selected groups using GraphPad Prism 5.0. In all cases, $P < 0.05$ was required for significance to identify specific differences.

5.3 Results

5.3.1 Sequencing

Sequencing traces showing the variation of SNPs (341T>C and 418C>T) in the NAT2 coding region of RAR and SAR plasmid constructs are presented in **Figure 5.5**. The complete sequencing traces of plasmid inserts for both plasmids are shown in Appendix A & B. Sequence analysis showed that no variant (wild type) was detected in the NAT2 coding region of RAR plasmid while SAR plasmid contained no other variant except for 341T>C and 481C>T (mutant alleles).

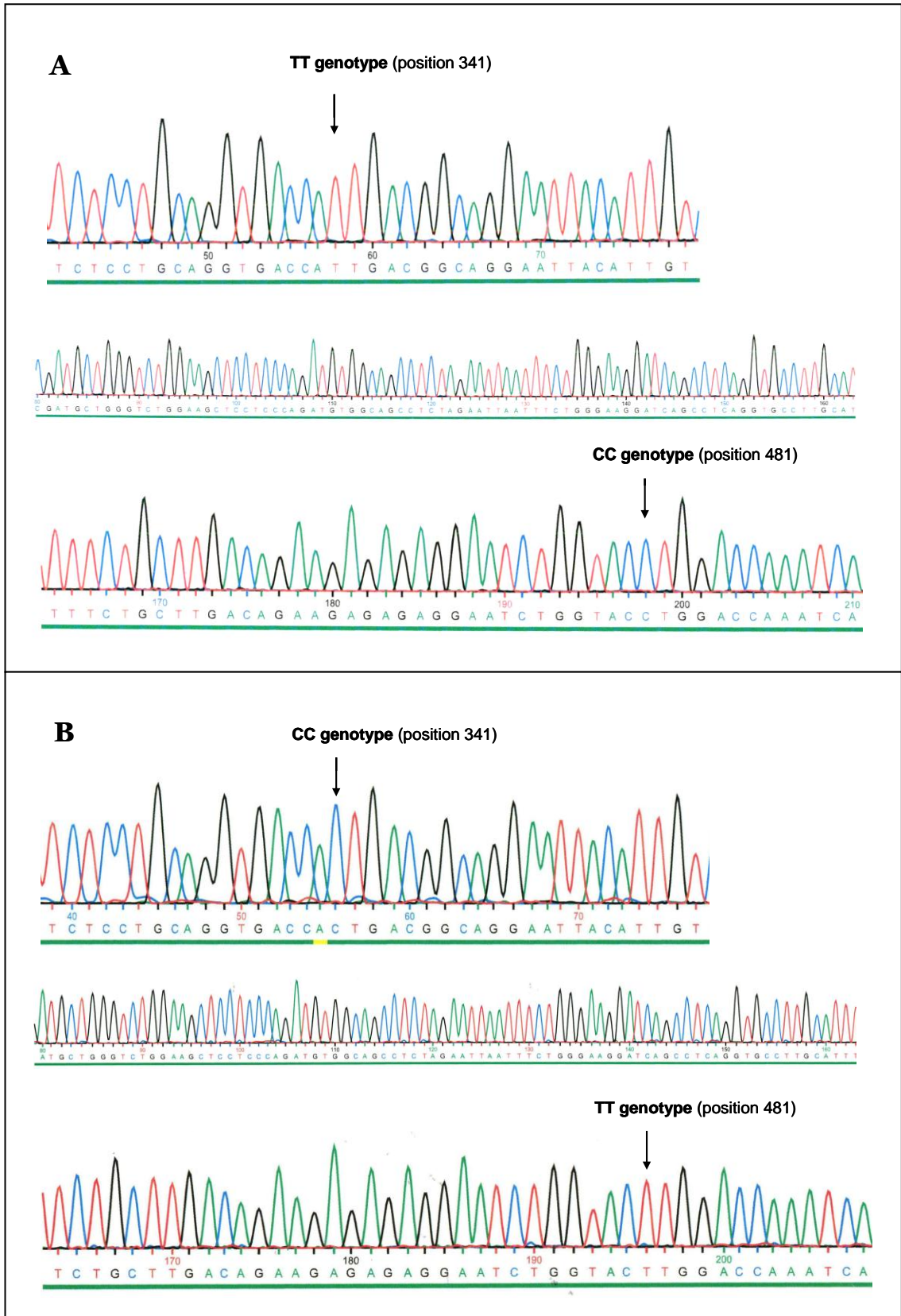


Figure 5.5 Sequencing result of the (A) rapid acetylator recombinant (RAR) plasmid containing the NAT2*4 wild-type allele and (B) slow acetylator recombinant (SAR) plasmid containing the NAT2*5 allele (341T>C and 481C>T)

NAT2 genotypes of HepG2, LS180 and Huh 7.5 cell lines were determined using PCR-RFLP methods. Huh7.5 was found to be a rapid acetylator (*NAT2**4/*4) while HepG2 and LS180 cells possess *NAT2**5/*6 slow acetylation genotypes. HepG2 was chosen for the expression studies and was stably transfected with RAR and SAR plasmids to study the effect of *NAT2* overexpression. *NAT2* overexpression efficacy of rapid acetylator recombinant (RAR) and slow acetylator recombinant (SAR) were assessed by RT-PCR and immunoblotting at mRNA and protein levels respectively. **Figure 5.6** shows the semiquantitative RT-PCR analysis of *NAT2* mRNA expressions in non-transfected, RAR and SAR cells. B-actin and GAPDH were used as a control. The *NAT2* mRNA level in RAR and SAR cells are markedly higher by the presence of the more intense bands when compared to the non-transfected cells. However, *NAT2* mRNA expression was similar between RAR and SAR cells. It was then further confirmed by quantitative RT-PCR analysis which showed no expression differences between RAR and SAR-stably transfected cells (**Table 5.2**). The *NAT2* mRNA expression in RAR and SAR were increased 364.76 ± 85.13 and 335.04 ± 74.31 fold respectively compared to the non-transfected cells. **Figure 5.7** shows the expression level of *NAT2* at protein level in (A) non-transfected, (B) RAR and (C) SAR cells. Relatively high level of *NAT2* expression was found in RAR and SAR cells compared to the non-transfected cells. However, *NAT2* protein expression in SAR is lower when compared to the RAR cells. Quantification of the *NAT2* bands in the immunoblot using ImageJ software revealed that *NAT2* protein expression in SAR was 39% of that for RAR though untransfected cells also showed a detectable band of intensity about 10% of the RAR cells (**Table 5.3**).

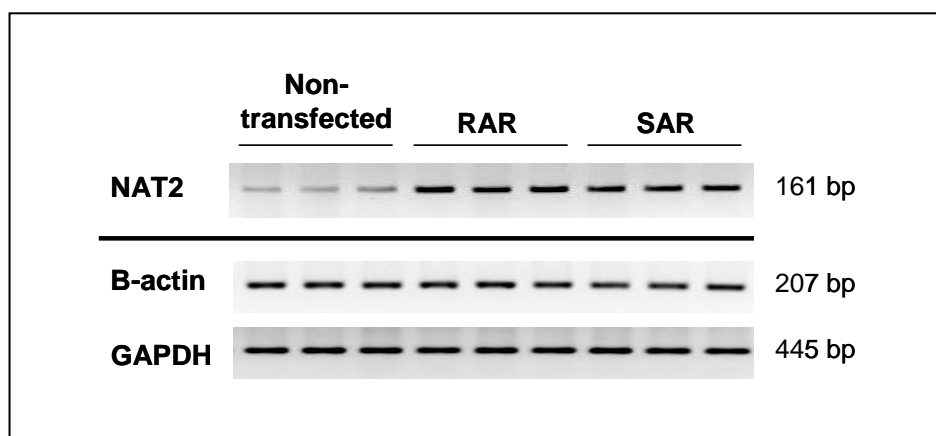


Figure 5.6 Semiquantitative RT-PCR analysis of NAT2 mRNA expressions

Table 5.2 Quantitative RT-PCR of NAT2 transcript level in non-transfected, RAR and SAR stably transfected cells

Cell lines	Average fold increase in mRNA expression
Non-transfected HepG2	1.00 ± 0.02
RAR-stably transfected HepG2	364.76 ± 85.13
SAR-stably transfected HepG2	335.04 ± 74.31

Data presented are means ± S.D. of triplicates from three independent experiments of the fold increase of NAT2 mRNA expression levels in RAR and SAR-stably transfected cells to corresponding levels in non-transfected cells, normalized with respect to GAPDH mRNA levels.

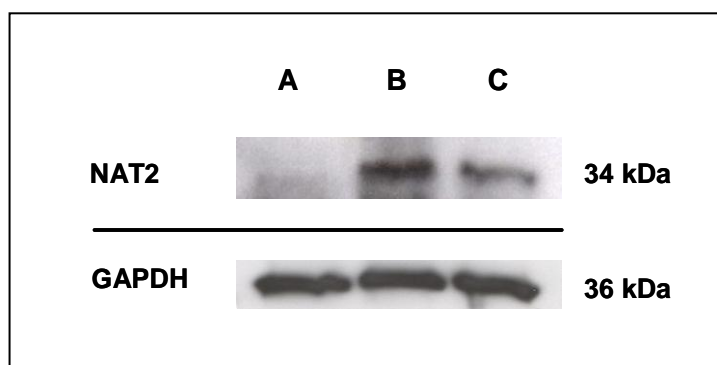


Figure 5.7 Western blot of NAT2 protein expressions in non-transfected (A), RAR-stably transfected (B) and SAR-stably transfected cells (C)

Table 5.3 Quantification of recombinant protein expressions of NAT2 alleles in HepG2 cells normalized to GAPDH expression using ImageJ software

Cell lines	Integrated density value*	Fold increase in NAT2 protein expression
Non-transfected HepG2	34465	1.0
RAR-stably transfected HepG2	345894	10.0
SAR-stably transfected HepG2	135169	3.9

* *Integrated density values of NAT2 was normalized to respective GAPDH level*

5.3.2 Determination of NAT2 enzyme activity

To determine whether overexpression of NAT2 enzyme results in catalytically active enzyme in RAR and SAR cells, the NAT2 enzyme activities were assayed and compared to the non-transfected cells (control). NAT2 enzyme activities were readily detectable in RAR, SAR and control cells incubated with 40 μ M Luciferin-NAT2 for 0-12 h. **Figure 5.8** displays the linearly increased of the relative luminescent units (RLU) over the entire time course with $r^2 > 0.9$ for all samples. NAT2 enzyme activity for each sample are presented in **Table 5.4** and expressed in relative luminescent units per mg protein per h (RLU/mg/h). A significantly higher NAT2 activity ($p < 0.05$) was detected in the RAR and SAR compared to the control cells, indicating the functional overexpression from both RAR and SAR plasmids. As shown in **Table 5.4**, RAR cells demonstrated a 4.3-fold increase in NAT2 activity over constitutive HepG2 activity compared with SAR where there was still an increase but this was significantly lower at 2.2 fold ($p < 0.05$). These data suggest that cell lines showing overexpression of NAT2 from the RAR and SAR clone have been created, with the RAR clone exhibiting significantly higher NAT2 activity than SAR.

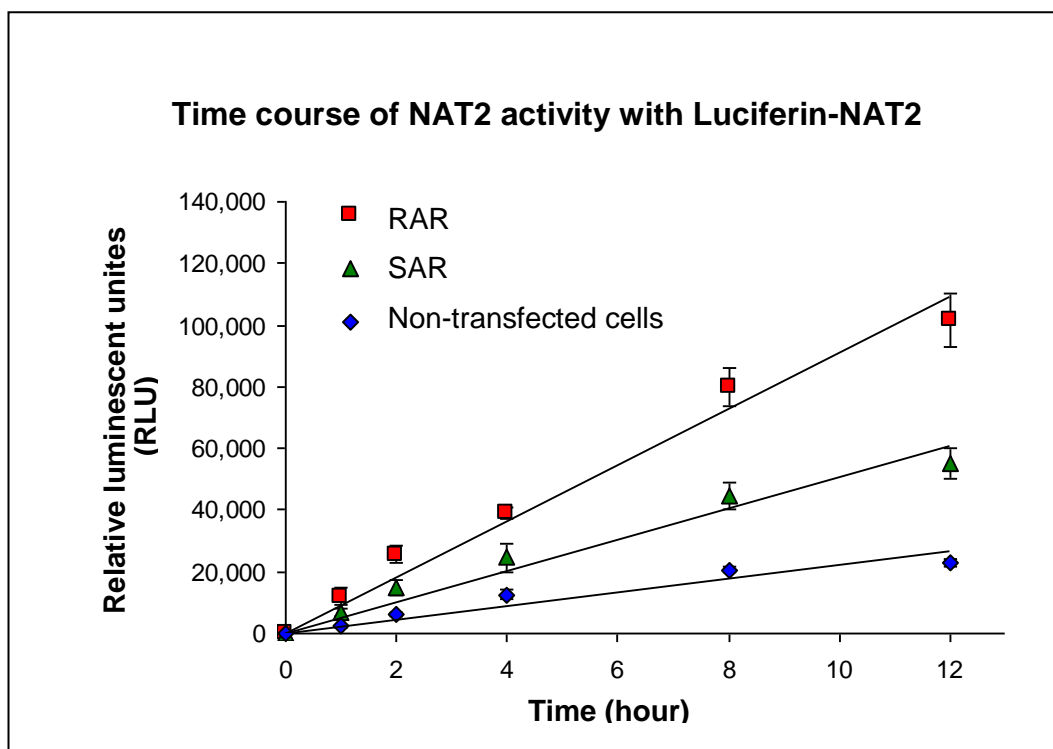


Figure 5.8 Time course of NAT2 activity with Luciferin-NAT2

Cell lysates of RAR, SAR and non-transfected cells were incubated with 40 μM Luciferin-NAT2 with or without the presence of 400 μM Acetyl-CoA for 0-12 h prior to adding LDR. Zero-time values were measured in samples where the acetyl-CoA was withheld until after LDR addition. Data presented are means \pm S.D. of triplicates from two independent experiments. The reactions were linear over the entire time course with $r^2 > 0.9$ for all samples.

Table 5.4 NAT2 activities of RAR, SAR and non-transfected cells as evaluated by the bioluminescent NAT2 enzyme assay

Cell lines	NAT2 activity (RLU/mg/h)	Fold increase
Non-transfected	367.60 \pm 22.76	1
SAR	825.66 \pm 82.16	2.2
RAR	1590.11 \pm 127.76	4.3

Data presented are means \pm S.D. of triplicates from two independent experiments
[†] Net NAT2 activities in RAR and SAR were calculated by subtracting the activity measured in the non-transfected cells

5.3.3 Functional characterisation of *NAT2* acetylation phenotypes

5.3.3.1 Effects of *NAT2* overexpression on cell proliferation

The functional consequences of difference *NAT2* acetylation phenotypes on INH toxicity were evaluated. MTT assays were performed and the EC₅₀ values were determined. As shown in **Figure 5.9**, no apparent differences were observed in RAR and SAR cells compared to the control cells. The EC₅₀ values of the control cells was slightly higher (28.43 mM) than the RAR (EC₅₀=24.73 mM) and SAR cells (24.76 mM). However, these differences were not statistically significant.

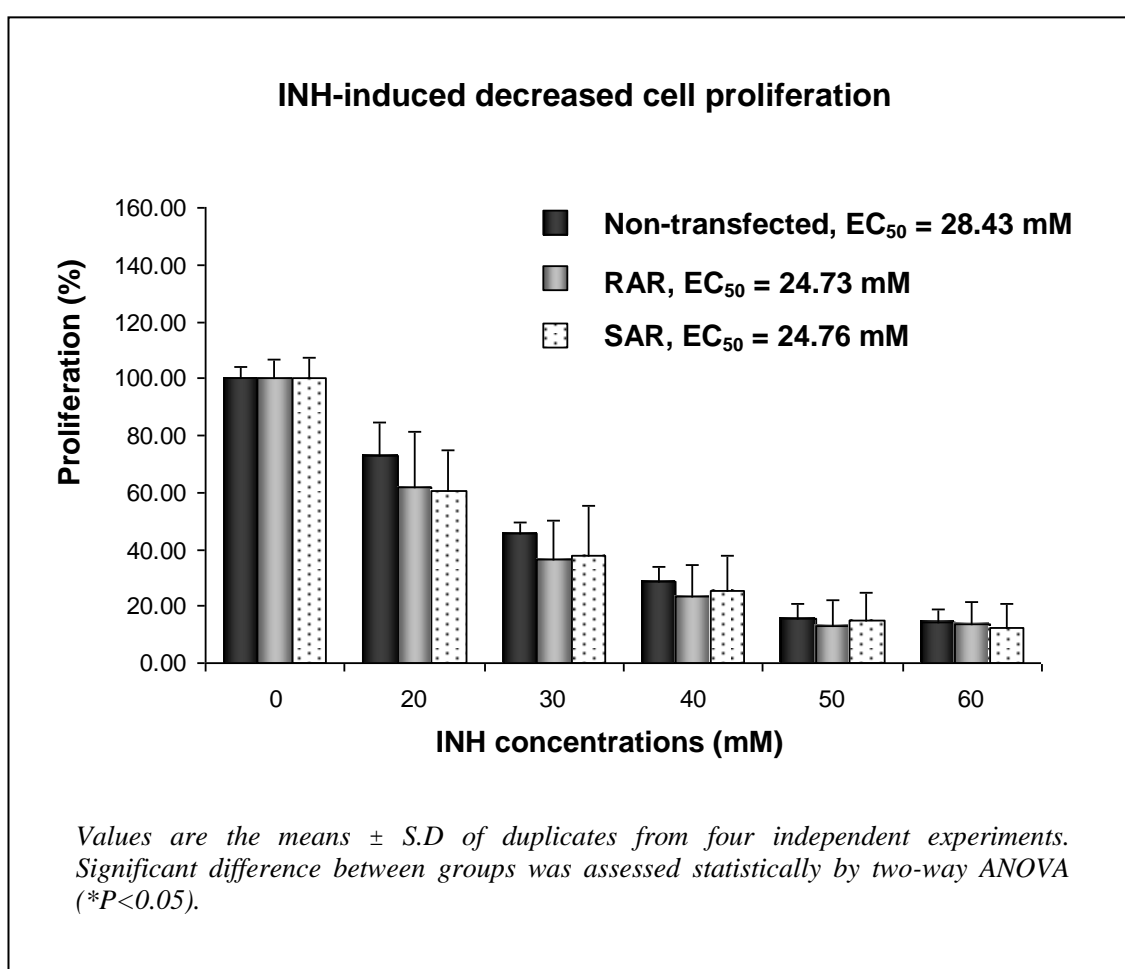


Figure 5.9 INH-induced decreased cell proliferation at 48 h in RAR, SAR and non-transfected cells

5.3.3.2 *Effects of NAT2 overexpression on cellular GSH and GSSG*

RAR, SAR and the non-transfected cells were assessed for cellular content of GSH and GSSG after 48 h exposure to INH. The effect of *NAT2* overexpression on total glutathione (GSH+GSSG) and GSH/GSSG ratio are summarized in **Figure 5.10** and **Figure 5.11** respectively. INH exposure decreases the total glutathione levels in all cell types. No significant differences in total glutathione levels were observed in RAR and SAR compared to the non-transfected cells. The GSH/GSSG ratio was further calculated and a significant decrease was found between RAR and the non-transfected cells at 20 mM INH ($p<0.05$) and 40 mM INH ($p<0.001$). Compared to the non-transfected cells, GSH/GSSG levels were lower in SAR and a significant decrease was observed at 40 mM INH treatment ($p<0.05$). GSH/GSSG levels in RAR appeared lower than SAR at various concentration of INH treatment but these differences were not statistically significant. These data indicate that overexpression of *NAT2* may slightly decrease the GSH/GSSG ratio, indicating an increased level of intracellular oxidative stress.

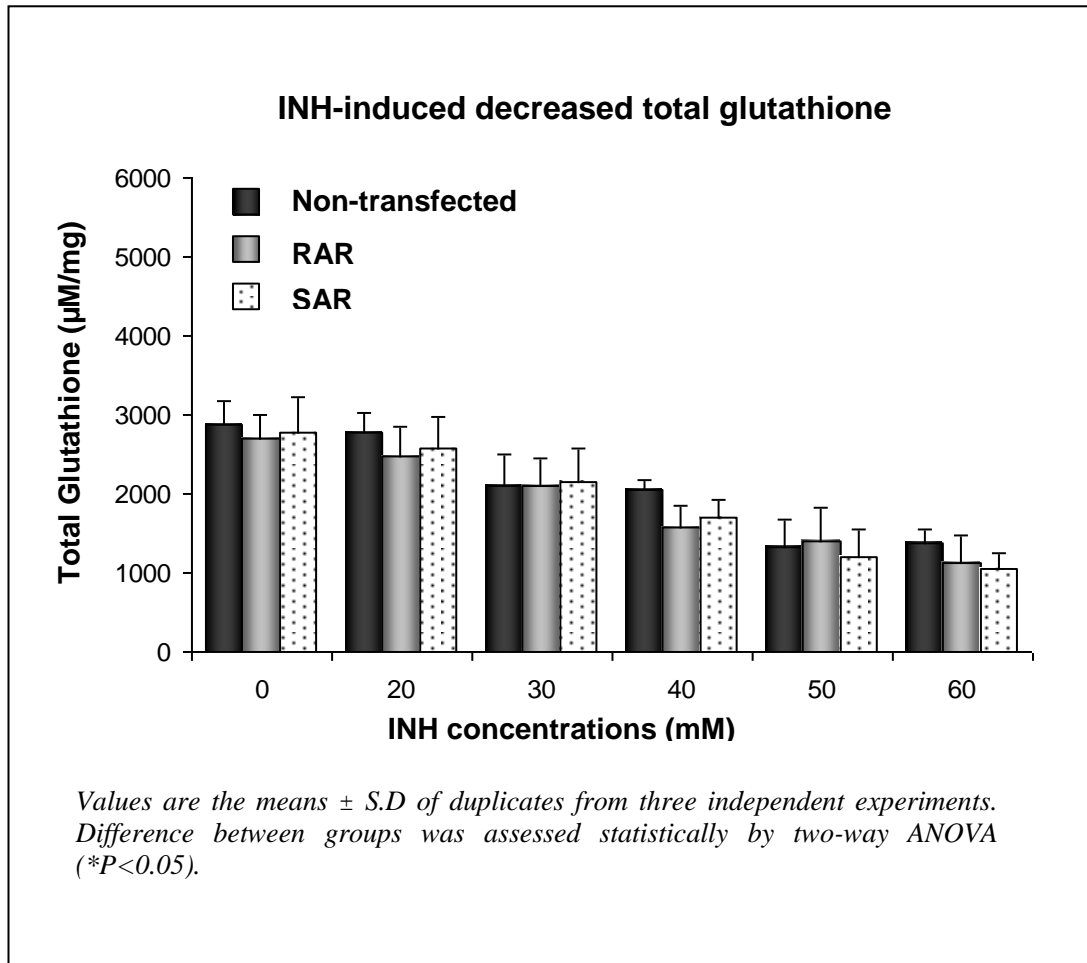


Figure 5.10 The effect of NAT2 overexpression on total glutathione depletion in RAR, SAR and non-transfected cells

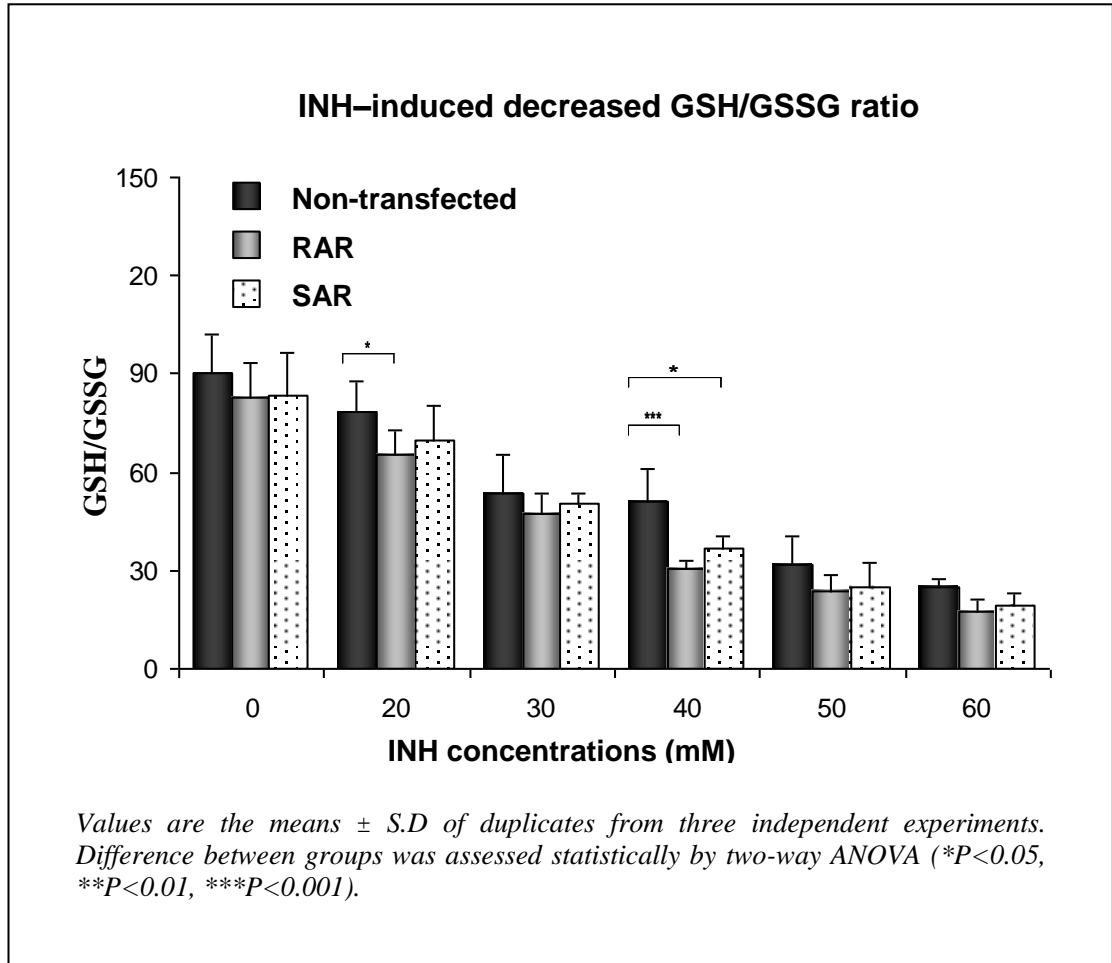


Figure 5.11 The effect of *NAT2* overexpression on GSH/GSSG ratio in RAR, SAR and non-transfected cells

5.3.3.3 Effects of NAT2 overexpression on INH-induced apoptosis

To investigate the functional role of NAT2 overexpression on INH-induced apoptosis, DNA fragmentation assay and caspase-3 activity assay were performed in RAR, SAR and non-transfected cells. As shown in **Figure 5.12**, apoptotic DNA laddering was observed in all cell types at the INH concentration of 50 and 60 mM. Nevertheless, an early apoptotic ladder pattern was seen in RAR at 40 mM of INH treatment. RAR are cells with higher acetylation capacity than SAR and appear to be more susceptible to INH-induced apoptotic DNA fragmentation. Caspase-3 activity assay was then performed to verify the findings of DNA fragmentation assay. **Figure 5.13** shows the significant increased of caspase-3 activity in RAR and SAR compared to the non-transfected cells ($p < 0.05$) when exposed to various concentration of INH. However there was no significant difference of caspase-3 activity observed between RAR and SAR cells. These findings suggest that RAR cells are marginally more susceptible to apoptosis at high INH concentrations.

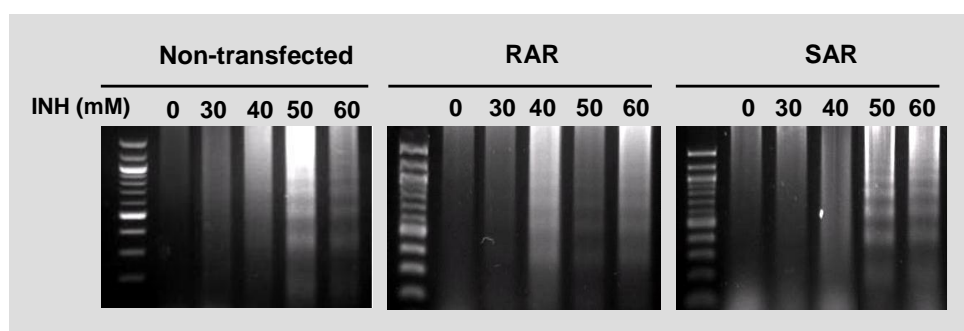


Figure 5.12 Effects of NAT2 overexpression on INH-induced DNA fragmentation

Image shown is the representative from one of two duplicates. DNA fragmentation assay was performed as indicators of apoptosis following 48 h of INH treatment. The apoptotic ladder patterns were seen in all cell types at 50 and 60 mM INH. However, RAR were found to be more susceptible to apoptosis induced by 40 mM INH compared to SAR and non-transfected cells as a more intense apoptotic DNA laddering was observed in these cells.

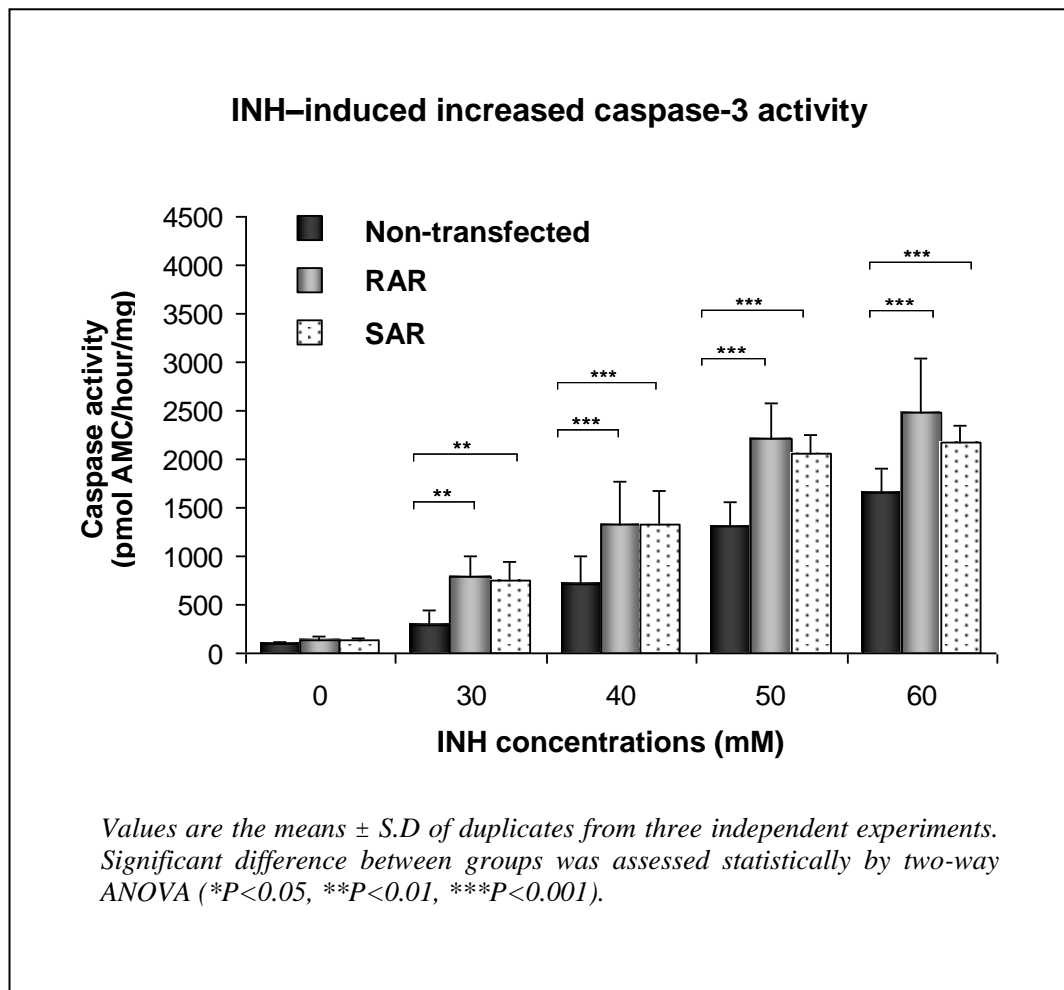


Figure 5.13 INH-induced increased caspase-3 activity in RAR, SAR and non-transfected cells

5.4 Discussion

These experiments aimed to look at the effect of stably expressing a wild-type NAT2 gene on isoniazid toxicity in a cell line that was homozygous for variant NAT2 alleles and therefore had a slow acetylator phenotype. As a control, a variant (*NAT2*5*) gene was expressed in a parallel experiment. The first step involved the isolation of HepG2 cell lines stably expressing the relevant genes. Previous studies have described the transient expression of *NAT2*4* and a few of the mutant NAT2 alleles or haplotypes including a combination of *NAT2*5* alleles (341T>C and 481C>T) in monkey kidney *COS-1* cells (Zang et al., 2007; Zang et al., 2004; Blum et al., 1991) and *E.coli* (Hein et al., 1994). The 341T>C polymorphism results in an amino acid change (Ile-114 to Thr) which substitutes a polar (Thr) for a non-polar (Ile) amino acid, whereas 481C>T is a synonymous SNP which has no effect on NAT2 mRNA, protein or catalytic activity (Zang et al., 2007). Blum and colleagues reported that the M1 allele which contain the 341T>C and 481C>T variants greatly reduced the expression of NAT2 protein without affecting mRNA expression (Blum et al., 1991). They concluded that the combined variants of these two SNPs together affected impaired translation of NAT2 protein when compared to the expression of *NAT2*4* allele using *COS-1* cells. However, Hein and colleagues did not observe any significant reduction of NAT2 protein in recombinant NAT2 containing both 341T>C and 481C>T variants in expression studies in *E.coli* (Hein et al., 1994), indicating the distinction between recombinant NAT2 protein expression system in prokaryotic and eukaryotic cells. Our present study showed that the stable expression of slow acetylator recombinant (SAR) featuring both NAT2 variants (341T>C and 481C>T) in HepG2 cells has a significantly reduced NAT2 protein expression level but a similar mRNA transcription level compared to the rapid acetylator recombinant (RAR), agreeing with the earlier finding using *COS-1* cells. However the level of NAT2 protein in cells overexpressing the *NAT2*4* reference allele was 6.1-fold higher than in *COS-1* cells overexpressing 341T>C variant (Zang et al., 2004). Zang and colleagues have also demonstrated the 341T>C variant showed eight-fold lower NAT2 catalytic activity compared to *COS-1* cells overexpressing *NAT2*4* allele using sulfamethazine as substrate (Zang et al., 2004). In another transfection study using sulfamethazine as NAT2 substrate, Blum and colleagues reported that NAT2 catalytic activity from the M1 allele (*NAT2*5*) was about 5-fold lower compared to that seen when the *NAT2*4* allele was transfected (Blum et al., 1991). It was proposed that

the lower NAT2 protein and enzyme activity due to 341T>C polymorphism resulted from enhanced protein degradation (Zang et al., 2004). Our current study has demonstrated a 2.7-fold statistically significant lower NAT2 activity in SAR stable transfected cells compared to RAR stable transfected cells. The observed lower NAT2 catalytic activity (2.7-fold) agrees well with the lower NAT2 protein expression (3.1-fold lower than expression from *NAT2*4*) by western blotting. Nevertheless, the observed difference in NAT2 catalytic activity in SAR compared to RAR using Luciferin-NAT2 as substrate was smaller than those reported previously. The significant overexpression of NAT2 enzymes in both SAR and RAR cells leads to a substantial net increase in NAT2 enzyme activity over background (non-transfected HepG2 cells) could be the reason why a smaller than expected difference was detected between the RAR and SAR cells. Ideally, a pTARGET empty plasmid or a nonsense vector should have been stably expressed in parallel to eliminate any non-specific effects which could have led to an underestimate of the difference in enzyme activity between RAR and SAR cells. A sensitive direct assay for isoniazid acetylation would have been more appropriate but this was not available for the current study. A comparison with a *NAT2*6* construct similar to the *NAT2*4* and **5* constructs used here would also be of interest.

We studied three different cell lines, the original "slow acetylator genotype" HepG2 cells, HepG2 cells with increased expression of mutated NAT2 and HepG2 cells with expression of wild-type NAT2. Previous studies showed that INH treatment could decrease cell proliferation and increase oxidative stress with mitochondrial dysfunction accompanied by apoptosis seen in HepG2 cells as well as in other cell lines (Bhadoria et al., 2010; Schwab and Tuschl, 2003). Both studies have demonstrated that INH could produce apoptosis in HepG2 cells at millimolar concentrations (26 mM) and therefore a comparable concentration in the range of 20 to 60 mM was used in our present study. The results from MTT assay showed that overexpression of either wild-type or variant *NAT2* has no effect on cell proliferation as no significant differences of the EC₅₀ values were observed in RAR and SAR cells compared to the control cells. However, when the cells were assessed for cellular content of GSH and GSSG, the GSH/GSSG ratio in both RAR and SAR cells were significantly lower than the controls, indicating that overexpression of NAT2 may increase the level of intracellular oxidative stress. However, the effect in RAR cells seems greater than for SAR. Overexpression of either

NAT2 construct also increased INH-induced apoptosis in HepG2 cells. These results suggested that the INH reactive metabolites generated by *NAT2* rather than the parent drug might be responsible for the development of INH-induced toxicity in HepG2. Acetylhydrazine, a toxic metabolite of INH has been suggested to be the cause of INH-induced hepatotoxicity, especially in slow acetylation phenotype (Lauterburg et al., 1985; Timbrell et al., 1980; Ellard et al., 1978). Individuals with rapid acetylator phenotype were suggested to be less susceptible to INH-induced DILI as they convert acetylhydrazine more rapidly into non-toxic diacetylhydrazine and decrease acetylhydrazine accumulation. On the other hand, slow acetylators with reduced *NAT2* enzyme convert acetylhydrazine to diacetylhydrazine more slowly and thus increase acetylhydrazine accumulation. Acetylhydrazine can be hydrolysed into hydrazine, a major INH toxic metabolite and it has been shown that hydrazine is of greater quantitative significance in slow than in rapid acetylator (Sarich et al., 1996). Slow acetylators with increased acetylhydrazine accumulation will hydrolyse some of the acetylisoniazid to hydrazine via this alternate pathway. More recent studies have suggested that hydrazine rather than acetylhydrazine could be the cause of INH-induced hepatotoxicity (Sarich et al., 1996; Gent et al., 1992; Noda et al., 1983).

In our present study, there was no statistically significant difference in functional consequences of *NAT2* acetylation phenotypes on INH toxicity observed between RAR and SAR cells though some suggestions that toxicity was greater in RAR were seen. The relatively small effects and lack of specificity could be due to the short duration of INH treatment (48 hours) in these cells and perhaps a longer duration for the cells exposed to INH is needed to allow the possibility for accumulation of more toxic effects of hydrazine and acetylhydrazine. Another reason could be due to that the amount of hydrazine formed indirectly by this alternate pathway via hydrolysis of acetylisoniazid was very little and may not cause serious toxicity to the cells. Conceivably, hydrazine formed directly by direct hydrolysis of INH may play an important role in the development of hepatotoxicity. It has been demonstrated that RMP enhance idiosyncratic hepatocellular reactions in slow acetylators by inducing formation of hydrazine from isoniazid (Sarma et al., 1986). A more recent study has also demonstrated that serum concentration of hydrazine was significantly higher in subjects with *NAT2* slow acetylator phenotypes, high concentration of serum RMP, and *GSTM1* null genotype (Fukino et al., 2008). These may suggest that polymorphisms in the

NAT2 alone may not fully account for the development of ATD-DILI and there could be another ATD metabolising enzymes or additional factors that contribute the idiosyncratic nature of liver toxicity caused by anti-tuberculosis medication. Though these preliminary findings suggesting overexpression of NAT2 results in increased INH toxicity are interesting, there are a number of limitations. In particular, HepG2 cells are not a perfect model for liver metabolism because they show relatively low levels of P450 and other xenobiotic metabolising enzyme expression (Westerink and Schoonen, 2007). However, it would not have been possible to perform these stable transfection studies in primary hepatocytes and HepG2 was the best alternative available.

Chapter 6. The Protective Role of Glutathione S-transferase
A Class Isoforms against Cytotoxic Effects of Isoniazid

6 The protective role of glutathione S-transferase A class against cytotoxic effects of isoniazid

6.1 Introduction

As described in chapter 5, INH-induced hepatotoxicity appears to be associated with reactive metabolites produced by NAT2, a major drug-metabolizing enzyme in INH metabolism. Exposure to reactive INH metabolites is believed to play a central role in accumulation of reactive oxygen species (ROS) within hepatocytes that may promote intracellular oxidative stress and lead to hepatocyte death via apoptosis and necrosis. Thus several enzyme systems including glutathione S-transferase enzymes (GSTs) and superoxide dismutase 2 (*SOD2*) may play a major role against liver injury by its detoxification effects through the conjugation of glutathione with harmful electrophiles generated during oxidative stress and lipid peroxidation. The inter-individual differences in the ability to detoxify certain drugs and their toxic intermediates could increase susceptibility to DILI due to toxic metabolites accumulation. As described in section 1.7.3, genetic polymorphisms of *GSTM1*, *GSTT1* and *SOD2* have previously found to be associated with ATD-DILI. In our present genotyping study (Chapter 3), some evidence for associations between polymorphisms in the glutathione S-transferase genes, particularly *GSTM1* and *GSTA4* and ATD-DILI was found, suggesting a protective role of these enzymes in preventing ATD-DILI. The aim of this chapter is to assess the protective role of glutathione S-transferase (GSTs) and their association with INH-induced DILI by using *in vitro* overexpression and siRNA knockdown approaches. In view of the well characterised role of *GSTA4* in detoxification of 4-hydroxynonenal (Hubatsch et al., 1998), a product of lipid peroxidation, the main aim of the experiments described in this chapter was to perform *in vitro* studies on this isoform in relation to INH toxicity.

6.2 Materials and Methods

6.2.1 The overexpression effect of hGSTA4 on INH toxicity

6.2.1.1 Construction of hGSTA4 recombinant stable cell lines

Total RNA was isolated from human primary hepatocytes and reverse transcription of mRNA was performed to synthesize cDNA (see section 2.5). Amplification of hGSTA4 cDNA was performed by using PCR. The PCR conditions were 35 cycles at 95°C for 60s, 51°C for 90s and 72°C for 90s; forward primer: 5'-AAGCTATCATGGCAGCAAG G-3' and reverse primer: 5'- GACAATACCATCTCTAGGA -3'. The PCR product (729 bp) was analysed in a 2% agarose gel and purified using Qiagen Gel Extraction Kit. It was used as the DNA insert for the recombinant plasmid construction (**Figure 6.1**) and cloned into the mammalian expression vector pTARGET (Promega). The presence of the recombinant construct was confirmed by digesting the plasmid DNA (3 µl) with *EcoRI* restriction enzyme (**Figure 5.2**) and the nucleotide sequence of the plasmid containing the DNA inserts were confirmed by sequencing (see section 2.4.6). The plasmid was then stably transfected into HepG2 cells using GeneJuice transfection reagent and the cells were selected with 500 µg/ml G418 antibiotic for 3-4 weeks until the G418-resistant clones were established (see section 2.5.4). The stably transfected cells were maintained in 250 µg/ml until further analysis. The overexpression of GSTA4 in the stably transfected cells were evaluated using quantitative RT-PCR and western blotting. The non-transfected HepG2 cells were used as a control.

6.2.1.2 Functional analysis of GSTA4 overexpression in HepG2 cell line against isoniazid hepatotoxicity

To test whether hGSTA4 overexpressing cell lines have a protective role against isoniazid hepatotoxicity, hGSTA4-stable transfected cell lines were harvested prior to apoptosis markers and cell viability analyses. G-418 selective culture medium were removed and replaced with fresh growth medium for 2 days. Cells were then subjected to MTT test, DNA fragmentation assay and Caspase-3 fluorometric assay (see section 2.8, 2.10 and 2.11).

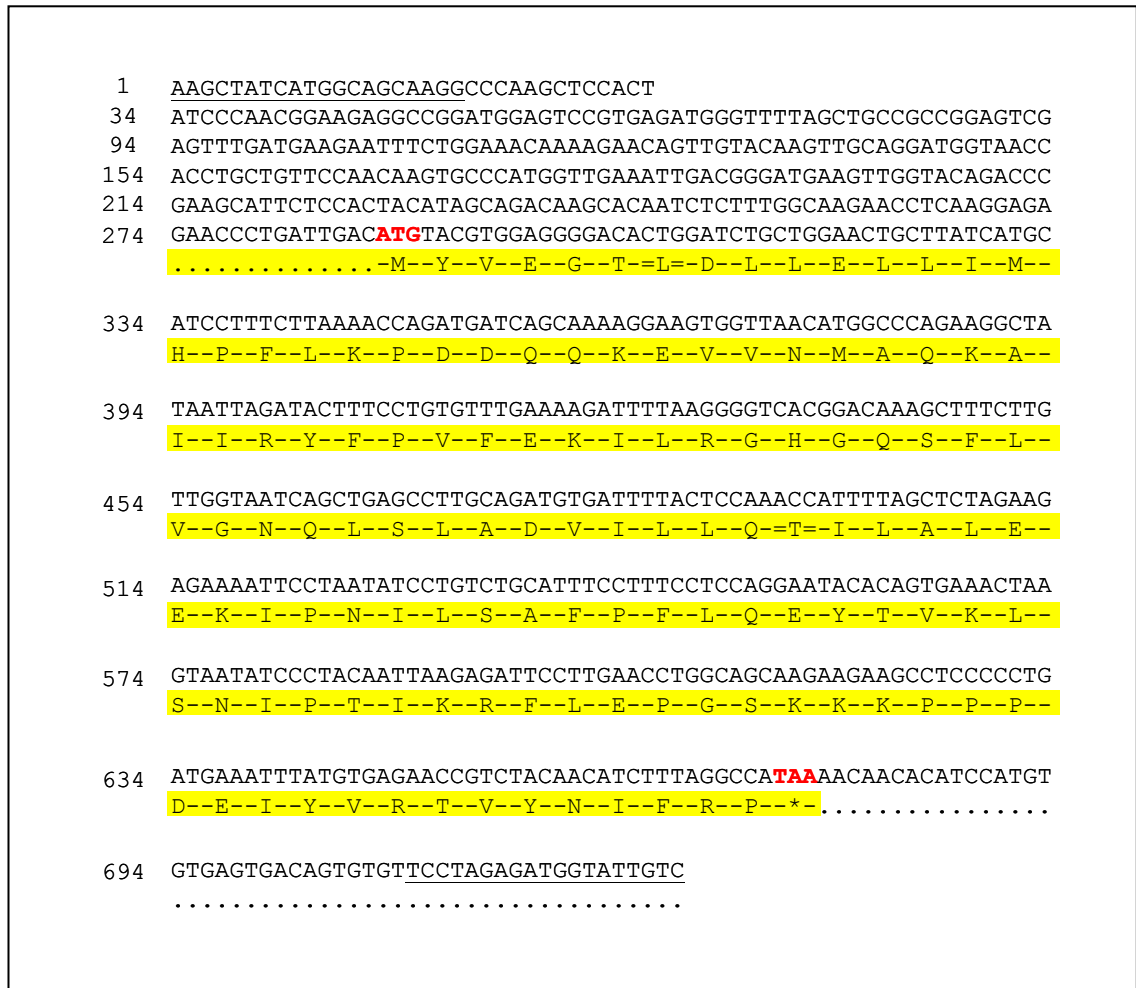


Figure 6.1 Nucleotide sequences of plasmid insert possessing *GSTA4* coding region.

*Figure shown is the nucleotide sequences of plasmid insert (729bp) containing *GSTA4* coding region. Primers used to amplify the DNA fragments are shown in underline; the start codon (ATG) and stop codon (TAG) are shown in red bold letters; the protein sequences are highlighted in yellow.*

6.2.2 Effects of GSTA1 inhibition in INH Cytotoxicity

6.2.2.1 Detection of GSTA1 expression in mammalian cells

To assess the significance of *GSTA1* mRNA and protein expression, HepG2, LS180, Caco-2, and Huh 7.5 cell lines were evaluated using quantitative RT-PCR and western blotting. Cell line with the presence of highly abundant GSTA1 protein was used for siRNA studies.

6.2.2.2 Small interfering RNA (siRNA) knockdown of GSTA1

Small interfering RNA (siRNA) *GSTA1* knockdown experiment was performed using validated Silencer Select predesigned siRNA (Ambion, Applied Biosystems). The siRNA sequences consisted of sense: r(AAUAAAGUACUUUACCUGA)dTdT and antisense: r(UUAGGUAAAGUACUUUAUU)dGdT, targeting the exon 7 of the *GSTA1*. A reverse transfection technique was performed using RiboJuice siRNA transfection reagent (Novagen, Merck Biosciences). Cell lines were passaged every 2-3 days to ensure rapid growth and doses were optimised to ensure highest transfection efficiency. Briefly, cells were detached from the flask to form a suspension of 1,000,000 cells per well in a 6-well plate format. For each well, 2 µl of RiboJuice were mixed thoroughly in 224 µl of serum free medium in a sterile tube and incubated for 5 min at room temperature. The optimized concentration of siRNA was then added into the mixture and incubated further at room temperature for 10 min. The siRNA/RiboJuice/medium complex mixture was then added into the cell suspension in 1.25 ml of antibiotic-free complete medium. After 4-8 h incubation, the transfection mixture were removed and replaced with complete growth medium. The cells were incubated for 72 h to allow optimal silencing of the *GSTA1* expression and *GSTA1* knockdown was assessed by both RTPCR and immunoblotting.

Pilot experiments included internal controls of untreated cells, mock-transfected cells with no siRNA, and a non-silencing siRNA control (Silencer Select Negative Control siRNA, Ambion). The Silencer Select Negative Control siRNAs are siRNAs with sequences that do not target any gene product to determine siRNA transfection efficiency and to control for the effects of siRNA delivery. A positive control using Silencer Select GAPDH siRNA (Ambion) was tested to develop and optimizing the

transfection condition. Optimisation of gene silencing was performed by quantifying *GSTA1* mRNA levels by Q-RT-PCR and GSTA1 protein levels by immunoblotting.

6.2.2.3 Analysis of the effects of *GSTA1* inhibition in INH cytotoxicity

The effect of *GSTA1* silencing on INH cytotoxicity was tested by performing the apoptosis marker and cell viability analyses. Cells were transfected with *GSTA1* siRNA or non-silencing siRNA control for 72 h and subjected to MTT test, DNA fragmentation assay and Caspase3 fluorometric assay (see section 2.8, 2.10, 2.11).

6.3 Result

6.3.1 The effect of hGSTA4 in INH toxicity

6.3.1.1 Evaluation of *GSTA4* expression in stably transfected HepG2 cells with *GSTA4* plasmid

The *GSTA4* overexpression efficacy of stably transfected HepG2 cells with *GSTA4* plasmid at mRNA and protein levels was assessed by RT-PCR and immunoblotting respectively. **Figure 6.2** shows the semiquantitative RT-PCR analysis of *GSTA4* mRNA expression in (A) non-transfected and (B) hGSTA4-stably transfected HepG2 cells. B-actin and GAPDH were used as a control. *GSTA4* mRNA level in hGSTA4-stably transfected HepG2 cells are increased by the presence of the more intense bands when compared to the non-transfected cells. The semiquantitative RT-PCR findings were further quantified by quantitative RT-PCR analysis as shown in **Table 6.1**. The hGSTA4-stably transfected cells have shown an approximately 60 fold increase in *GSTA4* transcript level when compared with the non-transfected cells. Data presented are means \pm S.D. of triplicates from three independent experiments of the fold increase of *GSTA4* mRNA expression levels in hGSTA4-stably transfected cells to corresponding levels in non-transfected cells, normalized with respect to GAPDH mRNA levels.

The expression level of *GSTA4* at protein level reflected mRNA findings, with a relatively high level of *GSTA4* expression in hGSTA4-stably transfected cells compared to the non-transfected cells (**Figure 6.3**).

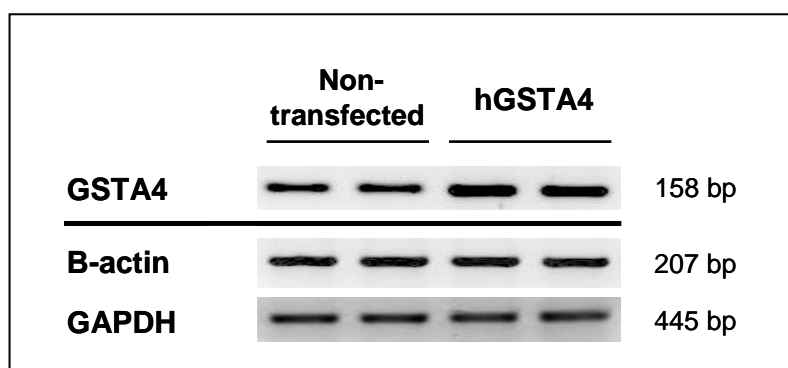


Figure 6.2 Semiquantitative RT-PCR analysis of GSTA4 mRNA expressions in non-transfected (A) and hGSTA4-stably transfected

Table 6.1 Quantitative RT-PCR of GSTA4 transcript level in non-transfected and stably transfected HepG2 with hGSTA4 plasmid

Cell lines	Average fold increase in mRNA expression
Non-transfected HepG2	1.00 ± 0.02
hGSTA4-stably transfected HepG2	60.29 ± 6.41

Data presented are means ± S.D. of triplicates from three independent experiments of the fold increase of GSTA4 mRNA expression levels in hGSTA4-stably transfected cells to corresponding levels in non-transfected cells, normalized with respect to GAPDH mRNA levels.

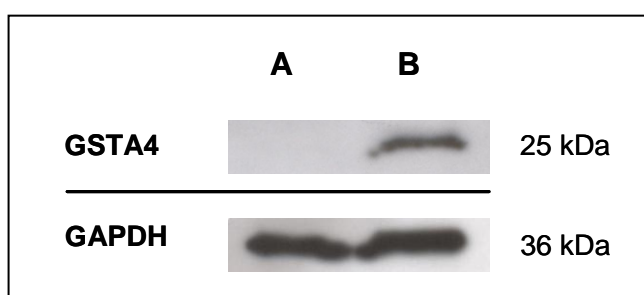


Figure 6.3 Immunoblot of GSTA4 protein expressions in non-transfected (A) and GSTA4-stably transfected HepG2

6.3.1.2 Functional role of GSTA4 against INH-decreased cell proliferation in HepG2 cells

To evaluate the functional consequences of hGSTA4 overexpression on cell proliferation, MTT assays were performed and the EC₅₀ values were determined. The hGSTA4-stably transfected cells have significantly reduced cell proliferation inhibition caused by INH at 20, 30, 40, 50 and 60 mM, compared with the non-transfected cells ($P < 0.05$). The EC₅₀ values of the hGSTA4-stably transfected cells was 38.64 mM which was higher than the non-transfected cells (29.16 mM), indicating that GSTA4 has a protective role against toxicants generated by INH (**Figure 6.4**).

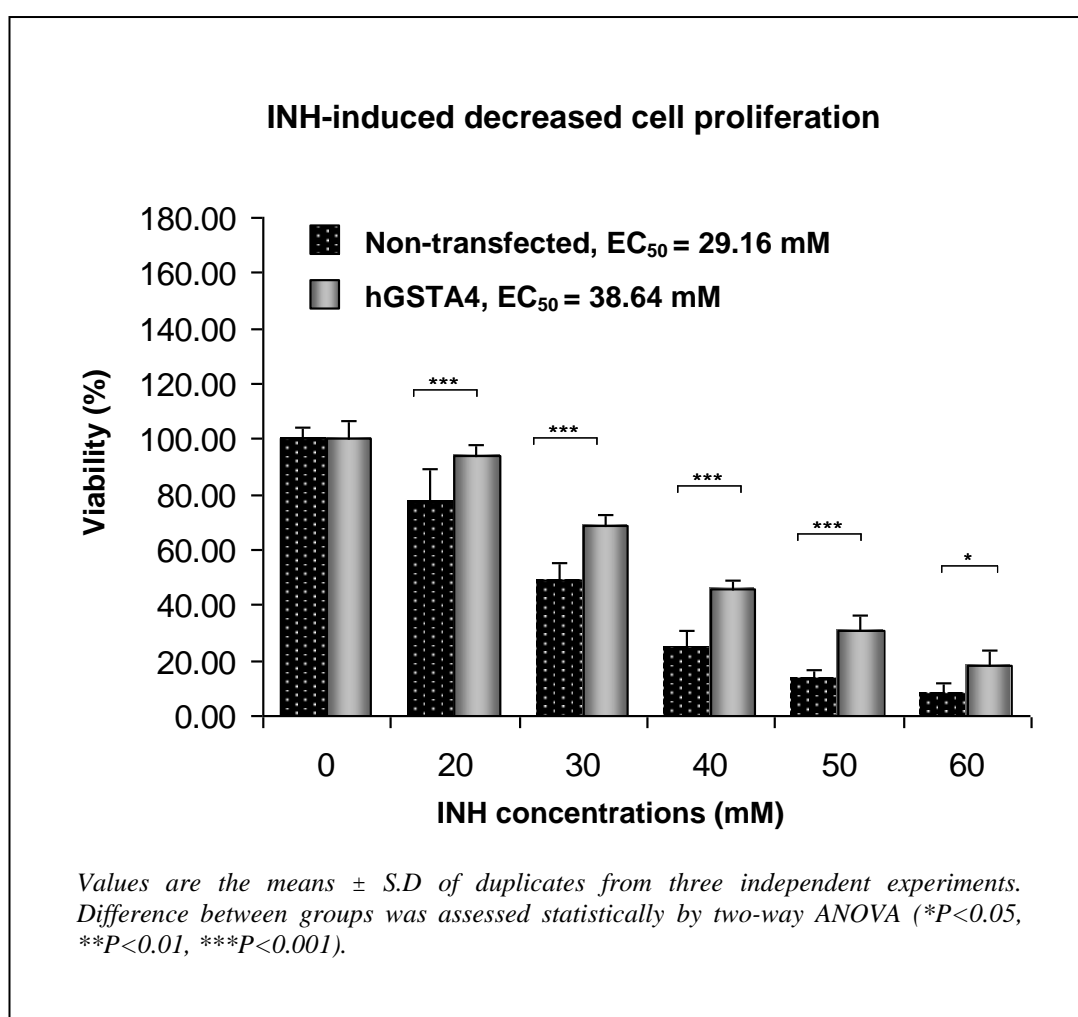


Figure 6.4 INH-induced decreased cell proliferation at 48 h in hGSTA4-transfected and non-transfected HepG2 cells

6.3.1.3 *Inhibitory effect of INH-induced apoptosis in HepG2 overexpressing GSTA4*

DNA fragmentation assay and caspase-3 activities were determined as indicators of apoptosis following 48 h of INH treatment in hGSTA4-stably transfected and non-transfected cells. DNA fragmentation was detected by an ethidium bromide stained gel following INH treatment (**Figure 6.5**). In non-transfected cells, obvious DNA fragmentation was observed at the concentration of 50 mM and 60 mM INH. However, DNA fragmentation ladder pattern of hGSTA4-stably transfected cells was only evident after INH treatment at 60 mM. This result was consistent with the findings in caspase-3 activity assay as reduced caspase-3 activity was observed in hGSTA4-stably transfected cells compared to the non-transfected cells (**Figure 6.6**). Significantly reduced ($P < 0.05$) caspase-3 activity was observed in hGSTA4-stably transfected cells at 50 mM INH treatment. This result is concordant with the results of MTT and DNA fragmentation assay, suggesting the inhibitory effect of INH-induced cytotoxicity in HepG2 by the overexpression of GSTA4.

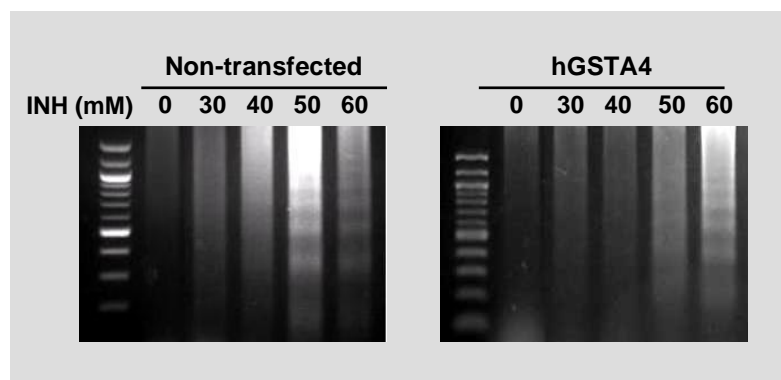


Figure 6.5 INH-induced DNA fragmentation in hGSTA4-stably transfected cells

Early detection of apoptotic DNA fragmentation was seen in non-transfected cells treated with 50 mM INH, whilst 60 mM INH in hGSTA4-transfected cells. Shown is a representative gel from two experiments.

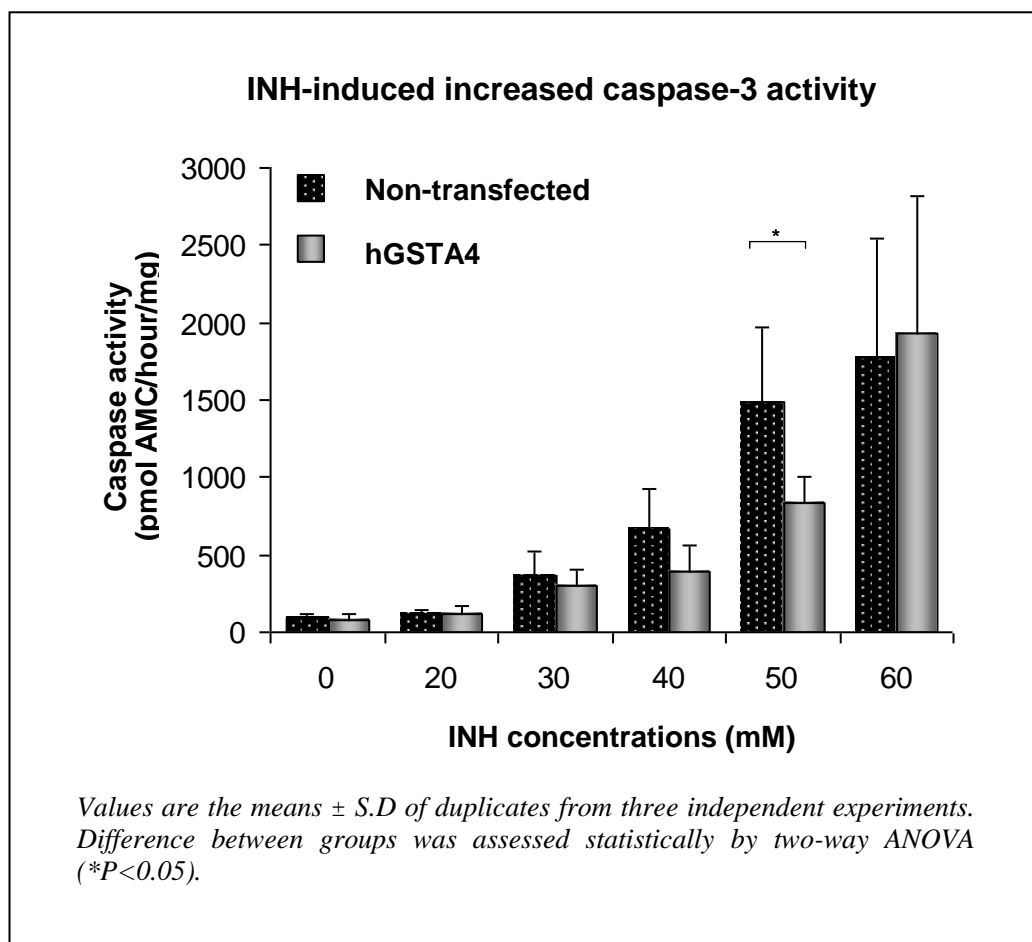


Figure 6.6 INH-induced increased caspase-3 activity in hGSTA4- and non-transfected HepG2 cells

6.3.2 The effect of isoniazid on *GSTA1* expression profile in human cell line

To examine whether the toxicity of INH is enhanced in GSTs-knockdown cells, small interfering RNA (siRNA) *GSTA4* knockdown experiment was initially performed in HepG2 and LS180 cells. *GSTA4* mRNA and protein expression were evaluated in both cell lines. However due to the lack of *GSTA4* expression in both cell lines (data not shown), *GSTA1* was then chosen as the candidate gene to study the toxicity profile of INH in *GSTA1*-knockdown cells.

6.3.2.1 GSTA1 expression in mammalian cell lines

The expression of *GSTA1* transcripts in mammalian cell lines was investigated using quantitative RT-PCR and *GSTA1* protein levels were assessed by immunoblotting. The *GSTA1* transcript expression level in the HepG2, LS180 and Huh7.5 is relatively low to corresponding level in Caco-2 cells (**Table 6.2**). The Caco-2 cell line has shown to express higher *GSTA1* transcript expression levels. The expression level of total *GSTA1* at protein level reflected mRNA findings, with relatively low levels of expression in (A) HepG2, (B) LS180 and (D) Huh7.5 and higher levels in (C) Caco-2 cell lines (**Figure 6.7**).

Table 6.2 Quantitative RT-PCR of GSTA1 transcript level in Caco-2, HepG2, Huh7.5, and LS180 cell lines

Cell lines	Average fold reduction in mRNA expression
Caco-2	1.000 ± 0.129
HepG2	0.072 ± 0.063
Huh7.5	0.019 ± 0.012
LS180	0.001 ± 0.001

Data presented are means ± S.D. of triplicates from two independent experiments of the fold increase of GSTA1 mRNA expression levels in HepG2, Huh7.5 and LS180 to corresponding levels in Caco-2 cells, normalized with respect to GAPDH mRNA levels.

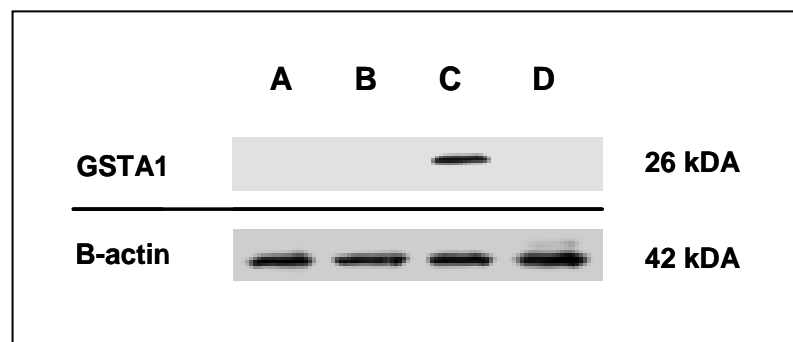


Figure 6.7 Immunoblot of GSTA1 protein level in mammalian cell lines

Immunoblotting was used to determine GSTA1 expression levels in (A) HepG2, (B) LS180, (C) Caco-2 and (D) Huh 7.5 cells. No GSTA1 protein level was detectable in HepG2, LS180 and Huh7.5 except for Caco-2 cell lines.

6.3.2.2 *GSTA1* silencing decreased *GSTA1* transcript levels

Caco-2 cell line was chosen as the cell line for *GSTA1* silencing work, due to its high expression levels of *GSTA1*. The efficiency of *GSTA1* knockdown was analyzed by quantitative RT-PCR 72 h after transfection. Cells were transfected with 5 nM, 10 nM and 25 nM *GSTA1* siRNA for 72 h. Comparison was made between non-silencing siRNA controls (NSCs) and the *GSTA1* siRNA. Internal controls included no treatment and mock-transfected cells with RiboJuice only. The *GSTA1* knockdown efficiency at the mRNA transcript level was shown in **Table 6.3** and **Figure 6.8**. Neither mock-transfected nor no treatment cells had significantly reduced *GSTA1* transcript levels compared to NSCs. Both 10 nM and 25 nM *GSTA1* siRNAs significantly reduced the expression levels of *GSTA1* by 77% and 81% respectively when compared to the NSCs.

Table 6.3 Quantitative RT-PCR analysis of the effect of *GSTA1* siRNA on *GSTA1* transcript levels at 72 h

Treatment	Average fold reduction in mRNA expression
Non-silencing siRNA controls (NSCs)	1.00 ± 0.12
Mock-transfection	0.87 ± 0.17
No treatment	0.97 ± 0.10
5 nM <i>GSTA1</i> siRNAs	0.41 ± 0.21
10 nM <i>GSTA1</i> siRNAs	0.23 ± 0.12
25 nM <i>GSTA1</i> siRNAs	0.19 ± 0.05

Data presented are means ± S.D. of triplicates from two independent experiments.

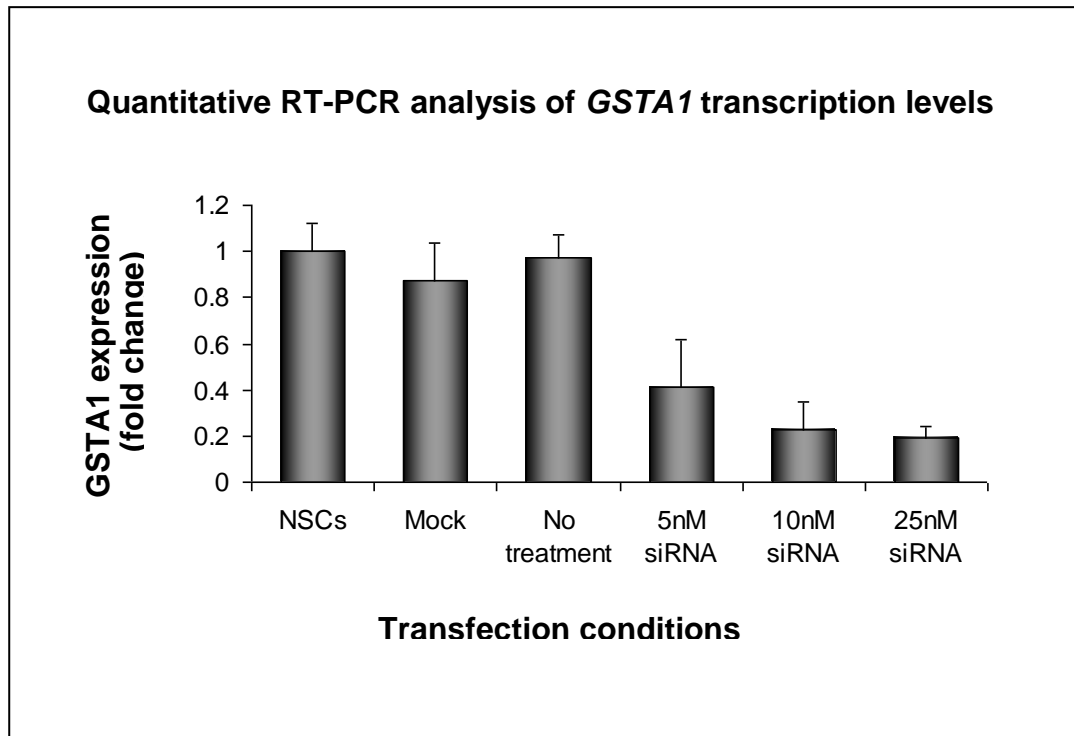


Figure 6.8 Silencing effect of *GSTA1* siRNA on *GSTA1* transcription levels at 72 hours by quantitative RT-PCR

GSTA1 transcription levels in Caco-2 cells transfected with 5, 10 and 25 nM of *GSTA1* siRNA, comparing with non-silencing siRNA controls (NSCs), mock transfection with RiboJuice only and no treatment control. All mRNA levels were normalized to GAPDH levels. The mRNA level for NSCs was set at 1 and fold reduction in the respective mRNA levels in the presence of corresponding siRNAs were determined. As shown, 25 nM *GSTA1* siRNA efficiently silences the *GSTA1* mRNA levels by greater than 80%. The *GSTA1* transcript levels remained unchanged in all controls.

6.3.2.3 *GSTA1* silencing decreased *GSTA1* total protein levels

Having determined that *GSTA1* siRNA successfully reduced *GSTA1* at transcript levels, the effect on protein expression was assessed by immunoblotting after 72 h. In keeping with mRNA finding, *GSTA1* protein levels remained unaltered in mock transfected NSCs and no treatment controls (**Figure 6.9**) (**Table 6.4**). Quantification of the *GSTA1* bands using ImageJ software revealed 5 nM, 10 nM and 25 nM *GSTA1* siRNAs reduced the protein expression levels of *GSTA1* by 32%, 79% and 89% respectively when compared to the NSCs. Knockdown efficiency of *GSTA1* is increased when cells were transfected with higher concentration of *GSTA1* siRNA (25 nM). Therefore 25 nM siRNA was used for efficient knockdown of *GSTA1* functional analyses.

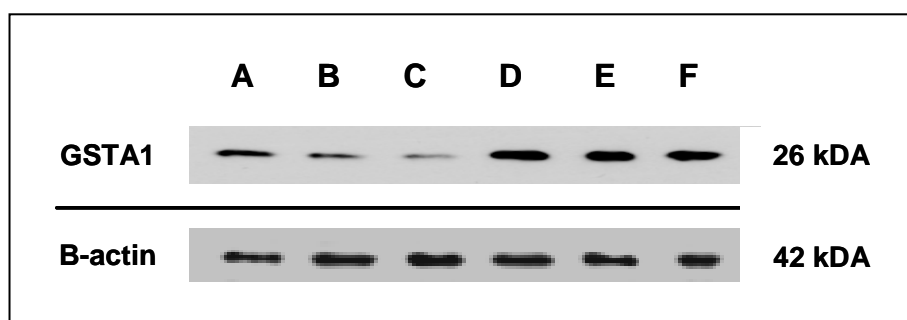


Figure 6.9 Effect of GSTA1 siRNA on GSTA1 protein levels

Immunoblotting was used to determine GSTA1 expression levels in Caco-2 cells transfected with (A) 5, (B) 10 and (C) 25 nM of GSTA1 siRNA, comparing with (D) no treatment (control), (E) mock transfection with RiboJuice only and (F) non-silencing siRNA controls (NSCs) at 72 h. Knockdown of GSTA1 protein was obvious by the GSTA1 siRNA at the concentration of 25 nM, and GSTA1 expression was unaltered in all control treatments

Table 6.4 Quantification of protein expression of GSTA1 normalized to β -actin level using ImageJ software

Treatment	Absolute peak area value*	Fold reduction in GSTA1 expression
Non-silencing siRNA controls (NSCs)	22.88	1.00
Mock-transfection	22.66	0.99
No treatment	23.20	1.01
5 nM GSTA1 siRNAs	15.66	0.68
10 nM GSTA1 siRNAs	4.90	0.21
25 nM GSTA1 siRNAs	2.52	0.11

* Absolute peak area value of GSTA1 were normalized to β -actin level

6.3.2.4 *GSTA1* silencing abolished protection against INH-induced cell proliferation inhibition

MTT assays were performed to determine the functional consequences of *GSTA1* silencing on cell proliferation in Caco-2 cells. Treatment with INH causes a dose-dependent inhibition of cell proliferation in both NSCs and *GSTA1* siRNA knockdown cells (*GSTA1*s). As shown in **Figure 6.10**, *GSTA1* silencing has significantly enhanced cell proliferation inhibition in *GSTA1*s compared to the NSCs when treated with 30, 45, 60, 75 and 90 mM INH ($p < 0.001$). The EC_{50} value of the *GSTA1*s was 48.82 mM lower than the NSCs (68.88 mM) which indicates that *GSTA1*s were more susceptible to INH-mediated cell proliferation inhibition compared to NSCs.

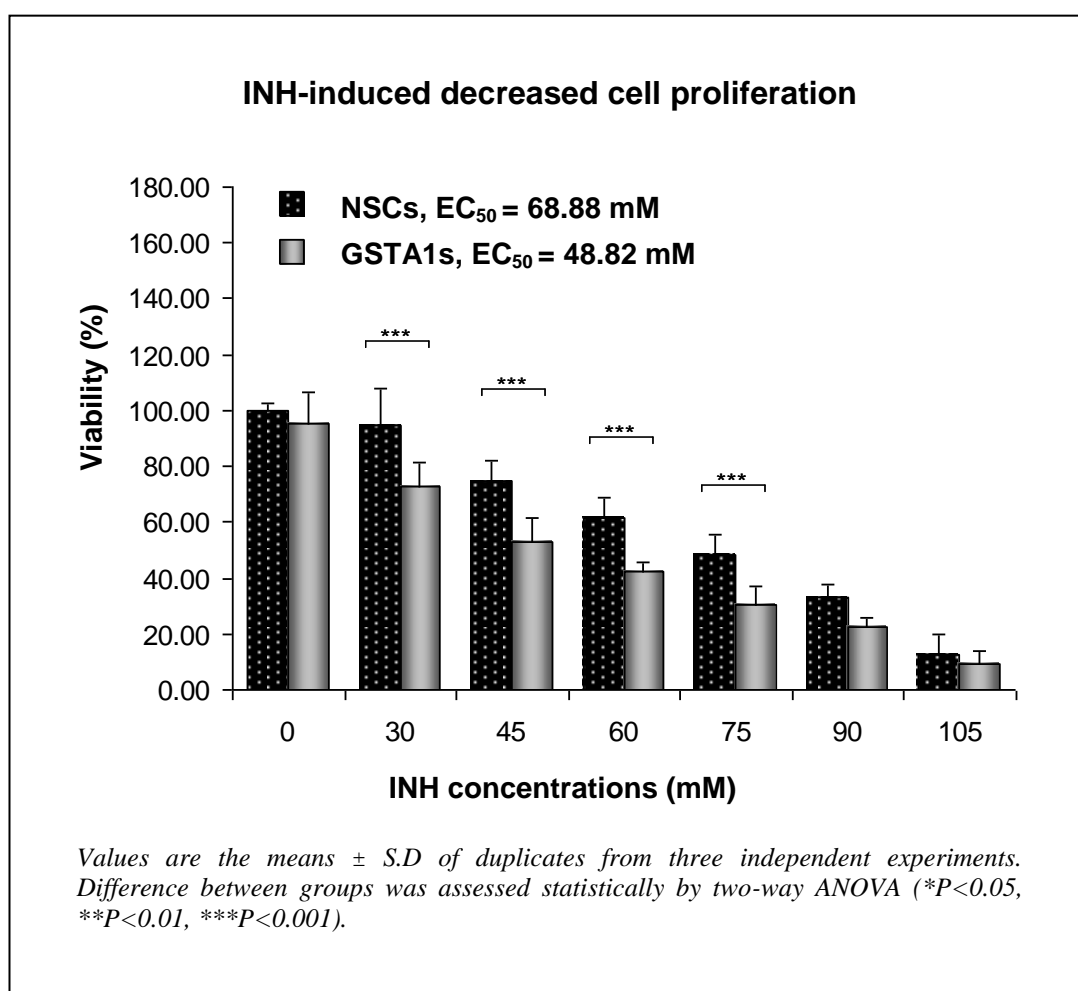


Figure 6.10 INH-induced decreased cell proliferation in *GSTA1* siRNA knockdown cells (*GSTA1*s)

6.3.2.5 *GSTA1* silencing promotes INH-induced apoptosis

To investigate the functional role of *GSTA1* in INH-induced apoptosis, DNA fragmentation assay and caspase-3 activity assay were performed in NSCs and *GSTA1*s. As shown in **Figure 6.11**, DNA fragmentation ladder pattern of *GSTA1*s was evident after INH treatment at 30, 45 and 60 mM. In NSCs, intense DNA laddering was observed at the concentration of 45 and 60 mM INH and a faint ladder pattern was seen at 30 mM INH. None of the apoptotic DNA laddering was observed in NSCs and *GSTA1*s cells, neither in *caco-2* cells without INH treatment. Caspase-3 activity assay was performed to confirm the findings of DNA fragmentation assay. **Figure 6.12** shows the increased of caspase-3 activity in NSCs and *GSTA1*s when exposed to 15, 30, 45 and 60 mM INH. A significant induction of caspase-3 activity was observed in *GSTA1*s at 15, 30 and 45 mM INH ($P < 0.001$) compared to NSCs. These findings confirmed the results of MTT and DNA fragmentation assay, suggesting *GSTA1* silencing increased INH-induced cytotoxicity in *Caco-2* cells.

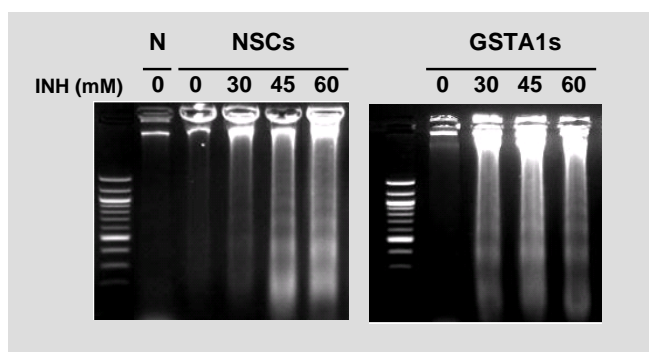


Figure 6.11 DNA fragmentation analyses in *Caco-2* cells transfected with NSCs and *GSTA1*s cells

*The apoptotic DNA fragmentation was detected in NSCs and *GSTA1*s treated with 30, 45 and 60 mM INH. However, less apoptotic DNA laddering was observed in NSCs compared to *GSTA1*s when treated with 30 mM INH, suggesting the protective role of *GSTA1* against INH-induced apoptosis. No DNA fragmentation was detected in *caco-2* cells (N), NSCs and *GSTA1*s in the absence of INH treatment.*

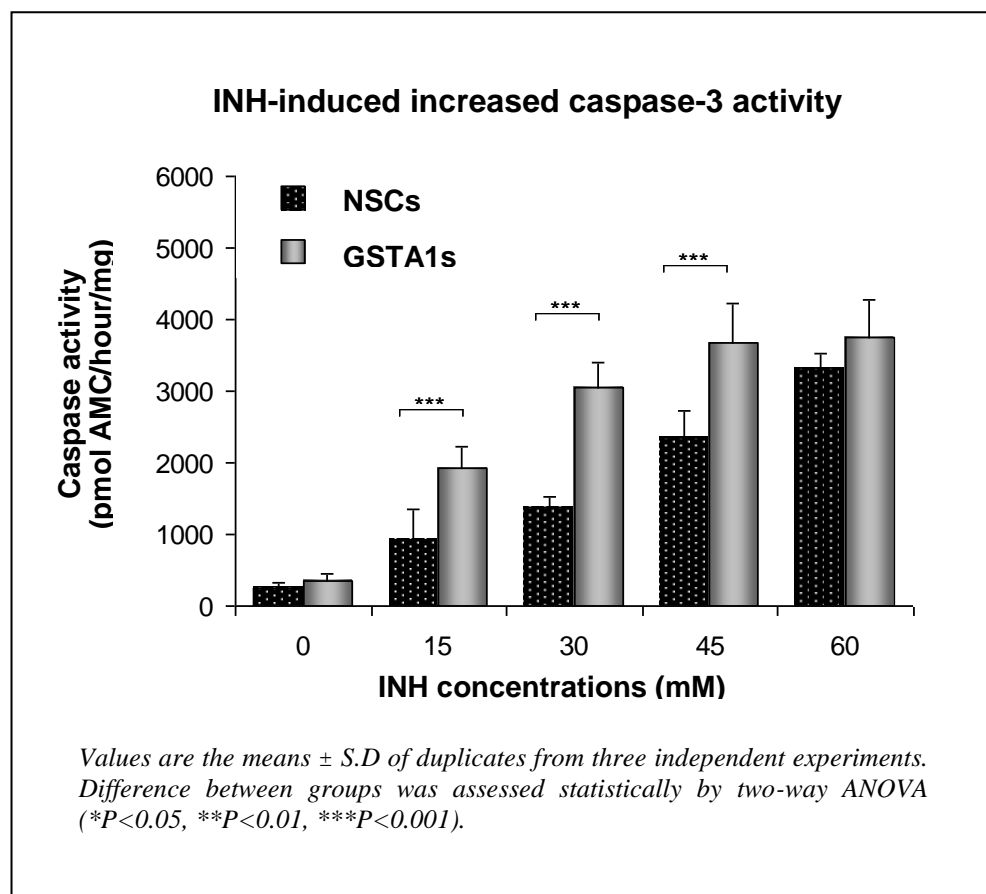


Figure 6.12 INH-induced increased caspase-3 activity in GSTA1 siRNA knockdown cells (GSTA1s)

6.4 Discussion

Though P450 mediated metabolism usually biotransforms drugs into water-soluble metabolites which are easier to eliminate, in some cases it causes the activation of a drug to a hepatotoxic metabolite and increases drug toxicity. In the case of isoniazid, polymorphisms in metabolic enzymes such as NAT2 and CYP2E1 may be associated with isoniazid-induced liver injury due to the increased level of toxic metabolites of isoniazid. Thus, GST enzymes may play an important role to limit or prevent ATD-DILI by reducing INH toxic metabolites or neutralising toxic products of oxidative stress such as 4-hydroxynonenal, particularly in slow acetylators. The present study aimed to examine in detail the possible relevance of *GSTA4* to protection against INH-related toxicity. *GSTA4* appears to be the main GST isoform that protects against 4-hydroxynonenal toxicity (Balogh and Atkins, 2011). Transfection of HepG2 cells with

GSTA4 has also been shown previously to protect against 4-hydroxynonenal-mediated oxidative injury (Gallagher et al., 2007) but the effect of its stable expression on INH-related toxicity has not been previously investigated. The current study has shown clearly that GSTA4 expression in HepG2 cells does result in decreased INH-related toxicity. This is of interest in view of the borderline significant associations seen for some GSTA4 SNPs for ATD-DILI (Chapter 3).

To confirm the *GSTA4* protective effect, we sought to assess INH toxicity after siRNA transfection to knockout *GSTA4*. Unfortunately, it was not possible to do this in any of the available cell lines as none were found to express GSTA4 constitutively at detectable levels. As an alternative and further investigation on the role of GSTA isoforms in protection against INH toxicity, siRNA studies were performed to knockout *GSTA1*. GSTA1 is not able to conjugate 4-hydroxynonenal but has been shown to decrease reduction of lipid peroxides due to having GSH peroxidase activity (Balogh and Atkins, 2011). This means it may have a role in preventing the formation of 4-hydroxynonenal. As for GSTA4, GSTA1 was expressed at low levels in several cell lines including HepG2. However, levels of expression in the epithelial colorectal adenocarcinoma cell line Caco-2 were relatively high and it was therefore decided to do the siRNA studies in these cells although a liver cell line would have been a better model for INH-related DILI. *GSTA1* silencing significantly abolished protection against INH-induced cell proliferation inhibition and increased INH-induced apoptosis in Caco-2 cells.

Therefore, though the GSTA isoforms were not able to prevent completely toxicity induced by INH, these results demonstrated that expression of GSTA1 or A4 could function to limit the effect of INH on the extent of apoptosis/necrosis. This finding suggests that lipid peroxidation could play a role in the mechanism for ATD-DILI. In Chapter 3, some evidence that individuals with the *GSTM1* null genotype are more susceptible to ATD-DILI was also obtained. There is evidence that *GSTM1* may also contribute to detoxification of 4-hydroxyalkenals from lipid peroxidation as well as having GSH peroxidase activity (Berhane et al., 1994) and it would also have been interesting to have performed expression and siRNA studies for this isoform. GSTA1, GSTA4 and GSTM1 are all expressed in human hepatocytes (Aninat et al., 2006) and are therefore very relevant to ATD-DILI.

As well as the findings reported in Chapter 3, it has been shown that the homozygous null genotype of *GSTM1* and *GSTT1* is implicated in methotrexate, troglitazone and carbamazepine-induced liver injury as well as DILI relating to a range of different drugs (Lucena et al., 2008a; Imanishi et al., 2007; Ueda et al., 2007; Watanabe et al., 2003). Therefore it is worth undertaking further studies on the possible role of GST in DILI using the types of approaches described in this chapter. In this present study, overexpression of *GSTA4* have significantly reduced cell proliferation inhibition caused by INH and decreased INH-induced apoptosis in HepG2 cells. *GSTA1* silencing has significantly abolished protection against INH-induced cell proliferation inhibition and increased INH-induced apoptosis in Caco-2 cells. Though the GSTs were not able to revert completely hepatic injury induced by INH, these results enabled to conclude that expression of GSTs could function to limit the effect of INH to the extent of apoptosis/necrosis. Individuals with GSTs deficiency are suggested to be less capable of detoxifying reactive metabolites thus, causing their hepatocytes to be less protective against oxidative damage during INH metabolism. In the previous chapter, some evidence for associations between polymorphisms in the GSTs, particularly *GSTM1* and *GSTA4* and ATD-DILI were found, suggesting a protective role of these enzymes in preventing ATD-DILI. It has been shown that homozygous null mutations of *GSTM1* and *GSTT1* implicated in methotrexate, troglitazone and carbamazepine-induced liver injury (Imanishi et al., 2007; Ueda et al., 2007; Watanabe et al., 2003). Genetic polymorphisms of GSTs have also been associated with many diseases including cancer and alcoholic liver disease (Andrade et al., 2009). Therefore it is worth undertaking further studies on the possible role of the polymorphisms in anti-oxidative stress genes which may influence their expression and consequently predict susceptibility and severity of DILI in individuals.

Chapter 7. General Discussion

7 General Discussion

Drug-induced liver injury (DILI) is one of the most commonly detected adverse drug reactions both during drug development and in clinical practice. Idiosyncratic adverse drug reactions such as DILI have received much attention because they are unpredictable and are often the key reason for useful drug withdrawals from the pharmaceutical market. Genetic factors in idiosyncratic DILI remain poorly understood. Over the past few decades, the association of genetic polymorphisms in drug metabolising enzymes with various ADRs have been extensively studied. Recent progress in pharmacogenetics research suggests that patients with specific genetic characteristics may be prone to specific ADRs and personalized drug therapy with pharmacogenetics can therefore lead to safer, more effective drugs and reduce ADRs. The evaluation of predisposing factors of ADRs may not fully prevent the occurrence of ADRs, but it can reduce the incidence and severity of ADRs, reduce the overall cost of healthcare and improve patient outcomes.

First-line anti-TB drugs used for disease treatment and latent TB infection (LTBI) are isoniazid (INH), rifampicin (RMP), pyrazinamide (PZA), ethambutol and streptomycin. The fact that multiple drugs are used is vital in treating the disease effectively but also means that assigning an adverse drug reaction to a particular drug is more difficult. DILI due to ATD is more common than most other forms of idiosyncratic DILI with the frequency of overt clinical hepatitis caused by INH and RMP coadministration reported to be 2.6%, but only 1.1% with rifampicin alone and 1.6% with INH alone (Steele et al., 1991). The frequency of anti-TB drugs hepatotoxicity increases greatly when they are used simultaneously (van Hest et al., 2004). These findings contrast with the reported frequencies of DILI due to flucloxacillin as 8.5 in every 100,000 new users (Daly et al., 2009) and co-amoxiclav as 1 in every 10,000 prescriptions (Donaldson et al., 2010). Despite the higher frequency for ATD-DILI, progress in identifying genetic risk factors and understanding the underlying mechanism has been slower than for other forms of DILI. However, it is important to point out that most of the other strong genetic associations described so far are with HLA alleles and any evidence for HLA involvement in ATD-DILI is very limited.

There has been some progress in identifying genetic risk factors for DILI with reported associations with genes such as *NAT2*, *CYP2E1* and *GSTM1* now reported and replicated, though not all studies have reported positive associations (see Chapter 1). The *NAT2* and *GSTM1* associations have been replicated in the current study but the overall effects are not particularly high with odds ratios of 4.6 for *NAT2* slow acetylators and 2.9 for *GSTM1* null detected. The current study has considerable limitations with numbers of cases studied small and subject to ethnic heterogeneity. The positive associations with *NAT2* and *GSTM1* seem to be particularly driven by the South Asian subjects, with less overall effect in Europeans and this needs further study in larger patient groups, especially since a lack of association between *NAT2* slow acetylators and European ATD-DILI cases has been reported previously by others (Yamada et al., 2009; Vuilleumier et al., 2006).

Using the data from the current study, it was possible to determine negative and positive predictive values for *NAT2* genotyping to prevent DILI from isoniazid. The negative predictive value of 0.99 suggests that genotyping would lead to a decrease in the number of cases but the low positive predictive value of 0.03 showed that large numbers of patients would be deprived of isoniazid treatment unnecessarily. Despite a much higher odds ratio for the association of flucloxacillin-related DILI with HLA B*5701 than for isoniazid DILI with *NAT2* slow acetylation, the positive predictive value for B*5701 for DILI is only 0.002 (Daly et al., 2009) so is lower than that for *NAT2* slow acetylator alleles for isoniazid DILI. This difference arises mainly because the risk of developing DILI from flucloxacillin is much lower than from isoniazid. Flucloxacillin DILI affects only 1 in every 500 individuals who are B*5701-positive whereas isoniazid-related DILI affects approximately 4 in every 100 individuals who are slow acetylators. There is therefore no clinical value in genotyping for either risk factor before the particular drugs are prescribed. *NAT2* typing could be included in a range of genotyping tests if additional genetic risk factors for DILI due to isoniazid could be identified and this increased the overall positive predictive value of a genotyping test.

Metabolic idiosyncrasy is generally postulated as the basis for the development of INH-induced hepatotoxicity. Our present study using an *in vitro* overexpression approach has suggested that toxic metabolites of INH caused more cytotoxicity than the parent drug in HepG2 cells overexpressing *NAT2* enzymes. Hydrazine, acetylhydrazine and

isonicotinic acid are potentially hepatotoxic metabolites of INH and accumulation of these reactive metabolites in patients may cause DILI (Metushi et al., 2011). However, it has been suggested recently (Metushi et al., 2011) that in addition to factors determining reactive metabolite formation, an immune component to isoniazid DILI is also a possibility. These workers suggest that this is partly suggested from features such as the delay in development of DILI following exposure to the drug and the appearance of liver biopsies from ATD-DILI patients which often have an appearance similar to those from patients with autoimmune hepatitis. A previous report of an HLA association is also cited as evidence for an immune association (Sharma et al., 2002) but a recent genome-wide association study (GWAS) involving some of the cases included in the current study has failed to detect any *HLA* association (Daly and Shen, unpublished). Nevertheless, the possibility of some involvement from either the innate or adaptive immune system in ATD-DILI as recently suggested (Metushi et al., 2011) deserves further study.

Most of the genetic studies up to now on ATD-DILI have focussed on INH, probably because this tends to be the common drug used in the patients who develop DILI though some also receive pyrazinamide which is known to increase the risk of DILI when included in a ATD regimen (Stout et al., 2003). Occasionally patients who receive PZA but not INH also develop DILI but such cases tend to be rare in the UK because PZA without INH will be mainly only used where the mycobacteria are found to be INH-resistant. It is also sometimes possible to identify cases where the DILI is likely to have been due to PZA not INH on the basis of successful reintroduction of ATD following DILI. However, this also raises the complication of adaptation where patients may suffer ATD-DILI which meets the phenotypic requirements used in studies such as the DILIGEN study but then do not suffer recurrence of symptoms when the drugs are reintroduced (Watkins, 2005). All these factors make genetic studies on ATD-DILI, including the present one, very challenging, though it may be possible to find cases where the DILI can be shown to be clearly due to either INH or PZA if sufficient numbers of ATD-DILI cases with good clinical information can be collected.

Recent success in identifying strong genetic associations for particular adverse drug reactions including DILI, myotoxicity and skin reactions have involved genome-wide association studies, not candidate gene association studies. For example associations

with *HLA-B*5701* have been detected for DILI due to flucloxacillin (Daly et al., 2009), with *HLA-DRB1*1501* and *A*0201* for DILI due to co-amoxiclav (Lucena et al., 2011), with *SLCO1B1* for simvastatin-induced myopathy (Link et al., 2008) and with *HLA-A*3101* for carbamazepine-induced skin rash (McCormack et al., 2011). A similar study to understand genetic factors affecting susceptibility to ATD-DILI seems the best way forward. A small GWAS study on the available European ATD-DILI samples in the present study has been negative apart from the *NATI* association described in Section 3.3.3 (Daly and Shen, unpublished) but efforts to increase recruitment and collaborate with other international DILI networks including EUDRAGENE (Molokhia and McKeigue, 2006) and DILIN (Fontana et al., 2009) should enable a larger GWAS study to be performed and hopefully detect specific genetic associations which can be replicated (Daly AK, personal communication).

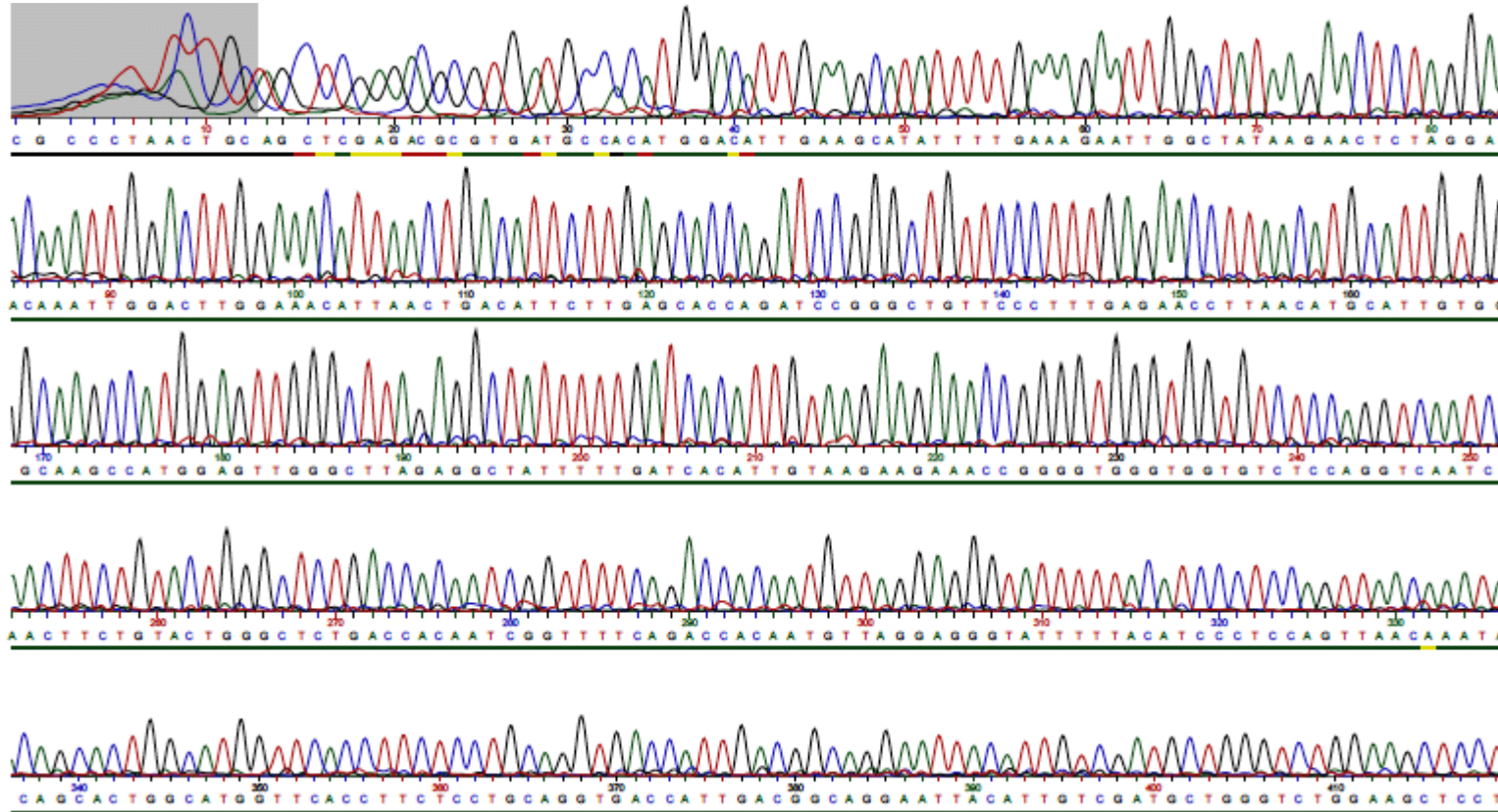
The *in vitro* studies described in this thesis (Chapters 4 to 6) have provided some novel findings concerning increased INH toxicity when *NAT2* is overexpressed but decreased toxicity when *GSTA4* is expressed. The finding that RMP pretreatment decreases INH toxicity while inducing expression of genes such as *CES2* in at least some human hepatocyte preparations is also interesting. Whether *CES2* can catalyse the formation of hydrazine from INH is still unclear and this aspect needs further study. A general limitation of all the *in vitro* studies is that millimolar concentrations of INH are needed to cause detectable toxic effects in either primary cultures or established cell lines. The maximum recommended dosage of INH is 300 mg/day and this will typically result in plasma levels of approximately 10 ug/ml which would give a molar concentration of approx. 100 uM. Hepatocytes could be exposed to slightly higher concentrations than those seen in plasma but they are unlikely to be as high as those needed *in vitro* to see detectable toxicity. It would be helpful to find more sensitive indicators for toxicity. Examining changes in mRNA expression by use of expression microarrays as reported recently in studies on flucloxacillin DILI (Andrews et al., 2010) or at the protein level by proteomics analysis after treating hepatocytes or other cell cultures with lower INH concentrations would be interesting. If a change in gene expression at a physiological INH concentration was seen, the transfection studies described here could be repeated to see if they could either prevent the change or make it larger.

In conclusion, the candidate gene studies described in this thesis provide further confirmation that *NAT2* genotype affects susceptibility to ATD-DILI, though this risk factor only accounts for a small proportion of total susceptibility. Approx. 50% of the UK population are positive for the slow acetylator *NAT2* genotype but only 1 or 2% are likely to develop ATD-DILI should they need treatment for TB. Therefore, susceptibility must involve a combination of *NAT2* slow acetylator genotype and several other susceptibility genes along with non-genetic risk factors. Considerable further work is needed both to understand the mechanism by which ATD-DILI occurs and to develop a genotyping test that would have adequate sensitivity and specificity to detect those at risk of ATD-DILI. A test of this type would be helpful since it would be possible to use alternatives to INH in TB treatment if it could be shown that this would prevent a patient developing DILI.

Chapter 8. Appendices

Appendix A

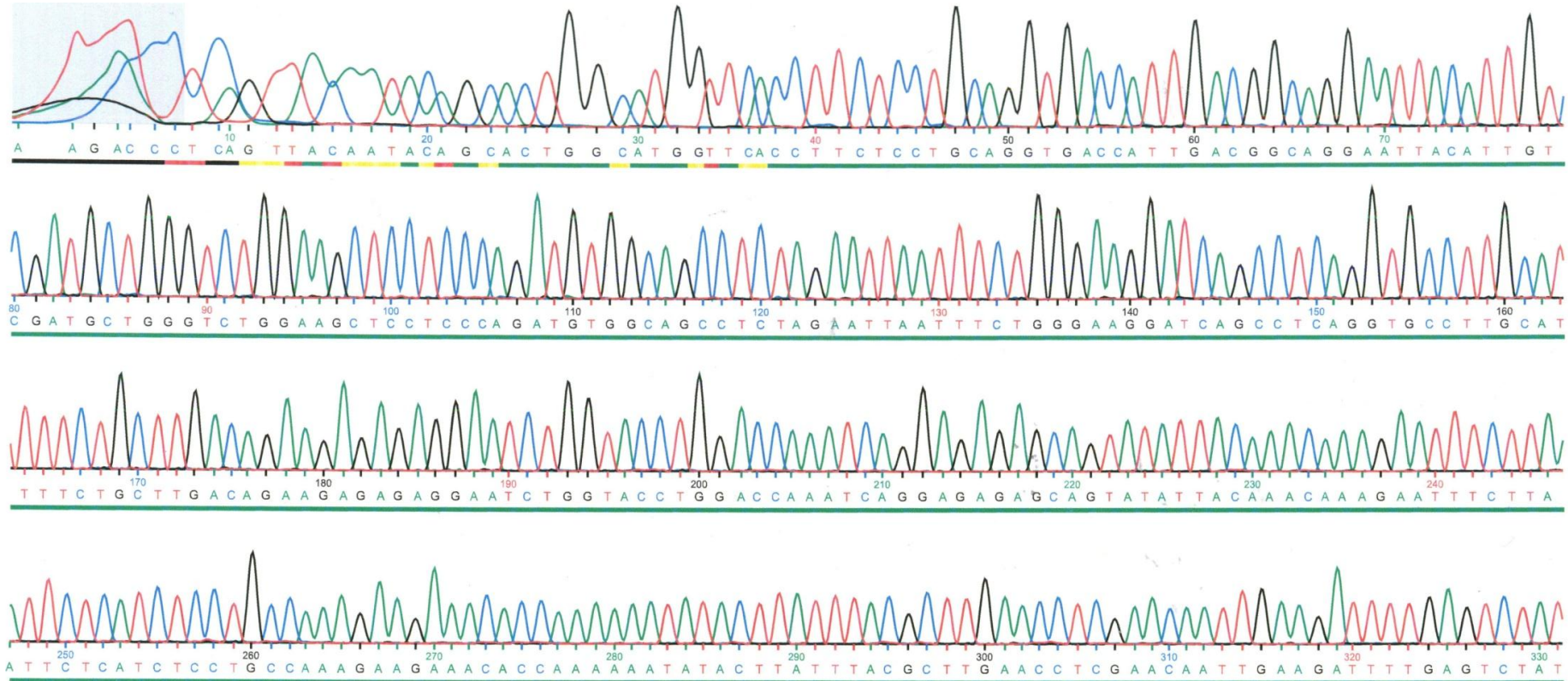
Start codon



Appendix A (i) Electropherogram for rapid acetylator recombinant (RAR) plasmid

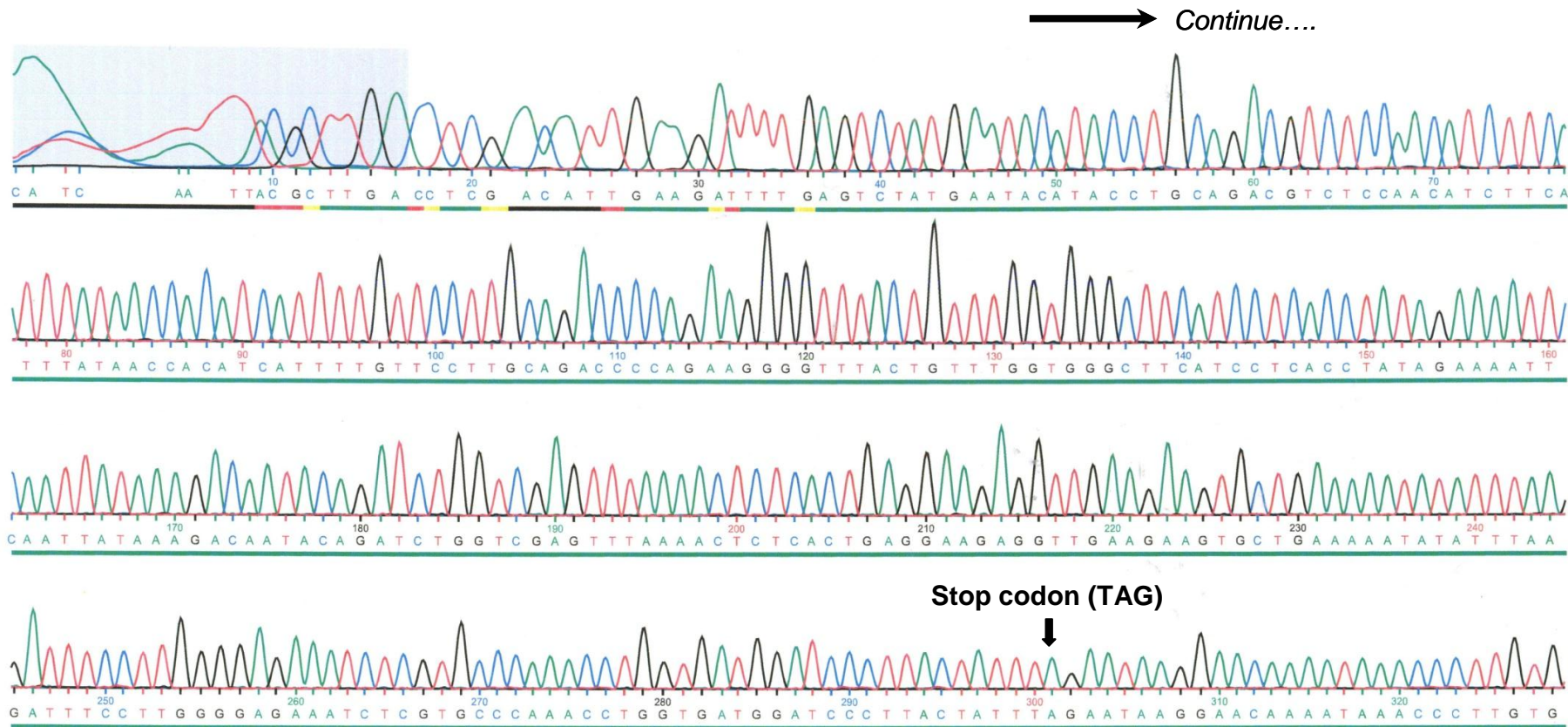
Electropherogram shown is the sequencing traces of RAR plasmid using T7 primer (5'-TAATACGACTCACTATAGGG-3').

→ Continue....



Appendix B (ii) Electropherogram for rapid acetylator recombinant (RAR) plasmid

Electropherogram shown is the sequencing traces of RAR plasmid using second primer (5'-TAATACGACTCACTATAGGG-3'), located 251 to 271 bp downstream of the start codon (ATG).

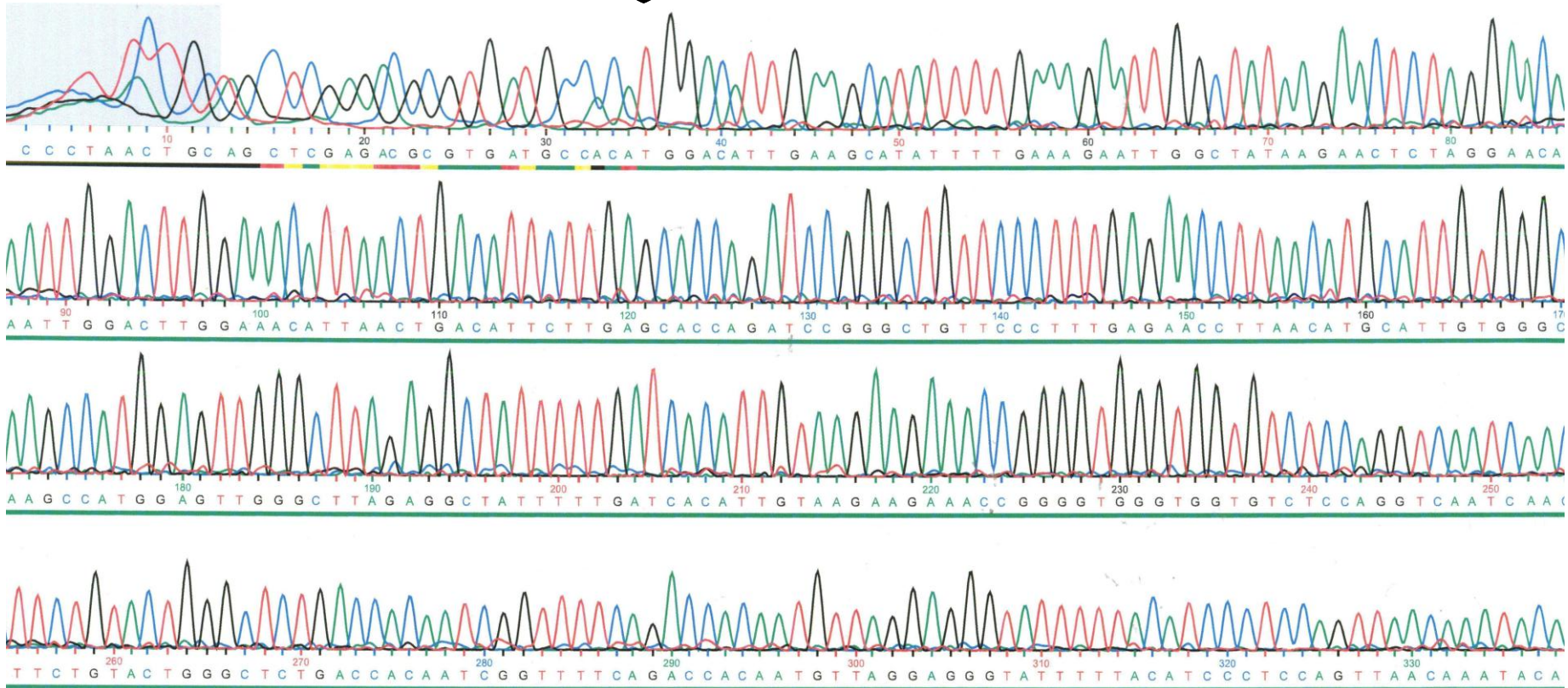


Appendix A (iii) Electropherogram for rapid acetylator recombinant (RAR) plasmid

Electropherogram shown is the sequencing traces of RAR plasmid using third primer (5'-TCCTGCCAAAGAAGAAACAC-3'), located 538 to 558 bp downstream of the start codon (ATG).

Appendix B

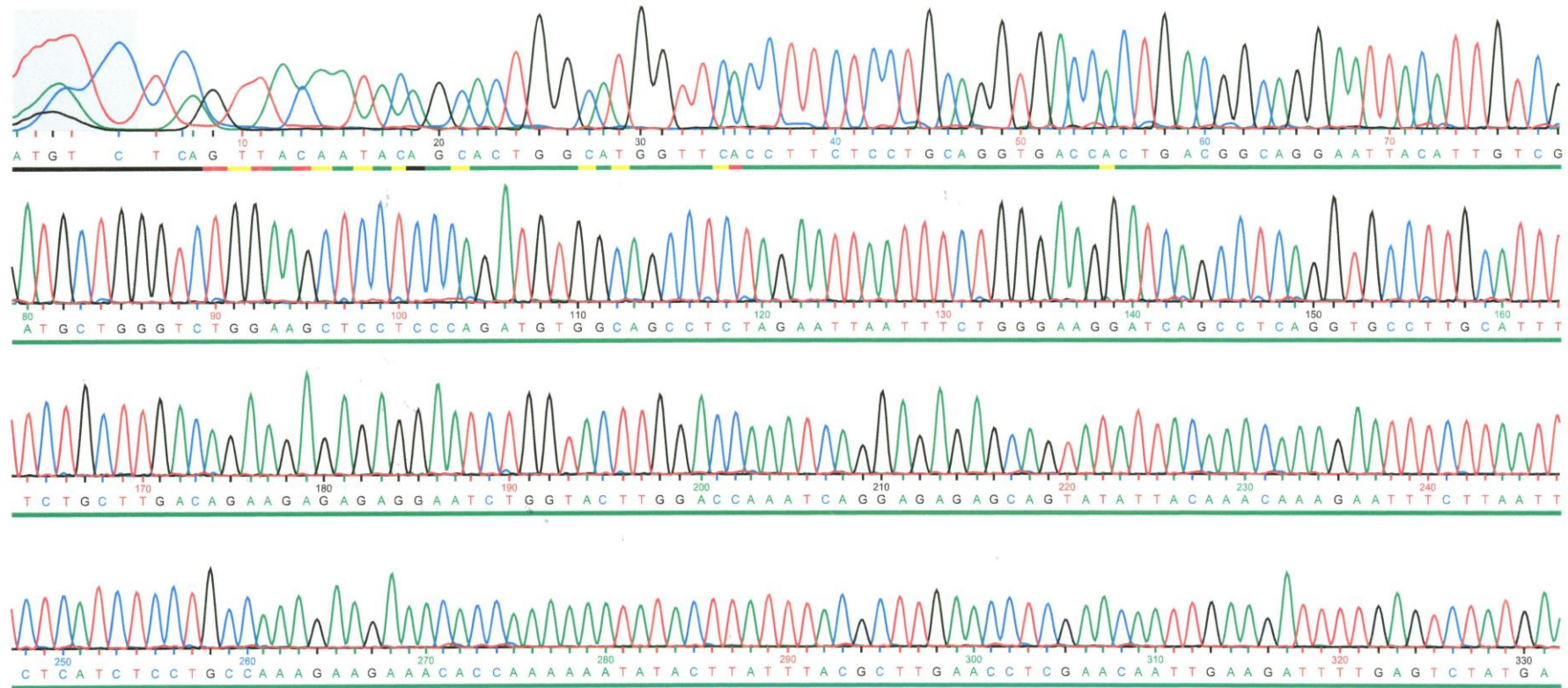
Start codon



Appendix B (i) Electropherogram for slow acetylator recombinant (SAR) plasmid

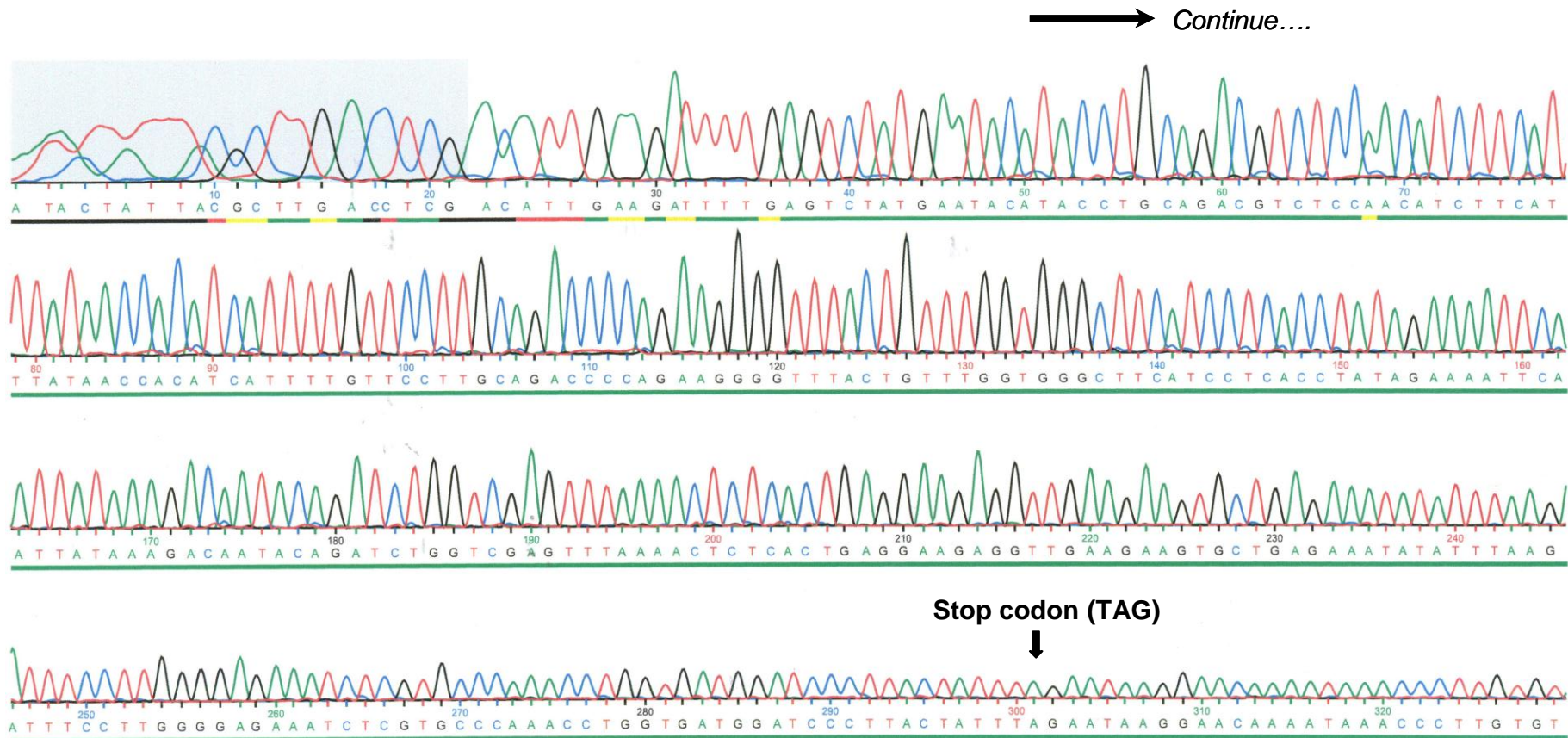
Electropherogram shown is the sequencing traces of SAR plasmid using T7 primer (5'-TAATACGACTCACTATAGGG-3').

→ Continue....



Appendix B (ii) Electropherogram for slow acetylator recombinant (SAR) plasmid

Electropherogram shown is the sequencing traces of SAR plasmid using second primer (5'-TAATACGACTCACTATAGGG-3'), located 251 to 271 bp downstream of the start codon (ATG).



Appendix B (iii) Electropherogram for slow acetylator recombinant (SAR) plasmid

Electropherogram shown is the sequencing traces of SAR plasmid using third primer (5'-TCCTGCCAAAGAAGAAACAC-3'), located 538 to 558 bp downstream of the start codon (ATG).

Chapter 9. References

9 References

- Abboud, G. and Kaplowitz, N. (2007) 'Drug-induced liver injury', *Drug Saf*, 30, (4), pp. 277-94.
- Abdel-Rahman, S. Z., Anwar, W. A., Abdel-Aal, W. E., Mostafa, H. M. and Au, W. W. (1998) 'GSTM1 and GSTT1 genes are potential risk modifiers for bladder cancer', *Cancer Detect Prev*, 22, (2), pp. 129-38.
- Accorsi, S., Fabiani, M., Nattabi, B., Corrado, B., Iriso, R., Ayella, E. O., Pido, B., Onek, P. A., Ogwang, M. and Declich, S. (2005) 'The disease profile of poverty: morbidity and mortality in northern Uganda in the context of war, population displacement and HIV/AIDS', *Trans R Soc Trop Med Hyg*, 99, (3), pp. 226-33.
- Acuna, G., Foernzler, D., Leong, D., Rabbia, M., Smit, R., Dorflinger, E., Gasser, R., Hoh, J., Ott, J., Borroni, E., To, Z., Thompson, A., Li, J., Hashimoto, L. and Lindpaintner, K. (2002) 'Pharmacogenetic analysis of adverse drug effect reveals genetic variant for susceptibility to liver toxicity', *Pharmacogenomics J*, 2, (5), pp. 327-34.
- Aithal, G. P., Ramsay, L., Daly, A. K., Sonchit, N., Leathart, J. B., Alexander, G., Kenna, J. G., Caldwell, J. and Day, C. P. (2004) 'Hepatic adducts, circulating antibodies, and cytokine polymorphisms in patients with diclofenac hepatotoxicity', *Hepatology*, 39, (5), pp. 1430-40.
- Aithal, G. P., Watkins, P.B, Andrade, R.J, Larrey, D., Molokhia, M., Takikawa, H., Hunt, C.M., Wilke, R.A., Avigan, M., Kaplowitz, N., Bjornsson, E., Daly, A. . (2011) 'Case definition and phenotype standardisation in drug-induced liver injury', *In press*.
- Andersson, T. B. (2010) 'The application of HepRG cells in evaluation of cytochrome P450 induction properties of drug compounds', *Methods Mol Biol*, 640, pp. 375-87.
- Andrade, R. J., Agundez, J. A., Lucena, M. I., Martinez, C., Cueto, R. and Garcia-Martin, E. (2009) 'Pharmacogenomics in drug induced liver injury', *Curr Drug Metab*, 10, (9), pp. 956-70.

- Andrade, R. J., Camargo, R., Lucena, M. I. and Gonzalez-Grande, R. (2004) 'Causality assessment in drug-induced hepatotoxicity', *Expert Opin Drug Saf*, 3, (4), pp. 329-44.
- Andrade, R. J., Guilarte, J., Salmeron, F. J., Lucena, M. I. and Bellot, V. (2001) 'Benzylpenicillin-induced prolonged cholestasis', *Ann Pharmacother*, 35, (6), pp. 783-4.
- Andrade, R. J., Lucena, M. I., Fernandez, M. C., Vega, J. L., Garcia-Cortes, M., Casado, M., Guerrero-Sanchez, E. and Pulido-Fernandez, F. (2002) 'Cholestatic hepatitis related to use of irbesartan: a case report and a literature review of angiotensin II antagonist-associated hepatotoxicity', *Eur J Gastroenterol Hepatol*, 14, (8), pp. 887-90.
- Andrade, R. J., Lucena, M. I., Kaplowitz, N., Garcia-Munoz, B., Borraz, Y., Pachkoria, K., Garcia-Cortes, M., Fernandez, M. C., Pelaez, G., Rodrigo, L., Duran, J. A., Costa, J., Planas, R., Barriocanal, A., Guarner, C., Romero-Gomez, M., Munoz-Yague, T., Salmeron, J. and Hidalgo, R. (2006) 'Outcome of acute idiosyncratic drug-induced liver injury: Long-term follow-up in a hepatotoxicity registry', *Hepatology*, 44, (6), pp. 1581-8.
- Andrade, R. J., Robles, M., Fernandez-Castaner, A., Lopez-Ortega, S., Lopez-Vega, M. C. and Lucena, M. I. (2007) 'Assessment of drug-induced hepatotoxicity in clinical practice: a challenge for gastroenterologists', *World J Gastroenterol*, 13, (3), pp. 329-40.
- Andrews, C. A. (2010) 'Natural Selection, Genetic Drift, and Gene Flow Do Not Act in Isolation in Natural Populations', *Nature Education Knowledge*, 1, (10).
- Andrews, E., Armstrong, M., Tugwood, J., Swan, D., Glaves, P., Pirmohamed, M., Aithal, G. P., Wright, M. C., Day, C. P. and Daly, A. K. (2010) 'A role for the pregnane X receptor in flucloxacillin-induced liver injury', *Hepatology*, 51, (5), pp. 1656-64.
- Aninat, C., Piton, A., Glaise, D., Le Charpentier, T., Langouet, S., Morel, F., Guguen-Guillouzo, C. and Guillouzo, A. (2006) 'Expression of cytochromes P450, conjugating enzymes and nuclear receptors in human hepatoma HepaRG cells', *Drug Metab Dispos*, 34, (1), pp. 75-83.

- Askgaard, D. S., Wilcke, T. and Dossing, M. (1995) 'Hepatotoxicity caused by the combined action of isoniazid and rifampicin', *Thorax*, 50, (2), pp. 213-4.
- Association, B. T. (1981) 'A controlled trial of 6-months isoniazid and rifampin therapy for pulmonary tuberculosis: first report: results during drug therapy', *Br J Dis Chest*, 75, pp. 141-153.
- Baker, M. A., Cerniglia, G. J. and Zaman, A. (1990) 'Microtiter plate assay for the measurement of glutathione and glutathione disulfide in large numbers of biological samples', *Anal Biochem*, 190, (2), pp. 360-5.
- Balogh, L. M. and Atkins, W. M. (2011) 'Interactions of glutathione transferases with 4-hydroxynonenal', *Drug Metab Rev*, 43, (2), pp. 165-78.
- Batra, J., Sharma, S. K. and Ghosh, B. (2006) 'Arylamine N-acetyltransferase gene polymorphisms: markers for atopic asthma, serum IgE and blood eosinophil counts', *Pharmacogenomics*, 7, (5), pp. 673-82.
- Benichou, C. (1990) 'Criteria of drug-induced liver disorders. Report of an international consensus meeting', *J Hepatol*, 11, (2), pp. 272-6.
- Benichou, C., Danan, G. and Flahault, A. (1993) 'Causality assessment of adverse reactions to drugs--II. An original model for validation of drug causality assessment methods: case reports with positive rechallenge', *J Clin Epidemiol*, 46, (11), pp. 1331-6.
- Benjamini, Y. and Hochberg, Y. (1995) 'Controlling the False Discovery Rate: A Practical and Powerful Approach to Multiple Testing', *Journal of the Royal Statistical Society B*, 57, pp. 289-300.
- Berhane, K., Widersten, M., Engstrom, A., Kozarich, J. W. and Mannervik, B. (1994) 'Detoxication of base propeals and other alpha, beta-unsaturated aldehyde products of radical reactions and lipid peroxidation by human glutathione transferases', *Proc Natl Acad Sci U S A*, 91, (4), pp. 1480-4.

- Berkowitz, F. E., Henderson, S. L., Fajman, N., Schoen, B. and Naughton, M. (1998) 'Acute liver failure caused by isoniazid in a child receiving carbamazepine', *Int J Tuberc Lung Dis*, 2, (7), pp. 603-6.
- Bhadoria, S., Mishra, R., Kanchan, R., Tripathi, C., Srivastava, A., Tiwari, A. and Sharma, S. (2010) 'Isoniazid-induced apoptosis in HepG2 cells: generation of oxidative stress and Bcl-2 down-regulation', *Toxicol Mech Methods*, 20, (5), pp. 242-51.
- Bjornsson, E. (2010) 'Review article: drug-induced liver injury in clinical practice', *Aliment Pharmacol Ther*, 32, (1), pp. 3-13.
- Bjornsson, E. and Olsson, R. (2005) 'Outcome and prognostic markers in severe drug-induced liver disease', *Hepatology*, 42, (2), pp. 481-9.
- Bjornsson, E., Talwalkar, J., Treeprasertsuk, S., Kamath, P. S., Takahashi, N., Sanderson, S., Neuhauser, M. and Lindor, K. (2010) 'Drug-induced autoimmune hepatitis: clinical characteristics and prognosis', *Hepatology*, 51, (6), pp. 2040-8.
- Black, M., Mitchell, J. R., Zimmerman, H. J., Ishak, K. G. and Epler, G. R. (1975) 'Isoniazid-associated hepatitis in 114 patients', *Gastroenterology*, 69, (2), pp. 289-302.
- Blazka, M. E., Elwell, M. R., Holladay, S. D., Wilson, R. E. and Luster, M. I. (1996) 'Histopathology of acetaminophen-induced liver changes: role of interleukin 1 alpha and tumor necrosis factor alpha', *Toxicol Pathol*, 24, (2), pp. 181-9.
- Blazka, M. E., Wilmer, J. L., Holladay, S. D., Wilson, R. E. and Luster, M. I. (1995) 'Role of proinflammatory cytokines in acetaminophen hepatotoxicity', *Toxicol Appl Pharmacol*, 133, (1), pp. 43-52.
- Blum, M., Grant, D. M., McBride, W., Heim, M. and Meyer, U. A. (1990) 'Human arylamine N-acetyltransferase genes: isolation, chromosomal localization, and functional expression', *DNA Cell Biol*, 9, (3), pp. 193-203.

- Blum, M., Demierre, A., Grant, D. M., Heim, M. and Meyer, U. A. (1991) 'Molecular mechanism of slow acetylation of drugs and carcinogens in humans', *Proc Natl Acad Sci U S A*, 88, (12), pp. 5237-41.
- Boelsterli, U. A. (2003) 'Idiosyncratic drug hepatotoxicity revisited: New insights from mechanistic toxicity', *Toxicology mechanisms & Methods*, 13, pp. 3-20.
- Boelsterli, U. A. and Lim, P. L. (2007) 'Mitochondrial abnormalities--a link to idiosyncratic drug hepatotoxicity?', *Toxicol Appl Pharmacol*, 220, (1), pp. 92-107.
- Bose, P. D., Sarma, M. P., Medhi, S., Das, B. C., Husain, S. A. and Kar, P. (2011) 'Role of polymorphic N-acetyl transferase2 and cytochrome P4502E1 gene in antituberculosis treatment-induced hepatitis', *J Gastroenterol Hepatol*, 26, (2), pp. 312-8.
- Bourdi, M., Masubuchi, Y., Reilly, T. P., Amouzadeh, H. R., Martin, J. L., George, J. W., Shah, A. G. and Pohl, L. R. (2002) 'Protection against acetaminophen-induced liver injury and lethality by interleukin 10: role of inducible nitric oxide synthase', *Hepatology*, 35, (2), pp. 289-98.
- Bozok Cetintas, V., Erer, O. F., Kosova, B., Ozdemir, I., Topcuoglu, N., Aktogu, S. and Eroglu, Z. (2008) 'Determining the relation between N-acetyltransferase-2 acetylator phenotype and antituberculosis drug induced hepatitis by molecular biologic tests', *Tuberk Toraks*, 56, (1), pp. 81-6.
- Buch, H., Buzello, W., Heymann, E. and Krisch, K. (1969) 'Inhibition of phenacetin- and acetanilide-induced methemoglobinemia in the rat by the carboxylesterase inhibitor bis-[p-nitrophenyl] phosphate', *Biochem Pharmacol*, 18, (4), pp. 801-11.
- Burk, O., Koch, I., Raucy, J., Hustert, E., Eichelbaum, M., Brockmoller, J., Zanger, U. M. and Wojnowski, L. (2004) 'The induction of cytochrome P450 3A5 (CYP3A5) in the human liver and intestine is mediated by the xenobiotic sensors pregnane X receptor (PXR) and constitutively activated receptor (CAR)', *J Biol Chem*, 279, (37), pp. 38379-85.

- Byrne, J. A., Strautnieks, S. S., Mieli-Vergani, G., Higgins, C. F., Linton, K. J. and Thompson, R. J. (2002) 'The human bile salt export pump: characterization of substrate specificity and identification of inhibitors', *Gastroenterology*, 123, (5), pp. 1649-58.
- Caro, A. A. and Cederbaum, A. I. (2004) 'Oxidative stress, toxicology, and pharmacology of CYP2E1', *Annu Rev Pharmacol Toxicol*, 44, pp. 27-42.
- Carr, D. F., Alfirevic, A., Tugwood, J. D., Barratt, B. J., Sherwood, J., Smith, J., Pirmohamed, M. and Park, B. K. (2007) 'Molecular and genetic association of interleukin-6 in tacrine-induced hepatotoxicity', *Pharmacogenet Genomics*, 17, (11), pp. 961-72.
- CDC. (2003) 'Update: adverse event data and revised American Thoracic Society/CDC recommendations against the use of rifampin and pyrazinamide for treatment of latent tuberculosis infection--United States, 2003', *MMWR Morb Mortal Wkly Rep*, 52, (31), pp. 735-9.
- Chalasanani, N., Fontana, R. J., Bonkovsky, H. L., Watkins, P. B., Davern, T., Serrano, J., Yang, H. and Rochon, J. (2008) 'Causes, clinical features, and outcomes from a prospective study of drug-induced liver injury in the United States', *Gastroenterology*, 135, (6), pp. 1924-34, 1934 e1-4.
- Chang, K. C., Leung, C. C., Yew, W. W. and Tam, C. M. (2007) 'Standard anti-tuberculosis treatment and hepatotoxicity: do dosing schedules matter?', *Eur Respir J*, 29, (2), pp. 347-51.
- Chatterjee, S., Lyle, N., Mandal, A. and Kundu, S. (2010) 'GSTT1 and GSTM1 gene deletions are not associated with hepatotoxicity caused by antitubercular drugs', *J Clin Pharm Ther*, 35, (4), pp. 465-70.
- Cho, H. J., Koh, W. J., Ryu, Y. J., Ki, C. S., Nam, M. H., Kim, J. W. and Lee, S. Y. (2007) 'Genetic polymorphisms of NAT2 and CYP2E1 associated with antituberculosis drug-induced hepatotoxicity in Korean patients with pulmonary tuberculosis', *Tuberculosis (Edinb)*, 87, (6), pp. 551-6.
- Choi, J. H., Ahn, B. M., Yi, J., Lee, J. H., Nam, S. W., Chon, C. Y., Han, K. H., Ahn, S. H., Jang, I. J., Cho, J. Y., Suh, Y., Cho, M. O., Lee, J. E., Kim, K. H. and Lee,

- M. G. (2007) 'MRP2 haplotypes confer differential susceptibility to toxic liver injury', *Pharmacogenet Genomics*, 17, (6), pp. 403-15.
- Coles, B. F., Morel, F., Rauch, C., Huber, W. W., Yang, M., Teitel, C. H., Green, B., Lang, N. P. and Kadlubar, F. F. (2001) 'Effect of polymorphism in the human glutathione S-transferase A1 promoter on hepatic GSTA1 and GSTA2 expression', *Pharmacogenetics*, 11, (8), pp. 663-9.
- Coppede, F., Armani, C., Bidia, D. D., Petrozzi, L., Bonuccelli, U. and Migliore, L. (2005) 'Molecular implications of the human glutathione transferase A-4 gene (hGSTA4) polymorphisms in neurodegenerative diseases', *Mutat Res*, 579, (1-2), pp. 107-14.
- Crippin, J. S. (1993) 'Acetaminophen hepatotoxicity: potentiation by isoniazid', *Am J Gastroenterol*, 88, (4), pp. 590-2.
- Cummins, C. L., Salphati, L., Reid, M. J. and Benet, L. Z. (2003) 'In vivo modulation of intestinal CYP3A metabolism by P-glycoprotein: studies using the rat single-pass intestinal perfusion model', *J Pharmacol Exp Ther*, 305, (1), pp. 306-14.
- Daly, A. K. (2003) 'Pharmacogenetics of the major polymorphic metabolizing enzymes', *Fundam Clin Pharmacol*, 17, (1), pp. 27-41.
- Daly, A. K. (2010) 'Drug-induced liver injury: past, present and future', *Pharmacogenomics*, 11, (5), pp. 607-11.
- Daly, A. K., Aithal, G. P., Leathart, J. B., Swainsbury, R. A., Dang, T. S. and Day, C. P. (2007) 'Genetic susceptibility to diclofenac-induced hepatotoxicity: contribution of UGT2B7, CYP2C8, and ABCC2 genotypes', *Gastroenterology*, 132, (1), pp. 272-81.
- Daly, A. K., Donaldson, P. T., Bhatnagar, P., Shen, Y., Pe'er, I., Floratos, A., Daly, M. J., Goldstein, D. B., John, S., Nelson, M. R., Graham, J., Park, B. K., Dillon, J. F., Bernal, W., Cordell, H. J., Pirmohamed, M., Aithal, G. P. and Day, C. P. (2009) 'HLA-B*5701 genotype is a major determinant of drug-induced liver injury due to flucloxacillin', *Nat Genet*, 41, (7), pp. 816-9.

- Danan, G. and Benichou, C. (1993) 'Causality assessment of adverse reactions to drugs--I. A novel method based on the conclusions of international consensus meetings: application to drug-induced liver injuries', *J Clin Epidemiol*, 46, (11), pp. 1323-30.
- Davies, E. C., Green, C. F., Taylor, S., Williamson, P. R., Mottram, D. R. and Pirmohamed, M. (2009) 'Adverse drug reactions in hospital in-patients: a prospective analysis of 3695 patient-episodes', *PLoS One*, 4, (2), pp. e4439.
- de Abajo, F. J., Montero, D., Madurga, M. and Garcia Rodriguez, L. A. (2004) 'Acute and clinically relevant drug-induced liver injury: a population based case-control study', *Br J Clin Pharmacol*, 58, (1), pp. 71-80.
- De Valle, M. B., Av Klinteberg, V., Alem, N., Olsson, R. and Bjornsson, E. (2006) 'Drug-induced liver injury in a Swedish University hospital out-patient hepatology clinic', *Aliment Pharmacol Ther*, 24, (8), pp. 1187-95.
- Desai, P. B., Nallani, S. C., Sane, R. S., Moore, L. B., Goodwin, B. J., Buckley, D. J. and Buckley, A. R. (2002) 'Induction of cytochrome P450 3A4 in primary human hepatocytes and activation of the human pregnane X receptor by tamoxifen and 4-hydroxytamoxifen', *Drug Metab Dispos*, 30, (5), pp. 608-12.
- Dickinson, D. S., Bailey, W. C., Hirschowitz, B. I., Soong, S. J., Eidus, L. and Hodgkin, M. M. (1981) 'Risk factors for isoniazid (INH)-induced liver dysfunction', *J Clin Gastroenterol*, 3, (3), pp. 271-9.
- Donaldson, P. T., Daly, A. K., Henderson, J., Graham, J., Pirmohamed, M., Bernal, W., Day, C. P. and Aithal, G. P. (2010) 'Human leucocyte antigen class II genotype in susceptibility and resistance to co-amoxiclav-induced liver injury', *J Hepatol*, 53, (6), pp. 1049-53.
- Dorak, M. T. (2006) Real-time PCR. Taylor and Francis.
- Dworkin, M. S., Adams, M. R., Cohn, D. L., Davidson, A. J., Buskin, S., Horwitch, C., Morse, A., Sackoff, J., Thompson, M., Wotring, L., McCombs, S. B. and Jones, J. L. (2005) 'Factors that complicate the treatment of tuberculosis in HIV-infected patients', *J Acquir Immune Defic Syndr*, 39, (4), pp. 464-70.

- Elaut, G., Henkens, T., Papeleu, P., Snykers, S., Vinken, M., Vanhaecke, T. and Rogiers, V. (2006) 'Molecular mechanisms underlying the dedifferentiation process of isolated hepatocytes and their cultures', *Curr Drug Metab*, 7, (6), pp. 629-60.
- Eliasson, E., Gardner, I., Hume-Smith, H., de Waziers, I., Beaune, P. and Kenna, J. G. (1998) 'Interindividual variability in P450-dependent generation of neoantigens in halothane hepatitis', *Chem Biol Interact*, 116, (1-2), pp. 123-41.
- Eliasson, E. and Kenna, J. G. (1996) 'Cytochrome P450 2E1 is a cell surface autoantigen in halothane hepatitis', *Mol Pharmacol*, 50, (3), pp. 573-82.
- Ellard, G. A., Mitchison, D. A., Girling, D. J., Nunn, A. J. and Fox, W. (1978) 'The hepatic toxicity of isoniazid among rapid and slow acetylators of the drug', *Am Rev Respir Dis*, 118, (3), pp. 628-9.
- Esterbauer, H., Schaur, R. J. and Zollner, H. (1991) 'Chemistry and biochemistry of 4-hydroxynonenal, malonaldehyde and related aldehydes', *Free Radic Biol Med*, 11, (1), pp. 81-128.
- Evans, W. E. and McLeod, H. L. (2003) 'Pharmacogenomics--drug disposition, drug targets, and side effects', *N Engl J Med*, 348, (6), pp. 538-49.
- Farcas, A. and Bojita, M. (2009) 'Adverse drug reactions in clinical practice: a causality assessment of a case of drug-induced pancreatitis', *J Gastrointestin Liver Dis*, 18, (3), pp. 353-8.
- Fernandez-Villar, A., Sopena, B., Fernandez-Villar, J., Vazquez-Gallardo, R., Ulloa, F., Leiro, V., Mosteiro, M. and Pineiro, L. (2004) 'The influence of risk factors on the severity of anti-tuberculosis drug-induced hepatotoxicity', *Int J Tuberc Lung Dis*, 8, (12), pp. 1499-505.
- Fontana, R. J., Seeff, L. B., Andrade, R. J., Bjornsson, E., Day, C. P., Serrano, J. and Hoofnagle, J. H. (2010) 'Standardization of nomenclature and causality assessment in drug-induced liver injury: summary of a clinical research workshop', *Hepatology*, 52, (2), pp. 730-42.

- Fontana, R. J., Watkins, P. B., Bonkovsky, H. L., Chalasani, N., Davern, T., Serrano, J. and Rochon, J. (2009) 'Drug-Induced Liver Injury Network (DILIN) prospective study: rationale, design and conduct', *Drug Saf*, 32, (1), pp. 55-68.
- Forget, E. J. and Menzies, D. (2006) 'Adverse reactions to first-line antituberculosis drugs', *Expert Opin Drug Saf*, 5, (2), pp. 231-49.
- Fretland, A. J., Leff, M. A., Doll, M. A. and Hein, D. W. (2001) 'Functional characterization of human N-acetyltransferase 2 (NAT2) single nucleotide polymorphisms', *Pharmacogenetics*, 11, (3), pp. 207-15.
- Fromm, M. F. (2003) 'Importance of P-glycoprotein for drug disposition in humans', *Eur J Clin Invest*, 33 Suppl 2, pp. 6-9.
- Fukino, K., Sasaki, Y., Hirai, S., Nakamura, T., Hashimoto, M., Yamagishi, F. and Ueno, K. (2008) 'Effects of N-acetyltransferase 2 (NAT2), CYP2E1 and Glutathione-S-transferase (GST) genotypes on the serum concentrations of isoniazid and metabolites in tuberculosis patients', *J Toxicol Sci*, 33, (2), pp. 187-95.
- Gallagher, E. P., Huisden, C. M. and Gardner, J. L. (2007) 'Transfection of HepG2 cells with hGSTA4 provides protection against 4-hydroxynonenal-mediated oxidative injury', *Toxicol In Vitro*, 21, (8), pp. 1365-72.
- Gardner, J. L., Doi, A. M., Pham, R. T., Huisden, C. M. and Gallagher, E. P. (2003) 'Ontogenic differences in human liver 4-hydroxynonenal detoxification are associated with in vitro injury to fetal hematopoietic stem cells', *Toxicol Appl Pharmacol*, 191, (2), pp. 95-106.
- Gent, W. L., Seifart, H. I., Parkin, D. P., Donald, P. R. and Lamprecht, J. H. (1992) 'Factors in hydrazine formation from isoniazid by paediatric and adult tuberculosis patients', *Eur J Clin Pharmacol*, 43, (2), pp. 131-6.
- Giacomini, K. M., Huang, S. M., Tweedie, D. J., Benet, L. Z., Brouwer, K. L., Chu, X., Dahlin, A., Evers, R., Fischer, V., Hillgren, K. M., Hoffmaster, K. A., Ishikawa, T., Keppler, D., Kim, R. B., Lee, C. A., Niemi, M., Polli, J. W., Sugiyama, Y.,

Swaan, P. W., Ware, J. A., Wright, S. H., Yee, S. W., Zamek-Gliszczynski, M. J. and Zhang, L. (2010) 'Membrane transporters in drug development', *Nat Rev Drug Discov*, 9, (3), pp. 215-36.

Gibson, G. G., Plant, N. J., Swales, K. E., Ayrton, A. and El-Sankary, W. (2002) 'Receptor-dependent transcriptional activation of cytochrome P4503A genes: induction mechanisms, species differences and interindividual variation in man', *Xenobiotica*, 32, (3), pp. 165-206.

Goidin, D., Mamessier, A., Staquet, M. J., Schmitt, D. and Berthier-Vergnes, O. (2001) 'Ribosomal 18S RNA prevails over glyceraldehyde-3-phosphate dehydrogenase and beta-actin genes as internal standard for quantitative comparison of mRNA levels in invasive and noninvasive human melanoma cell subpopulations', *Anal Biochem*, 295, (1), pp. 17-21.

Grange, J. M., Winstanley, P. A. and Davies, P. D. (1994) 'Clinically significant drug interactions with antituberculosis agents', *Drug Saf*, 11, (4), pp. 242-51.

Greiner, B., Eichelbaum, M., Fritz, P., Kreichgauer, H. P., von Richter, O., Zundler, J. and Kroemer, H. K. (1999) 'The role of intestinal P-glycoprotein in the interaction of digoxin and rifampin', *J Clin Invest*, 104, (2), pp. 147-53.

Griffith, O. W. (1980) 'Determination of glutathione and glutathione disulfide using glutathione reductase and 2-vinylpyridine', *Anal Biochem*, 106, (1), pp. 207-12.

Guengerich, F. P. (1999) 'Cytochrome P-450 3A4: regulation and role in drug metabolism', *Annu Rev Pharmacol Toxicol*, 39, pp. 1-17.

Hamanishi, T., Furuta, H., Kato, H., Doi, A., Tamai, M., Shimomura, H., Sakagashira, S., Nishi, M., Sasaki, H., Sanke, T. and Nanjo, K. (2004) 'Functional variants in the glutathione peroxidase-1 (GPx-1) gene are associated with increased intima-media thickness of carotid arteries and risk of macrovascular diseases in Japanese type 2 diabetic patients', *Diabetes*, 53, (9), pp. 2455-60.

Haouzi, D., Lekehal, M., Moreau, A., Moulis, C., Feldmann, G., Robin, M. A., Letteron, P., Fau, D. and Pessayre, D. (2000) 'Cytochrome P450-generated reactive metabolites cause mitochondrial permeability transition, caspase activation, and apoptosis in rat hepatocytes', *Hepatology*, 32, (2), pp. 303-11.

- Hardy, G. H. (1908) 'Mendelian Proportions in a Mixed Population', *Science*, 28, (706), pp. 49-50.
- Hartley, D. P. and Petersen, D. R. (1997) 'Co-metabolism of ethanol, ethanol-derived acetaldehyde, and 4-hydroxynonenal in isolated rat hepatocytes', *Alcohol Clin Exp Res*, 21, (2), pp. 298-304.
- Hautekeete, M. L., Horsmans, Y., Van Waeyenberge, C., Demanet, C., Henrion, J., Verbist, L., Brenard, R., Sempoux, C., Michielsen, P. P., Yap, P. S., Rahier, J. and Geubel, A. P. (1999) 'HLA association of amoxicillin-clavulanate--induced hepatitis', *Gastroenterology*, 117, (5), pp. 1181-6.
- Hayashi, S., Watanabe, J. and Kawajiri, K. (1991) 'Genetic polymorphisms in the 5'-flanking region change transcriptional regulation of the human cytochrome P450IIE1 gene', *J Biochem*, 110, (4), pp. 559-65.
- Hein, D. W., Doll, M. A., Rustan, T. D. and Ferguson, R. J. (1995) 'Metabolic activation of N-hydroxyarylamines and N-hydroxyarylamides by 16 recombinant human NAT2 allozymes: effects of 7 specific NAT2 nucleic acid substitutions', *Cancer Res*, 55, (16), pp. 3531-6.
- Hein, D. W., Ferguson, R. J., Doll, M. A., Rustan, T. D. and Gray, K. (1994) 'Molecular genetics of human polymorphic N-acetyltransferase: enzymatic analysis of 15 recombinant wild-type, mutant, and chimeric NAT2 allozymes', *Hum Mol Genet*, 3, (5), pp. 729-34.
- Helin-Salmivaara, A., Saarelainen, S., Gronroos, J. M., Vesalainen, R., Klaukka, T. and Huupponen, R. (2007) 'Risk of upper gastrointestinal events with the use of various NSAIDs: a case-control study in a general population', *Scand J Gastroenterol*, 42, (8), pp. 923-32.
- Hirata, K., Takagi, H., Yamamoto, M., Matsumoto, T., Nishiya, T., Mori, K., Shimizu, S., Masumoto, H. and Okutani, Y. (2008) 'Ticlopidine-induced hepatotoxicity is associated with specific human leukocyte antigen genomic subtypes in Japanese patients: a preliminary case-control study', *Pharmacogenomics J*, 8, (1), pp. 29-33.

- Holm, S. (1979) 'A simple sequentially rejective multiple test procedure', *Scand J Statistics*, 6, (2), pp. 65-70.
- Holt, M. P. and Ju, C. (2006) 'Mechanisms of drug-induced liver injury', *AAPS J*, 8, (1), pp. E48-54.
- HPA. (2007) *Annual report on tuberculosis surveillance and control in the UK 2007*. London: Health Protection Agency
- Hu, Y., Oscarson, M., Johansson, I., Yue, Q. Y., Dahl, M. L., Tabone, M., Arinco, S., Albano, E. and Ingelman-Sundberg, M. (1997) 'Genetic polymorphism of human CYP2E1: characterization of two variant alleles', *Mol Pharmacol*, 51, (3), pp. 370-6.
- Huang, R., Okuno, H., Takasu, M., Shiozaki, Y. and Inoue, K. (1995) 'Protective effect of rifampicin against acute liver injury induced by carbon tetrachloride in mice', *Jpn J Pharmacol*, 69, (4), pp. 325-34.
- Huang, Y. S., Chern, H. D., Su, W. J., Wu, J. C., Chang, S. C., Chiang, C. H., Chang, F. Y. and Lee, S. D. (2003) 'Cytochrome P450 2E1 genotype and the susceptibility to antituberculosis drug-induced hepatitis', *Hepatology*, 37, (4), pp. 924-30.
- Huang, Y. S., Chern, H. D., Su, W. J., Wu, J. C., Lai, S. L., Yang, S. Y., Chang, F. Y. and Lee, S. D. (2002) 'Polymorphism of the N-acetyltransferase 2 gene as a susceptibility risk factor for antituberculosis drug-induced hepatitis', *Hepatology*, 35, (4), pp. 883-9.
- Huang, Y. S., Su, W. J., Huang, Y. H., Chen, C. Y., Chang, F. Y., Lin, H. C. and Lee, S. D. (2007) 'Genetic polymorphisms of manganese superoxide dismutase, NAD(P)H:quinone oxidoreductase, glutathione S-transferase M1 and T1, and the susceptibility to drug-induced liver injury', *J Hepatol*, 47, (1), pp. 128-34.
- Hubatsch, I., Ridderstrom, M. and Mannervik, B. (1998) 'Human glutathione transferase A4-4: an alpha class enzyme with high catalytic efficiency in the conjugation of 4-hydroxynonenal and other genotoxic products of lipid peroxidation', *Biochem J*, 330 (Pt 1), pp. 175-9.

- Hussaini, S. H., O'Brien, C. S., Despott, E. J. and Dalton, H. R. (2007) 'Antibiotic therapy: a major cause of drug-induced jaundice in southwest England', *Eur J Gastroenterol Hepatol*, 19, (1), pp. 15-20.
- Ibanez, L., Perez, E., Vidal, X. and Laporte, J. R. (2002) 'Prospective surveillance of acute serious liver disease unrelated to infectious, obstructive, or metabolic diseases: epidemiological and clinical features, and exposure to drugs', *J Hepatol*, 37, (5), pp. 592-600.
- Imanishi, H., Okamura, N., Yagi, M., Noro, Y., Moriya, Y., Nakamura, T., Hayakawa, A., Takeshima, Y., Sakaeda, T., Matsuo, M. and Okumura, K. (2007) 'Genetic polymorphisms associated with adverse events and elimination of methotrexate in childhood acute lymphoblastic leukemia and malignant lymphoma', *J Hum Genet*, 52, (2), pp. 166-71.
- Ishida, Y., Kondo, T., Ohshima, T., Fujiwara, H., Iwakura, Y. and Mukaida, N. (2002) 'A pivotal involvement of IFN-gamma in the pathogenesis of acetaminophen-induced acute liver injury', *Faseb J*, 16, (10), pp. 1227-36.
- Iyer, L., Das, S., Janisch, L., Wen, M., Ramirez, J., Karrison, T., Fleming, G. F., Vokes, E. E., Schilsky, R. L. and Ratain, M. J. (2002) 'UGT1A1*28 polymorphism as a determinant of irinotecan disposition and toxicity', *Pharmacogenomics J*, 2, (1), pp. 43-7.
- Ju, C., Reilly, T. P., Bourdi, M., Radonovich, M. F., Brady, J. N., George, J. W. and Pohl, L. R. (2002) 'Protective role of Kupffer cells in acetaminophen-induced hepatic injury in mice', *Chem Res Toxicol*, 15, (12), pp. 1504-13.
- Kaivosaaari, S., Finel, M. and Koskinen, M. (2011) 'N-glucuronidation of drugs and other xenobiotics by human and animal UDP-glucuronosyltransferases', *Xenobiotica*.
- Kaplowitz, N. (2002) 'Biochemical and cellular mechanisms of toxic liver injury', *Semin Liver Dis*, 22, (2), pp. 137-44.
- Kaplowitz, N. (2005) 'Idiosyncratic drug hepatotoxicity', *Nat Rev Drug Discov*, 4, (6), pp. 489-99.

- Kayanja, H. K., Debanne, S., King, C. and Whalen, C. C. (2005) 'Tuberculosis infection among health care workers in Kampala, Uganda', *Int J Tuberc Lung Dis*, 9, (6), pp. 686-8.
- Kim, S. H., Bahn, J. W., Kim, Y. K., Chang, Y. S., Shin, E. S., Kim, Y. S., Park, J. S., Kim, B. H., Jang, I. J., Song, J., Park, H. S., Min, K. U. and Jee, Y. K. (2009) 'Genetic polymorphisms of drug-metabolizing enzymes and anti-TB drug-induced hepatitis', *Pharmacogenomics*, 10, (11), pp. 1767-79.
- Kindmark, A., Jawaid, A., Harbron, C. G., Barratt, B. J., Bengtsson, O. F., Andersson, T. B., Carlsson, S., Cederbrant, K. E., Gibson, N. J., Armstrong, M., Lagerstrom-Fermer, M. E., Dellsen, A., Brown, E. M., Thornton, M., Dukes, C., Jenkins, S. C., Firth, M. A., Harrod, G. O., Pinel, T. H., Billing-Clason, S. M., Cardon, L. R. and March, R. E. (2008) 'Genome-wide pharmacogenetic investigation of a hepatic adverse event without clinical signs of immunopathology suggests an underlying immune pathogenesis', *Pharmacogenomics J*, 8, (3), pp. 186-95.
- Kliwer, S. A., Goodwin, B. and Willson, T. M. (2002) 'The nuclear pregnane X receptor: a key regulator of xenobiotic metabolism', *Endocr Rev*, 23, (5), pp. 687-702.
- Kocabas, N. A., Sardas, S., Cholerton, S., Daly, A. K. and Karakaya, A. E. (2004) 'N-acetyltransferase (NAT2) polymorphism and breast cancer susceptibility: a lack of association in a case-control study of Turkish population', *Int J Toxicol*, 23, (1), pp. 25-31.
- Kolars, J. C., Lown, K. S., Schmiedlin-Ren, P., Ghosh, M., Fang, C., Wrighton, S. A., Merion, R. M. and Watkins, P. B. (1994) 'CYP3A gene expression in human gut epithelium', *Pharmacogenetics*, 4, (5), pp. 247-59.
- Kolars, J. C., Schmiedlin-Ren, P., Schuetz, J. D., Fang, C. and Watkins, P. B. (1992) 'Identification of rifampin-inducible P450III_{A4} (CYP3A₄) in human small bowel enterocytes', *J Clin Invest*, 90, (5), pp. 1871-8.
- Konno, K., Feldmann, F. M. and McDermott, W. (1967) 'Pyrazinamide susceptibility and amidase activity of tubercle bacilli', *Am Rev Respir Dis*, 95, (3), pp. 461-9.

- Kretz-Rommel, A. and Boelsterli, U. A. (1995) 'Cytotoxic activity of T cells and non-T cells from diclofenac-immunized mice against cultured syngeneic hepatocytes exposed to diclofenac', *Hepatology*, 22, (1), pp. 213-22.
- Krishnaswamy, K., Prasad, C. E. and Murthy, K. J. (1991) 'Hepatic dysfunction in undernourished patients receiving isoniazid and rifampicin', *Trop Geogr Med*, 43, (1-2), pp. 156-60.
- Kumar, R., Bhatia, V., Khanal, S., Sreenivas, V., Gupta, S. D., Panda, S. K. and Acharya, S. K. (2010) 'Antituberculosis therapy-induced acute liver failure: magnitude, profile, prognosis, and predictors of outcome', *Hepatology*, 51, (5), pp. 1665-74.
- Kumari, S. and Ram, V. J. (2004) 'Advances in molecular targets and chemotherapy of tuberculosis', *Drugs Today (Barc)*, 40, (6), pp. 487-500.
- Lacroix, C., Guyonnaud, C., Chaou, M., Duwoos, H. and Lafont, O. (1988) 'Interaction between allopurinol and pyrazinamide', *Eur Respir J*, 1, (9), pp. 807-11.
- Lacroix, C., Hoang, T. P., Nouveau, J., Guyonnaud, C., Laine, G., Duwoos, H. and Lafont, O. (1989) 'Pharmacokinetics of pyrazinamide and its metabolites in healthy subjects', *Eur J Clin Pharmacol*, 36, (4), pp. 395-400.
- Laemmli, U. K. (1970) 'Cleavage of structural proteins during the assembly of the head of bacteriophage T4', *Nature*, 227, (5259), pp. 680-5.
- Lakehal, F., Dansette, P. M., Becquemont, L., Lasnier, E., Delelo, R., Ballardur, P., Poupon, R., Beaune, P. H. and Housset, C. (2001) 'Indirect cytotoxicity of flucloxacillin toward human biliary epithelium via metabolite formation in hepatocytes', *Chem Res Toxicol*, 14, (6), pp. 694-701.
- Landsteiner, K. and Jacobs, J. (1935) 'Studies on the Sensitization of Animals with Simple Chemical Compounds', *J Exp Med*, 61, (5), pp. 643-56.

- Lang, C., Meier, Y., Stieger, B., Beuers, U., Lang, T., Kerb, R., Kullak-Ublick, G. A., Meier, P. J. and Pauli-Magnus, C. (2007) 'Mutations and polymorphisms in the bile salt export pump and the multidrug resistance protein 3 associated with drug-induced liver injury', *Pharmacogenet Genomics*, 17, (1), pp. 47-60.
- Larrey, D. (2000) 'Drug-induced liver diseases', *J Hepatol*, 32, (1 Suppl), pp. 77-88.
- Larrey, D. (2002) 'Epidemiology and individual susceptibility to adverse drug reactions affecting the liver', *Semin Liver Dis*, 22, (2), pp. 145-55.
- Lasser, K. E., Allen, P. D., Woolhandler, S. J., Himmelstein, D. U., Wolfe, S. M. and Bor, D. H. (2002) 'Timing of new black box warnings and withdrawals for prescription medications', *JAMA*, 287, (17), pp. 2215-20.
- Lauterburg, B. H., Smith, C. V., Todd, E. L. and Mitchell, J. R. (1985) 'Pharmacokinetics of the toxic hydrazino metabolites formed from isoniazid in humans', *J Pharmacol Exp Ther*, 235, (3), pp. 566-70.
- Lazarou, J., Pomeranz, B. H. and Corey, P. N. (1998) 'Incidence of adverse drug reactions in hospitalized patients: a meta-analysis of prospective studies', *JAMA*, 279, (15), pp. 1200-5.
- Lee, A. M., Mennone, J. Z., Jones, R. C. and Paul, W. S. (2002) 'Risk factors for hepatotoxicity associated with rifampin and pyrazinamide for the treatment of latent tuberculosis infection: experience from three public health tuberculosis clinics', *Int J Tuberc Lung Dis*, 6, (11), pp. 995-1000.
- Lee, S. W., Chung, L. S., Huang, H. H., Chuang, T. Y., Liou, Y. H. and Wu, L. S. (2010) 'NAT2 and CYP2E1 polymorphisms and susceptibility to first-line anti-tuberculosis drug-induced hepatitis', *Int J Tuberc Lung Dis*, 14, (5), pp. 622-6.
- Lee, S., Kasif, S., Weng, Z. and Cantor, C. R. (2008) 'Quantitative analysis of single nucleotide polymorphisms within copy number variation', *PLoS One*, 3, (12), pp. e3906
- Lee, W. M. (2003) 'Drug-induced hepatotoxicity', *N Engl J Med*, 349, (5), pp. 474-85.

- Leiro, V., Fernandez-Villar, A., Valverde, D., Constenla, L., Vazquez, R., Pineiro, L. and Gonzalez-Quintela, A. (2008) 'Influence of glutathione S-transferase M1 and T1 homozygous null mutations on the risk of antituberculosis drug-induced hepatotoxicity in a Caucasian population', *Liver Int*, 28, (6), pp. 835-9.
- Li, A. P., Reith, M. K., Rasmussen, A., Gorski, J. C., Hall, S. D., Xu, L., Kaminski, D. L. and Cheng, L. K. (1997) 'Primary human hepatocytes as a tool for the evaluation of structure-activity relationship in cytochrome P450 induction potential of xenobiotics: evaluation of rifampin, rifapentine and rifabutin', *Chem Biol Interact*, 107, (1-2), pp. 17-30.
- Lienhardt, C., Fielding, K., Sillah, J., Tunkara, A., Donkor, S., Manneh, K., Warndorff, D., McAdam, K. P. and Bennett, S. (2003) 'Risk factors for tuberculosis infection in sub-Saharan Africa: a contact study in The Gambia', *Am J Respir Crit Care Med*, 168, (4), pp. 448-55.
- Link, E., Parish, S., Armitage, J., Bowman, L., Heath, S., Matsuda, F., Gut, I., Lathrop, M. and Collins, R. (2008) 'SLCO1B1 variants and statin-induced myopathy--a genomewide study', *N Engl J Med*, 359, (8), pp. 789-99.
- Livak, K. J. and Schmittgen, T. D. (2001) 'Analysis of relative gene expression data using real-time quantitative PCR and the 2(-Delta Delta C(T)) Method', *Methods*, 25, (4), pp. 402-8.
- Lucena, M. I., Andrade, R. J., Martinez, C., Ulzurrun, E., Garcia-Martin, E., Borraz, Y., Fernandez, M. C., Romero-Gomez, M., Castiella, A., Planas, R., Costa, J., Anzola, S. and Agundez, J. A. (2008a) 'Glutathione S-transferase m1 and t1 null genotypes increase susceptibility to idiosyncratic drug-induced liver injury', *Hepatology*, 48, (2), pp. 588-96.
- Lucena, M. I., Camargo, R., Andrade, R. J., Perez-Sanchez, C. J. and Sanchez De La Cuesta, F. (2001) 'Comparison of two clinical scales for causality assessment in hepatotoxicity', *Hepatology*, 33, (1), pp. 123-30.
- Lucena, M. I., Garcia-Cortes, M., Cueto, R., Lopez-Duran, J. and Andrade, R. J. (2008b) 'Assessment of drug-induced liver injury in clinical practice', *Fundam Clin Pharmacol*, 22, (2), pp. 141-58.

- Lucena, M. I., Garcia-Martin, E., Andrade, R. J., Martinez, C., Stephens, C., Ruiz, J. D., Ulzurrun, E., Fernandez, M. C., Romero-Gomez, M., Castiella, A., Planas, R., Duran, J. A., De Dios, A. M., Guarner, C., Soriano, G., Borraz, Y. and Agundez, J. A. (2010) 'Mitochondrial superoxide dismutase and glutathione peroxidase in idiosyncratic drug-induced liver injury', *Hepatology*, 52, (1), pp. 303-12.
- Lucena, M. I., Molokhia, M., Shen, Y., Urban, T. J., Aithal, G. P., Andrade, R. J., Day, C. P., Ruiz-Cabello, F., Donaldson, P. T., Stephens, C., Pirmohamed, M., Romero-Gomez, M., Navarro, J. M., Fontana, R. J., Miller, M., Groome, M., Bondon-Guitton, E., Conforti, A., Stricker, B. H., Carvajal, A., Ibanez, L., Yue, Q. Y., Eichelbaum, M., Floratos, A., Pe'er, I., Daly, M. J., Goldstein, D. B., Dillon, J. F., Nelson, M. R., Watkins, P. B. and Daly, A. K. (2011) 'Susceptibility to Amoxicillin-Clavulanate-Induced Liver Injury Is Influenced by Multiple HLA Class I and II Alleles', *Gastroenterology*, 141, (1), pp. 338-47.
- Lunetta, K. L. (2008) 'Genetic association studies', *Circulation*, 118, (1), pp. 96-101.
- Mallal, S., Nolan, D., Witt, C., Masel, G., Martin, A. M., Moore, C., Sayer, D., Castley, A., Mamotte, C., Maxwell, D., James, I. and Christiansen, F. T. (2002) 'Association between presence of HLA-B*5701, HLA-DR7, and HLA-DQ3 and hypersensitivity to HIV-1 reverse-transcriptase inhibitor abacavir', *Lancet*, 359, (9308), pp. 727-32.
- Maria, V. A. and Victorino, R. M. (1998) 'Immunological investigation in hepatic drug reactions', *Clin Exp Allergy*, 28 Suppl 4, pp. 71-7.
- Martignoni, M., Groothuis, G. M. and de Kanter, R. (2006) 'Species differences between mouse, rat, dog, monkey and human CYP-mediated drug metabolism, inhibition and induction', *Expert Opin Drug Metab Toxicol*, 2, (6), pp. 875-94.
- Martinez-Jimenez, C. P., Jover, R., Donato, M. T., Castell, J. V. and Gomez-Lechon, M. J. (2007) 'Transcriptional regulation and expression of CYP3A4 in hepatocytes', *Curr Drug Metab*, 8, (2), pp. 185-94.
- Marquard, V., Beckmann, L., Heid, I. M., Lamina, C. and Chang-Claude, J. (2009) 'Impact of genotyping errors on the type I error rate and the power of haplotype-based association methods', *BMC Genet*, 10, pp. 3.

- Masubuchi, Y. (2006) 'Metabolic and non-metabolic factors determining troglitazone hepatotoxicity: a review', *Drug Metab Pharmacokinet*, 21, (5), pp. 347-56.
- Masubuchi, Y., Bourdi, M., Reilly, T. P., Graf, M. L., George, J. W. and Pohl, L. R. (2003) 'Role of interleukin-6 in hepatic heat shock protein expression and protection against acetaminophen-induced liver disease', *Biochem Biophys Res Commun*, 304, (1), pp. 207-12.
- Matzinger, P. (1994) 'Tolerance, danger, and the extended family', *Annu Rev Immunol*, 12, pp. 991-1045.
- McCarver, D. G., Byun, R., Hines, R. N., Hichme, M. and Wegenek, W. (1998) 'A genetic polymorphism in the regulatory sequences of human CYP2E1: association with increased chlorzoxazone hydroxylation in the presence of obesity and ethanol intake', *Toxicol Appl Pharmacol*, 152, (1), pp. 276-81.
- McCormack, M., Alfirevic, A., Bourgeois, S., Farrell, J. J., Kasperaviciute, D., Carrington, M., Sills, G. J., Marson, T., Jia, X., de Bakker, P. I., Chinthapalli, K., Molokhia, M., Johnson, M. R., O'Connor, G. D., Chaila, E., Alhusaini, S., Shianna, K. V., Radtke, R. A., Heinzen, E. L., Walley, N., Pandolfo, M., Pichler, W., Park, B. K., Depondt, C., Sisodiya, S. M., Goldstein, D. B., Deloukas, P., Delanty, N., Cavalleri, G. L. and Pirmohamed, M. (2011) 'HLA-A*3101 and carbamazepine-induced hypersensitivity reactions in Europeans', *N Engl J Med*, 364, (12), pp. 1134-43.
- McFarland, R., Hudson, G., Taylor, R. W., Green, S. H., Hodges, S., McKiernan, P. J., Chinnery, P. F. and Ramesh, V. (2008) 'Reversible valproate hepatotoxicity due to mutations in mitochondrial DNA polymerase gamma (POLG1)', *Arch Dis Child*, 93, (2), pp. 151-3.
- Meier, Y., Cavallaro, M., Roos, M., Pauli-Magnus, C., Folkers, G., Meier, P. J. and Fattinger, K. (2005) 'Incidence of drug-induced liver injury in medical inpatients', *Eur J Clin Pharmacol*, 61, (2), pp. 135-43.
- Menzies, D., Dion, M. J., Rabinovitch, B., Mannix, S., Brassard, P. and Schwartzman, K. (2004) 'Treatment completion and costs of a randomized trial of rifampin for 4 months versus isoniazid for 9 months', *Am J Respir Crit Care Med*, 170, (4), pp. 445-9.

- Metushi, I. G., Cai, P., Zhu, X., Nakagawa, T. and Uetrecht, J. P. (2011) 'A fresh look at the mechanism of isoniazid-induced hepatotoxicity', *Clin Pharmacol Ther*, 89, (6), pp. 911-4.
- Mitchell, J. R., Thorgeirsson, U. P., Black, M., Timbrell, J. A., Snodgrass, W. R., Potter, W. Z., Jollow, H. R. and Keiser, H. R. (1975) 'Increased incidence of isoniazid hepatitis in rapid acetylators: possible relation to hydrazine metabolites', *Clin Pharmacol Ther*, 18, (1), pp. 70-9.
- Mitchell, J. R., Zimmerman, H. J., Ishak, K. G., Thorgeirsson, U. P., Timbrell, J. A., Snodgrass, W. R. and Nelson, S. D. (1976) 'Isoniazid liver injury: clinical spectrum, pathology, and probable pathogenesis', *Ann Intern Med*, 84, (2), pp. 181-92.
- Mo, Z., Gao, Y., Cao, Y., Gao, F. and Jian, L. (2009) 'An updating meta-analysis of the GSTM1, GSTT1, and GSTP1 polymorphisms and prostate cancer: a HuGE review', *Prostate*, 69, (6), pp. 662-88.
- Molokhia, M. and McKeigue, P. (2006) 'EUDRAGENE: European collaboration to establish a case-control DNA collection for studying the genetic basis of adverse drug reactions', *Pharmacogenomics*, 7, (4), pp. 633-8.
- Moskvina, V., Craddock, N., Holmans, P., Owen, M. J. and O'Donovan, M. C. (2006) 'Effects of differential genotyping error rate on the type I error probability of case-control studies', *Hum Hered*, 61, (1), pp. 55-64.
- Naveen, A. T., Adithan, C., Padmaja, N., Shashindran, C. H., Abraham, B. K., Satyanarayanamoorthy, K., Anitha, P., Gerard, N. and Krishnamoorthy, R. (2004) 'Glutathione S-transferase M1 and T1 null genotype distribution in South Indians', *Eur J Clin Pharmacol*, 60, (6), pp. 403-6.
- Nei, M. (1975) 'The bottleneck effect and genetic variability in population', *Evolutin*, 29, pp. 10.
- Nelson, D. R., Koymans, L., Kamataki, T., Stegeman, J. J., Feyereisen, R., Waxman, D. J., Waterman, M. R., Gotoh, O., Coon, M. J., Estabrook, R. W., Gunsalus, I. C.

- and Nebert, D. W. (1996) 'P450 superfamily: update on new sequences, gene mapping, accession numbers and nomenclature', *Pharmacogenetics*, 6, (1), pp. 1-42.
- Noda, A., Hsu, K. Y., Noda, H., Yamamoto, Y. and Kurozumi, T. (1983) 'Is isoniazid-hepatotoxicity induced by the metabolite, hydrazine?', *J UOEH*, 5, (2), pp. 183-90.
- Nomura, F., Itoga, S., Uchimoto, T., Tomonaga, T., Nezu, M., Shimada, H. and Ochiai, T. (2003) 'Transcriptional activity of the tandem repeat polymorphism in the 5'-flanking region of the human CYP2E1 gene', *Alcohol Clin Exp Res*, 27, (8 Suppl), pp. 42S-46S.
- O'Donohue, J., Oien, K. A., Donaldson, P., Underhill, J., Clare, M., MacSween, R. N. and Mills, P. R. (2000) 'Co-amoxiclav jaundice: clinical and histological features and HLA class II association', *Gut*, 47, (5), pp. 717-20.
- Ohno, M., Yamaguchi, I., Yamamoto, I., Fukuda, T., Yokota, S., Maekura, R., Ito, M., Yamamoto, Y., Ogura, T., Maeda, K., Komuta, K., Igarashi, T. and Azuma, J. (2000) 'Slow N-acetyltransferase 2 genotype affects the incidence of isoniazid and rifampicin-induced hepatotoxicity', *Int J Tuberc Lung Dis*, 4, (3), pp. 256-61.
- Ostapowicz, G., Fontana, R. J., Schiodt, F. V., Larson, A., Davern, T. J., Han, S. H., McCashland, T. M., Shakil, A. O., Hay, J. E., Hynan, L., Crippin, J. S., Blei, A. T., Samuel, G., Reisch, J. and Lee, W. M. (2002) 'Results of a prospective study of acute liver failure at 17 tertiary care centers in the United States', *Ann Intern Med*, 137, (12), pp. 947-54.
- Page, K. R., Sifakis, F., Montes de Oca, R., Cronin, W. A., Doherty, M. C., Federline, L., Bur, S., Walsh, T., Karney, W., Milman, J., Baruch, N., Adelakun, A. and Dorman, S. E. (2006) 'Improved adherence and less toxicity with rifampin vs isoniazid for treatment of latent tuberculosis: a retrospective study', *Arch Intern Med*, 166, (17), pp. 1863-70.
- Pahl, R. and Schafer, H. (2010) 'PERMORY: an LD-exploiting permutation test algorithm for powerful genome-wide association testing', *Bioinformatics*, 26, (17), pp. 2093-100.

- Papay, J. I., Clines, D., Rafi, R., Yuen, N., Britt, S. D., Walsh, J. S. and Hunt, C. M. (2009) 'Drug-induced liver injury following positive drug rechallenge', *Regul Toxicol Pharmacol*, 54, (1), pp. 84-90.
- Parthasarathy, R., Sarma, G. R., Janardhanam, B., Ramachandran, P., Santha, T., Sivasubramanian, S., Somasundaram, P. R. and Tripathy, S. P. (1986) 'Hepatic toxicity in South Indian patients during treatment of tuberculosis with short-course regimens containing isoniazid, rifampicin and pyrazinamide', *Tubercle*, 67, (2), pp. 99-108.
- Passarelli, M. C., Jacob-Filho, W. and Figueras, A. (2005) 'Adverse drug reactions in an elderly hospitalised population: inappropriate prescription is a leading cause', *Drugs Aging*, 22, (9), pp. 767-77.
- Patel, H., Bell, D., Molokhia, M., Srishanmuganathan, J., Patel, M., Car, J. and Majeed, A. (2007) 'Trends in hospital admissions for adverse drug reactions in England: analysis of national hospital episode statistics 1998-2005', *BMC Clin Pharmacol*, 7, pp. 9.
- Pearson, W. R. (2005) 'Phylogenies of glutathione transferase families', *Methods Enzymol*, 401, pp. 186-204.
- Pessayre, D., Mansouri, A., Haouzi, D. and Fromenty, B. (1999) 'Hepatotoxicity due to mitochondrial dysfunction', *Cell Biol Toxicol*, 15, (6), pp. 367-73.
- Possuelo, L. G., Castelan, J. A., de Brito, T. C., Ribeiro, A. W., Cafrune, P. I., Picon, P. D., Santos, A. R., Teixeira, R. L., Gregianini, T. S., Hutz, M. H., Rossetti, M. L. and Zaha, A. (2008) 'Association of slow N-acetyltransferase 2 profile and anti-TB drug-induced hepatotoxicity in patients from Southern Brazil', *Eur J Clin Pharmacol*, 64, (7), pp. 673-81.
- Rae, J. M., Johnson, M. D., Lippman, M. E. and Flockhart, D. A. (2001) 'Rifampin is a selective, pleiotropic inducer of drug metabolism genes in human hepatocytes: studies with cDNA and oligonucleotide expression arrays', *J Pharmacol Exp Ther*, 299, (3), pp. 849-57.
- Rao D. C., G. C. (2008) Genetic dissection of complex traits. Oxford: Elsevier Inc.

- Raucy, J. L., Lasker, J., Ozaki, K. and Zoleta, V. (2004) 'Regulation of CYP2E1 by ethanol and palmitic acid and CYP4A11 by clofibrate in primary cultures of human hepatocytes', *Toxicol Sci*, 79, (2), pp. 233-41.
- Reau, N. S. and Jensen, D. M. (2008) 'Vanishing bile duct syndrome', *Clin Liver Dis*, 12, (1), pp. 203-17, x.
- Reed, J. C. (2001) 'Apoptosis-regulating proteins as targets for drug discovery', *Trends Mol Med*, 7, (7), pp. 314-9.
- Reuben, A., Koch, D. G. and Lee, W. M. (2010) 'Drug-induced acute liver failure: results of a U.S. multicenter, prospective study', *Hepatology*, 52, (6), pp. 2065-76.
- Robin, M. A., Le Roy, M., Descatoire, V. and Pessayre, D. (1997) 'Plasma membrane cytochromes P450 as neoantigens and autoimmune targets in drug-induced hepatitis', *J Hepatol*, 26 Suppl 1, pp. 23-30.
- Rochon, J., Protiva, P., Seeff, L. B., Fontana, R. J., Liangpunsakul, S., Watkins, P. B., Davern, T. and McHutchison, J. G. (2008) 'Reliability of the Roussel Uclaf Causality Assessment Method for assessing causality in drug-induced liver injury', *Hepatology*, 48, (4), pp. 1175-83.
- Roy, B., Chowdhury, A., Kundu, S., Santra, A., Dey, B., Chakraborty, M. and Majumder, P. P. (2001) 'Increased risk of antituberculosis drug-induced hepatotoxicity in individuals with glutathione S-transferase M1 'null' mutation', *J Gastroenterol Hepatol*, 16, (9), pp. 1033-7.
- Ryan, D. E., Ramanathan, L., Iida, S., Thomas, P. E., Haniu, M., Shively, J. E., Lieber, C. S. and Levin, W. (1985) 'Characterization of a major form of rat hepatic microsomal cytochrome P-450 induced by isoniazid', *J Biol Chem*, 260, (10), pp. 6385-93.
- Salazar-Paramo, M., Rubin, R. L. and Garcia-De La Torre, I. (1992) 'Systemic lupus erythematosus induced by isoniazid', *Ann Rheum Dis*, 51, (9), pp. 1085-7.

- Sarich, T. C., Adams, S. P., Petricca, G. and Wright, J. M. (1999) 'Inhibition of isoniazid-induced hepatotoxicity in rabbits by pretreatment with an amidase inhibitor', *J Pharmacol Exp Ther*, 289, (2), pp. 695-702.
- Sarich, T. C., Youssefi, M., Zhou, T., Adams, S. P., Wall, R. A. and Wright, J. M. (1996) 'Role of hydrazine in the mechanism of isoniazid hepatotoxicity in rabbits', *Arch Toxicol*, 70, (12), pp. 835-40.
- Sarma, G. R., Immanuel, C., Kailasam, S., Narayana, A. S. and Venkatesan, P. (1986) 'Rifampin-induced release of hydrazine from isoniazid. A possible cause of hepatitis during treatment of tuberculosis with regimens containing isoniazid and rifampin', *Am Rev Respir Dis*, 133, (6), pp. 1072-5.
- Satoh, T., Taylor, P., Bosron, W. F., Sanghani, S. P., Hosokawa, M. and La Du, B. N. (2002) 'Current progress on esterases: from molecular structure to function', *Drug Metab Dispos*, 30, (5), pp. 488-93.
- Schuetz, E. G., Schinkel, A. H., Relling, M. V. and Schuetz, J. D. (1996) 'P-glycoprotein: a major determinant of rifampicin-inducible expression of cytochrome P4503A in mice and humans', *Proc Natl Acad Sci U S A*, 93, (9), pp. 4001-5.
- Schwab, C. E. and Tuschl, H. (2003) 'In vitro studies on the toxicity of isoniazid in different cell lines', *Hum Exp Toxicol*, 22, (11), pp. 607-15.
- Sgro, C., Clinard, F., Ouazir, K., Chanay, H., Allard, C., Guilleminet, C., Lenoir, C., Lemoine, A. and Hillon, P. (2002) 'Incidence of drug-induced hepatic injuries: a French population-based study', *Hepatology*, 36, (2), pp. 451-5.
- Shama, L. N., Kubow, K. B., Jokela, J. and Robinson, C. T. (2011) 'Bottlenecks drive temporal and spatial genetic changes in alpine caddisfly metapopulations', *BMC Evol Biol*, 11, pp. 278.
- Sharma, S. K., Balamurugan, A., Saha, P. K., Pandey, R. M. and Mehra, N. K. (2002) 'Evaluation of clinical and immunogenetic risk factors for the development of

hepatotoxicity during antituberculosis treatment', *Am J Respir Crit Care Med*, 166, (7), pp. 916-9.

Shen, C., Meng, Q., Zhang, G. and Hu, W. (2008) 'Rifampicin exacerbates isoniazid-induced toxicity in human but not in rat hepatocytes in tissue-like cultures', *Br J Pharmacol*, 153, (4), pp. 784-91.

Shimada, T., Yamazaki, H., Mimura, M., Inui, Y. and Guengerich, F. P. (1994) 'Interindividual variations in human liver cytochrome P-450 enzymes involved in the oxidation of drugs, carcinogens and toxic chemicals: studies with liver microsomes of 30 Japanese and 30 Caucasians', *J Pharmacol Exp Ther*, 270, (1), pp. 414-23.

Simon, T., Becquemont, L., Mary-Krause, M., de Waziers, I., Beaune, P., Funck-Brentano, C. and Jaillon, P. (2000) 'Combined glutathione-S-transferase M1 and T1 genetic polymorphism and tacrine hepatotoxicity', *Clin Pharmacol Ther*, 67, (4), pp. 432-7.

Sinclair, J., Jeffery, E., Wrighton, S., Kostrubsky, V., Szakacs, J., Wood, S. and Sinclair, P. (1998) 'Alcohol-mediated increases in acetaminophen hepatotoxicity: role of CYP2E and CYP3A', *Biochem Pharmacol*, 55, (10), pp. 1557-65.

Singer, J. B., Lewitzky, S., Leroy, E., Yang, F., Zhao, X., Klickstein, L., Wright, T. M., Meyer, J. and Paulding, C. A. (2010) 'A genome-wide study identifies HLA alleles associated with lumiracoxib-related liver injury', *Nat Genet*, 42, (8), pp. 711-4.

Skakun, N. P. and Shman'ko, V. V. (1985) '[Synergistic effect of rifampicin on hepatotoxicity of isoniazid]', *Antibiot Med Biotekhnol*, 30, (3), pp. 185-9.

Soars, M. G., Petullo, D. M., Eckstein, J. A., Kasper, S. C. and Wrighton, S. A. (2004) 'An assessment of udp-glucuronosyltransferase induction using primary human hepatocytes', *Drug Metab Dispos*, 32, (1), pp. 140-8.

Song, X., Xie, M., Zhang, H., Li, Y., Sachdeva, K. and Yan, B. (2004) 'The pregnane X receptor binds to response elements in a genomic context-dependent manner,

and PXR activator rifampicin selectively alters the binding among target genes', *Drug Metab Dispos*, 32, (1), pp. 35-42.

Spracklin, D. K., Hankins, D. C., Fisher, J. M., Thummel, K. E. and Kharasch, E. D. (1997) 'Cytochrome P450 2E1 is the principal catalyst of human oxidative halothane metabolism in vitro', *J Pharmacol Exp Ther*, 281, (1), pp. 400-11.

Steele, M. A., Burk, R. F. and DesPrez, R. M. (1991) 'Toxic hepatitis with isoniazid and rifampin. A meta-analysis', *Chest*, 99, (2), pp. 465-71.

Stewart, J. D., Horvath, R., Baruffini, E., Ferrero, I., Bulst, S., Watkins, P. B., Fontana, R. J., Day, C. P. and Chinnery, P. F. (2010) 'Polymerase gamma gene POLG determines the risk of sodium valproate-induced liver toxicity', *Hepatology*, 52, (5), pp. 1791-6.

Stout, J. E., Engemann, J. J., Cheng, A. C., Fortenberry, E. R. and Hamilton, C. D. (2003) 'Safety of 2 months of rifampin and pyrazinamide for treatment of latent tuberculosis', *Am J Respir Crit Care Med*, 167, (6), pp. 824-7.

Sun, F., Chen, Y., Xiang, Y. and Zhan, S. (2008) 'Drug-metabolising enzyme polymorphisms and predisposition to anti-tuberculosis drug-induced liver injury: a meta-analysis', *Int J Tuberc Lung Dis*, 12, (9), pp. 994-1002.

Suzuki, T., Higgins, P. J. and Crawford, D. R. (2000) 'Control selection for RNA quantitation', *Biotechniques*, 29, (2), pp. 332-7.

Tafazoli, S., Mashregi, M. and O'Brien, P. J. (2008) 'Role of hydrazine in isoniazid-induced hepatotoxicity in a hepatocyte inflammation model', *Toxicol Appl Pharmacol*, 229, (1), pp. 94-101.

Takeda, K., Watanabe, J., Inoue, K. and Kanamura, S. (2000) 'Rifampicin suppresses hepatic CYP2E1 expression and minimizes DNA injury caused by carbon tetrachloride in perivenular hepatocytes of mice', *Alcohol Clin Exp Res*, 24, (4 Suppl), pp. 87S-92S.

- Takikawa, H., Takamori, Y., Kumagi, T., Onji, M., Watanabe, M., Shibuya, A., Hisamochi, A., Kumashiro, R., Ito, T., Mitsumoto, Y., Nakamura, A. and Sakaguchi, T. (2003) 'Assessment of 287 Japanese cases of drug induced liver injury by the diagnostic scale of the International Consensus Meeting', *Hepatol Res*, 27, (3), pp. 192-195.
- Temple, R. J. and Himmel, M. H. (2002) 'Safety of newly approved drugs: implications for prescribing', *Jama*, 287, (17), pp. 2273-5.
- Timbrell, J. A., Mitchell, J. R., Snodgrass, W. R. and Nelson, S. D. (1980) 'Isoniazid hepatotoxicity: the relationship between covalent binding and metabolism in vivo', *J Pharmacol Exp Ther*, 213, (2), pp. 364-9.
- Tostmann, A., Aarnoutse, R. E., Peters, W. H., Richard, P. N. and Boeree, M. J. (2010) 'Xanthine oxidase inhibition by allopurinol increases in vitro pyrazinamide-induced hepatotoxicity in HepG2 cells', *Drug Chem Toxicol*, 33, (3), pp. 325-8.
- Tostmann, A., Boeree, M. J., Peters, W. H., Roelofs, H. M., Aarnoutse, R. E., van der Ven, A. J. and Dekhuijzen, P. N. (2008) 'Isoniazid and its toxic metabolite hydrazine induce in vitro pyrazinamide toxicity', *Int J Antimicrob Agents*, 31, (6), pp. 577-80.
- Trauner, M., Meier, P. J. and Boyer, J. L. (1998) 'Molecular pathogenesis of cholestasis', *N Engl J Med*, 339, (17), pp. 1217-27.
- Ueda, K., Ishitsu, T., Seo, T., Ueda, N., Murata, T., Hori, M. and Nakagawa, K. (2007) 'Glutathione S-transferase M1 null genotype as a risk factor for carbamazepine-induced mild hepatotoxicity', *Pharmacogenomics*, 8, (5), pp. 435-42.
- Uetrecht, J. (2008) 'Idiosyncratic drug reactions: past, present, and future', *Chem Res Toxicol*, 21, (1), pp. 84-92.
- Ungo, J. R., Jones, D., Ashkin, D., Hollender, E. S., Bernstein, D., Albanese, A. P. and Pitchenik, A. E. (1998) 'Antituberculosis drug-induced hepatotoxicity. The role of hepatitis C virus and the human immunodeficiency virus', *Am J Respir Crit Care Med*, 157, (6 Pt 1), pp. 1871-6.

- Urban, T., Shen, Y., Chalasani, N. P., Fontana, R. J., Rochon, J., Stolz, A., Serrano, J. A., Aithal, G. P., Daly, A., Dillon, J. E., Floraros, A., Molokhia, M., Lucena, M. I., Goldstein, D. B. and Watkins, P. B. (2011) Conference on Digestive Disease Week 2011. Chicago, May. Philadelphia:Gastroenterology, W B Saunders Co-Elsevier INC.
- van Hest, R., Baars, H., Kik, S., van Gerven, P., Trompenaars, M. C., Kalisvaart, N., Keizer, S., Borgdorff, M., Mensen, M. and Cobelens, F. (2004) 'Hepatotoxicity of rifampin-pyrazinamide and isoniazid preventive therapy and tuberculosis treatment', *Clin Infect Dis*, 39, (4), pp. 488-96.
- Vanhoof, J., Landewe, S., Van Wijngaerden, E. and Geusens, P. (2003) 'High incidence of hepatotoxicity of isoniazid treatment for tuberculosis chemoprophylaxis in patients with rheumatoid arthritis treated with methotrexate or sulfasalazine and anti-tumour necrosis factor inhibitors', *Ann Rheum Dis*, 62, (12), pp. 1241-2.
- Vatsis, K. P., Martell, K. J. and Weber, W. W. (1991) 'Diverse point mutations in the human gene for polymorphic N-acetyltransferase', *Proc Natl Acad Sci U S A*, 88, (14), pp. 6333-7.
- Velaga, M. R., Wilson, V., Jennings, C. E., Owen, C. J., Herington, S., Donaldson, P. T., Ball, S. G., James, R. A., Quinton, R., Perros, P. and Pearce, S. H. (2004) 'The codon 620 tryptophan allele of the lymphoid tyrosine phosphatase (LYP) gene is a major determinant of Graves' disease', *J Clin Endocrinol Metab*, 89, (11), pp. 5862-5.
- Venkatesan, K. (1989) 'Clinical pharmacokinetic considerations in the treatment of patients with leprosy', *Clin Pharmacokinet*, 16, (6), pp. 365-86.
- Verma, S. and Kaplowitz, N. (2009) 'Diagnosis, management and prevention of drug-induced liver injury', *Gut*, 58, (11), pp. 1555-64.
- Vignati, L., Turlizzi, E., Monaci, S., Grossi, P., Kanter, R. and Monshouwer, M. (2005) 'An in vitro approach to detect metabolite toxicity due to CYP3A4-dependent bioactivation of xenobiotics', *Toxicology*, 216, (2-3), pp. 154-67.
- Vuilleumier, N., Rossier, M. F., Chiappe, A., Degoumois, F., Dayer, P., Mermillod, B., Nicod, L., Desmeules, J. and Hochstrasser, D. (2006) 'CYP2E1 genotype and

isoniazid-induced hepatotoxicity in patients treated for latent tuberculosis', *Eur J Clin Pharmacol*, 62, (6), pp. 423-9.

Wackerly D., M. W., Scheaffer R. (2008) *Mathematical statistics with applications*. California: Brooks/Cole.

Walraven, J. M., Zang, Y., Trent, J. O. and Hein, D. W. (2008) 'Structure/function evaluations of single nucleotide polymorphisms in human N-acetyltransferase 2', *Curr Drug Metab*, 9, (6), pp. 471-86.

Wang, T., Yu, H. T., Wang, W., Pan, Y. Y., He, L. X. and Wang, Z. Y. (2010) 'Genetic polymorphisms of cytochrome P450 and glutathione S-transferase associated with antituberculosis drug-induced hepatotoxicity in Chinese tuberculosis patients', *J Int Med Res*, 38, (3), pp. 977-86.

Watanabe, I., Tomita, A., Shimizu, M., Sugawara, M., Yasumo, H., Koishi, R., Takahashi, T., Miyoshi, K., Nakamura, K., Izumi, T., Matsushita, Y., Furukawa, H., Haruyama, H. and Koga, T. (2003) 'A study to survey susceptible genetic factors responsible for troglitazone-associated hepatotoxicity in Japanese patients with type 2 diabetes mellitus', *Clin Pharmacol Ther*, 73, (5), pp. 435-55.

Watanabe, J., Hayashi, S. and Kawajiri, K. (1994) 'Different regulation and expression of the human CYP2E1 gene due to the RsaI polymorphism in the 5'-flanking region', *J Biochem*, 116, (2), pp. 321-6.

Watkins, P. B. (2005) 'Idiosyncratic liver injury: challenges and approaches', *Toxicol Pathol*, 33, (1), pp. 1-5.

Watkins, P. B., Murray, S. A., Winkelman, L. G., Heuman, D. M., Wrighton, S. A. and Guzelian, P. S. (1989) 'Erythromycin breath test as an assay of glucocorticoid-inducible liver cytochromes P-450. Studies in rats and patients', *J Clin Invest*, 83, (2), pp. 688-97.

Weiner, I. M. and Tinker, J. P. (1972) 'Pharmacology of pyrazinamide: metabolic and renal function studies related to the mechanism of drug-induced urate retention', *J Pharmacol Exp Ther*, 180, (2), pp. 411-34.

- Weinberg, W. (1963) 'On the demonstration of heredity in man', *Papers on Human Genetics*, Prentice-Hall, Original: 1908; Translation by S.H. Boyer.
- Wester, K., Jonsson, A. K., Spigset, O., Druid, H. and Hagg, S. (2008) 'Incidence of fatal adverse drug reactions: a population based study', *Br J Clin Pharmacol*, 65, (4), pp. 573-9.
- Westerink, W. M. and Schoonen, W. G. (2007) 'Cytochrome P450 enzyme levels in HepG2 cells and cryopreserved primary human hepatocytes and their induction in HepG2 cells', *Toxicol In Vitro*, 21, (8), pp. 1581-91.
- Westfall, P. H. and Young, S. S. (1993) *Resampling-based multiple testing: examples and methods for p-value adjustment*. 1st Edition ed New York: John Wiley & Sons.
- WHO. (2002) *WHO safety of medicines. A guide to detecting and reporting adverse drug reactions. Why health professionals need to take action*. Geneva: World Health Organisation (WHO/EDM/QSM/2002.2).
- WHO. (2004) *Pharmacovigilance: ensuring the safe use of medicines. WHO Policy Perspectives on Medicines*. Geneva: World Health Organisation
- WHO. (2010a) *Global Tuberculosis Control* Geneva: World Health Organisation
- WHO (2010b) *Tuberculosis Fact sheet N°104 - Infection and transmission*. Available at: <http://www.who.int/mediacentre/factsheets/fs104/en/> (Accessed:
- Wigginton, J. E., Cutler, D. J. and Abecasis, G. R. (2005) 'A note on exact tests of Hardy-Weinberg equilibrium', *Am J Hum Genet*, 76, (5), pp. 887-93.
- Woo, J., Chan, C. H., Walubo, A. and Chan, K. K. (1992) 'Hydrazine--a possible cause of isoniazid--induced hepatic necrosis', *J Med*, 23, (1), pp. 51-9.

- Xie, W., Yeuh, M. F., Radomska-Pandya, A., Saini, S. P., Negishi, Y., Bottroff, B. S., Cabrera, G. Y., Tukey, R. H. and Evans, R. M. (2003) 'Control of steroid, heme, and carcinogen metabolism by nuclear pregnane X receptor and constitutive androstane receptor', *Proc Natl Acad Sci U S A*, 100, (7), pp. 4150-5.
- Xu, C., Li, C. Y. and Kong, A. N. (2005) 'Induction of phase I, II and III drug metabolism/transport by xenobiotics', *Arch Pharm Res*, 28, (3), pp. 249-68.
- Yamada, S., Tang, M., Richardson, K., Halaschek-Wiener, J., Chan, M., Cook, V. J., Fitzgerald, J. M., Elwood, R. K., Brooks-Wilson, A. and Marra, F. (2009) 'Genetic variations of NAT2 and CYP2E1 and isoniazid hepatotoxicity in a diverse population', *Pharmacogenomics*, 10, (9), pp. 1433-45.
- Yamamoto, T., Higashino, K., Kono, N., Kawachi, M., Nanahoshi, M., Takahashi, S., Suda, M. and Hada, T. (1989) 'Metabolism of pyrazinamide and allopurinol in hereditary xanthine oxidase deficiency', *Clin Chim Acta*, 180, (2), pp. 169-75.
- Yamamoto, T., Suou, T. and Hirayama, C. (1986) 'Elevated serum aminotransferase induced by isoniazid in relation to isoniazid acetylator phenotype', *Hepatology*, 6, (2), pp. 295-8.
- Yang, D., Pearce, R. E., Wang, X., Gaedigk, R., Wan, Y. J. and Yan, B. (2009) 'Human carboxylesterases HCE1 and HCE2: ontogenic expression, inter-individual variability and differential hydrolysis of oseltamivir, aspirin, deltamethrin and permethrin', *Biochem Pharmacol*, 77, (2), pp. 238-47.
- Yang, J. and Yan, B. (2007) 'Photochemotherapeutic agent 8-methoxypsoralen induces cytochrome P450 3A4 and carboxylesterase HCE2: evidence on an involvement of the pregnane X receptor', *Toxicol Sci*, 95, (1), pp. 13-22.
- Yee, D., Valiquette, C., Pelletier, M., Parisien, I., Rocher, I. and Menzies, D. (2003) 'Incidence of serious side effects from first-line antituberculosis drugs among patients treated for active tuberculosis', *Am J Respir Crit Care Med*, 167, (11), pp. 1472-7.
- Younossian, A. B., Rochat, T., Ketterer, J. P., Wacker, J. and Janssens, J. P. (2005) 'High hepatotoxicity of pyrazinamide and ethambutol for treatment of latent tuberculosis', *Eur Respir J*, 26, (3), pp. 462-4.

- Yue, J. and Peng, R. (2009) 'Does CYP2E1 play a major role in the aggravation of isoniazid toxicity by rifampicin in human hepatocytes?', *Br J Pharmacol*, 157, (3), pp. 331-3.
- Yue, J., Peng, R., Chen, J., Liu, Y. and Dong, G. (2009) 'Effects of rifampin on CYP2E1-dependent hepatotoxicity of isoniazid in rats', *Pharmacol Res*, 59, (2), pp. 112-9.
- Yue, J., Peng, R. X., Yang, J., Kong, R. and Liu, J. (2004) 'CYP2E1 mediated isoniazid-induced hepatotoxicity in rats', *Acta Pharmacol Sin*, 25, (5), pp. 699-704.
- Zang, Y., Doll, M. A., Zhao, S., States, J. C. and Hein, D. W. (2007a) 'Functional characterization of single-nucleotide polymorphisms and haplotypes of human N-acetyltransferase 2', *Carcinogenesis*, 28, (8), pp. 1665-71.
- Zang, Y., Zhao, S., Doll, M. A., Christopher States, J. and Hein, D. W. (2007b) 'Functional characterization of the A411T (L137F) and G364A (D122N) genetic polymorphisms in human N-acetyltransferase 2', *Pharmacogenet Genomics*, 17, (1), pp. 37-45.
- Zang, Y., Zhao, S., Doll, M. A., States, J. C. and Hein, D. W. (2004) 'The T341C (Ile114Thr) polymorphism of N-acetyltransferase 2 yields slow acetylator phenotype by enhanced protein degradation', *Pharmacogenetics*, 14, (11), pp. 717-23.
- Zhong, S., Wyllie, A. H., Barnes, D., Wolf, C. R. and Spurr, N. K. (1993) 'Relationship between the GSTM1 genetic polymorphism and susceptibility to bladder, breast and colon cancer', *Carcinogenesis*, 14, (9), pp. 1821-4.
- Zhu, W., Song, L., Zhang, H., Matoney, L., LeCluyse, E. and Yan, B. (2000) 'Dexamethasone differentially regulates expression of carboxylesterase genes in humans and rats', *Drug Metab Dispos*, 28, (2), pp. 186-91.
- Zimmerman, H. J. (1981) *Drug Hepatotoxicity: Spectrum of clinical lesions*. London: Pitman Medical.

Zimmerman, H. J. (1999) *Drug-induced liver disease*. 2nd ed Philadelphia: Lippincott Williams & Wilkins.

Zimniak, P., Singhal, S. S., Srivastava, S. K., Awasthi, S., Sharma, R., Hayden, J. B. and Awasthi, Y. C. (1994) 'Estimation of genomic complexity, heterologous expression, and enzymatic characterization of mouse glutathione S-transferase mGSTA4-4 (GST 5.7)', *J Biol Chem*, 269, (2), pp. 992-1000.